LA-UR-16-30[illegible]

Landscape History and Processes on the Pajarito Plateau, Northern New Mexico

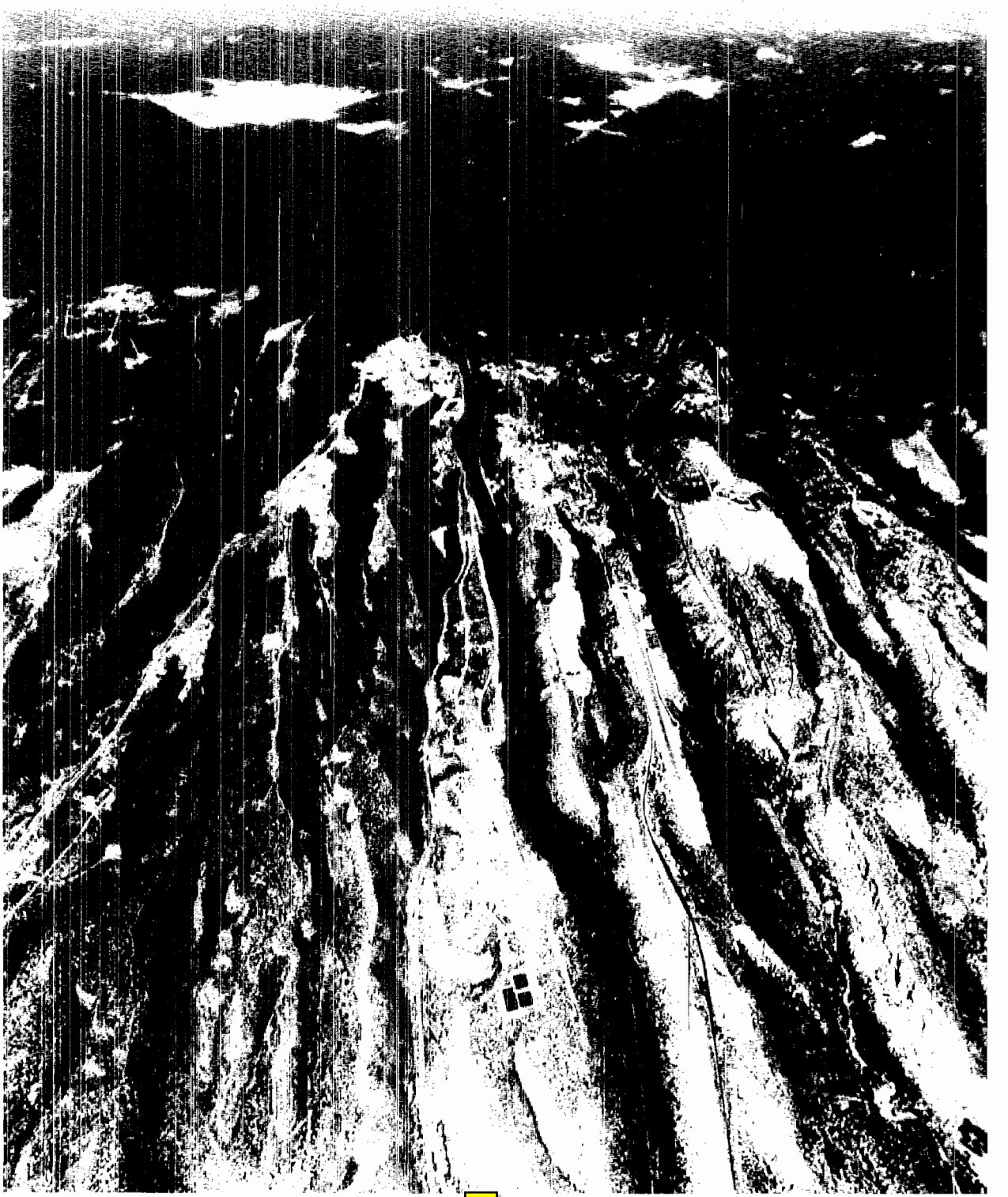

LOS ALAMOS NATIONAL LABORATORY
3 9338 00422 6329

LA-UR-96-3035

Landscape History and Processes on the Pajarito Plateau, Northern New Mexico

Rocky Mountain Cell, Friends of the Pleistocene
Field Trip Guidebook
September 12-15, 1996

Steven L. Reneau[1] and Eric V. McDonald[1]

Co-Leaders:

Craig D. Allen[2], David E. Broxton[1], Jamie N. Gardner[1], Rory P. Gauthier[3], Keith I. Kelson[4], William M. Phillips[5], Bradford P. Wilcox[6]

[1]Geology and Geochemistry Group, MS D462, Los Alamos National Laboratory, Los Alamos, NM 87545

[2]National Biological Service, Bandelier National Monument, Los Alamos, New Mexico, 87544

[3]Chaco Canyon National Historical Park, Nageezi, New Mexico 87037

[4]William Lettis and Associates, 1777 Botelho Drive, Suite 262, Walnut Creek, CA 94596

[5] Department of Geosciences, University of Arizona, Tucson, AZ 8572, and Environmental Science and Waste Technology Group, MS J514, Los Alamos National Laboratory, Los Alamos, NM 87545

[6]Environmental Sciences Group, MS J495, Los Alamos National Laboratory, Los Alamos, NM 87545

LOS ALAMOS NATL. LAB. LIBS.
3 9338 00422 6329

Guidebook supported by the Seismic Hazards Investigation Program and the Environmental Restoration Project of Los Alamos National Laboratory

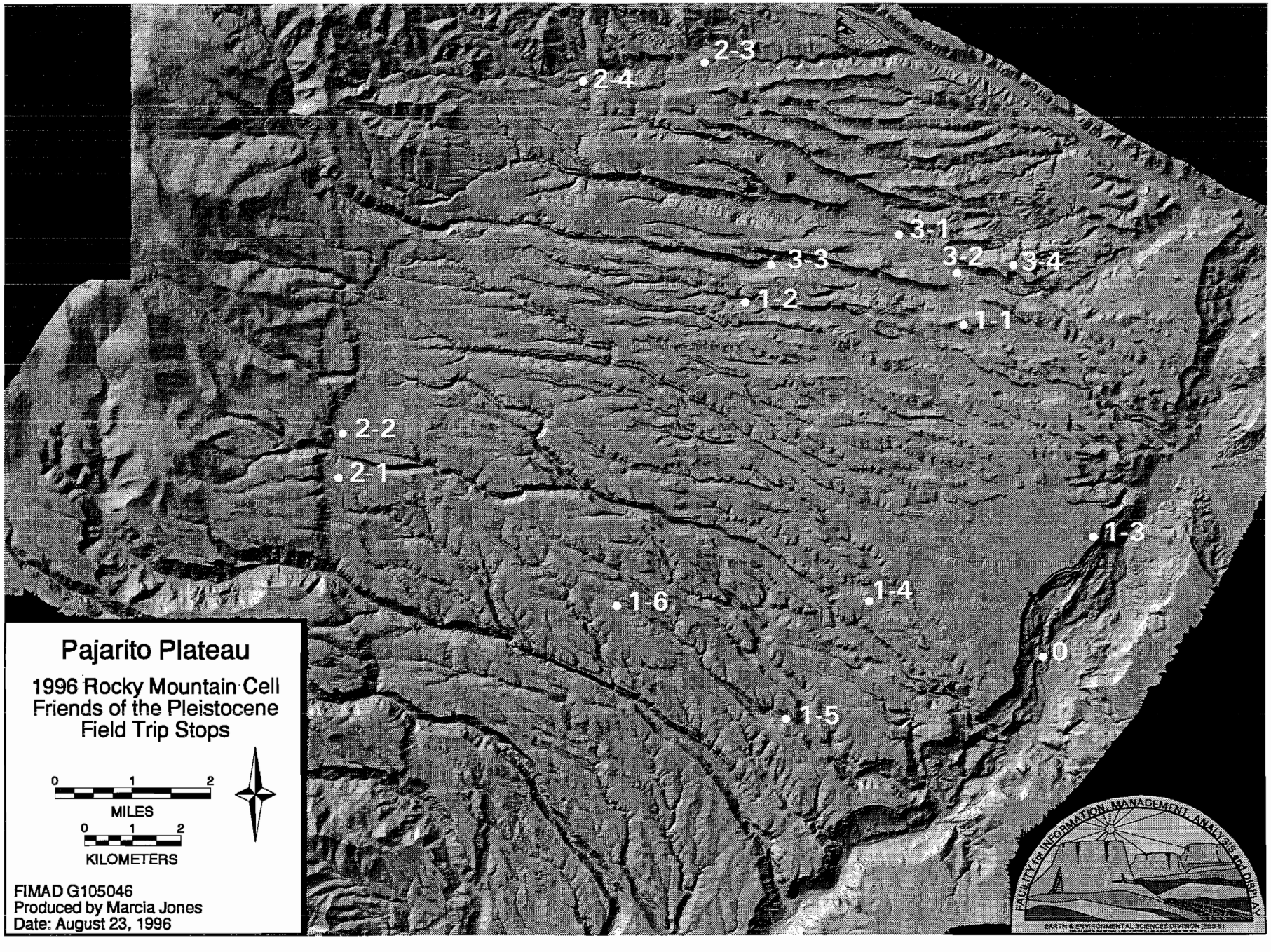
2-3
2-4
3-1
3-3
3-2
3-4
1-2
1-1
2-2
2-1
1-3
1-4
1-6
0
1-5
Pajarito Plateau
1996 Rocky Mountain Cell
Friends of the Pleistocene
Field Trip Stops
0 1 2
MILES
0 1 2
KILOMETERS
FIMAD G105046
Produced by Marcia Jones
Date: August 23, 1996
FACILITY FOR INFORMATION MANAGEMENT, ANALYSIS, AND DISPLAY
EARTH & ENVIRONMENTAL SCIENCES DIVISION (EES-5)

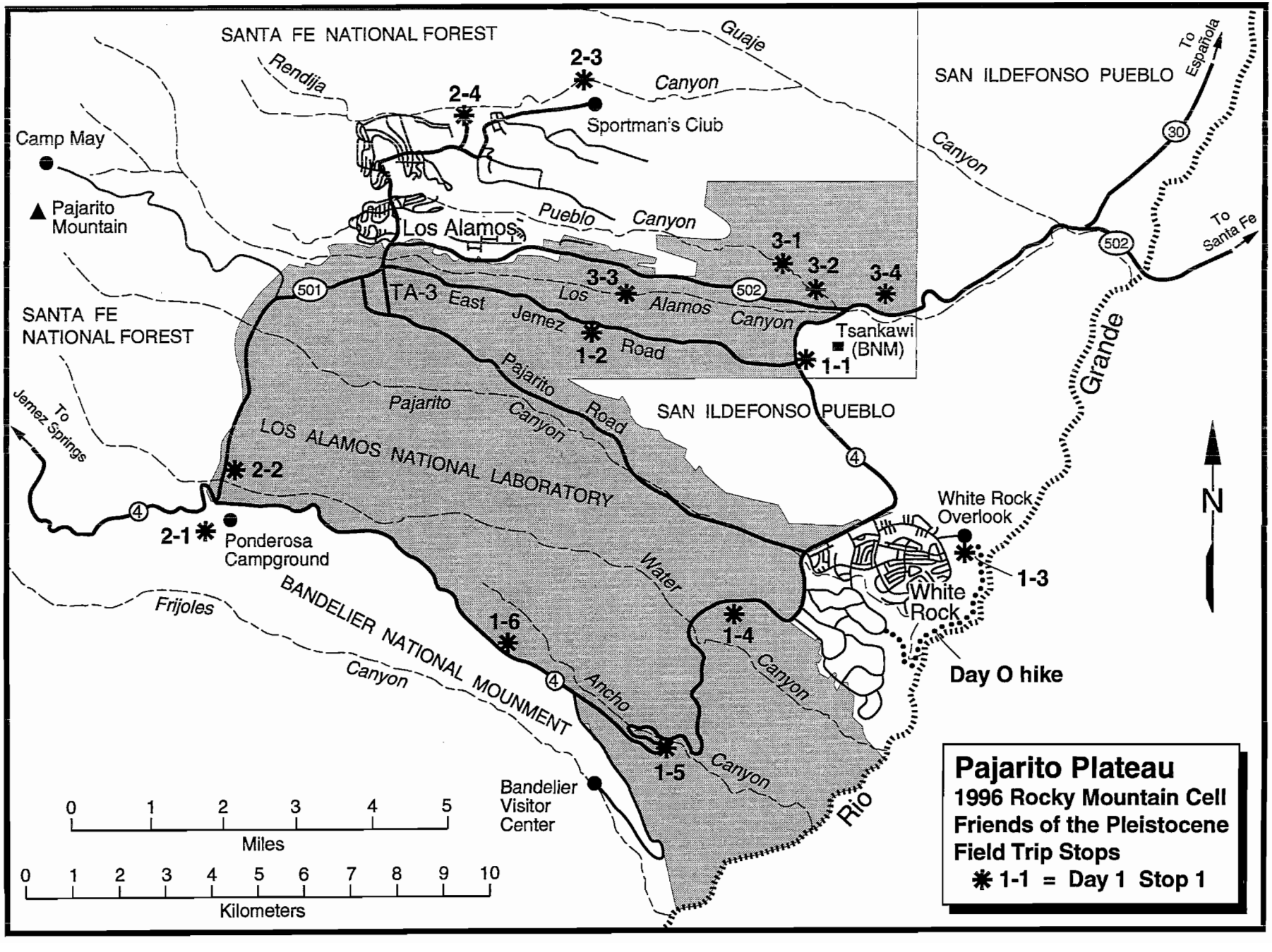
SANTA FE NATIONAL FOREST
Rendija
Guaje
Canyon
2-3
2-4
Sportman's Club
SAN ILDEFONSO PUEBLO
To Española
30
Camp May
Pajarito Mountain
Pueblo
Canyon
Los Alamos
3-1
3-2
3-4
3-3
501
502
TA-3
East
Jemez
Road
Los
Alamos
Canyon
Tsankawi (BNM)
1-1
1-2
SANTA FE NATIONAL FOREST
To Santa Fe
Grande
Pajarito
Canyon
Pajarito
Road
SAN ILDEFONSO PUEBLO
To Jemez Springs
LOS ALAMOS NATIONAL LABORATORY
2-2
4
2-1
Ponderosa Campground
White Rock Overlook
1-3
White Rock
Water
Frijoles
Canyon
BANDELIER NATIONAL MOUNMENT
1-6
1-4
Canyon
Ancho
Canyon
1-5
Rio
Day O hike
Bandelier Visitor Center
N
0 1 2 3 4 5
Miles
0 1 2 3 4 5 6 7 8 9 10
Kilometers
Pajarito Plateau
1996 Rocky Mountain Cell
Friends of the Pleistocene
Field Trip Stops
1-1 = Day 1 Stop 1

ACKNOWLEDGMENTS

Most of the work discussed in this guidebook was funded by the U.S. Department of Energy through the Los Alamos National Laboratory Environmental Restoration Project and Seismic Hazards Investigation Program. Support from numerous individuals in these programs has been vital, including Jim Aldrich, Dave Broxton, Darrell Bultman, Keith Dowler, Gary Eller, Jamie Gardner, Chuck Harrington, Dean Keller, Don Krier, Bill Laughlin, Roy Michelotti, Dean Nelson, Allyn Pratt, Marty Price, Robert Raymond, Cheryl Rofer, Everett Springer, and Doug Volkman. Support from the National Park Service in conducting field work in Bandelier National Monument has been greatly appreciated, and San Ildefonso Pueblo has also generously permitted access onto their lands for some geologic and environmental activities.

Colleagues who have made important contributions to this work on the Pajarito Plateau, in addition to the leaders of this field trip, include David Dethier of Williams College; Tom Kolbe, Susan Olig, and Ivan Wong of Woodward-Clyde Federal Services; Steve Forman of the University of Illinois; Will Graf of Arizona State University; Les McFadden and Paula Watt of the University of New Mexico; Paul Drakos of Glorietta Geoscience; Mark Hemphill-Haley of the University of Oregon; Dave Simpson of Woodward-Clyde Consultants; Sue Cannon of the U.S. Geological Survey; and Scott Baldridge, Karen Carter, Fraser Goff, Pat Longmire, Dave Vaniman, and Giday WoldeGabriel of Los Alamos National Laboratory. Participants in the "Canyons" investigations have included Jeff Blossom, Dave Broxton, Flori Caporuscio, Deba Daymon, Jenny Harris, Johnnye Lewis, Pat Longmire, Gerald Martinez, Orrin Myers, Mary Mullen, Randy Ryti, Linnea Wahl, and Brad Wilcox, and field rad teams from ERG in Albuquerque (Dave Hunter, Darrio Rocha, John Taylor) and Chemrad in Oak Ridge, Tennessee (Mike Blair, Chuck Flynn, Brett Lawrence). We have learned and continue to learn a lot from all of you.

Field, laboratory, and computer assistance from a number of people have been essential, including Diana Anderson, Kirk Anderson, Jeff Blossom, John Carney, Kerry Cummings, Marcia Fronterhouse, Rose Gallaway, Antonio Garcia, Penny Gomez, Kevin Reid, Matt Rice, and Karen Shaffon. Special thanks goes to the personnel of the Facility for Information, Management, Analysis, and Display (FIMAD), LANL's Geographic Information System team, for their continual support in providing maps and other products, including: Tom Garrison, Marcia Jones, Nancy Marusak, Belinda Scheber, and Doug Walther. Review comments on various sections of this guidebook by Jamie Gardner, David Dethier, Dave Broxton, Craig Allen, and Brad Wilcox are also much appreciated. We would also like to express great appreciation to Dan Thomas for his efforts in trying to allow soil pits to be excavated and investigated while meeting ever-changing safety requirements.

Last but not least, this guidebook would have not been possible except for the outstanding support provided by Anthony Garcia and Lanny Piotrowski with illustrations and word processing under a ridiculously short deadline. Thanks!

CAUTIONARY PREFACE

Much of this field trip is on Department of Energy land, passing through many areas posted with DOE "No Trespassing" signs. Several field trip stops are in such areas, and these stops should not be made without being in the company of Laboratory or other authorized personnel on official business. The consumption of alcohol is prohibited on DOE land, so please wait until appropriate times to imbibe (lunch stops are on Los Alamos County lands, where no such restrictions apply). Some stops are within Bandelier National Monument, so please respect their regulations as well (no rock hammers!). Part of the field trip also passes through lands of San Ildefonso Pueblo, closed to the public, and we ask that their boundaries be respected. Archaeological sites are scattered throughout the field trip area, and are protected under Federal law: feel free to admire artifacts, but please leave them where you found them!! Finally, be warned that the police of Los Alamos County show great diligence in their job: speeding, open containers, minors with alcohol, etc., are an invitation for trouble, so, please use common sense on this field trip.

INTRODUCTION

The Pajarito Plateau is a dissected landscape of alternating mesas and canyons that is located on the east flank of the Jemez Mountains (the Sierra de los Valles), draining eastward to White Rock Canyon of the Rio Grande (Fig. 1). The defining feature of the Plateau is the Tshirege Member of the Bandelier Tuff, a massive series of ignimbrites (also called "ash-flow tuffs") erupted from the Jemez Mountains at ca. 1.22 Ma and associated with development of the Valles caldera. The Tshirege Member buried most of the former topography between the mountains and the Rio Grande, almost instantaneously creating a new landscape and providing an excellent early Pleistocene datum which aids in an examination of neotectonics and drainage evolution.

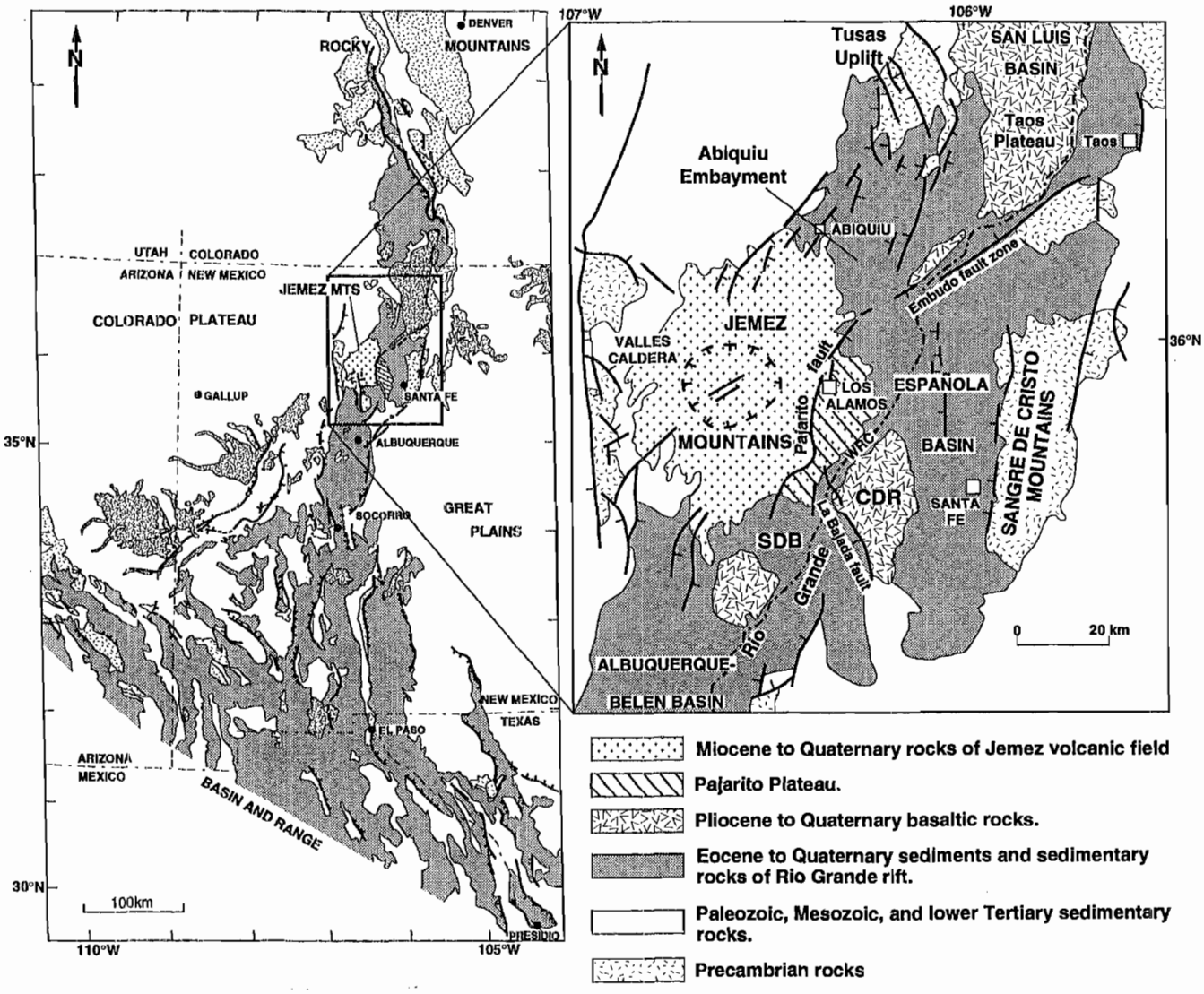

Fig. 1. Generalized geologic map showing the distribution of Cenozoic sediments of the Rio Grande rift and adjacent Basin and Range province, Cenozoic volcanic rocks of the rift and the Jemez lineament, and major faults. Inset shows general geologic and geographic features in the Los Alamos area. CDR: Cerros del Rio volcanic field; SDB: Santo Domingo basin; WRC: White Rock Canyon of the Rio Grande (modified from Baldridge et al., 1994).

This area is widely known and studied by volcanologists, with the Valles caldera being the "type-example" of a resurgent caldera, and with the Bandelier Tuff providing world-class examples of high-volume (>10^2 km^3) silicic ignimbrites (Smith and Bailey, 1966, 1968; see field trip guides to this area by Bailey and Smith, 1978; Self et al., 1987; Goff et al., 1989, 1996; Self and Sykes, 1996). The Pajarito Plateau is also renowned for its archaeological sites, possessing an exceptionally high density of ancestral Puebloan (Anasazi) ruins both in Bandelier National Monument and in surrounding areas. The Plateau has also entered history books as the home of "Project Y" of the "Manhattan Engineering District", the top-secret World War II project to develop the first atomic bombs which has evolved into the present Los Alamos National Laboratory ("LANL", a Department of Energy facility operated by the University of California).

Research on Quaternary geology and surface processes on the Pajarito Plateau has accelerated over the last 5-10 years, driven in large part by seismic hazard and environmental concerns at LANL. A Seismic Hazards Investigation Program was initiated in 1984 (Gardner and House, 1987), and has subsequently resulted in an increased understanding of many aspects of Pajarito Plateau geology. Field work for the LANL Environmental Restoration Project was begun in 1992, part of a nationwide DOE program whose ambitious goal is to systematically evaluate and clean up contaminated sites throughout the DOE complex, and has further spurred detailed earth science investigations across the Laboratory.

This field trip will focus on select aspects of the geology of the Pajarito Plateau, particularly the late Quaternary geomorphic history and soils, supplemented by briefer discussion of a range of topics pertaining to Quaternary geology, surface processes, and archaeology. No attempt is made on the field trip to cover all related topics, although references contained in this introduction and in the logs are intended to direct the reader to much of the recent and earlier work, including work that has not yet been published outside the internal LANL literature (but which is generally available for distribution).

Modern Climate

The Pajarito Plateau has a semiarid, temperate mountain climate (Bowen, 1990, 1992). The average temperature is about 8.8°C (47.8°F) in Los Alamos (7380', 2250 m elev.) and 9.6°C (49.3°F) in White Rock (6380', 1945 m elev.), with maximum and minimum temperatures occurring in July and January, respectively (Fig. 2). The average annual precipitation is about 45 cm (17.8 in) in Los Alamos and 34 cm (13.3 in) in White Rock. Precipitation has a strong maximum in July and August, corresponding with the "summer monsoon" and providing ~40% of the average annual total. Summer moisture is derived from the south, primarily the Gulf of Mexico, and is associated with thunderstorms that can develop on an almost daily basis, producing locally intense but spatially variable rainfall. Analyses of Los Alamos precipitation data by Bowen (1990) indicate that 1-hr rainfalls of ~3-4 cm and 15-min rainfalls of ~2-3 cm occur every 10 yrs on different parts of the Plateau (with higher average intensities occurring to the west). These intense rainfalls can generate very rapid surface runoff and flashy flood peaks.

Snowfall is primarily derived from frontal storms that originate to the west over the Pacific Ocean, and is highly variable from year to year (Bowen, 1990, 1992). A historic minimum of 24 cm occurred in Los Alamos in 1949-1950, and a maximum of 389 cm in 1986-1987. On average, winter is the driest season on the Pajarito Plateau, with the minimum average monthly precipitation occur-

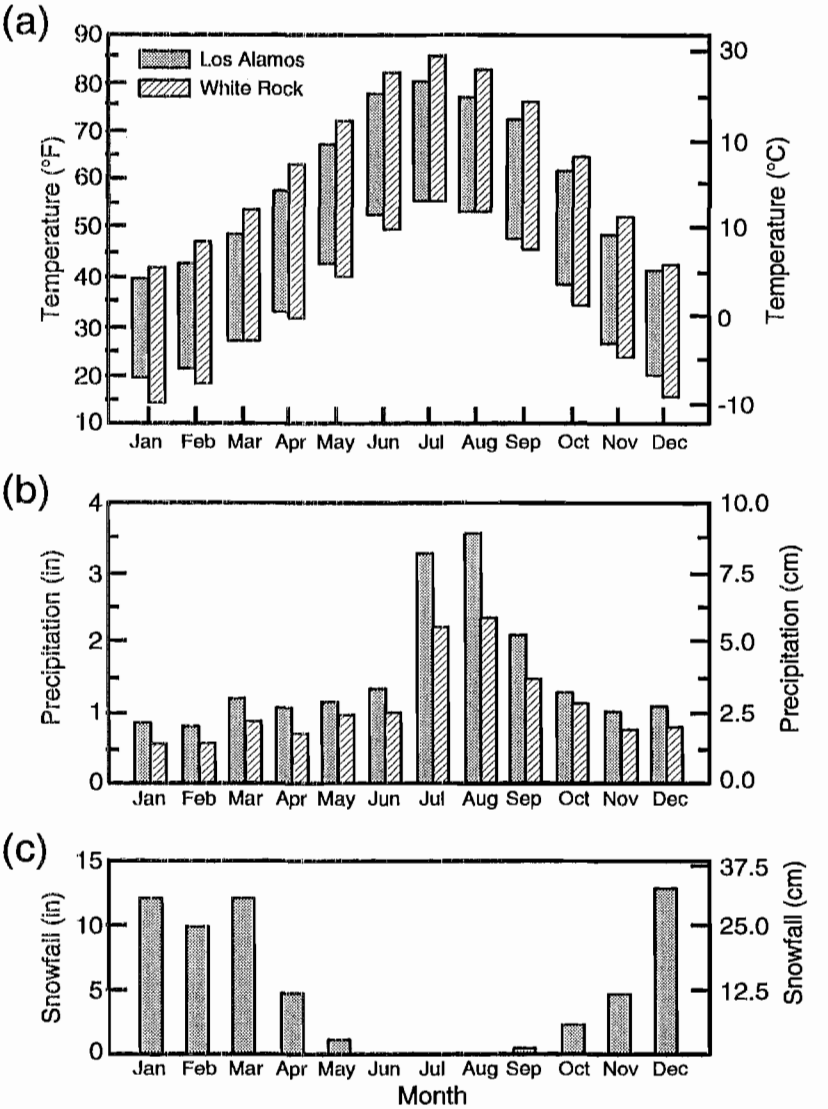

Fig. 2. Summary of "normal weather" in Los Alamos (1961-1990) and White Rock (1965-1990). (a) average daily minimum and maximum temperature, and (b) average monthly precipitation for both sites; and (c) average monthly Los Alamos snowfall (from Bowen, 1992).

ring in February (Fig. 2). However, plant-available water is much less in the spring due to higher evapotranspiration rates, and extended dry periods in May and June are common.

Systematic variations in precipitation occur between the lower elevation, eastern Pajarito Plateau and the higher elevation, western Plateau, with both mean summer and mean annual precipitation increasing to the west towards the Jemez Mountains (Fig. 3, Bowen 1990, 1992). Relations between elevation and annual precipitation for the area have been prepared by Spiegel and Baldwin (1963) and Rogers (1994), as shown in Figure 4.

Modern Vegetation

The modern vegetation of the Pajarito Plateau is dominated by piñon-juniper ("PJ") woodlands to the east and ponderosa pine forests to the west, modified by variations in soils, slope aspect, and other factors such as anthropogenic disturbances (Foxx and Tierney, 1984; Allen, 1989). The east-

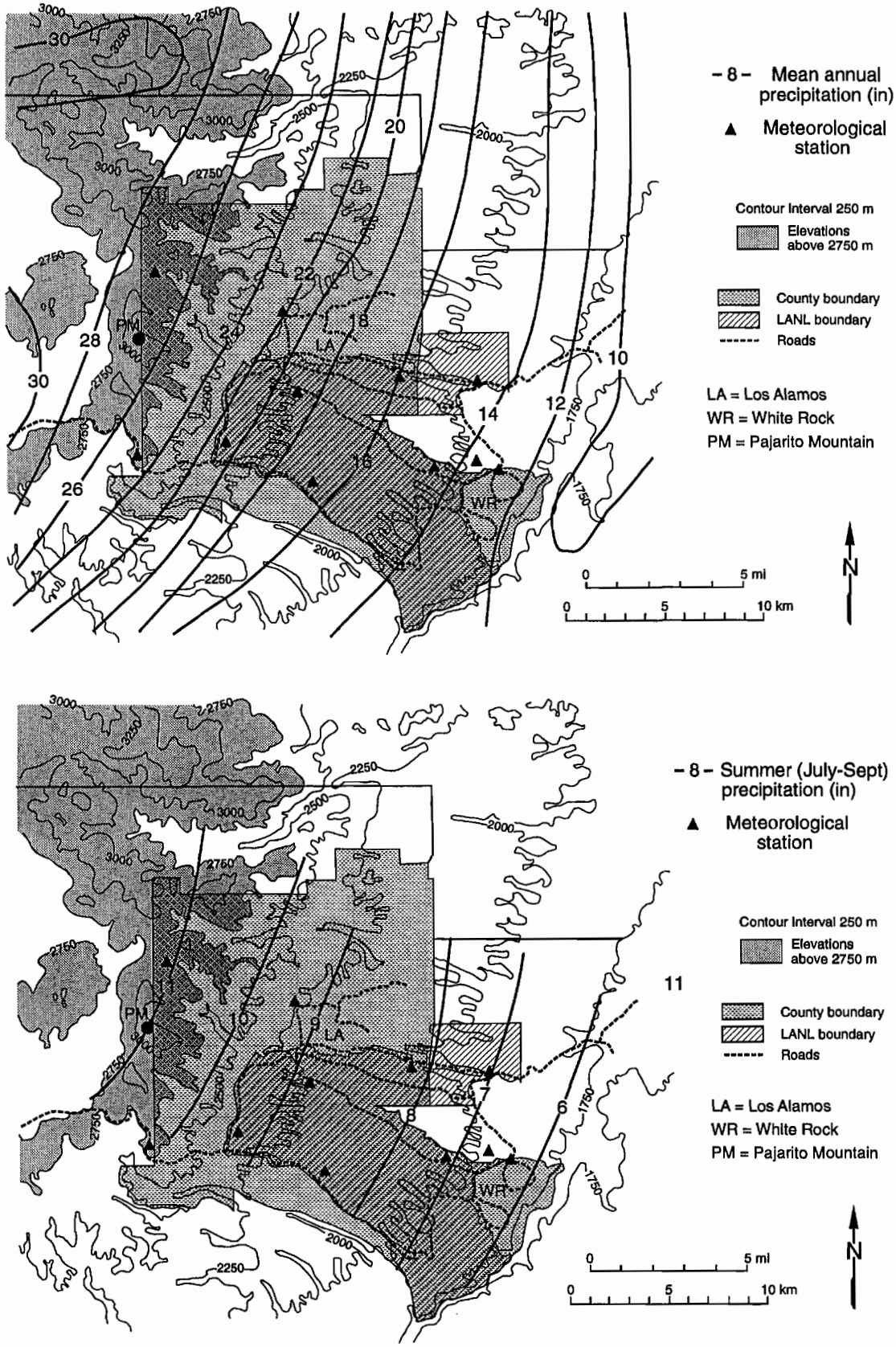

Fig. 3. Maps showing east to west variations in (a) mean annual precipitation across the Pajarito Plateau, and (b) July to September mean precipitation (the "summer monsoon"). From Rogers (1994), as modified from Bowen (1990) and Williams (1986).

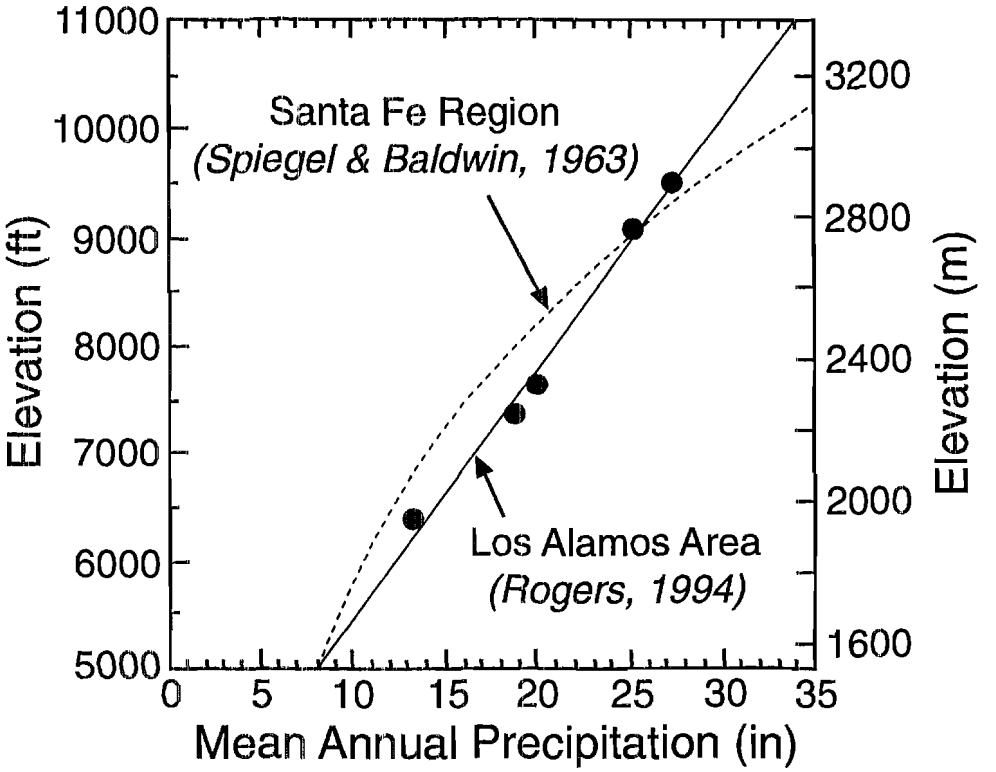

Fig. 4. Elevation-precipitation relationships for the Santa Fe region estimated by Spiegel and Baldwin (1963) and for the Los Alamos area by Rogers (1994)..

west orientations of the canyons produce strong variations between north-facing and south-facing canyon walls, and vegetation more typical of montane forests in the Jemez Mountains can extend significant distances to the east on north-facing slopes, contrasting with relatively arid conditions on opposing south-facing walls. Cold air drainage from the Sierra de los Valles also helps create relatively moist environments in the canyons, particularly their western parts. On mesas, ponderosa pines often extend farther east in relatively thick and porous pumice-rich soils, adjacent to piñon pines and junipers where thinner soils overlie tuff bedrock. Ponderosa pines can also be common in some sandy canyon bottoms to the east.

The general east-west variations in vegetation communities between the Rio Grande and the summits of the Jemez Mountains, from Allen (1989), are shown below.

Elevation	General Vegetation Communities
1600-1900 m	Juniper grasslands (*Juniperus monosperma, Bouteluoa* sp.)
1900-2100 m	Piñon-juniper woodlands (*Pinus edulis, Juniperus monosperma*)
2100-2300 m	Ponderosa pine forests (*Pinus ponderosa*)
2300-2900 m	Mixed conifer forests of ponderosa pine, Douglas-fir (*Pseudotsuga menziesii*), white fir (*Abies concolor*), aspen (*Populus tremuloides*), and limber pine (*Pinus flexilis*)
2900-3500 m	North-facing slopes: Spruce-fir forests of Engelmann spruce (*Picea engelmanni*) and corkbark fir (*Abies lasiocarpa* var. *arizonica*)
	South-facing mountain slopes: local areas of high elevation grasslands (*Festuca thurberi, Danthonia parryi*)

Paleoenvironments

Paleoclimatic data are sparse in the immediate vicinity of the Pajarito Plateau and the Jemez Mountains, with no long site-specific records presently existing (Spaulding, 1992). Inferences about late Quaternary changes in vegetation and climate thus must be based on work in surrounding regions, subject to the uncertainties imparted by the original records and by extrapolation to the Plateau.

Many of the available paleoclimatic records indicate that the late Pleistocene climate of the Southwest was generally wetter than today, with precipitation probably dominated by winter frontal storms (Spaulding et al., 1983; Hall, 1985; Van Devender et al., 1987; Allen, 1991; Phillips et al., 1992; Thompson et al., 1993). There is also some indication from pollen records that the full-glacial climate (ca. 22-16 ^{14}C ka) was colder and drier than the latest Pleistocene, with little summer rainfall (Spaulding, 1992). Late Pleistocene vegetation at the elevation of the Pajarito Plateau elsewhere in the Southwest included montane forests or parklands of spruce and fir (Wright et al., 1973; Betancourt, 1990; Anderson, 1993), and similar vegetation communities presumably occurred on the Plateau.

Vegetation more closely resembling modern communities became established perhaps around 10 ^{14}C ka, associated with a warmer, drier climate than in the latest Pleistocene and greatly enhanced summer precipitation. A variety of paleoclimate records from the Rocky Mountains of Colorado, the Colorado Plateau, and the southwestern deserts imply that summer rainfall in the early Holocene was higher than today, indicating stronger monsoonal circulation at that time (e.g., Markgraf and Scott, 1981; Friedman et al., 1988; Betancourt, 1990; Davis and Shafer, 1992; Thompson et al., 1993). For the middle Holocene, particularly ca. 7.5-5.5 ^{14}C ka, Spaulding (1992) points out a contrast in available records between apparently warmer and moister conditions to the north and west of the Pajarito Plateau and pronounced aridity to the south, compounding the uncertainty as to the middle Holocene climate on the Plateau.

Archaeology

The archaeological record of the Pajarito Plateau and surrounding areas is dominated by relatively late stages of ancestral Puebloan or Anasazi culture. Most of the ruins date to after about A.D. 1200, post-dating the peak of Anasazi culture in areas to the west such as Chaco Canyon and Mesa Verde. Records of earlier periods are relatively sparse. A brief discussion of the major prehistoric periods follows, with the general chronology from Cordell (1979, 1984) and Stuart and Gauthier (1981).

The PaleoIndian Period is dated to ca. 10,000 B.C. to ca. 5500-4000 B.C., and is poorly understood on the Pajarito Plateau. Elsewhere it includes the big-game hunters of the Clovis and later Folsom cultures. Rare Folsom points (ca. 8000-9000 B.C.) provide evidence of early prehistoric occupation on the Plateau (Steen, 1977, 1982). Two buried fire pits that were recently exposed in trenches on Pajarito Mesa, dated at ca. 9.3-9.5 ^{14}C ka (ca. 8200-8600 cal B.C.; Kolbe et al., 1994; Reneau et al., 1995b), provide confirmation of prehistoric occupation during this period.

The Archaic Period is considered to extend from ca. 5500-4000 B.C. to ca. A.D. 400-600. The most common evidence from this period on the Pajarito Plateau consists of surface lithic scatters which are undated or poorly dated. Some recent dates from buried sites have been obtained from investigations of late Quaternary deposits on the Plateau, specifically a date of ca. 3.94 ^{14}C ka (~2460 cal B.C.) from a site in Frijoles Canyon and a date of ca. 4.66 ^{14}C ka (~3370-3470 cal B.C.) from a hearth in the Fence Canyon area.

The local Rio Grande Anasazi (prehistoric Pueblo) record begins with the relatively poorly understood Developmental Period, which extended from ca. A.D. 600-1175. The successive Coalition Period (ca. A.D. 1175-1325) is better understood, and included major increases in prehistoric populations in this area. Peak occupation of relatively high elevation mesas on the Pajarito Plateau occurred in the Late Coalition Period, ca. A.D. 1250-1325, and ruins from this period occur on most mesa tops (Stuart and Gauthier, 1981; Orcutt, 1991). The Classic Period of the Rio Grande Anasazi extended from ca. A.D. 1325-1600, and during this period populations consolidated into relatively large pueblos at lower elevations, including Tshirege, Tyuonyi, Otowi, and Tsankawi (Stop 1-1). These sites were apparently abandoned shortly before the arrival of Spaniards, and the modern pueblos of San Ildefonso, Santa Clara, and Cochiti along the Rio Grande trace their ancestry to the prehistoric inhabitants of the Pajarito Plateau.

History

The first Europeans to visit the Pajarito Plateau region were Spaniards with the Coronado expedition in 1541, although they likely remained to the east within the Rio Grande valley. Brief visits up the Rio Grande were next made in 1581 and 1582 by the Rodriguez and Espejo expeditions, with actual conquest of the region by Onate in 1598. The Spanish were expelled during the Pueblo revolt of 1680, but the area was reconquered by de Vargas in 1692.

Much of the Pajarito Plateau was given to the Sanchez family as a Spanish Land Grant in 1742, part of which was later known as the Ramon Vigil Grant, beginning a period of small-scale subsistence farming. However, significant and wide-spread land-use changes probably did not occur on the Pajarito Plateau until at least the 1860s, with Navaho and Apache raiding parties restricting use first by the Spanish and later by Americans (this area became a United States territory with the Mexican Cession in 1848). Large numbers of sheep and cattle were being grazed in the area by the 1880s, and commercial logging began in 1897. Grazing, logging, and farming continued until 1942 when part of the area was taken over by the U.S. Government for the Manhattan Project, whose purpose was to develop the first atomic bombs. Many areas were developed beginning in 1943 with the WW II activities, and then for subsequent growth of the Los Alamos Scientific Laboratory, the Los Alamos townsite, and the initial construction camp and later bedroom community of White Rock (see summaries in Foxx and Tierney, 1984, Allen, 1989, and Rothman, 1992).

Tectonic Setting

The Pajarito Plateau is located within the Española basin of the Rio Grande rift, a major north-south trending continental rift that extends from near the Mexican border into southern Colorado (Fig. 1). The rift has been active since perhaps ~27-28 Ma, with major rift basins forming by ~15 Ma (e.g., Chapin, 1988; Ingersoll et al., 1990; Chapin and Cather, 1994).

The Española basin is bounded to the north by the Embudo fault and to the south by the La Bajada fault, which are interpreted as accommodation zones that transfer displacement between the Española basin, the San Luis basin and the Abiquiu embayment to the north, and the Santo Domingo basin to the south (Kelley, 1979; Muehlberger, 1979; Aldrich, 1986; Baldridge et al., 1994; Chapin and Cather, 1994; Gonzalez, 1995). The Pajarito fault zone forms the active western boundary of the Española basin and the Rio Grande rift, crossing the western Pajarito Plateau on and adjacent to LANL (Manley, 1979; Golombek, 1983; Golombek et al., 1983; Gardner and Goff, 1984; Gardner

and House, 1978; Wong et al., 1995; Olig et al., 1996). It is believed to have been active since at least around 5 Ma on the northern Plateau, with deformation along the southern part of the fault beginning prior to 16.5 Ma (Gardner and Goff, 1984).

The Española basin is often referred to as a half-graben, as it only displays major Quaternary faulting on its western border (the Pajarito fault system), and the structurally deepest part of the basin lies near its western margin. However, the use of the term "half-graben" for the Española basin has been questioned because it may oversimplify the basin's structure and result in use of an inappropriate conceptual model (see discussion in Goff et al., 1996, Day 1, Stop 6). In detail, geophysical studies and examination of subsurface drill hole data indicate that the structurally deepest part of the basin, occurring under the western Pajarito Plateau (Ferguson et al., 1995), is bounded to the east by a series of mainly down-to-the-west normal faults that underlie much of the Plateau (Dransfield and Gardner, 1985). Quaternary extension rates in this part of the Rio Grande rift are estimated to be ~0.11 mm/yr, with most of this represented by offset on the Pajarito fault system (Kelson and Olig, 1995).

The Pajarito fault system largely occurs in areas underlain by the ca. 1.22 Ma Tshirege Member of the Bandelier Tuff ($^{40}Ar/^{39}Ar$ age from Izett and Obradovich, 1994), which provides an excellent datum for evaluating Quaternary faulting. The fault system includes: 1) the ~41 km long east-facing Pajarito fault zone, with an estimated maximum vertical displacement of ~155 m and an average along-strike displacement of ~80 m since 1.22 Ma; 2) the ~9-14 km long west-facing Rendija Canyon fault zone, with an estimated maximum vertical displacement of ~36 m and an average displacement of ~22 m since 1.22 Ma; and 3) the ~9-12 km long west-facing Guaje Mountain fault zone, with an estimated maximum vertical displacement of ~27 m and an average displacement of ~15 m since 1.22 Ma (Fig. 5) (Gardner and House, 1987; Wong et al., 1995; Olig et al., 1996).

Despite a considerable amount of recent work on the Pajarito fault system (Kolbe et al., 1994, 1995; Carter and Gardner, 1995; Carter and Winter, 1995; McCalpin, 1995; Reneau et al., 1995b; Wong et al., 1995, 1996; Kelson et al., 1996; and Olig et al., 1996), many uncertainties remain concerning its kinematics and paleoseismic history. Some of these uncertainties will be addressed on this field trip, along with visits to sites where useful paleoseismic information has been obtained (Day 2 stops and road log).

Geologic Units

The primary geologic units exposed on or adjacent to the Pajarito Plateau consist of Miocene to early Pleistocene sediments and volcanic rocks associated with the Rio Grande rift and the Jemez and Cerros del Rio volcanic fields (Fig. 1). Geologic maps of the entire area of this field trip were prepared by Griggs (1964) and Smith et al. (1970), and more detailed maps of select areas have been prepared by many subsequent workers. A highly generalized cross section indicating the relationships of these units is shown in Figure 6, and these units are discussed briefly below.

Santa Fe Group. Miocene rift-filling sediments of the Santa Fe Group (Tesuque and/or Chamita Formations of Galusha and Blick, 1971), dominantly composed of friable sandstones, underlie the Pajarito Plateau and outcrop locally in White Rock Canyon (Griggs, 1964; Smith et al., 1970; Dethier, 1996). Although poorly exposed, these sediments are geomorphically significant as they probably host many of the failure planes of the massive landslide complexes within White Rock Canyon (Reneau et al., 1995a; Dethier, 1996) (discussed on Day 0 hike, and at Stop 1-3).

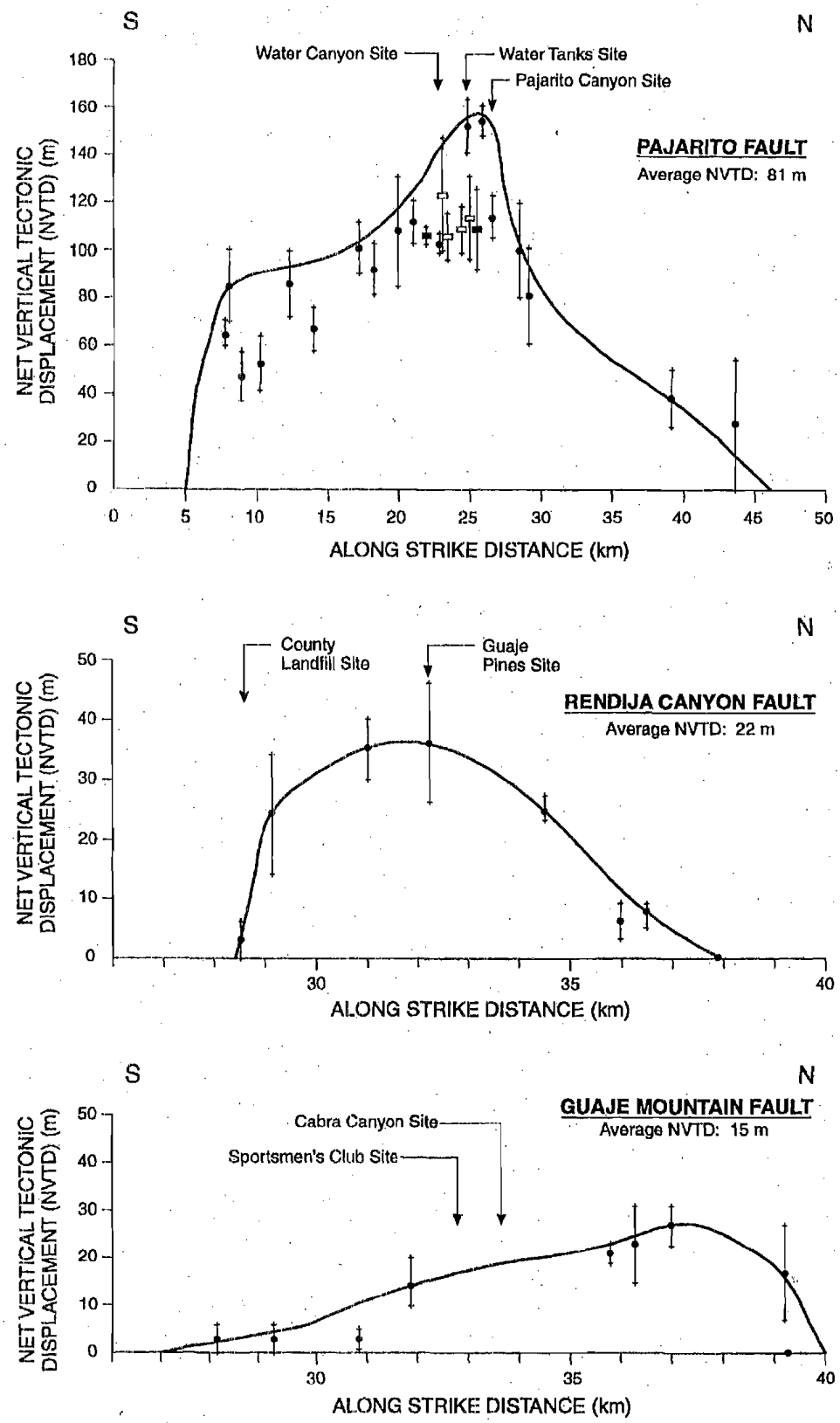

Fig. 5. Displacement curves for the Pajarito fault system showing estimated net vertical tectonic displacement (NVTD) of the top of the Bandelier Tuff. Solid circles show data from profiles constructed from 7.5' quadrangles; solid rectangles show data from profiles measured in the field; open rectangles show data from profiles constructed from 1:1200 scale topographic maps (from Olig et al., 1996).

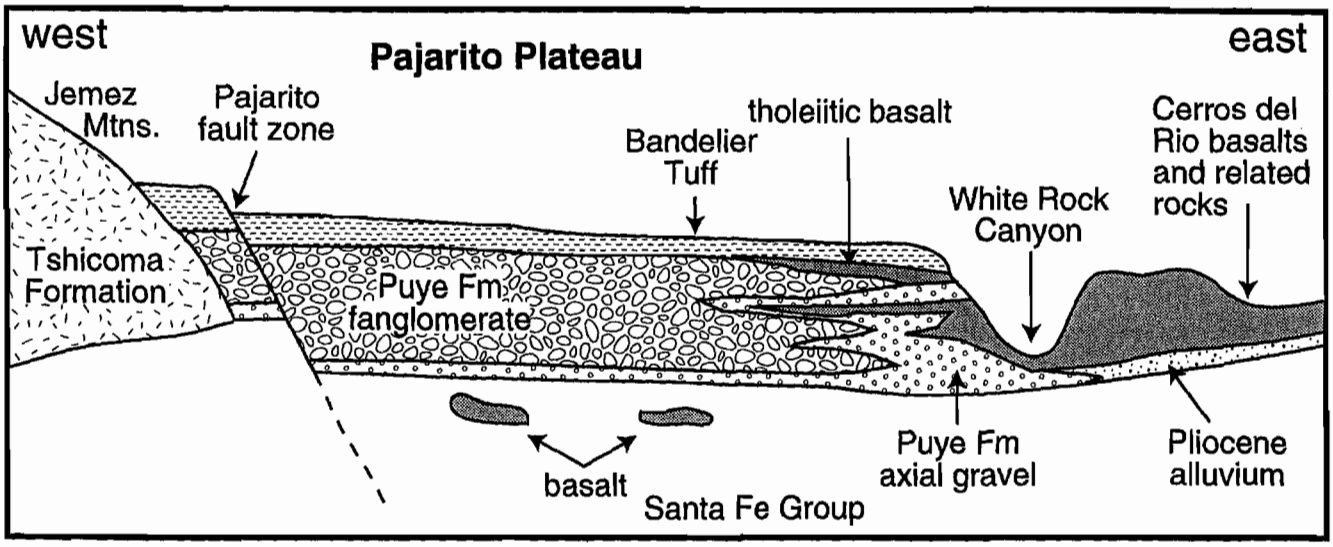

Fig. 6. Schematic geologic cross section showing relationships of the primary geologic units exposed in the vicinity of the Pajarito Plateau. (Modified from Waresback and Turbeville, 1990).

Tschicoma Formation. The Miocene to Pliocene Tschicoma Formation, part of the Polvadera Group, is dominated by dacitic lavas and is the primary bedrock unit in the Sierra de los Valles east of the Plateau (Griggs, 1964; Smith et al., 1970). K-Ar analyses from these lavas indicate ages of about 3-7.5 Ma (Dalrymple et al., 1967; Leudke and Smith, 1978; Gardner et al., 1986; Singer and Kudo, 1986; Aldrich and Dethier, 1990). The rugged, higher elevation Tschicoma terrain provides the upper watersheds for many of the Plateau streams, and Tschicoma clasts often dominate the gravel component of alluvium along these streams as they are more resistant than most of the Bandelier Tuff.

Basaltic rocks of the Cerros del Rio volcanic field. Basaltic rocks of the late Pliocene Cerros del Rio volcanic field outcrop widely on the eastern Plateau, and are well exposed within White Rock Canyon (Griggs, 1964; Smith et al., 1970; Dethier, 1996). In addition to extensive flows that range in composition from hawaiite to andesite, erupted from numerous vents, the Cerros del Rio is marked by deposits from numerous maar volcanoes, the product of phreatomagmatic eruptions generated from the interaction of rising magma with shallow groundwater near the Pliocene Rio Grande (Aubele, 1978, 1979; Dethier, 1996; Heiken et al., 1996). Recent $^{40}Ar/^{39}Ar$ analyses indicate that most of the Cerros del Rio rocks near the Pajarito Plateau were erupted between about 2.3 and 2.8 Ma, particularly between 2.4 and 2.6 Ma (WoldeGabriel et al., 1996). Most streams draining the Plateau in the Los Alamos area have prominent knickpoints where they cross the basalts, and the Cerros del Rio rocks thus provide important local base level controls, isolating the Plateau streams from base level changes along the Rio Grande (discussed at Stops 1-2, 1-5, 3-1). The basaltic rocks also typically form the cap rocks for the massive White Rock Canyon landslides (Day 0 hike; Stop 1-3).

Puye Formation. The Puye Formation is primarily a large Pliocene alluvial fan complex derived from erosion of the Tschicoma highlands in the northeastern Jemez Mountains (Griggs, 1964; Bailey et al., 1969; Smith et al., 1970; Turbeville et al., 1989; Waresback and Turbeville, 1990). As defined by Griggs (1964) and Bailey et al. (1969), the Puye Formation pre-dates the Otowi Member of the Bandelier Tuff, although deposition of Puye-like gravels has continued to the present. The Puye Formation is often referred to as a "rift-filling" unit, although this may be a misnomer as the bulk of the Puye sediments may have been deposited in a basin with a volcanic rather than a tectonic origin,

being formed by blockage of the Rio Grande valley by Cerros del Rio volcanism (Reneau and Dethier, 1996). Streams traversing areas of Puye outcrops are typically steeper than other Plateau streams, associated with an abundant local supply of dacite boulders (discussed at Stop 2-3; the Puye Formation is also seen at Stop 3-1).

Otowi Member, Bandelier Tuff. The Otowi Member of the Bandelier Tuff, named by Griggs (1964) and Bailey et al. (1969), is a massive sequence of ignimbrites erupted from the Jemez Mountains at ca. 1.61 Ma ($^{40}Ar/^{39}Ar$ analyses from Izett and Obradovich, 1994, and Spell et al., 1995), and associated with development of the Toledo caldera (Smith and Bailey, 1966, Heiken et al., 1990). On the Pajarito Plateau, the Otowi Member is entirely non-welded and easily eroded, often forming slopes on lower canyon walls and probably constituting a significant source of sand-size sediment. In the Los Alamos area it ranges from 0->140 m in thickness; these thickness variations result in part from irregular deposition over the prior topography, and in part from erosion of the ignimbrites in the ~400 ky that preceded eruption of the Tshirege Member (Broxton and Reneau, 1996). The basal Plinian deposit of the Otowi Member, the Guaje Pumice Bed (Bailey et al., 1969), is up to 7-10 m thick where exposed on the Plateau (Self et al, 1986). The Otowi Member can be seen at Stops 1-5, 2-3, and 3-4 on this field trip.

Cerro Toledo interval. Deposits occurring stratigraphically between the Otowi and Tshirege Members of the Bandelier Tuff in the Los Alamos area are referred to as the "Cerro Toledo interval" (Broxton and Reneau, 1995; Broxton et al., 1995a; Goff, 1995). In some areas, particularly to the north, the Cerro Toledo interval is dominated by primary and reworked pumice deposits associated with the Cerro Toledo Rhyolite, which originated mainly from Cerro Toledo and related vents in the northern Jemez Mountains (Smith et al., 1970; Heiken et al., 1986). In other areas this interval is dominated by dacite-rich alluvium deposited by streams draining the Sierra de los Valles. The Cerro Toledo-age landscape in the Los Alamos area apparently had relatively low relief, with streams generally incised only about 15-30 m below local drainage divides, and included extensive areas of stream terraces buried by pumice beds (Broxton and Reneau, 1996). Cerro Toledo pumice beds have yielded recent $^{40}Ar/^{39}Ar$ ages of 1.22-1.59 Ma, spanning virtually the entire time span between the Otowi and Tshirege Members (Spell et al., 1995). Some aspects of the Cerro Toledo paleotopography are discussed at Stops 1-1 and 1-5, and also at various places on the road logs.

Tshirege Member, Bandelier Tuff. The Tshirege Member of the Bandelier Tuff, named by Griggs (1964) and Bailey et al. (1969), is a massive sequence of ignimbrites erupted from the Jemez Mountains at ca. 1.22 Ma ($^{40}Ar/^{39}Ar$ age from Izett and Obradovich, 1994), and associated with development of the Valles caldera (e.g., Smith and Bailey, 1966, 1968; Heiken et al., 1990). On the Pajarito Plateau, the Tshirege Member is a compound cooling unit that possesses pronounced lateral and vertical variations in welding and alteration. Differential erosion associated with variations in welding and vapor-phase alteration in vertical sections result in a "benched topography", with alternating cliffs and slopes along many canyon walls. The degree of welding generally increases to the west, towards the caldera, and the presence of densely welded tuff on the western Plateau provides a strong contrast with the eastern Plateau, where even the cliff-forming units are easily crushed with a hammer. In the Los Alamos area the Tshirege Member locally exceeds 260 m in thickness, with significant thickness variations occurring across the Plateau; thicknesses of 30-100 m are more common (Broxton and Reneau, 1996). The basal Plinian deposit of the Tshirege Member, the Tsankawi Pumice Bed (Bailey et al., 1969), is typically ~0.2-1.0 m thick on the Plateau (Self et al, 1986). The gently east-sloping mesas of the Pajarito Plateau are capped by relatively resistant,

variably welded flow units within the tuff, although the upper surface of the Plateau probably rarely or never represents the actual top of the ignimbrite sheet, as is sometimes assumed. This is due mainly to erosion of unknown thicknesses of the uppermost, non-welded tuff, although in a few areas the actual top of the ignimbrite sheet may be preserved beneath early post-Bandelier deposits.

In the Los Alamos area, the Tshirege Member has been subdivided into a series of mappable units by a number of workers who have used varying criteria and varying nomenclature, resulting in some confusion in the local literature (see discussion in Broxton and Reneau, 1995). The mapping units presently employed by LANL's Environmental Restoration Project are shown in Figure 7, based on inferred cooling breaks within the tuff. (The 6 major subdivisions of the Tshirege Member in Figure 7 generally correspond to units A through F of Rogers, 1995).

Tshirege unit 1g (Qbt-1g) is the lowermost non-welded tuff, the only unit with primary volcanic glass remaining in most areas (1g = glassy part of cooling unit 1). Qbt-1v consists of the upper part of cooling unit 1, which has been subject to pervasive vapor-phase alteration associated with early de-gassing of the ignimbrite; common vapor-phase minerals occurring here and in overlying units include alkali feldspar, cristobalite, and tridymite (Broxton et al., 1995a, 1995b). Qbt-2 is a prominent cliff-forming unit, forming the main cap rock for mesas on the eastern Pajarito Plateau (Stop 1-3, 3-4). Qbt-3 caps many mesas farther west, including the Los Alamos townsite, but is less welded than Qbt-2 and, where present to the east, has eroded into low mounds (Stop 1-4). Qbt-4, absent from the eastern Plateau, caps many mesas in the central Plateau (Stop 1-6) and thickens westward. Lastly, Qbt-5 is a relatively thin but densely welded unit that forms a prominent cap rock on parts of the western Plateau (Ponderosa Campground, Stop 2-1). (For more details on some of the chemical, mineralogic, and petrographic variations between these units, see Broxton et al., 1995a, 1995b). Some features of the Tshirege Member are discussed at Stop 1-1 and at various places in the road logs.

Post-Bandelier Landscape Development

Eruption of the Tshirege Member of the Bandelier Tuff at ca. 1.22 Ma effectively buried most of the former topography, reshaping the landscape between the Sierra de los Valles and the Rio Grande. Because the thickness of tuff varied significantly across the Plateau, the upper surface of the ignimbrite sheet possessed a somewhat different orientation than the previous landscape, and as a result the post-Bandelier drainage net is generally oblique to the pre-1.22 Ma streams, with more easterly orientations than prior to 1.22 Ma (Broxton and Reneau, 1996).

Also of significance is the fact that the pre-Tshirege paleocanyon of the Rio Grande was completely buried by the tuff, undoubtedly damming the river and creating a new local base level for streams draining the Plateau (Fig. 8; Reneau and Dethier, 1996b). The outlet to the tuff-dammed lake was apparently located about 2 km east of its former course, forcing the post-1.22 Ma Rio Grande to erode a new canyon through about 200 m of basaltic rocks to reach its pre-Tshirege grade. A persistent knickpoint probably existed along the Rio Grande as it slowly incised through the basalts, in turn impeding incision of streams on the Plateau. Part of the buried paleocanyon can be viewed at a distance from Stop 1-3.

Mesa-Top Alluvium and Canyon Incision. Isolated remnants of dacite-rich gravels deposited by streams draining the Sierra de los Valles occur widely over the upper surface of the central and eastern Plateau, often in shallow paleochannels (e.g., Reneau, 1995a; Reneau et al., 1995b). These

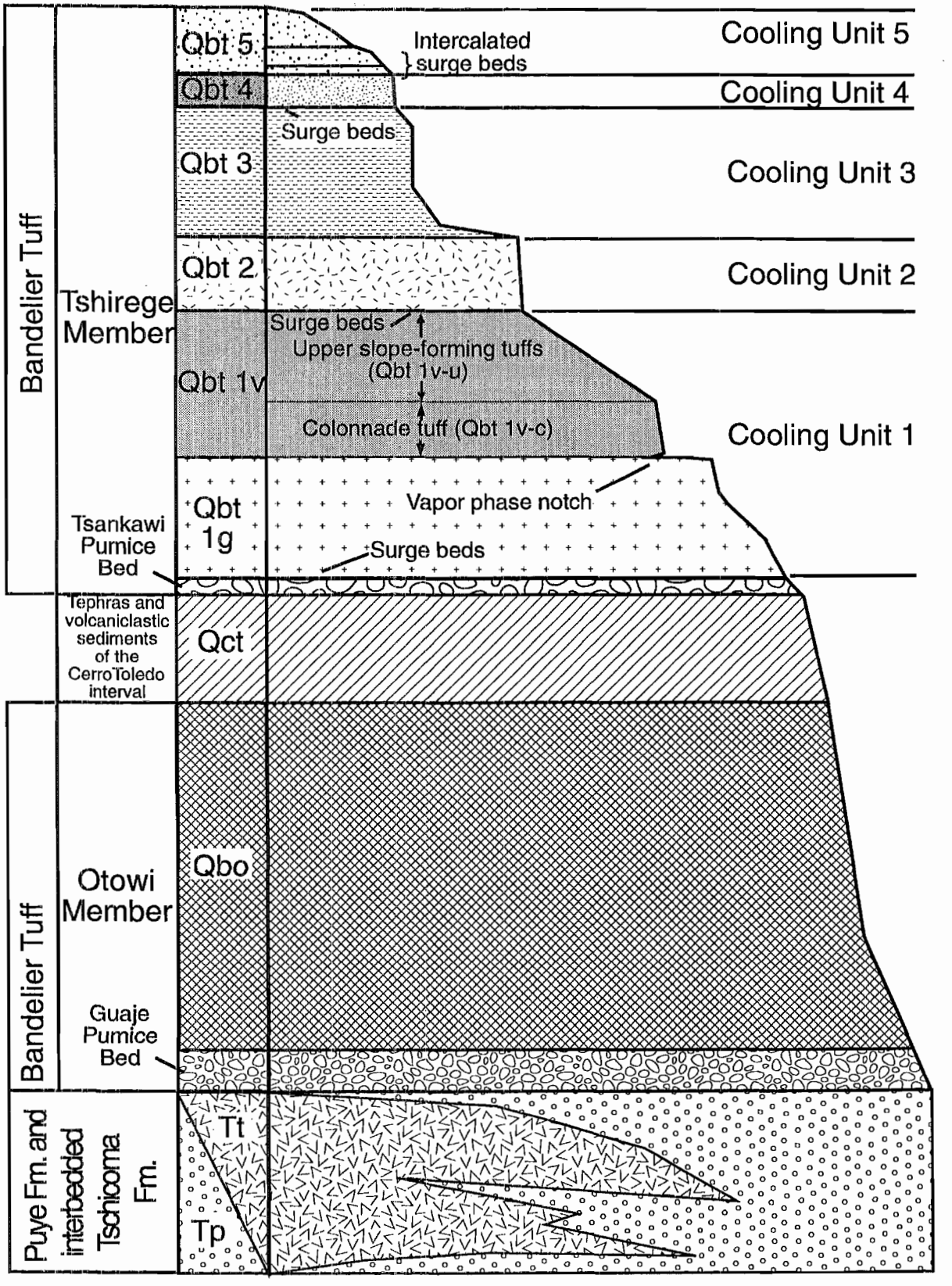

Fig. 7. Stratigraphic nomenclature of the Bandelier Tuff on the Pajarito Plateau. Modified from Broxton and Reneau (1995) to include "Qbt 5", which is only present on the western Plateau and which is probably equivalent to "unit F" of Rogers (1995).

deposits record the locations of dispersed, probable early Pleistocene streams that pre-dated incision of the canyons. To the west, such mesa-top alluvial deposits become more extensive, covering many of the mesas on the western Plateau. The timing of initial incision of the canyons on the Plateau is not yet known and undoubtedly varied greatly, although inferred early Pleistocene pumice beds associated with the Valles Rhyolite (the post-Bandelier volcanic rocks in the Valles caldera; Bailey et al., 1969; Smith et al., 1970) have been recently recognized in many areas and may ultimately allow age control for early post-Bandelier units (Dave Broxton, unpublished data). It is notable that some canyons on the western Plateau have not yet been incised into tuff (e.g., Cañon de Valle), and the "mesa-top alluvium" locally merges with late Quaternary fans near the base of the Pajarito fault escarpment. Initial incision of canyons through the Tshirege ignimbrites has thus occurred throughout the past 1.22 Ma in different areas, indicating that the mesa-top alluvium may record a long (but as of yet unresolved) history of sedimentation, drainage evolution, and time-transgressive canyon incision. An excellent example of one of the mesa-top paleochannels will be visited at Stop 3-4, and related deposits are mentioned in the Day 2 log.

Cliff Retreat. Cliff retreat rates on the Pajarito Plateau are poorly constrained at present, and likely show significant spatial and temporal variability across the Plateau. Cliff retreat along most canyons may be dominated by the dislodgment of individual fracture-bounded blocks, resulting in discrete rockfalls (e.g., Reneau, 1995a, 1995b). From casual observations of recent rockfall events, it is not obvious that they occur under any particular meteorological condition; for example, a rockfall in April 1993 from the south side of Mesita del Buey (north wall of Pajarito Canyon) occurred during a dry period long after the freeze-thaw cycles of winter. In some areas, mass wasting features along mesa edges indicate the potential for much larger failures. For example, partially-detached blocks up to 25 m wide and 100 m long occur on the south edge of DP Mesa, above Los Alamos Canyon (Reneau, 1995a), and a belt of mesa-edge instability ~30-60 m wide and 1.8 km long occurs along the north edge of Pajarito Mesa, above Pajarito Canyon (Reneau, 1995b). Available data suggest that these larger bedrock failures occur along canyons where a threshold combination of canyon depth and canyon-wall gradient has been exceeded, in turn suggesting that rates of mesa-edge retreat could accelerate once such a threshold has been crossed (Reneau, 1995b). In other areas, the widest parts of canyons correspond with areas of broad stream terraces, suggesting that canyon widening may be significantly aided by lateral erosion by streams. Finally, it seems likely that seismic shaking would be very effective at dislodging numerous partially-detached blocks and possibly destabilizing many previously intact areas of cliff, particularly given the proximity to traces of the Pajarito fault system, although there are no data to evaluate the relative importance of such events.

Late Quaternary Alluvial History. Sediments within the canyons of the Pajarito Plateau record significant temporal variations in fluvial processes through the late Quaternary, and also significant spatial variability between canyons (Reneau et al., 1996b). Abundant evidence exists for widespread sediment deposition throughout the Holocene, contrasting with the apparent rarity of latest Pleistocene alluvial deposits. The late Pleistocene stream channels in many canyons are buried many meters beneath the canyon floors, and we believe that this dramatic change in fluvial processes reflects major changes in sediment supply and flood characteristics accompanying the Pleistocene-Holocene climatic transition. A strong contrast also exists between net Holocene aggradation in many canyons and net Holocene incision in others, the latter accompanied by development of multiple Holocene terraces. Stratigraphic and geochronologic evidence pertaining to the late Quaternary alluvial history are examined at many stops on this field trip (Stops 1-2, 1-4, 1-5, 2-2, 2-3, 3-1, 3-3).

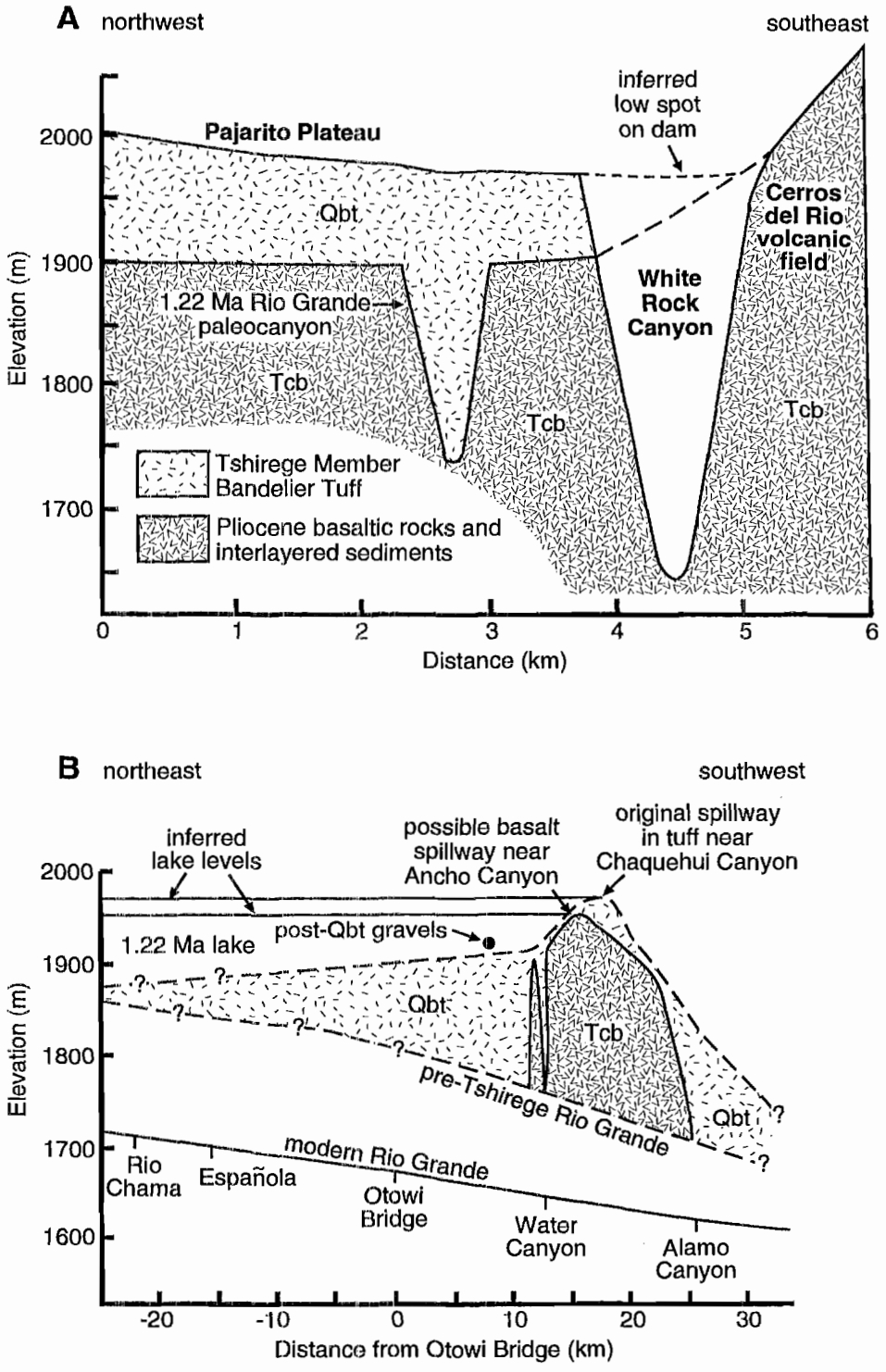

Fig. 8. A). Schematic cross section through the area of the ca. 1.22 Ma Bandelier Tuff dam near Chaquehui Canyon. The low point on dam was near the eastern margin of the Tshirege ignimbrite sheet about 2 km east of the buried early Pleistocene Rio Grande paleocanyon, superimposed on Cerros del Rio basaltic rocks. B) Profile of the Rio Grande at White Rock Canyon and adjacent parts of the Española basin at ca. 1.22 Ma, showing: the pre-Tshirege Member river level; the approximate topography immediately after eruption of the tuff and geologic units beneath the post-tuff channel; the location of spillways and approximate lake elevations; and the location of post-tuff Rio Grande gravels at White Rock (Stop 1-3) (from Reneau and Dethier, 1996b).

Post-1943 A.D. Alluvial History. As with the earlier record of late Quaternary fluvial change, significant spatial and temporal variability in streams on the Pajarito Plateau are recorded since major development began at LANL in 1943 (subsequently referred to as "historic" alluvium). These changes have been locally documented using examinations of sequential airphotos that extend back to 1935, using "exotic" materials contained within young sediment deposits as dating tools, using biological evidence such as trees partially buried by alluvium, and using radionuclide contaminants as tracers (e.g., Becker, 1991; Drake and Inoue, 1993; Drakos and Inoue, 1994; Aldrich and Harrington, 1995; Graf, 1995, 1996; Reneau, 1995a; and Drakos et al., 1996). In some drainages, 2 m or more of sediment was first deposited and then incised since WW II, producing historic fill terraces, whereas in others historic channels remain buried beneath aggrading valley bottoms. The recent behavior of Plateau streams is receiving increasing attention because of their significance for evaluating contaminant transport, and examples of channels that have experienced major historic channel changes will be visited on Day 3 of this field trip.

Soils

Soils on the Pajarito Plateau have developed from a diverse set of parent materials that include alluvial, colluvial, and eolian sediments, and fallout pumice, in addition to locally weathered bedrock. These soils have also been strongly affected by local variations in geomorphic history, with long-term (i.e., >100 ka) "stable" landscape positions being relatively rare. Many soils have either been partially stripped or buried by younger deposits, forming complex, superimposed soil profiles. General variations in soil characteristics across the Plateau were originally identified and mapped in a soil survey by Nyhan et al. (1978). Recently, many additional studies have examined pedologic, geomorphic, geochronologic, stratigraphic, geochemical, mineralogic, and isotopic aspects of soils and related fracture fills in greater detail (e.g., Davenport, 1993; Drake and Inoue, 1993; Drakos and Inoue, 1994; Kolbe et al., 1994, 1995; Davenport et al., 1995; Reneau et al., 1995b, 1996a, 1996b; Vaniman and Chipera, 1995; Wong et al., 1995; Drakos et al., 1996; Eberly et al., 1996; Kelson et al., 1996; Longmire et al., 1996; McDonald et al., 1996a, 1996b; McFadden et al., 1996; Newman, 1996; Watt, 1996). Many stops on this field trip will explore some of these aspects of soils, particularly as they pertain to evaluating the geomorphic history of the Pajarito Plateau (e.g., Stops 1-2, 1-4, 1-5, 1-6, 2-2, 2-3).

Day 0, White Rock Canyon hike: "Red Dot Trail" to "Blue Dot Trail"
(Piedra Loop to Overlook Park)

Leader: Steven Reneau (with many contributions to work by David Dethier)

The prime geologic attractions along this hike include well-dated lacustrine deposits associated with late Pleistocene landslide-dammed lakes along the Rio Grande. These deposits provide a record of the timing of the most recent major landsliding within White Rock Canyon and yield insights into local geomorphic responses to late Quaternary climatic changes (Dethier and Reneau, 1996; Reneau and Dethier, 1996a). The hike is through a terrain dominated by large-scale landsliding, and also features late Quaternary fluvial deposits. Abundant prehistoric Pueblo ("Anasazi") petroglyphs occur on and near this route, along with prehistoric field houses, farm fields, and irrigation ditches (note that to help protect them from vandalism, their exact locations are not specified in this guide).

This route involves ~6-8 miles of hiking on unmaintained trails in an arid canyon, with a rocky 900' descent to start and an equal climb at the end. Shade is sparse, afternoon temperatures can be quite warm, and abundant water should be carried. For those wishing an abbreviated hike, the trail down can be retraced to the rim after visiting sites near the river (on hot days, a dip in the pools of Pajarito Springs is highly recommended before hiking out). The area is covered by the USGS 7.5' White Rock quadrangle (Fig. 0-1), and is entirely on Los Alamos County lands.

- The meeting area is near the head of the Blue Dot Trail (**point 13, Fig. 0-1**), where some vehicles can be left and a shuttle made to the top of the Red Dot Trail. To reach the meeting area, turn southeast off NM State Rd 4 onto Rover Blvd. in White Rock, following signs to Overlook Park. At 0.1 mi, turn left onto Meadow Lane, following it for 0.9 mi to Overlook Road. Turn left and follow Overlook Rd for 0.4 mi past the concession stand (and restrooms), turning right after the last ballfield onto a paved road (a race course for mini-cars should be on your left; if you miss the turnoff, turn around at the end of Overlook Rd and take the first paved road to the left). Follow the paved road to the end, and park in the large parking lot. (The top of the Blue Dot Trail (unsigned) is immediately east, through the piñon-juniper woodland, down a shallow drainage, and through a gap in an old fence.)

- From the meeting area, drivers will retrace route to State Road 4, turn left on NM 4 for 0.3 mi to Sherwood Dr., turn left and follow Sherwood for 0.7 mi south to where it terminates at Piedra Loop. At Piedra Loop, turn left (east), following it for 0.7 mi to top of Red Dot Trail (signed) (after Mariposa Ct, between lots 161 & 162).

- The Red Dot Trail (named after the red paint used to mark the route) begins on Piedra Loop 1.4 mi east of State Road 4, and 0.7 mi east of the junction of Piedra Loop and Sherwood Dr. Park on the road, and walk ~0.2 km east to the rim of White Rock Canyon (1925 m, 6320' elev.), where the trail begins its descent (**point 1, Fig. 0-1**). Dacite-rich gravels cap the basalt at the top of the trail, which were deposited by the Pajarito Canyon stream before it cut its present narrow slot into the basalt (0.5 km to the north). From the rim it is ~2.5 km (1.5 mi) to the Rio Grande, dropping ~270 m (900 ft) in elevation, first passing down through the capping basalt cliffs, then switchbacking down to and over large back-tilted slumps capped by basalts, and finally past the lush oasis of Pajarito Springs (trail is also described by Hoard, 1981). This route follows the Red Dot Trail most of the way to the Rio Grande, turning right (south) near the bottom to visit late Pleistocene deposits a short distance downriver.

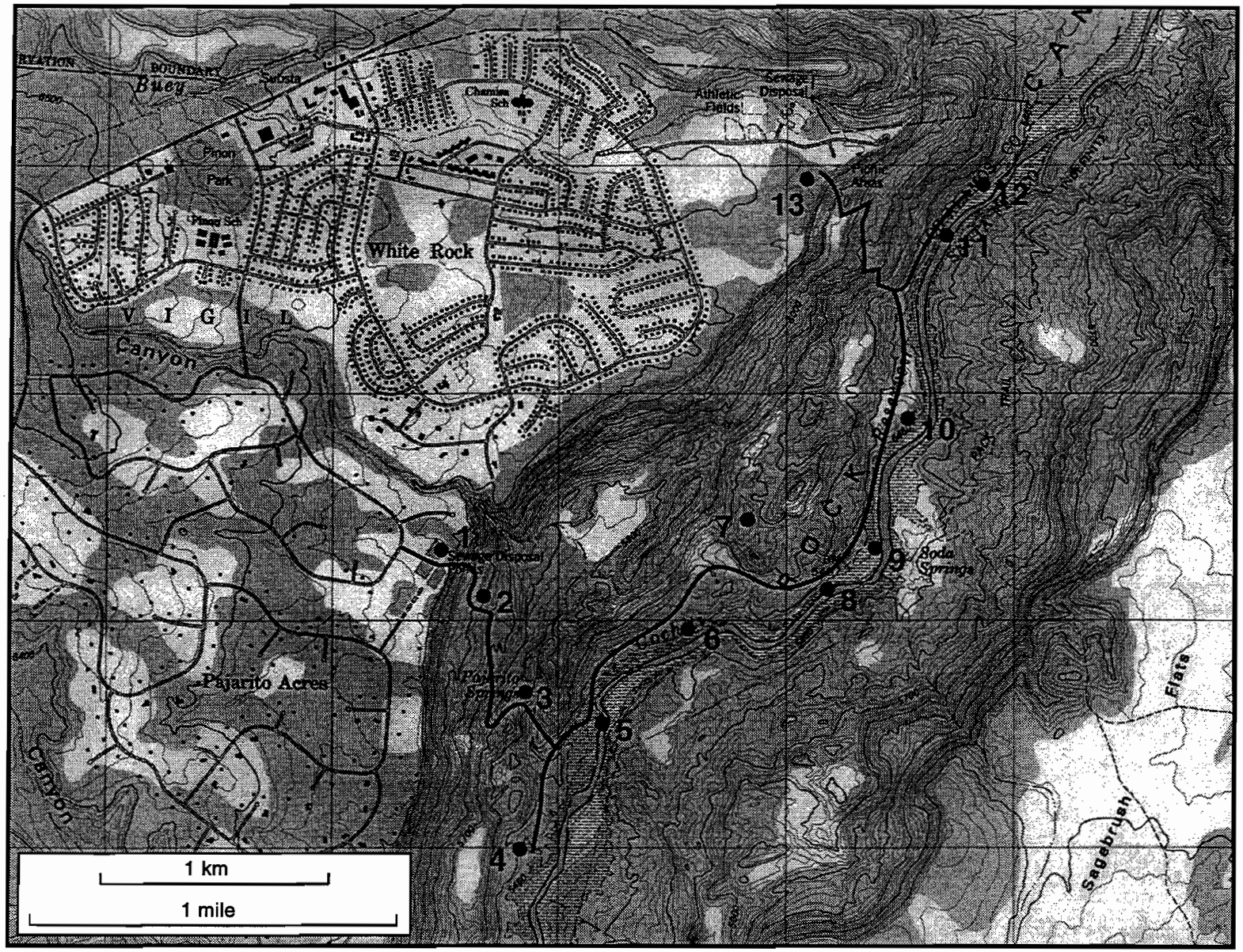

Fig. 0-1. Topographic map of part of White Rock Canyon showing route of Red Dot Trail to Blue Dot Trail hike, and points of interest mentioned in log. Base is USGS White Rock 7.5' quadrangle. Contour interval is 20 ft.

Bedrock Stratigraphy. The most prominent bedrock units present in this part of White Rock Canyon are late Pliocene basaltic rocks of the Cerros del Rio volcanic field (Griggs, 1964; Smith et al., 1970; Dethier, 1996). About 50 m of lava flows underlie the canyon rim, and are well exposed along the upper parts of both the Red Dot and Blue Dot Trails. The uppermost flow at White Rock is a tholeiitic basalt derived from vents to the west (unit Tcb3 of Dethier, 1996), dated at ca. 2.3-2.5 Ma by $^{40}Ar/^{39}Ar$ (WoldeGabriel et al., 1996). Underlying units are only rarely exposed due to extensive landsliding, but include: (1) quartzite-rich fluvial deposits of the ancestral Rio Grande, which comprise an axial facies of the Pliocene Puye Formation (*a la* Manley, 1976, 1979, and Dethier, 1996; called "Totavi Lentil" by Griggs, 1964, and "Totavi Formation" by Waresback and Turbeville, 1990); (2) dacite-rich Pliocene fanglomerates of the Puye Formation; and (3) friable sandstones and associated sedimentary rocks of the Miocene Santa Fe Group. Other Tertiary units in northern White Rock Canyon include late Pliocene lacustrine deposits, associated with damming of the ancestral Rio Grande by Cerros del Rio basalts ("Culebra lake clay" of Kelley, 1952), and Pliocene alluvium derived from granitic terrain to the east. The early Pleistocene Tshirege Member of the Bandelier Tuff locally overlies the Cerros del Rio basalts, most prominently east of the river southeast of the Red Dot Trail where it plugs the paleocanyon of the early Pleistocene Rio Grande (Reneau and Dethier, 1996b).

Pajarito Canyon Slump Complex. Most of the terrain between the rims and the river in this part of White Rock Canyon is composed of massive Pleistocene landslide complexes (Fig. 0-2; Smith et al., 1970; Reneau et al., 1995a; Dethier, 1996). These slides are generally slumps, with the capping basalts typically back-tilted 10-70°. Failure planes are rarely exposed, but are probably mainly within the Tertiary sedimentary rocks, particularly the Santa Fe Group, the Pliocene lacustrine sediments, and relatively weak beds within the Puye Formation.

Fig. 0-2. Oblique aerial photograph of slump complex along western side of White Rock Canyon at Pajarito Canyon, below White Rock, looking southwest. Canyon is 270 m deep. Largest slump block is tilted 35-45° to northwest. The Red Dot trail site is along the river at the left edge of the photograph Upriver, near prominent sandbar, Rio Grande is constricted by Pajarito Canyon fan..

The larger slump complexes are generally overlain by the ca. 50-60 ka El Cajete pumice (age from Toyoda et al., 1995; Reneau et al., 1996a), indicating that they were largely emplaced by this time. Pockets of the El Cajete pumice can be observed along the Red Dot Trail where it was deposited on the uppermost ridge of the slump complex (~6120' elev.), and on the slope to the east (the latter include stratified deposits that probably record local slope transport); at these sites the pumice is preserved where buried by colluvium containing basalt boulders (**point 2, Fig. 0-1**). At least some of these slumps have been episodically active since they formed, particularly in their toe zones. This is best shown by the record of multiple lakes formed upstream of landslide-dams, which we will examine on this hike.

The troughs and depressions formed behind individual slump blocks are typically filled with relatively fine-grained slopewash deposits. Deposits exposed in gullies on the Red Dot Trail are typical of those elsewhere in the canyon, with the uppermost sediments containing reworked El Cajete pumice and presumably being Holocene in age. The relatively fine texture also suggests reworking of wind-blown sediment. Primary fallout El Cajete pumice, overlying older deposits, is exposed in some areas. Other material filling the troughs and depressions include: rocky colluvium near the margins; alluvium near larger drainages (such as the Holocene fan along the Pajarito Canyon channel visible below the trail to the east); and lacustrine deposits near the Rio Grande (associated with the landslide-dammed lakes). No signs of ponds within the closed depressions have been found, possibly due to high infiltration rates in the underlying colluvium and fractured rock.

Petroglyphs. Outstanding examples of prehistoric Pueblo (Anasazi) rock art occur along the Red Dot Trail and at many other locations in White Rock Canyon, displaying a variety of motifs (Fig. 0-3). They are largely or entirely petroglyphs which were pecked into varnished basalt boulders, and remain well preserved (although vandalized at some sites, and drowned beneath Cochiti Reservoir at others). Petroglyphs seem to be most common near prehistoric farm fields and on major routes into the canyon (such as this trail), although isolated rock art can also be found almost anywhere in the canyon. The White Rock Canyon petroglyphs are considered to be part of the "Rio Grande Style", and are discussed by Schaafsma (1975, 1980) who studied them as part of archaeological work that preceded the initial filling of Cochiti Reservoir. They appear to have been largely created during the "Rio Grande Classic Period", ca. A.D. 1325-1600, and petroglyphs depicting men on horseback indicate that at least some were made after the first visit of Spaniards to the region in 1541. The Red Dot Trail petroglyphs may have been made by inhabitants of the Tshirege ruins, the largest Classic Period pueblo on the Pajarito Plateau, located only 3 km from the top of the trail (Hoard, 1981).

Pajarito Springs. Pajarito Springs (**point 3, Fig. 0-1**) are the largest in a series of springs that occur along the lower slopes of White Rock Canyon, and which have been believed to represent discharge from regional aquifers that are recharged from both the east and the west (Purtymun et al., 1980). Recent isotope analyses indicate that most springs on the west side of the river are associated with the deep aquifer beneath the Pajarito Plateau, and are recharged at relatively low elevations of ~2080-2465 m (Blake et al., 1995). In contrast, samples from some springs and water supply wells are chemically and isotopically distinct, indicating recharge at much higher elevations of ~3000 m and suggesting a source in the Sangre de Cristo Range. These include "Soda Springs", on the east side of the river, and water from a confined aquifer under artesian pressure on the west side of the river (Los Alamos well field). More recent chemical analyses indicate that Pajarito Springs could represent either discharge from an "intermediate" perched aquifer or from the top of the "main aquifer" (P. Longmire, pers. comm., 1996). Pajarito Springs is regularly sampled by both Los Alamos and State environmental groups, and analyses have not yet revealed any evidence of contamination from Laboratory activities.

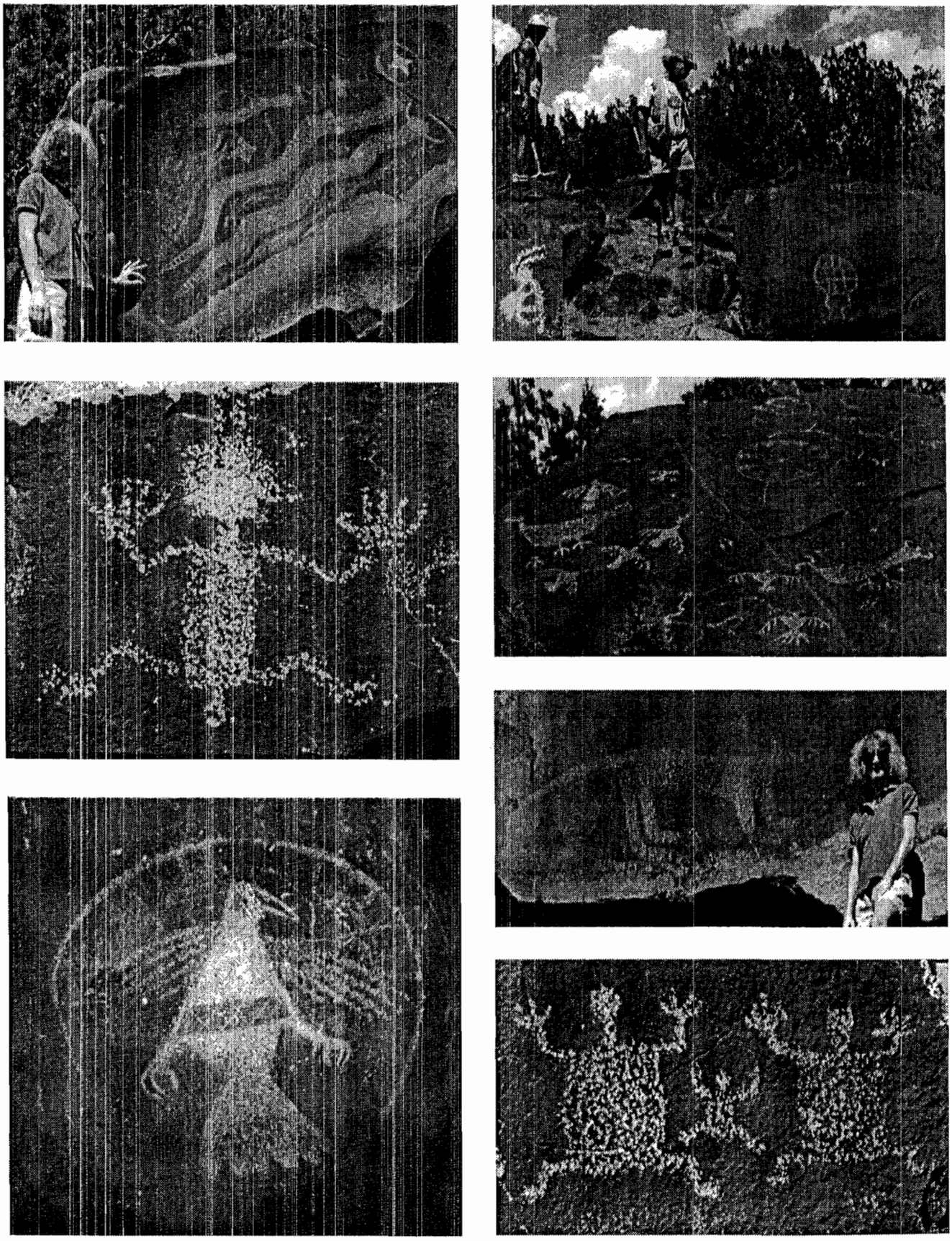

Fig. 0-3. Petroglyphs in White Rock Canyon.

Groundwater discharge at springs such as this one may have contributed to triggering slope failures, particularly during wetter periods in the past when recharge rates may have been greater than today (Dethier and Reneau, 1996; Reneau and Dethier, 1996a).

- After the first crossing of the stream below Pajarito Springs, the trail climbs up a slope to the east. Along this slope are laminated lacustrine deposits that are similar to those found at many sites within northern White Rock Canyon. The upper sediments apparently display soft-sediment deformation associated with contemporaneous emplacement of bouldery colluvium. This site was not discovered until the dry run for this field trip, and has not been studied in detail. The elevation of these sediments (~5550') is consistent with deposition in the largest and oldest landslide-dammed lake recognized in the canyon, with an estimated age of ca. 40-70 ka (Reneau and Dethier, 1996a). Notably, these sediments contain clasts of reworked pumice, probably from the El Cajete pumice, thus providing additional age control for this oldest lake.

- The trail continues up the slope and then drops again to the stream. Where the trail crosses the stream near a major bend to the northeast (@ ~5470' elev.), leave the main trail and head south up the slope and onto and across a flat. Keep towards the base of the slope to the west, following poorly-defined trails that lead south into an area of incised late Pleistocene Rio Grande terraces. Gullies about 0.4 km south of the stream provide excellent exposures of the youngest recognized lacustrine deposits in White Rock Canyon, dated at ca. 12.4 ^{14}C ka (**point 4, Fig. 0-1**).

Late Pleistocene Lacustrine and Fluvial Stratigraphy in "Red Dot Trail" Area. The area near the bottom of the Red Dot Trail provides excellent exposures of late Pleistocene lacustrine deposits (Fig. 0-4) that are both underlain and overlain by Rio Grande fluvial deposits. These deposits are similar to others that have been found along 14 km of White Rock Canyon, extending upstream from a landslide complex located west of lower Water Canyon where the Rio Grande was repeatedly dammed during the late Pleistocene (Figs. 0-5, 0-6; Reneau et al., 1995a; Dethier and Reneau, 1996; Reneau and Dethier, 1996a). The dam is located ~2.5 km downriver from here, and is accessible by an unnamed, unmaintained trail that follows the river. (The landslide dam will not be visited on this hike due to its relative inaccessibility, but is well worth a visit.)

Finely-laminated, horizontally-bedded, silt-rich sediment dominates the lower part of this 5-6 m thick lacustrine section, grading upwards into sandier beds (Fig. 0-7). The deposits at this site are part of the youngest lacustrine section that we have found in White Canyon, and are tightly dated at ~12.4 ^{14}C ka by five statistically indistinguishable radiocarbon dates (Reneau et al., 1995a; Reneau and Dethier, 1996a). These dates were on charcoal fragments collected from the tops of underlying buried soils (4 samples) or from basal lake sands (1 sample); three of the samples were collected from the Red Dot area. The highest lacustrine deposits at this site are about 1672 m (5485') in elevation, similar to the elevation of channels over the landslide dam and to the upper limit of other lacustrine deposits in the canyon (including the Blue Dot Trail area) (Fig. 0-6). The landslide dam that produced this lake and one or more earlier lakes was apparently stable, allowing the lake to completely fill with sediment before progradation of quartzite-rich Rio Grande bedload gravels over the lacustrine section.

The Rio Grande fluvial deposits that overlie and are inset into the lacustrine section are associated with terraces produced during downcutting through the landslide-dammed lake deposits, and may primarily represent "fill-cut terraces", although minor aggradation may also have occurred. At least two distinct inset terraces occur here (Fig. 0-8). The ages of these terraces are not well constrained, but a date of 9.96 ^{14}C ka from a fan that overlies the highest terrace ~1 km downriver, above a buried soil, indicates

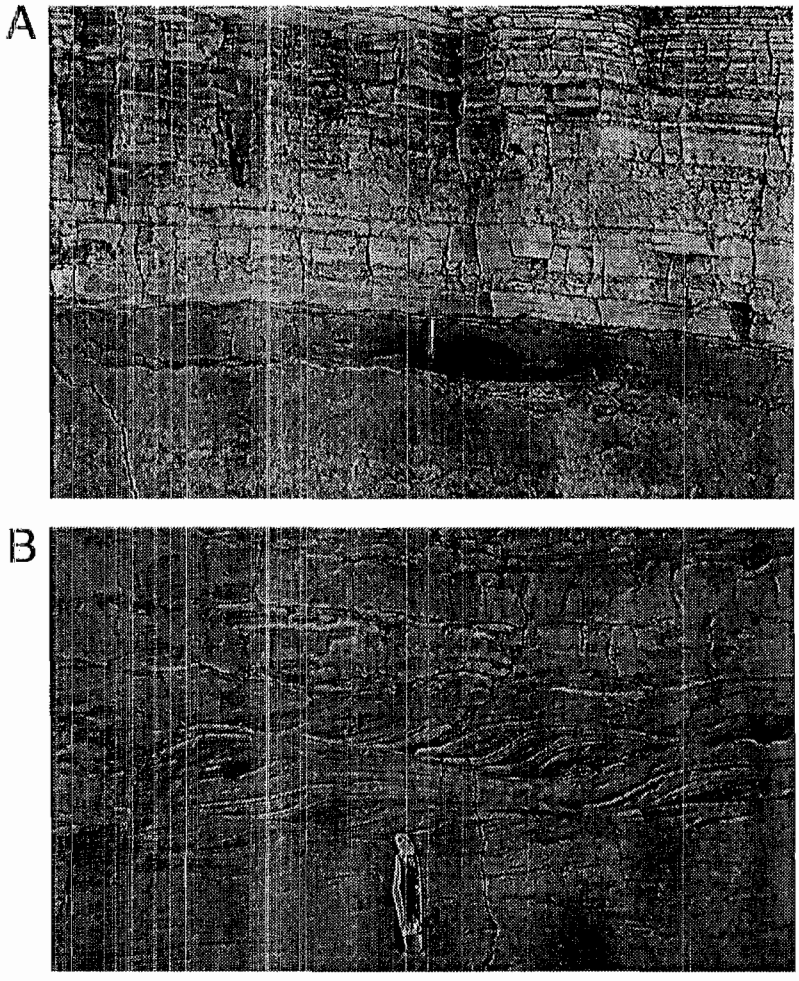

Fig. 0-4. Photographs of sediments at Red Dot Trail area. (A) Laminated, thin-bedded fine sands and silts overlie basal coarse sand layer of lacustrine deposit (at pocket knife). Lowermost unit is a bioturbated sand (Rio Grande flood plain deposit) dated at ca. 12.3 1^4C ka at a nearby exposure (WR-20). (B) Cross-bedded sands within lacustrine section.

that they are latest Pleistocene in age (Dethier and Reneau, 1996; Reneau and Dethier, 1996a). Behind the back (west) edge of the higher Red Dot terrace is a whitish diatomaceous bed that was presumably deposited in a pond within a trough or abandoned channel. The Rio Grande gravels that underlie the lacustrine section at the Red Dot site apparently represent a terrace formed after an earlier landslide-dammed lake, and are capped by a poorly-developed, bioturbated, sandy soil that may represent a floodplain deposit (Fig. 0-4a).

Data from elsewhere in White Rock Canyon suggest prior landslide-dammed lakes at ca. 13.1, 13.4, and 15-17.5 ^{14}C ka, and at about 40-70 ka. A particularly revealing section (first visited by Antonio Garcia) is exposed in bluffs on the east side of the river immediately upstream of the dam, where a sequence of lacustrine deposits separated by buried soils provides convincing evidence for 3 separate lakes between ca. 13.7 and 12.4 ^{14}C ka (Fig. 0-9), and thus repeated destabilization of the toe of the adjacent landslide complex. Estimates of the heights and ages of the late Pleistocene lakes and the prior and subsequent level of the Rio Grande are shown in Figure 0-10.

The ages of the latest Pleistocene landslide-dammed lakes correspond to highstands of pluvial Lake Estancia 120 km to the south (Fig. 0-10b), indicating that the same climatic conditions responsible for

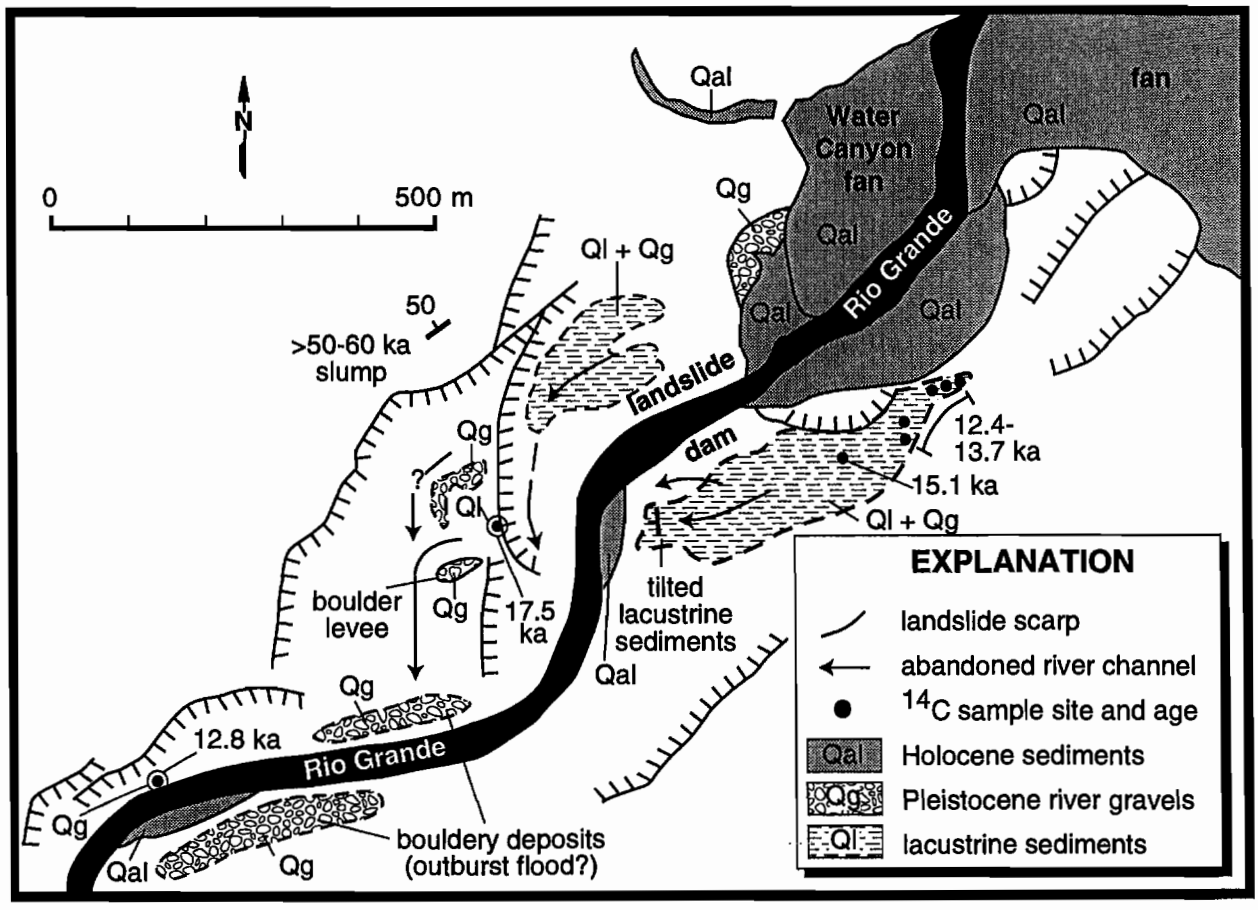

Fig. 0-5. Sketch map of Water Canyon-Chino Mesa landslide dam area. Slump to northwest (tilted 50° to the northwest) is overlain by the El Cajete pumice, indicating an age of >50-60 ka (from Reneau and Dethier, 1996a).

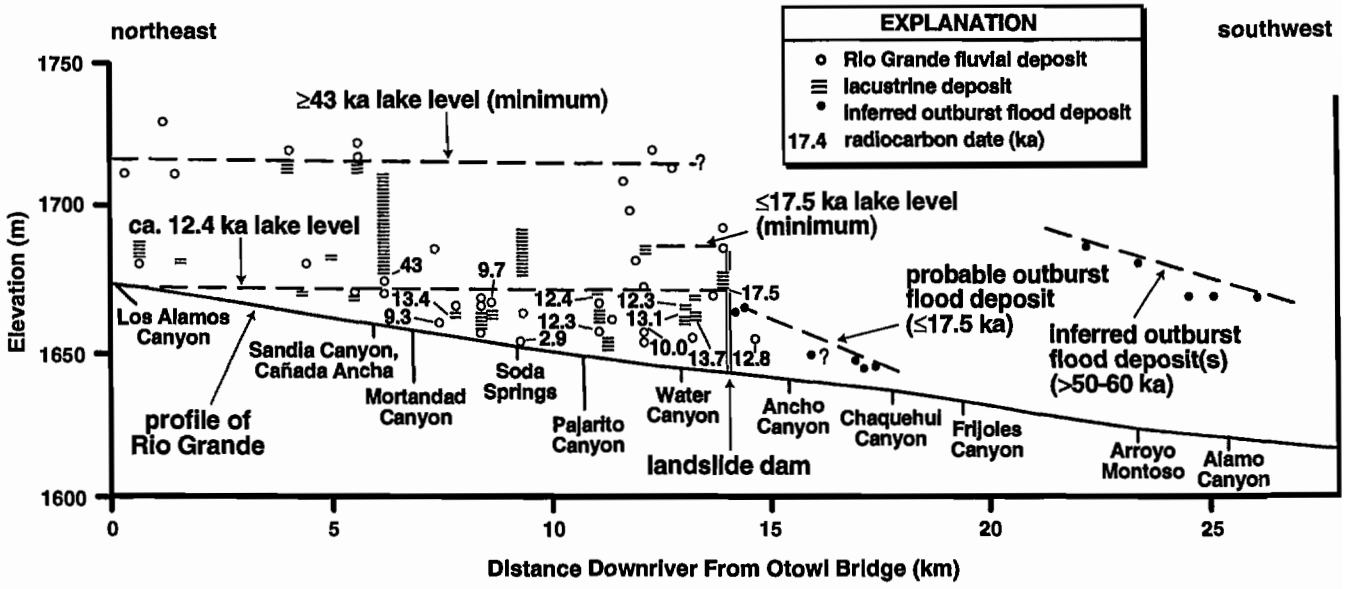

Fig. 0-6. Longitudinal profile of Rio Grande in northern White Rock Canyon showing locations of lacustrine deposits, Rio Grande fluvial deposits, probable outburst flood deposits, radiocarbon-dated samples, latest-Pleistocene landslide dam, and inferred lake levels (from Reneau and Dethier, 1996a).

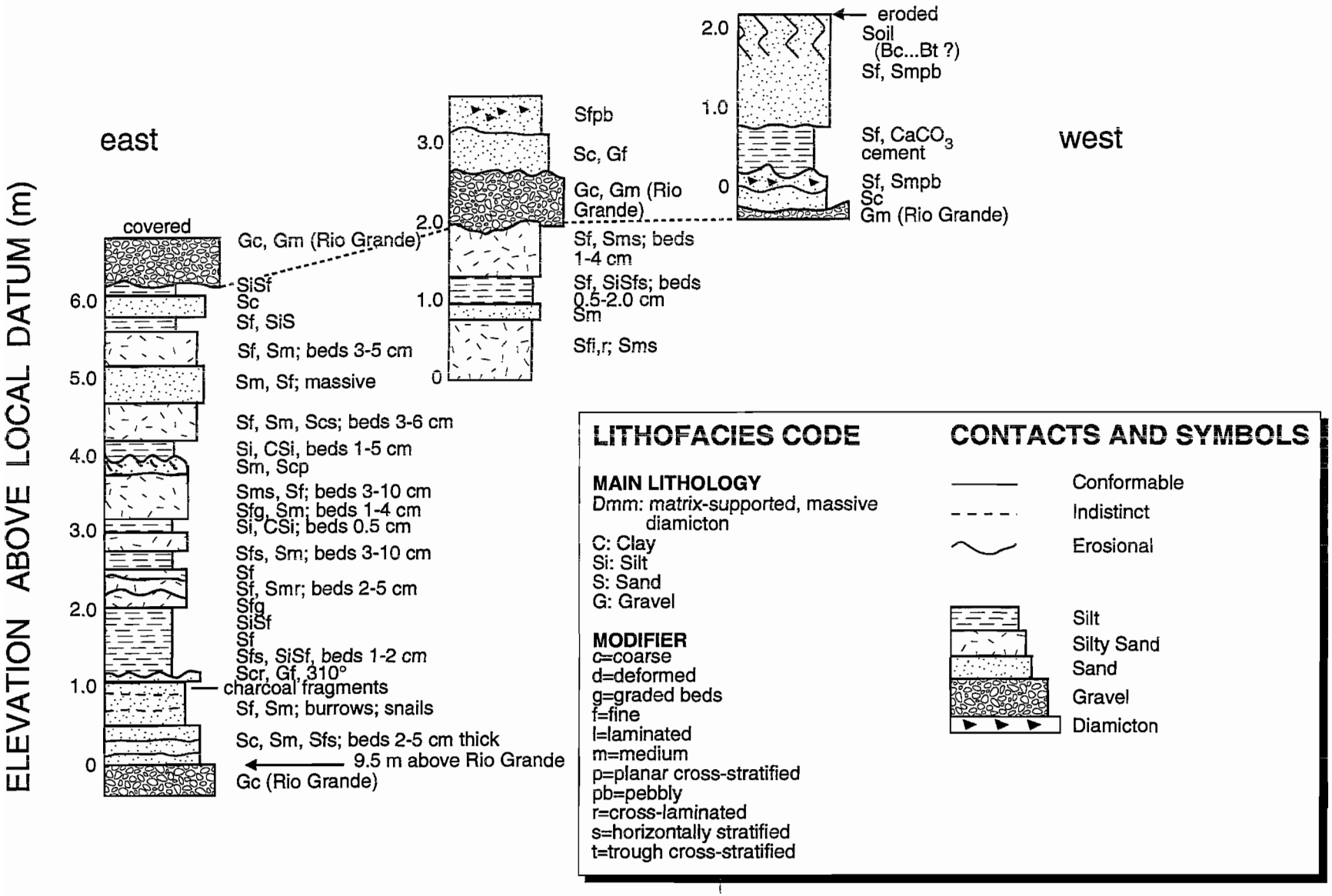

Fig. 0-7. Measured stratigraphic sections exposed in the Red Dot Trail area. Described by David Dethier (from Reneau et al., 1995a).

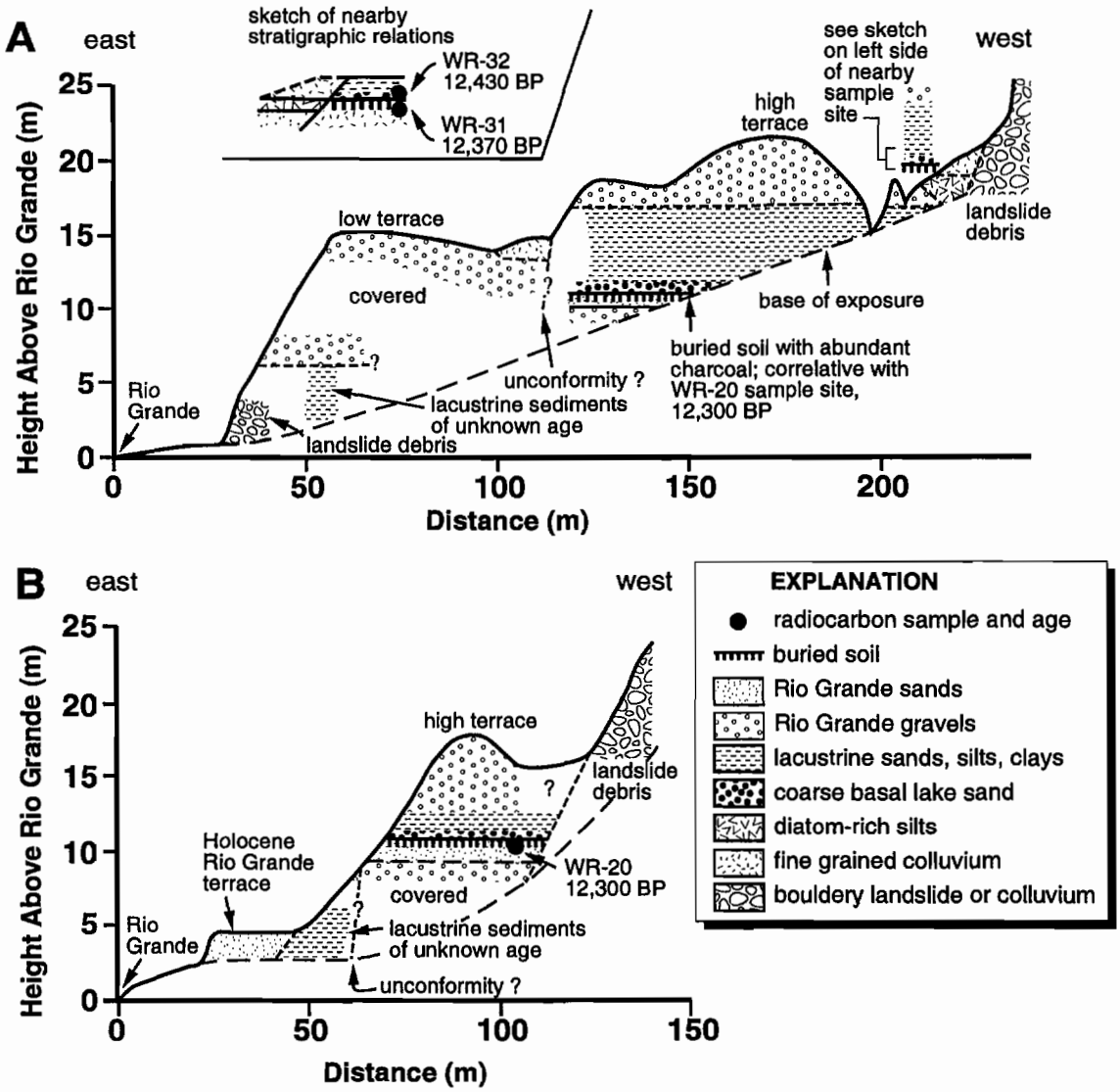

Fig. 0-8. Cross sections of Red Dot Trail area, showing stratigraphy and radiocarbon sample sites. (A) Northern section, with inset showing stratigraphic relations at nearby WR-31 and WR-32 sample sites, 30 m south of section. (B) Southern section, 150 m south of (A), showing WR-20 sample site. All radiocarbon dates overlap at 2σ (from Reneau and Dethier, 1996a).

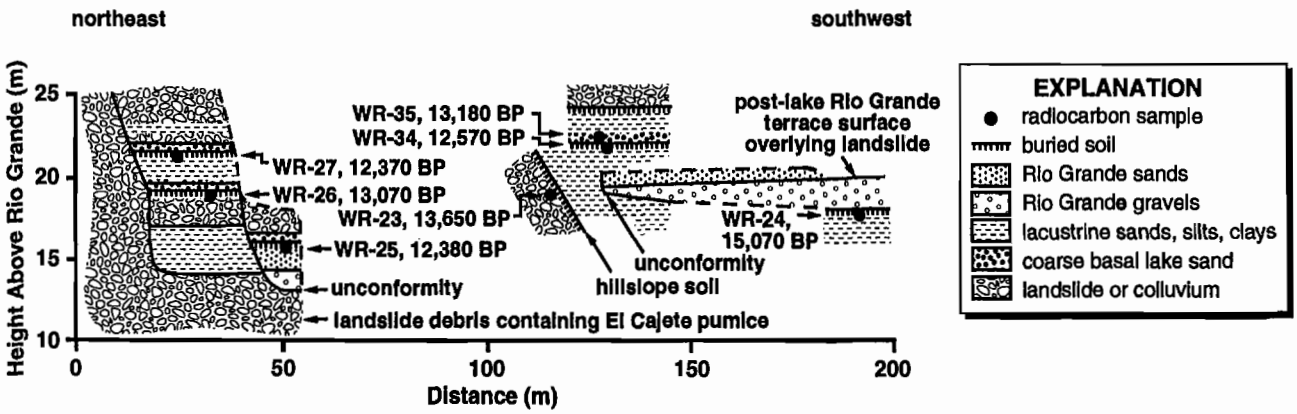

Fig. 0-9. Sketch of stratigraphy exposed below Chino Mesa in area of Water Canyon landslide dam, showing radiocarbon sample sites. Blank areas are covered (from Reneau and Dethier, 1996a).

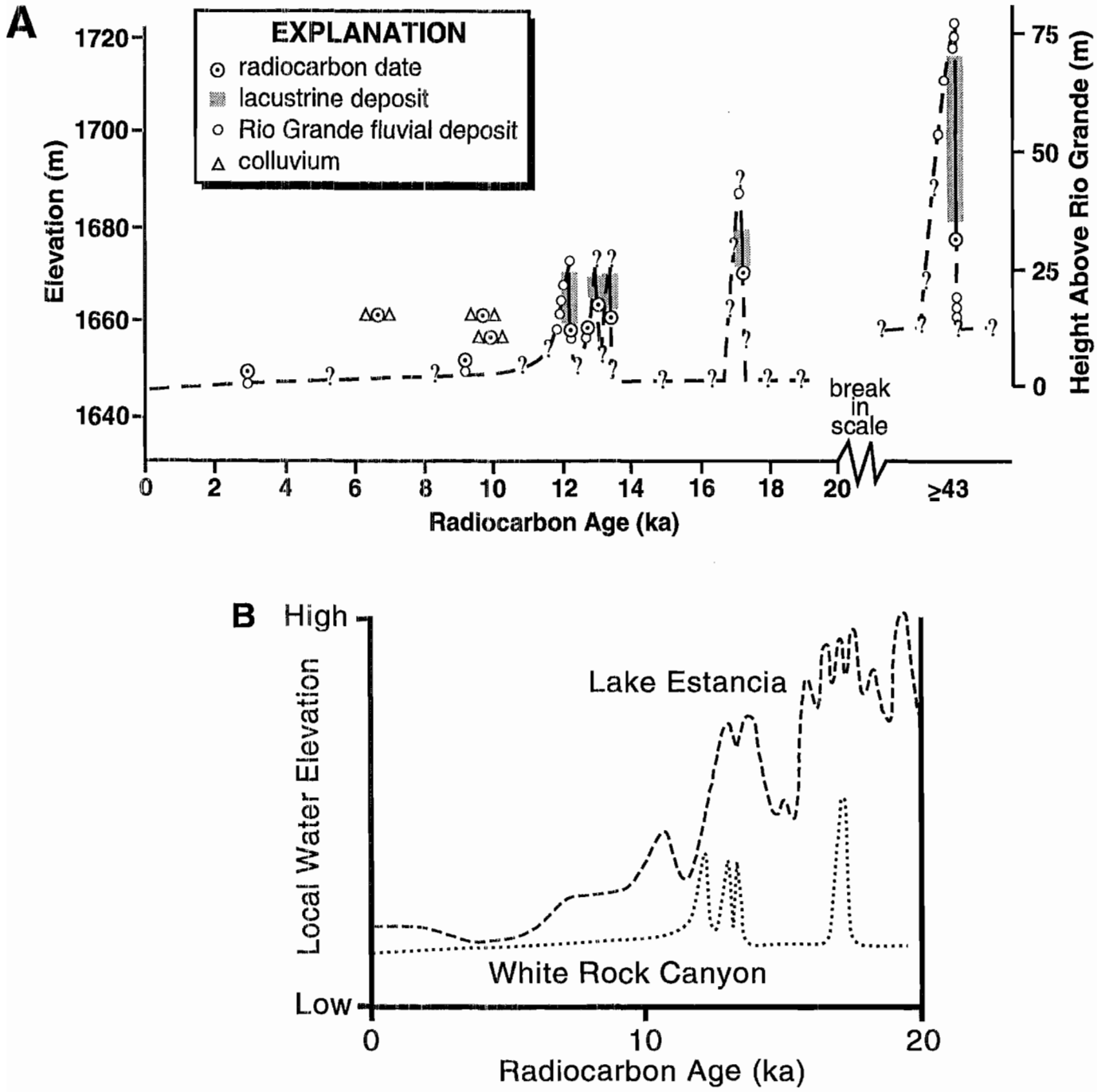

Fig. 0-10. A) Diagram showing inferred variations in water level in the Chino Mesa/Water Canyon West area. Data from sites elsewhere in White Rock Canyon are plotted using elevation for lake deposits and height above the modern Rio Grande for fluvial and colluvial deposits. B) Comparison of the estimated sizes and ages of the latest Pleistocene White Rock Canyon lakes with the history of pluvial Lake Estancia (Allen, 1991), 120 km to the south, showing synchroneity of lake-level high stands (from Reneau and Dethier, 1996a).

the filling of the pluvial lake basin (believed to be dominated by increased winter precipitation from the Pacific Ocean; Allen, 1991) led to reactivation of one or more of the White Rock Canyon slump complexes (Reneau et al., 1995a; Dethier and Reneau, 1996; Reneau and Dethier, 1996a). Although the exact triggering mechanisms are not known, we believe they included some combination of increased discharge from regional aquifers, increased infiltration directly onto the slump complexes, and increased incision and lateral erosion by the Rio Grande, all of which could contribute to slope destabilization.

Prehistoric Farm Fields. Many of the flats within White Rock Canyon, both fluvial terraces near the river and higher surfaces formed on the slump complexes, were farmed by the local prehistoric Pueblo people. Ruins in this area are small structures, containing one or several rooms, and are believed to have been seasonal "field houses" occupied only during the farming season by inhabitants of Tshirege and other large pueblos on the Pajarito Plateau. Evidence of the actual farm fields are provided by remnants of stone-bordered terraces, the terraces being effective at slowing runoff and enhancing infiltration. Of particular interest in the Red Dot Trail area are well-defined irrigation ditches, lined with basalt slabs, that were traced to their origin at Pajarito Springs by Rory Gauthier, former Bandelier National Monument archaeologist.

- From the late Pleistocene terraces south of Pajarito Canyon, retrace the route to the stream, and head downstream towards the Rio Grande along the west margin of the bouldery Pajarito Canyon fan. About halfway to the river, a pool where short waterfalls drop over basalt boulders makes an excellent lunch stop.

Pajarito Canyon Fan. The Rio Grande makes a slight bend at the mouth of Pajarito Canyon around the toe of a bouldery fan (**point 5, Fig. 0-1**). The boulders are dominated by basalt, suggesting a source downstream of the waterfalls (usually dry) where the stream drops into White Rock Canyon. No age control is available on this fan or other similar fans in White Rock Canyon, although their surfaces are presumed to be late Holocene in age due to their topographic position and their fresh morphology. The largest rapid on the Rio Grande in this area is Ancho Rapid, 4.7 km downriver, where the Ancho Canyon fan impinges on the river.

Rio Grande. The Rio Grande upstream of White Rock Canyon drains an area of about 37,000 km^2, and its headwaters are in the glaciated San Juan Mountains of southern Colorado. Modern floods typically occur either in the spring, of relatively long duration and derived from snowmelt runoff, or in the summer, generally of short duration and derived from summer thunderstorms (Nordin and Beverage, 1965; Allen et al., 1993; Graf, 1994). The largest floods on record at Otowi Bridge, at the head of White Rock Canyon, had discharges of about 700 m^3/s and occurred during the snowmelt seasons of 1920 and 1941. Although there are no estimates available for variations in the late Quaternary discharge of the Rio Grande, we expect that floods were typically larger in the late Pleistocene relative to the Holocene, associated with higher regional precipitation and larger snowpacks in the mountains. Channel incision and lateral erosion associated with such late Pleistocene floods may have contributed to the reactivation of landslide complexes recorded by the landslide-dammed lake deposits (Reneau et al., 1995a; Dethier and Reneau, 1996; Reneau and Dethier, 1996a).

- From the mouth of Pajarito Canyon a trail traverses up the slope to the south, passing small springs, and reaching a broad flat in ~0.5 km. This flat is developed on a late Pleistocene (?) landslide into which the Rio Grande is incised, as can be viewed from the edge of the flat to the east.

Possible Late Pleistocene (?) Landslide Dam. For ~0.7 km through here the Rio Grande has cut through the lower part of the Pajarito Canyon complex (**point 6, Fig. 0-1**). Morphologically, this inner canyon is similar to that formed 3.5 km downriver where the river has incised through the ca. 12.4 ^{14}C ka landslide dam, suggesting that this landslide also dammed the river. Coarse sands that may have been deposited along an overflow channel have been mapped upstream on top of the landslide complex, 13 m above the river, but these have not been dated. In addition, no lacustrine deposits or outburst flood deposits have been found in association with this landslide. If it did dam the river, we have no evidence for the age, size, or duration of the resultant lake. It is possible that sliding was slow and/or discontinuous, and that the landslide was relatively easily eroded by the river, preventing the formation of a large or long-lived lake.

- The trail heads northeast across the large flat, bending east around the south side of an anomalous 35-m high hill composed of quartzite-rich gravels (presumably a landslide block underlain by the axial facies of the Pliocene Puye Formation, although the absence of capping basalt is puzzling). North of this hill is a rock avalanche deposit that can provide a diversion for those that like rugged boulder fields.

Rock Avalanche. This rock avalanche deposit (**point 7, Fig. 0-1**) was derived from failure of the basalt cliffs to the west. The deposit is ~0.6 km long, and the avalanche likely descended ~200 m in elevation and traveled ~1 km horizontally from the canyon rim. It is morphologically similar to a much larger deposit that occurs just north of Ancho Canyon, both of which display characteristics common to long-runout rock avalanches (Reneau et al., 1995a). The age of this rock avalanche is unknown. Seismic shaking (*a la* Keefer, 1984) provides a plausible (but unconfirmed) triggering mechanism for the initial failure.

- The trail crosses a shallow southwest-draining trough between landslide blocks, reaching a narrow flat parallel to the Rio Grande (**point 8, Fig. 0-1**). A berm at the east edge of the flat contains some very well-rounded and sculpted basalt boulders, some of which appear to be imbricated, suggesting that it represents an ancient flood levee. This berm is similar in appearance to inferred outburst flood deposits downstream of the Water Canyon landslide dam. The berm is about 20 m above the river, and its elevation of about 5500' suggests it is older than the 12.4 ^{14}C ka lake and younger than the ca. 40-70 ka lake. A possible causative landslide dam upriver has not yet been identified.

- The trail continues to parallel the Rio Grande, traversing down to near the river west of "Soda Springs" (**point 9, Fig. 0-1**).

Late Quaternary Deposits in the Soda Springs Reach. The large barren area across the Rio Grande includes "Soda Springs", and vegetation is presumably sparse due to widespread deposition of salts in an area of long-term groundwater discharge (the best access to this area, on the east side of the river, is by hiking south from the mouth of Cañada Ancha). Soda Springs is a perennial spring that may have a recharge area in the Sangre de Cristo Range, based on stable isotope data that indicates an average recharge elevation of ~3000 m (Blake et al., 1995). (The name "Soda Springs", shown on the USGS White Rock 7.5' quadrangle, is apparently a misnomer as the waters do not contain the requisite chemical composition to be called "soda springs"; F. Goff, pers. comm., 1995)

The deposits in the Soda Springs area, east of the river, are poorly exposed and poorly understood. They appear to include extensive areas of fine-grained distal colluvial or fan deposits derived from the

slopes to the east, and may also include some lacustrine deposits. Well-laminated lacustrine deposits that may be correlated with the ca. 40-70 ka landslide-dammed lake are exposed in a drainage to the southeast, but no local age control is available. Local deposits of quartzite-rich gravels indicate remnants of late Pleistocene Rio Grande terraces, although their age and context is uncertain. The barren area includes a bed that is rich in gastropod fossils of the genera *Gyraulus* or *Valvata* (?), indicating a freshwater pond deposit and inferred to be associated with springs, perhaps produced during a time of enhanced groundwater discharge. An apparent age of 14,150 ± 80 ^{14}C BP (WR-40, Beta-72984) was obtained from these shells which does not seem to fit into the rest of the late Pleistocene chronology in White Rock Canyon. Other workers have found *Gyraulus* and other genera living at sites of deep groundwater discharge to provide unreliable radiocarbon dates as they can incorporate "old carbon" contained within the groundwater, resulting in apparent ages that are too old (J. Quade, pers. comm., 1994).

On the west side of the river the trail crosses an extensive late Holocene sand deposit that lacks obvious stratification. The origin of this deposit is not certain, but possibilities include Rio Grande overbank sediments, eolian sediments, distal fan sediments, or some combination of these. Where exposed in a cut bank at the west edge of a broad gravel bar, 2.1-2.6 m of sand directly overlies Rio Grande gravels, and we thus informally refer to them as "Rio Grande floodplain deposits". Abundant charcoal collected from the base of the sands, ~2 m above the present river level, yielded an age of 2880 ± 80 ^{14}C BP (~2980 cal BP or 1030 cal B.C.; Reneau et al., 1995a; Reneau and Dethier, 1996a). This date indicates that the Rio Grande at ca. 3000 BP was located within ~2 m of its modern level, providing a constraint on the late Holocene position of the river (Fig. 0-10a). Data from another site upriver (optional stop near end of hike) indicate that the river was within 5 m of its present grade at ca. 9.3 ^{14}C ka.

Immediately to the west of the sandy flat, ~1.5 m of Rio Grande gravels underlie an ~13-m high terrace remnant and overlie colluvial or landslide debris containing abundant basalt boulders. The terrace is similar in height to other terraces in northern White Rock Canyon that overlie the latest Pleistocene landslide-dammed lake deposits, and is thus presumed to be associated with reincision after one of the lakes.

Archaic Occupation of White Rock Canyon. The ca. 2880 ^{14}C BP charcoal in the Soda Springs reach was restricted to a small area and was associated with scattered fire-cracked rocks, indicating the location of a prehistoric campsite dating to the Archaic period. Such clusters of fire-cracked rocks are typical of late Archaic sites in White Rock Canyon that were described as part of archaeological investigations conducted prior to filling of Cochiti Reservoir (Chapman, 1979a, 1979b). As described by Chapman, the Archaic inhabitants heated "quartzite cobbles and basalt clasts for use in stone boiling. Stone boiling involves dropping heated rocks into containers filled with foodstuffs and water. It is a common food preparation technique used by people whose technological inventory does not include fire-resistant ceramic or metal cooking vessels. Repeated use of stones as heat retainers inevitably results in their fracture and generation of a discard pile of heat-fractured or firecracked rock pieces. Kinds of foodstuffs prepared through stone boiling include soups, stews, and mushes made from milled seeds" (Chapman, 1979b, p. 66).

The Archaic period includes the long time span after the big game hunters of the Paleo-Indian period and prior to widespread development of agriculture associated with the ancestral Pueblo or Anasazi cultures. Although details of this time period are sparse, Archaic peoples in New Mexico are believed to have had a hunter-gatherer lifestyle in relatively small, mobile groups (Chapman, 1979a, 1979b; Cordell, 1979, 1984; Stuart and Gauthier, 1981). Age control on other Archaic sites in White Rock

Canyon is sparse. No radiocarbon ages were obtained during the Cochiti Reservoir investigations, but projectile points mainly seemed to associated with the "Armijo" and "En Medio" phases of Irwin-Williams (1973), which have estimated ages of ca. 1800-800 B.C. and 800 B.C-A.D. 400, respectively (Chapman, 1979b), consistent with the radiocarbon date obtained in the Soda Springs reach. Excavation of a rock shelter during the National Park Service's Cochiti Reservoir project also yielded radiocarbon dates in this same general range, of ca. 1390-3100 ^{14}C BP or ~1750 B.C.-A.D. 560 (uncalibrated ages from Traylor et al., 1977, cited in Chapman, 1979b), suggesting repeated use of White Rock Canyon during this general period.

- From the Soda Springs reach, continue on the trail northward, paralleling the Rio Grande. In about 0.5 km the trail passes a spring and then reaches a shallow trough that is west of a late Pleistocene Rio Grande terrace remnant. For the next ~0.15 km the trail passes though an eroded area of fluvial, lacustrine, and colluvial deposits that share many similarities with exposures present in the Red Dot area, plus some additional features.

Late Quaternary Lacustrine, Fluvial, and Colluvial Stratigraphy in "Blue Dot Trail" Area. Two drainages that cross the trail in this area provide exposures of a variety of late Quaternary deposits (**point 10, Fig. 0-1**; Fig. 0-11)

.

At the first (southern) drainage, a stream bank exposure east of the trail displays well-laminated lacustrine sediment that overlie colluvial or landslide debris, and which are in turn unconformably overlain by Rio Grande gravels (Fig. 0-11b). As seen at the Red Dot Trail site, a relatively coarse sand layer is present immediately below the lake sediments, suggesting a transgressive beach deposit. No age control has been obtained from this exposure, but the lacustrine deposits are presumed to be between 12.4 and 13.7 ^{14}C ka in age based on a correlation with other deposits in White Rock Canyon.

To the west of the trail, a shallow incision along this drainage exposes organic-rich sediments that overlie the back edge of the terrace. These sediments are presumed to have been deposited in an area of groundwater discharge, similar to the springs occurring a short distance to the south. A date of 9.66 ^{14}C ka from charcoal fragments provides a minimum-limiting age for the terrace and the underlying lacustrine deposits (Fig. 0-11b; Reneau and Dethier, 1996a).

At the second (northern) drainage on the trail, a heavily eroded "badlands" has developed to the west. These are developed on a colluvial deposit which is grey in its lower part, indicative of prolonged saturation and presumably associated with springs. The middle section of this colluvial deposit contains unusually abundant fossil gastropods (the terrestrial genera *Succinea*, *Vallonia* (?), *Pupoides*, *Pupilla*), which are suggestive of a relatively lush grassland environment and which yielded a date of 6.68 ^{14}C ka (Fig. 0-11a). Heavily oxidized quartzite-rich cobbles, associated with the terrace to the east and exposed at the trail, project under these colluvial deposits. To the northwest the colluvium partially overlies an eroded remnant of well-laminated lacustrine sediments that in turn overlies bouldery colluvium. These lacustrine sediments are not dated, but their elevation and sedimentology suggests a correlation with the ca. 40-70 ka deposits which are best exposed 2 km upriver near the mouth of Cañada Ancha.

To the east of this trail the drainage is incised below a late Pleistocene terrace, exposing a section that is very similar to the Red Dot Trail sediments examined ~2.5 km downriver. Rio Grande gravels overlie well-laminated lacustrine sediment, which in turn overlie older Rio Grande gravels (Figs. 0-11a, 0-12). No dates have been obtained here.

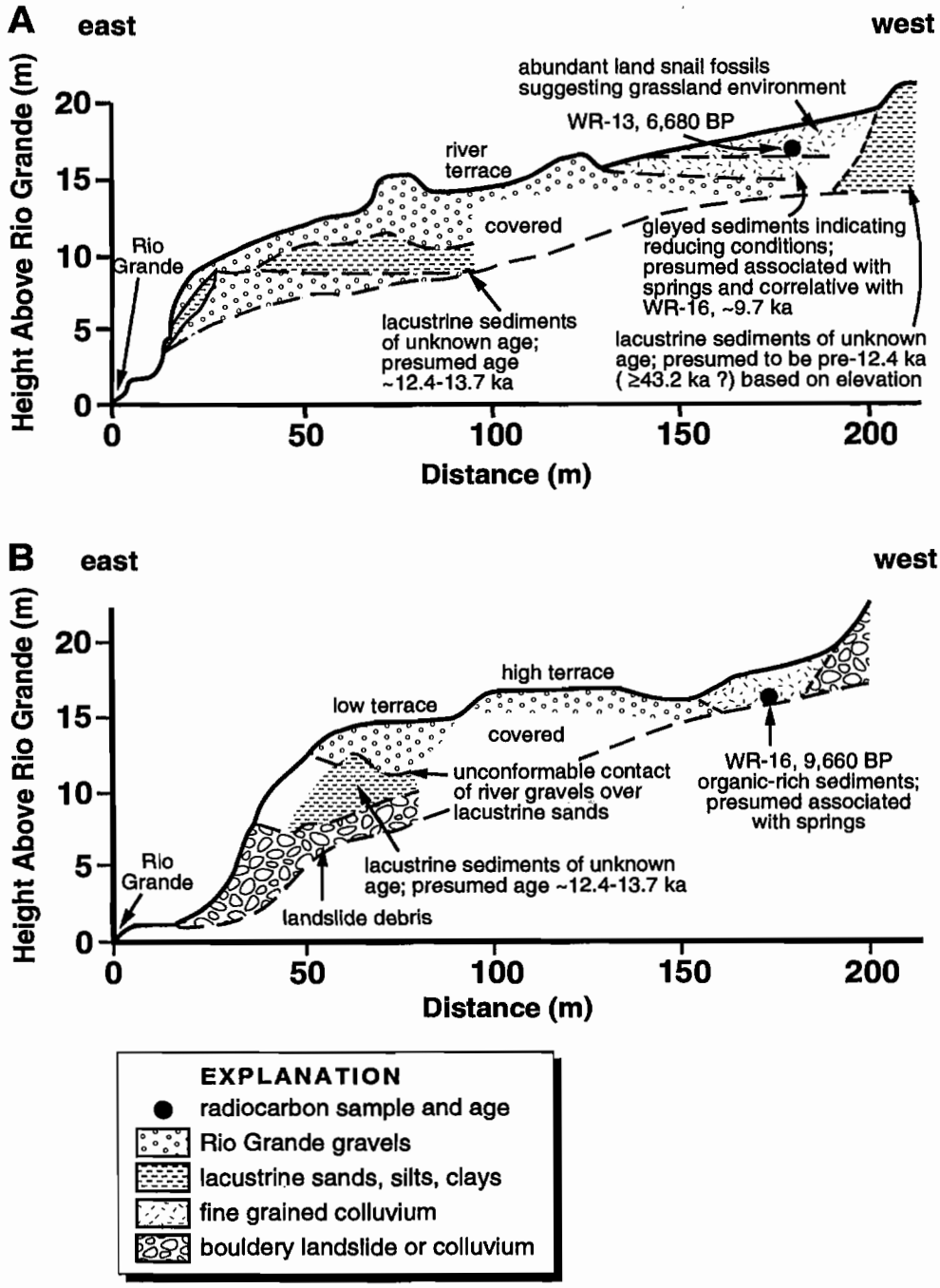

Fig. 0-11. Cross sections of Blue Dot Trail area, showing stratigraphy and radiocarbon sample sites. (A) Northern section, showing WR-13 sample site. (B) Southern section, 130 m south of (A), showing WR-16 sample site (from Reneau and Dethier, 1996a).

- The trail continues north over a late Pleistocene terrace remnant into a heavily-vegetated area, watered by a series of springs. In this area the Blue Dot Trail heads west, climbing about 800' (250 m) in ~1.5 km (1 mi) over landslide complexes to the rim at Overlook Park (**point 13, Fig. 0-1**). A trail can also be followed north parallel to the river for ~0.7 km to visit an early Holocene Rio Grande terrace remnant south of the Mortandad Canyon fan. (Note: upriver, on the south part of the Mortandad Canyon fan, begins San Ildefonso Pueblo lands, closed to the public).

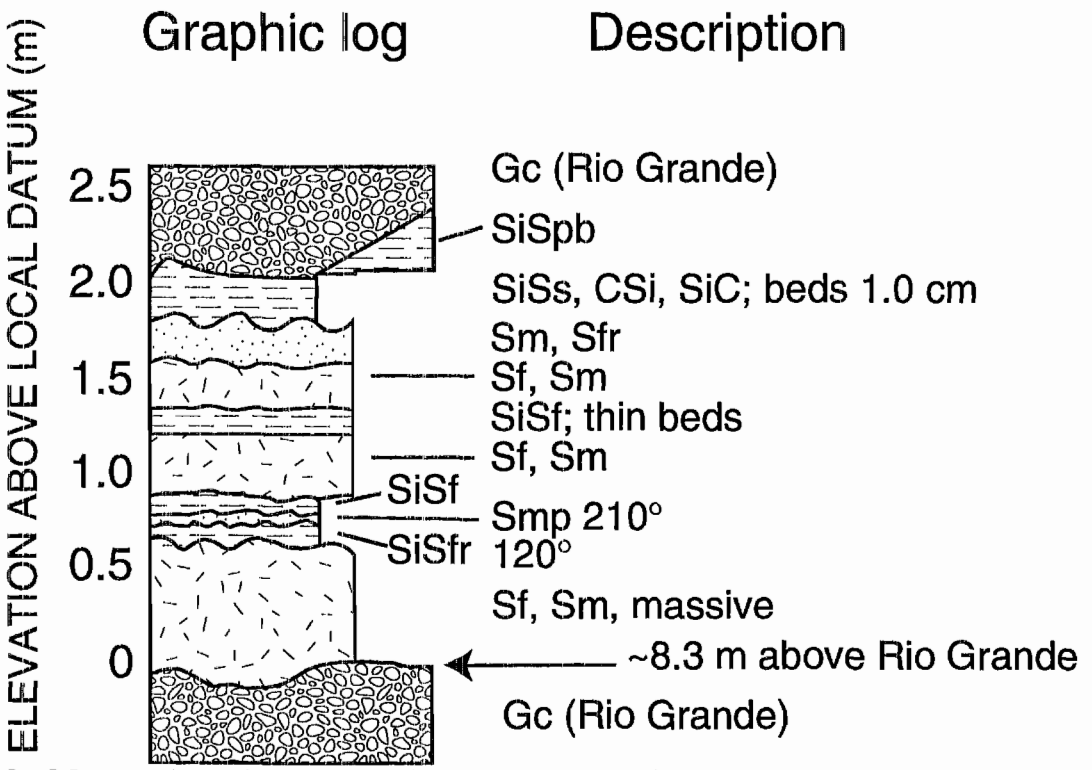

Fig. 0-12. Measured stratigraphic section exposed near the Blue Dot Trail area. Described by David Dethier. See Figure 0-7 for explanation of symbols and lithofacies codes (from Reneau et al., 1995a).

Future Landsliding Potential. The Rio Grande in this area is cutting against the west slope of White Rock Canyon at the toe of a narrow slump complex that extends up to the White Rock Overlook, resulting in a relatively steep average slope gradient (~0.5 m/m) between the canyon rim and the river (**point 11, Fig. 0-1**; Fig. 0-13). An evaluation of the potential for future landsliding involving presently intact areas along the canyon rims identified this as one of three locations on the southwest rim most susceptible to large-scale failure (Reneau et al., 1995a). This potential for instability is due to the combination of the steep slope and the likely presence of a thick section of relatively weak sediments which are involved in slumps in adjacent areas. Initiation of the Pleistocene slumps in White Rock Canyon often involved up to 0.5 km or more of retreat of the canyon rim, and a failure of this scale here would involve much of Overlook Park. In addition to widening the canyon and potentially damming the Rio Grande, such a failure would likely force the Rio Grande to the east. A reduction in the average slope gradient would result, diminishing the immediate potential for large-scale failures of the canyon rim. For example, the average slope gradient in the center of the Pajarito Canyon slump complex is only about 0.2 m/m (Fig. 0-13), and future slumping in that area would most likely be restricted to toe failures instead of new failures of the rim (for which local homeowners should be grateful).

Early Holocene Rio Grande Terrace Remnant. A narrow remnant of a 5-m high Rio Grande terrace, covered by colluvium, is exposed along the west bank of the river (**point 12, Fig. 0-1**; Fig. 0-14; Reneau and Dethier, 1996a). About 4 m of Rio Grande gravels overlie river-sculpted basalt boulders which are exposed near water level. The gravels are overlain by 1.5 m of fine sands that presumably represent overbank deposits. Fossil gastropods (*Succinea*) from these upper sands yielded an age of 9.34 ^{14}C ka, indicating that by the beginning of the Holocene the Rio Grande had abandoned the higher terrace levels and was within ~5 m of its present level (Fig. 0-10a).

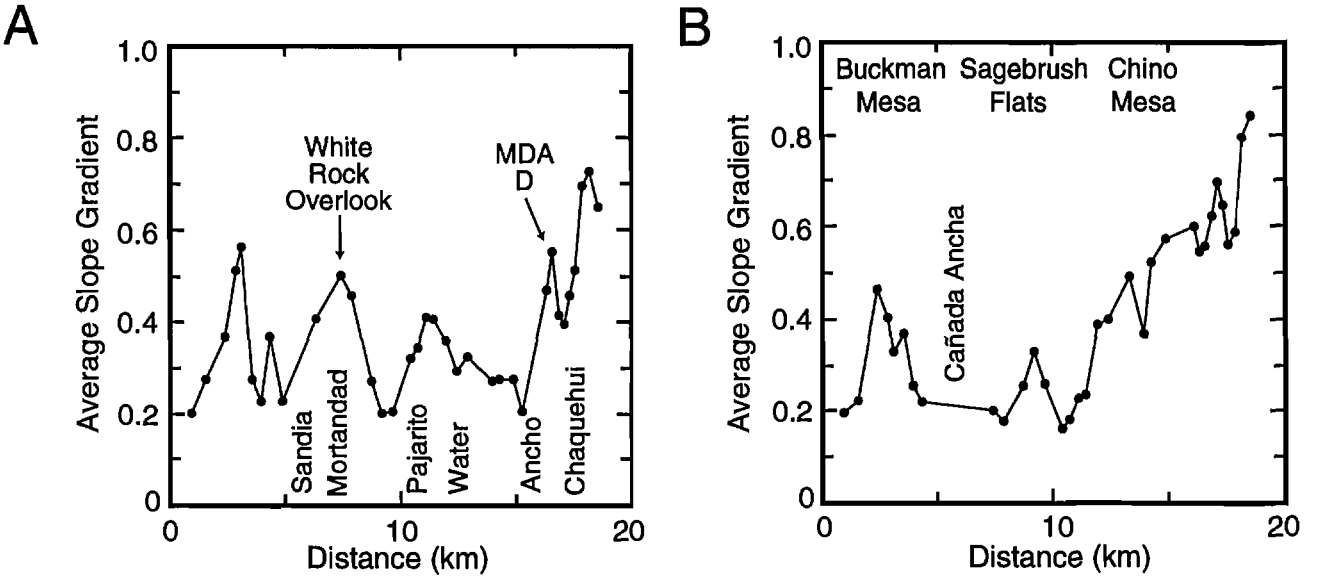

Fig. 0-13. Plots of average slope gradient in White Rock Canyon, defined as canyon depth divided by rim to floodplain distance, vs. distance downstream from Otowi Bridge. A) Northwest side of canyon. B) Southeast side of canyon. Areas with the steepest slopes are expected to be most susceptible to future failures involving the canyon rims, except for the areas to the southeast (downriver) where the sections are dominated by basaltic rocks (from Reneau et al., 1995a).

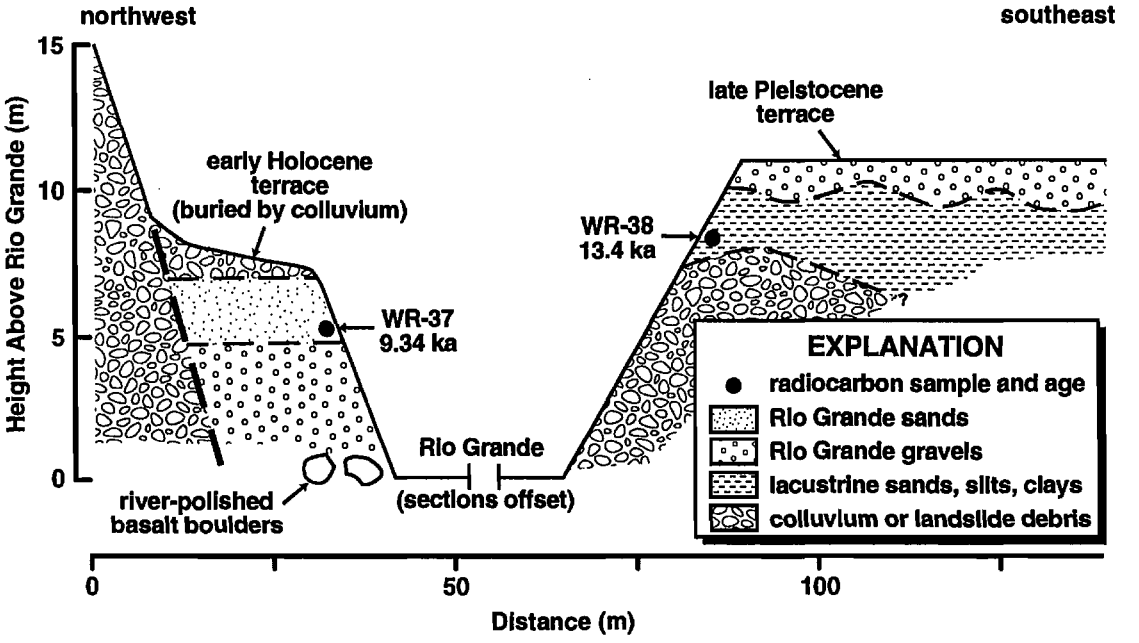

Fig. 0-14. Schematic cross section showing terraces, lacustrine sediments, and radiocarbon sample sites downriver of Mortandad Canyon (from Reneau and Dethier, 1996a).

- From the junction with the Blue Dot Trail, head west, climbing up to Overlook Park. Late Pliocene Rio Grande deposits (axial facies of Puye Formation), very similar in clast composition to the late Quaternary river deposits, are exposed within the landslide complex along the trail. At the top of the trail (**point 13, Fig. 0-1**), similar quartzite-rich gravels overlie both the basalt and the basal Tshirege Member of the Bandelier Tuff, recording an early Pleistocene river terrace (visited at Stop 1-3). From the canyon rim, hike west through the piñon-juniper woodland to the parking area.

Day 1, Tsankawi Unit of Bandelier National Monument to Ponderosa Campground

Leaders: Steven Reneau, Eric McDonald, Craig Allen, Dave Broxton, Jamie Gardner, Rory Gauthier, Brad Wilcox

Stop 1-1: Tsankawi Mesa

Field trip begins at parking lot for the Tsankawi unit of Bandelier National Monument, on the east side of NM State Road 4 (SR 4). Meeting area is 17 miles from Ponderosa Campground following SR 4, 3 miles from White Rock, 6 miles from Los Alamos, and 35 miles from Santa Fe. **Restrooms. No water. No shade.**

This stop involves an about 1.5 mile hike with 150' climb. Artifacts, rocks, plants, etc., are protected, so please leave your rock hammers behind and leave everything where you found it.

- Hike ~1/2 mi east up trail towards Tsankawi (tsank-ah-WEE) ruins. Trail begins at an elevation of ~6520' (1990 m) in a typical piñon-juniper ("PJ") woodland (dominated by *Pinus edulis* and *Juniperus monosperma*, with scattered *Pinus ponderosa* and rare *Juniperus scopulorum*). At signpost 2, the trail crosses a 2+ m deep gully through a loose, Holocene colluvial deposit, typical of the degree of erosion that is widespread across the eastern Pajarito Plateau.

- At signpost 3, the trail begins climbing through a narrow slot in orange tuff on a prehistoric Anasazi trail, flattening on a wide bench at signpost 4. This bench is developed at the transition between underlying glassy tuff of the lowest Tshirege Member of the Bandelier Tuff (unit Qbt-1g) and overlying pervasively vapor-phase altered tuff (Qbt-1v), and marks a prominent pseudo-stratigraphic marker on the Plateau (caused by alteration associated with initial de-gassing, and apparently not corresponding with a true depositional break; see Introduction for more discussion of tuff units) (Fig. 1-1). Note that the overlying tuff is pock-marked where devitrified pumice has been preferentially weathered, whereas glassy pumice stands out from the face of the underlying tuff, being more resistant than the matrix. The trail follows this bench to the east, then climbs up an incised Anasazi trail through grayish tuff of Qbt-1v.

- Signpost 6 is at the base of a 4-m high cliff formed in the overlying stratigraphic unit, Qbt-2, a relatively resistant unit that constitutes the main "cap rock" for many of the mesas on the eastern Plateau (Fig. 1-1). Many petroglyphs are carved into this cliff, including a version of "kokopelli", the legendary flute-player. Either climb up through the deep narrow slot in the tuff, or keep right to a 4-m high ladder. At the mesa top (signpost 7), turn left to the western tip of the mesa.

Station 1-1a, West end of Tsankawi Mesa

Geographic and Geologic Overview. From the west end of this isolated mesa is a wide view across part of the Pajarito Plateau, showing the typical topography of relatively narrow mesas alternating with steep-walled canyons carved in the Bandelier Tuff (Fig. 1-2). The buildings on the mesas to the west are part of the Los Alamos National Laboratory (LANL), which occupies most of the land between here and the base of the mountains.

The mountains on the skyline, 17 km west, are the Sierra de Los Valles, the eastern part of the Jemez Mountains and the eastern topographic rim of the Valles caldera. These mountains are underlain by

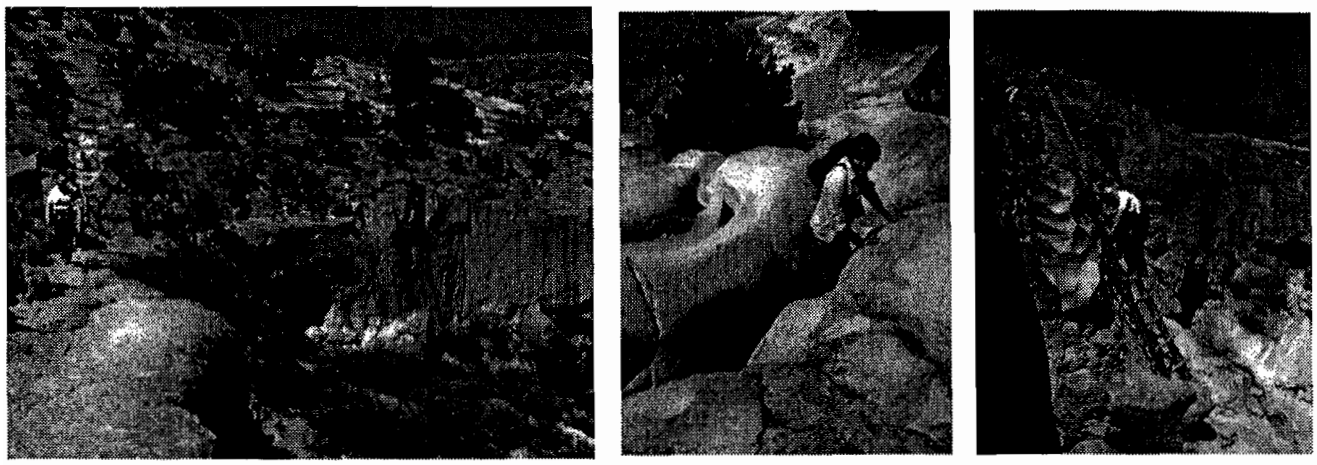

Fig. 1-1. Photographs of trails at Tsankawi, illustrating stratigraphic variations within the Tshirege Member (unit designations from Broxton and Reneau, 1995). Left photo: prominent bench developed on top of unit Qbt-1g (at "vapor-phase notch"); underlying tuff is glassy, and overlying tuff (Qbt-1v) has experienced pervasive vapor-phase alteration. Center photo: prehistoric trial is incised into non-welded, vapor-phase altered tuff of unit Qbt-1v. Right photo: ladder ascends cliff formed in unit Qbt-2, the most resistant unit on the eastern Pajarito Plateau; contact with underlying Qbt-1v (horizontal parting on lower cliff) represents a cooling break within the Tshirege Member and a pause in the eruptions.

Miocene-to-Pliocene dacitic lavas of the Tschicoma Formation which is named after Tschicoma Peak, the highest point in the Jemez at 11,561' (3524 m) (the mountain with the large south-facing grassland to the NW). Roughly at the base of the mountain front is the Pajarito fault zone, a major bounding structure of the Rio Grande rift with up to ~155 m of down-to-the-east normal displacement since 1.22 Ma. The prominent straight-walled canyon immediately to the northwest is ~100 m deep Los Alamos Canyon, heading in the Sierra de Los Valles (visited at Stop 3-3), and the shallower canyon to the southwest (with the paved road) is Sandia Canyon, heading on the Plateau (visited at Stop 1-2). On the southwest horizon is St. Peter's Dome in the San Miguel Mountains, in the center of the April 1996 Dome Fire area, and the isolated mountain to the north is Clara Peak. The eastern skyline is dominated by the Sangre de Cristo (Blood of Christ) Mountains, 45 km away on the eastern side of the Rio Grande rift, cored by a variety of Precambrian rocks and reaching elevations of >13,000' (~4000 m). To the southeast are late Pliocene vents of the Cerros del Rio volcanic field, and on the southern horizon are the Sandia Mountains east of Albuquerque, 75 km distant.

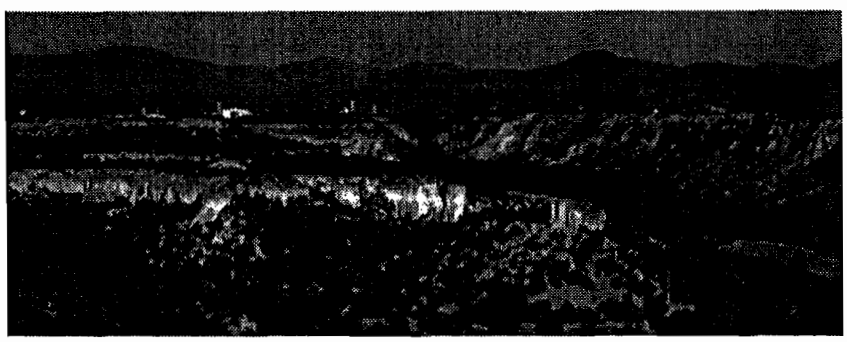

Fig. 1-2. View west from Tsankawi Mesa, Stop 1-1a, across Los Alamos Canyon. Tshirege Member of Bandelier Tuff (1.22 Ma) forms the cliffs; pumice beds and alluvium of Cerro Toledo interval (1.22-1.61 Ma) and Otowi Member of Bandelier Tuff (1.61 Ma) underlie the lower slopes. The Sierra de los Valles, the eastern rim of the Valles caldera, form the western skyline, with Pajarito Mountain to left.

Bandelier Tuff. The early Pleistocene Bandelier Tuff defines and dominates the Pajarito Plateau. It was erupted from the Jemez Mountains in two major caldera-forming eruptions at ca. 1.61 and 1.22 Ma, forming the Otowi (lower) and Tshirege (upper) Members, respectively. The Otowi Member is entirely non-welded where exposed on the Plateau, typically forming slopes on the lower canyon walls, including the lower ~40 m of Los Alamos Canyon immediately to the northwest. In contrast, the Tshirege Member is composed of multiple cooling units with varying degrees of welding and alteration, producing a benched topography of alternating cliffs and slopes as is well displayed on the trail to this stop (Fig. 1-1). Between the Otowi and Tshirege Members is a variable unit locally referred to as the "Cerro Toledo interval", which includes pumice beds, alluvium, colluvium, and soils that span the intervening ca. 400 ky. Small exposures of the Cerro Toledo interval can be seen on the south-facing wall of Los Alamos Canyon from this mesa, the stratified layers locally visible at the base of the Tshirege cliffs. (The rock units in Los Alamos Canyon to the west of here have been mapped by Goff, 1995, and Rogers, 1995, and detailed petrographic and mineralogic analyses are provided by Broxton et al., 1995a).

Eruption of each of the Members of the Bandelier Tuff profoundly changed the landscape in this area, burying the former topography with 10s to >100 m of ignimbrite, and subsequent drainage networks apparently had little relation to previous streams, with the exception that they continued to drain previously established basins in the Sierra de Los Valles and empty into the Rio Grande (Broxton and Reneau, 1996). A major north-south drainage that existed between the Tschicoma highlands and the Cerros del Rio volcanic field prior to 1.61 Ma was largely swamped by emplacement of the Otowi ignimbrites, and post-Otowi streams had more southeasterly trends. This landscape was again remade at ca. 1.22 Ma with emplacement of the Tshirege Member, and subsequent streams had a yet more easterly trend.

Also of note is the widespread occurrence of dacite-rich fluvial deposits derived from the Sierra de Los Valles that occur on top of the Tshirege Member on many mesas. These deposits record a very diffuse, perhaps braided drainage network on this part of the Plateau for some undefined length of time after 1.22 Ma, prior to initial incision of the canyons. One of the best examples of a mesa-top paleochannel occurs on the mesa 1.5 km northeast of this stop, which may be examined on an optional hike on the afternoon of Day 3.

- Walk east on the mesa crest ~1/4 mi to the Tsankawi ruins.

Station 1-1b, Tsankawi Ruins

Tsankawi is a large unexcavated ruin that is representative of many of the "Rio Grande Classic Period" ruins on the Pajarito Plateau (Fig. 1-3). Although not well dated, it is believed to have been built in the 1400s and perhaps abandoned in the late 1500s. The Tewa-speakers of San Ildefonso Pueblo, in the Rio Grande valley ~12 km northeast of here, consider it to be one of their ancestral villages, and San Ildefonso lands border this part of Bandelier National Monument. "Tsankawi" is a contraction of a longer Tewa name, *saekewikwaje onwikege*, which means "village between two canyons at the clump of sharp, round cactus" (Stuart, 1989).

As described by David Stuart: "Its four large roomblocks are arranged in an irregular rectangle around a central plaza, with nearly a dozen kivas at the site. It contained between 350 and 400 rooms and, like others nearby, was built of hand-cut volcanic tuff, mortared with adobe. Portions of Tsankawi were once several stories high. Photographs taken a century ago show how deterioration of such ruins has

Fig. 1-3. Oblique airphoto of Tsankawi Mesa. Tsankawi ruins to right.

accelerated in modern times. . . . Tsankawi gave its name to a distinctive Tewa Black-on-cream pottery and, although not adequately dated, flourished in the A.D. 1400s and 1500s. Most of its farmlands and the faint remains of small, one- or two-room "field" houses, typical of the Classic Period, are in the canyon bottoms surrounding Tsankawi's mesa" (Stuart, 1989, p. 109).

East of the ruins on the mesa top is the remains of a small reservoir that apparently impounded water that ran off the roof tops and the plaza, a feature also occurring at other Classic Period ruins in the area. The south side of the mesa contains abundant "cavate" ruins, carved into the tuff, which are common on many of the south-facing cliffs on the eastern Pajarito Plateau. The cavates often constituted a back room behind masonry structures built out from the cliffs, called "talus pueblos", although these outer rooms are not preserved (a reconstructed talus pueblo can be viewed in Frijoles Canyon).

- Retrace trail to parking lot.

<u>Mileage from Tsankawi</u>

0.0 Tsankawi parking lot

0.1 **East Jemez Road** ("Truck Route"). Keep in right lane before light, turning right up East Jemez Road into Sandia ("watermelon") Canyon. To right is water-supply well PM-1. Late Pliocene basalt of the Cerros del Rio volcanic field underlies the Otowi Member of the Bandelier Tuff here at a depth of 50 m (Purtymun, 1995). On the slopes to the northwest, dacite-rich gravels in the Cerro Toledo interval occur between the Tshirege and Otowi Members, indicating the location of a pre-Tshirege, ca. 1.22-1.61 Ma paleodrainage that trends roughly northwest-southeast, oblique to Sandia Canyon (Broxton and Reneau, 1996). East Jemez Road for the next mile is bordered by DOE land that is open to the public. The canyon bottom is underlain by ~5.5 m of Holocene alluvium in this area (Sandia Canyon observation well SCO-2; Purtymun, 1995). Many cavate ruins are visible at base of the south-facing canyon wall, carved into the lower non-welded part of Tshirege Member (Qbt-1g). Grey tuff higher on canyon wall is Qbt-1v, and the mesa is capped by Qbt-2.

1.0 A trail to Mortandad Canyon begins at gate to left (south), crossing gap in mesa. The trail passes a "deer trap", a rectangular pit excavated in tuff in gap where prehistoric hunters presumably hid beneath a brush blind to shoot deer chased up the saddle. Similar pits also occur on many canyon edges, and are believed to have been used to catch eagles for ceremonial purposes, using

rabbits or other bait tethered next to the pit as lures (Hoard, 1981). From the pit, the trail continues west along a tuff bench (top of Qbt-1g) to a series of cavate ruins, some containing excellen examples of "Mortandad-style" petroglyphs, carved into smoke-blackened ceilings (Fig. 1-4).

1.6 LANL Technical Area (TA) 72. Protective Force Live Firing Range to right. Land adjacent tc road here and to the west marked by DOE "No Trespassing" signs. Please respect signs, or risk the wrath of the LANL "Pro Force".

2.1 Aggrading channel to left, downstream of deeply incised channel.

2.5 **Stop 1-2: Sandia Canyon.** Park on shoulder before where west-bound lane divides, as close as possible to guard rail. Area marked by DOE "No Trespassing" signs, so do not make this stop unescorted. Watch for traffic. LANL TA-53 on mesa top to north (Mesita de Los Alamos), home of the Los Alamos Neutron Science Center (LANSCE), a facility for high energy particle research utilized by physicists from many universities (formerly called the Meson Physics Facility or LAMPF).

- Cross guardrail to south and walk across grassy canyon floor to a 3-4 m deep incised channel heading for a 6.5 m high north-facing stream bank exposure. The channel here was not incised in 1935, and the recent incision may record an increase in runoff from developed areas in the headwaters, including part of LANL's main Tech Area, TA-3. Incision may also have been aided by channel modifications associated with construction of East Jemez Road, which included straightening its course and restricting the channel to the south side of the canyon bottom.

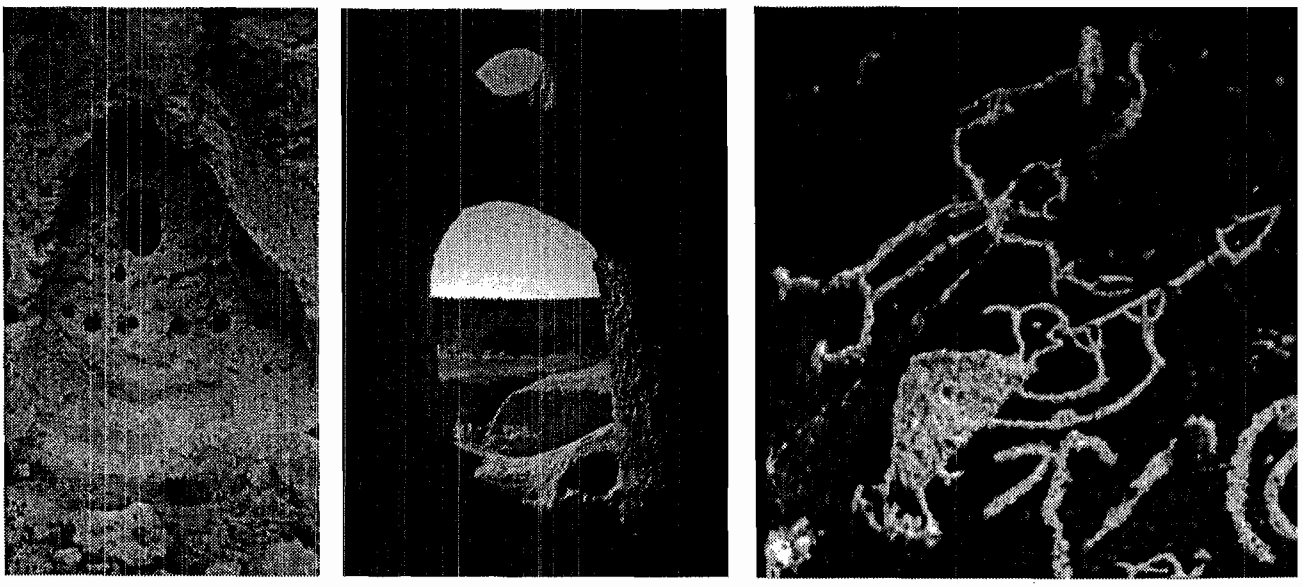

Fig. 1-4. Photographs of Mortandad Canyon archaeological sites. Left photo: split-level cavate ruin carved into tuff; the line of holes were for "vigas" (roof beams). Center photo: view from inside cavate ruin, with smoke hole. Right photo: "Mortandad-style" petroglyphs, etched into smoke-blackened ceiling (Maxwell and Kokopelli).

Station 1-2a: Late Quaternary Stratigraphy and Soils (6750', 2060 m elev.)

El Cajete Pumice Bed. The most striking unit in this exposure is the El Cajete pumice bed (Figs. 1-5, 1-6). Up to 0.75 m of generally unstratified, presumably primary fallout pumice is sandwiched between pre- and post-El Cajete colluvium, with the pumice bed dipping beneath the present channel. The El Cajete pumice is part of the Valles Rhyolite of Bailey et al. (1969), and was erupted from the El Cajete vent in the Valles caldera 28 km to the west. It is a product of the youngest eruptive sequence from the Valles caldera (the "El Cajete Series" of Self et al., 1988, or the "southwestern moat rhyolites" of Wolff and Gardner, 1995, and Wolff et al., 1996), and provides a key late Quaternary stratigraphic marker on much of the Pajarito Plateau, allowing precise correlation of horizons in diverse geomorphic settings (see also Stops 0-2, 1-4, 1-6, 2-2).

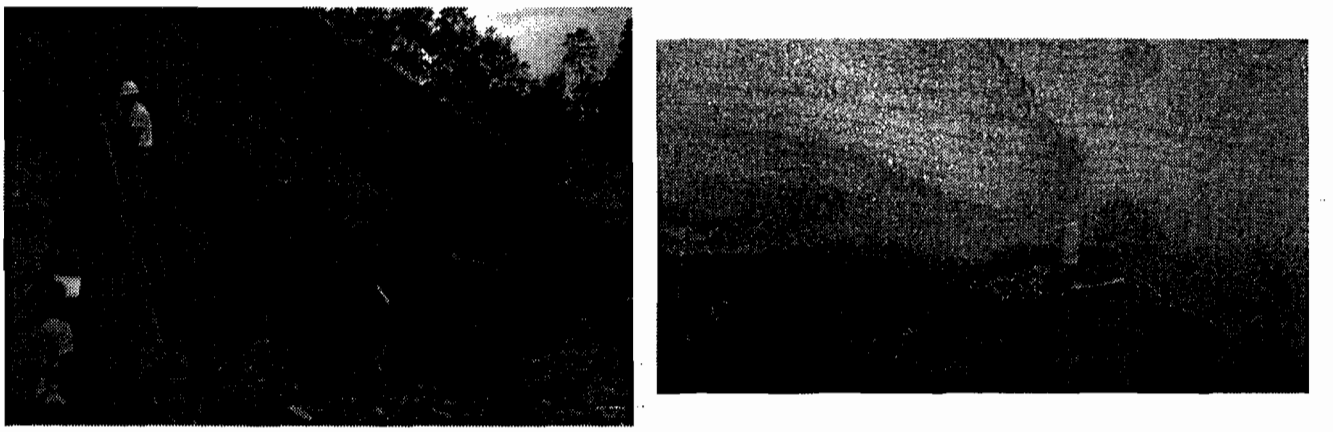

Fig. 1-5. Photographs of Sandia Canyon stream bank at Stop 1-2a. In left photo, base of El Cajete pumice is at hard hat, and slopes down to right. Right photo shows primary fallout El Cajete pumice, with lamellae, overlying pre-El Cajete soil (hammer for scale).

Age of El Cajete Pumice. The age of the El Cajete pumice has been difficult to determine with great accuracy. The El Cajete and associated units contain abundant xenocrysts, which have confounded K-Ar and $^{39}Ar/^{40}Ar$ analyses, and fission-track analyses also apparently had problems. At present, our best estimate of the age of the El Cajete pumice is ca. 50-60 ka, based on constraints provided by electron spin resonance (ESR) analyses of quartz phenocrysts (Toyoda et al., 1995), ^{14}C analyses of burnt logs entrained within surge beds near the vent, and thermoluminescence (TL) analyses of soils buried by the pumice on the Plateau (Reneau et al., 1996a). The TL analyses by Steve Forman yielded consistent results in two very different geomorphic settings, one a colluvial slope analogous to the buried soil at this stop (but occurring at the base of the Pajarito fault escarpment; see Day 2, Mile 1.2), and the other a gently-sloping mesa top, providing additional support for the accuracy of the analyses.

Stratigraphy and Late Quaternary Geomorphic History in Sandia Canyon. The El Cajete pumice at this stop overlies a 1.15 m thick, well developed soil that has formed in a colluvial deposit. The colluvium in turn overlies and truncates horizontally-stratified fine sands and silts that represent overbank deposits from a pre-El Cajete period of aggradation of Sandia Canyon (Fig. 1-6). At least three weakly developed soils have formed in these deposits. Fluvial coarse sands and gravels are interbedded with and underlie the overbank deposits, along with additional colluvial layers. (Note that the pre-El Cajete fluvial deposits are tilted to the north, indicating some slumping of the lower part of this section). The age of this aggradation period is not certain, but the degree of soil development in the buried colluvial deposit, much stronger than in the overlying colluvium, indicates perhaps 30-50 ky before burial (see next section). The age of the underlying stream deposits is thus estimated at >80-110 ka.

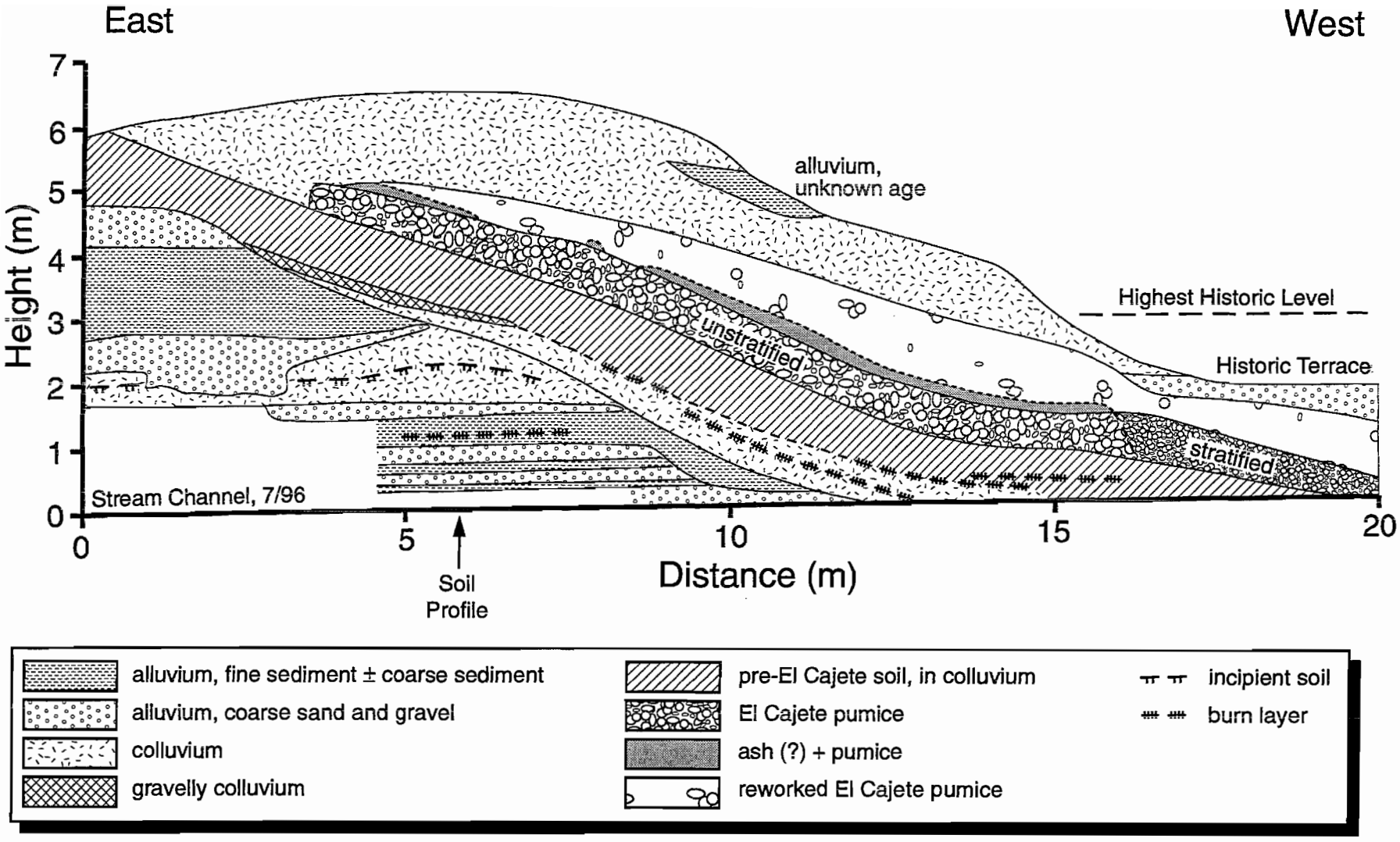

Fig. 1-6. Sketch of Sandia Canyon stream bank exposure with El Cajete pumice bed, at Stop 1-2a.

Overlying 0.6-0.75 m of pure, generally unstratified pumice is up to 1.1 m of stratified pumice that likely represents colluvial transport of the fallout pumice off the slope relatively soon after eruption. Separating these two units are lenses of ash (?) that may be correlative with an ash bed at the top of the pumice at Stop 1-6. The overlying colluvium contains common clasts of tuff, indicating exposure of the pre-eruption units following stripping of the pumice.

The stratigraphic context of the El Cajete pumice at this stop and at other canyon bottom sites on the Pajarito Plateau demonstrates significant late Quaternary aggradation. At the time of the El Cajete eruptions, the channel of Sandia Canyon here was located below the present channel, which in turn is located ~3 m below its highest historic level. The El Cajete pumice has also been encountered in drill holes beneath the floors of several other canyons (Reneau et al., 1996b). In Mortandad Canyon (0.7 km south of this stop), ^{14}C dates of 7.26 and 7.77 ka have been obtained on charcoal collected at depths of 10-12 m from 2 holes (Fig. 1-7), indicating the magnitude of Holocene aggradation there and suggesting that the bulk of the alluvial fills are Holocene in age. This and other evidence suggests a profound change in geomorphic processes on the Pajarito Plateau between the late Pleistocene and the early Holocene (see also Stops 1-4, 2-2, 2-3).

The local base level for this part of Sandia Canyon is a prominent knickpoint on late Pliocene basalt 7.5 km downstream (Fig. 1-8), which the Quaternary stream has been generally ineffective at eroding. Similar basalt knickpoints, providing local base levels, occur along most streams on this part of the Pajarito Plateau, isolating them from base level changes along the Rio Grande. The Holocene aggradation here and in other canyons has caused a steepening of stream gradients, and probably occurred in response to some combination of increased sediment supply and decreased stream flows associated with the Pleistocene-Holocene climatic transition.

Although the stream channel at the time of eruption of the El Cajete pumice here is some undetermined depth below the modern channel, relatively pure beds of stream-reworked El Cajete pumice are exposed in terrace remnants upstream, indicating net incision in the last ca. 50-60 ka. A terrace deposit containing similar pure beds of fluvially-reworked pumice in the north fork of Ancho Canyon (upstream of Day 1 Mile 16.0 on the Log) has yielded a radiocarbon-dead date of >46.7 ^{14}C ka, supporting the inference that such pumice-dominated beds were deposited relatively soon after eruption. The

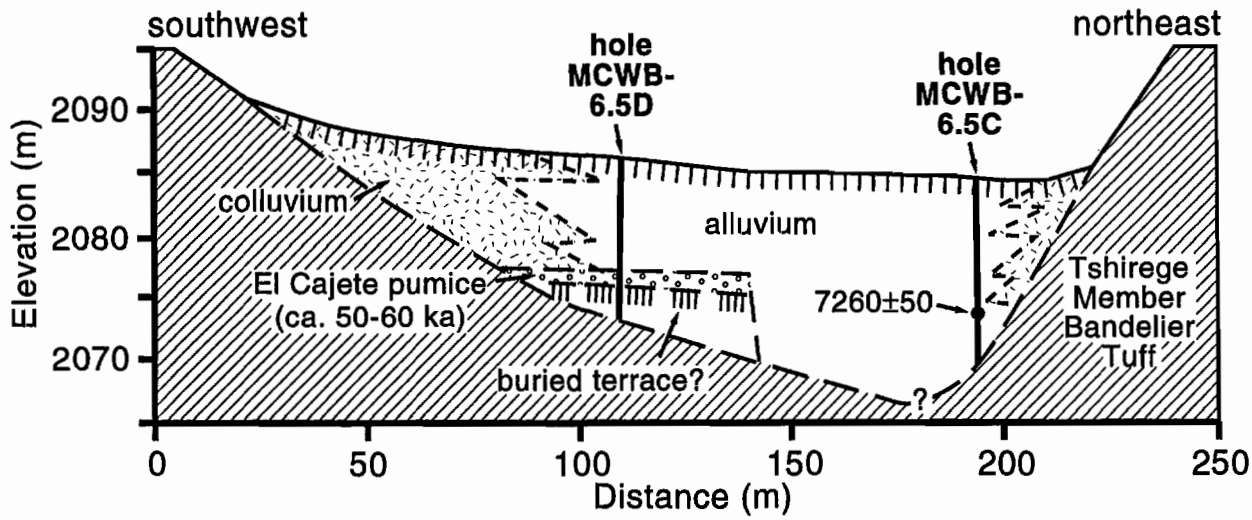

Fig. 1-7. Generalized cross section across Mortandad Canyon, 0.7 km south of Stop 1-2, showing radiocarbon date and inferred stratigraphic context of units exposed in core holes (from Reneau et al., 1996b, modified from unpublished core logs of S. McLin and others, 1994).

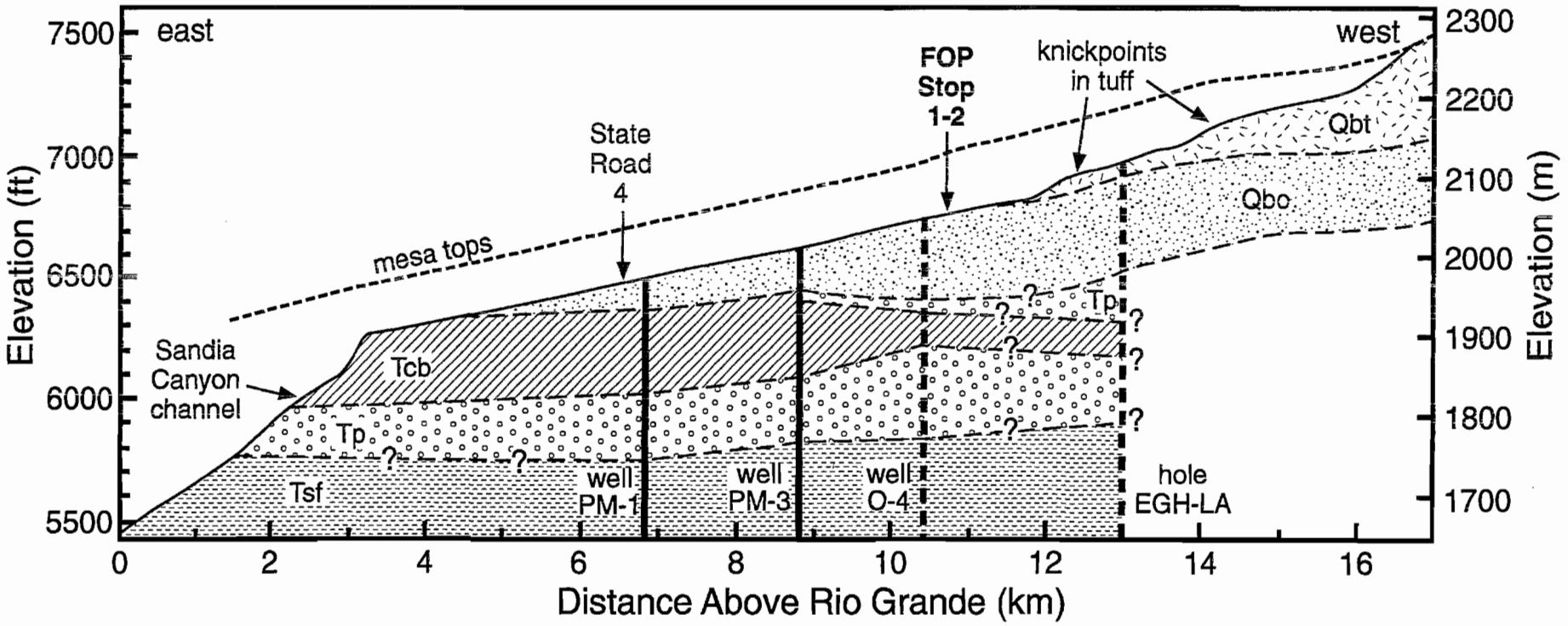

Fig. 1-8. Longitudinal profile of Sandia Canyon, showing simplified bedrock units. Approximate bedrock contacts based on Purtymun (1995), Broxton and Reneau (1996), and Dethier (1996), and are subject to revision pending reexamination of samples from these holes (J. Gardner, work in progress) and results from future drill holes. Contacts from well O-4 and hole EGH-LA projected to Sandia Canyon. Qbt: Tshirege Member of Bandelier Tuff; Qbo: Otowi Member of Bandelier Tuff; Tcb: Cerros del Rio basaltic rocks; Tp: Puye Formation; Tsf: Santa Fe Group, undivided.

contrast between net aggradation at this stop and net incision upstream demonstrates a reduction in the gradient of the buried late Quaternary bedrock-channel beneath the Holocene fill, showing continued evolution of the channels into tuff, presumably associated with migration of knickpoints in the tuff upstream (Fig. 1-8).

Soil-Stratigraphy of Profile SC-1: The El Cajete pumice at this stop overlies a moderately developed, buried soil complex consisting of perhaps three superimposed soil profiles that have largely formed in three thin layers of hillslope colluvium. This soil in turn overlies a 3+ m sequence of colluvium and alluvium that contains three weakly developed soils. In combination, this exposure illustrates both the complexity of the soil stratigraphy developed at diverse geomorphic settings on the Pajarito Plateau, and the prominence of the pre-El Cajete soil, which constitutes a significant time stratigraphic marker across much of the Plateau.

Buried Soils b1-b3: The top of the uppermost soil is a thin (10 cm) E horizon (Etb1, Fig. 1-9) that is considerably lighter in color than the underlying horizons (Table 1-1). An E horizon is a horizon in which either the removal or the segregation of iron oxyhydroxides and clay has occurred to the extent that the color of the horizon is dominated by the primary color of sand and silt particles rather than by the color of coatings on these particles (Soil Survey Staff, 1981). Coatings of clay and iron oxides do occur in places in the E horizons exposed in this stream cut; however, the formation of these cutans represent illuviation subsequent to burial by younger deposits.

The first sequence of Bt horizons (b1) extends to 75 cm below the base of the pumice. The Bt horizons have soil colors ranging from hues of 6.25 YR to 7.5 YR, prismatic structure that parts to subangular blocky structure, and common to few argillans along pores and ped faces, especially along prismatic ped faces. A second E horizon (Etb2, 75-84 cm) marks the top of the next thin buried soil (b2). This E horizon is generally similar to the upper one, but has a greater abundance of argillans, especially along prismatic ped faces, resulting from translocation of clay subsequent to burial by younger colluvium. The base of this soil (or colluvial layer) is denoted by a thin layer of gravely-loam with an abrupt lower boundary. The nature of the deposit and contact indicates burial of the underlying soil by colluvium. The underlying soil (b3) has a weakly developed Bt horizon that grades downward into generally unaltered colluvium and/or stream alluvium.

A Profile Development Index (PDI) value of 50.1 for this sequence of buried soils implies that this section may represent 30-50,000 years of soil formation PDI values were determined using the Soil Development Index of Harden (1982) and Harden and Taylor (1983). Age estimates for PDI values are based on development of a local soil chronosequence in nearby Rendija Canyon and TA-16 (McDonald, et al., 1996b) that will be one focus of Stops 2-2 and 2-3.

Prominence of Pre-El Cajete Soil: At this site, as well as at many locations across the Pajarito Plateau, the El Cajete pumice overlies a moderately- to well-developed buried soil. At most sites, the top of the buried soil is denoted by a sharp contact with the overlying pumice and the preservation of a light colored E horizon. This soil-stratigraphic contact will be exposed at several stops on this field trip (Stops 1-4, 1-6, 2-2). The widespread occurrence of a moderately- to well-developed buried soil below the ca. 50-60 ka El Cajete pumice indicates that a Plateau-wide period of relative landscape stability favoring soil development preceded deposition of the pumice. Particularly notable at this site is the moderate development of Bt horizons on a relatively steep hillslope, a landscape position that is generally unstable over time intervals that would allow the development of such horizons. For example, the present surface soil at this site, by comparison, is of considerably weaker development, consisting of A

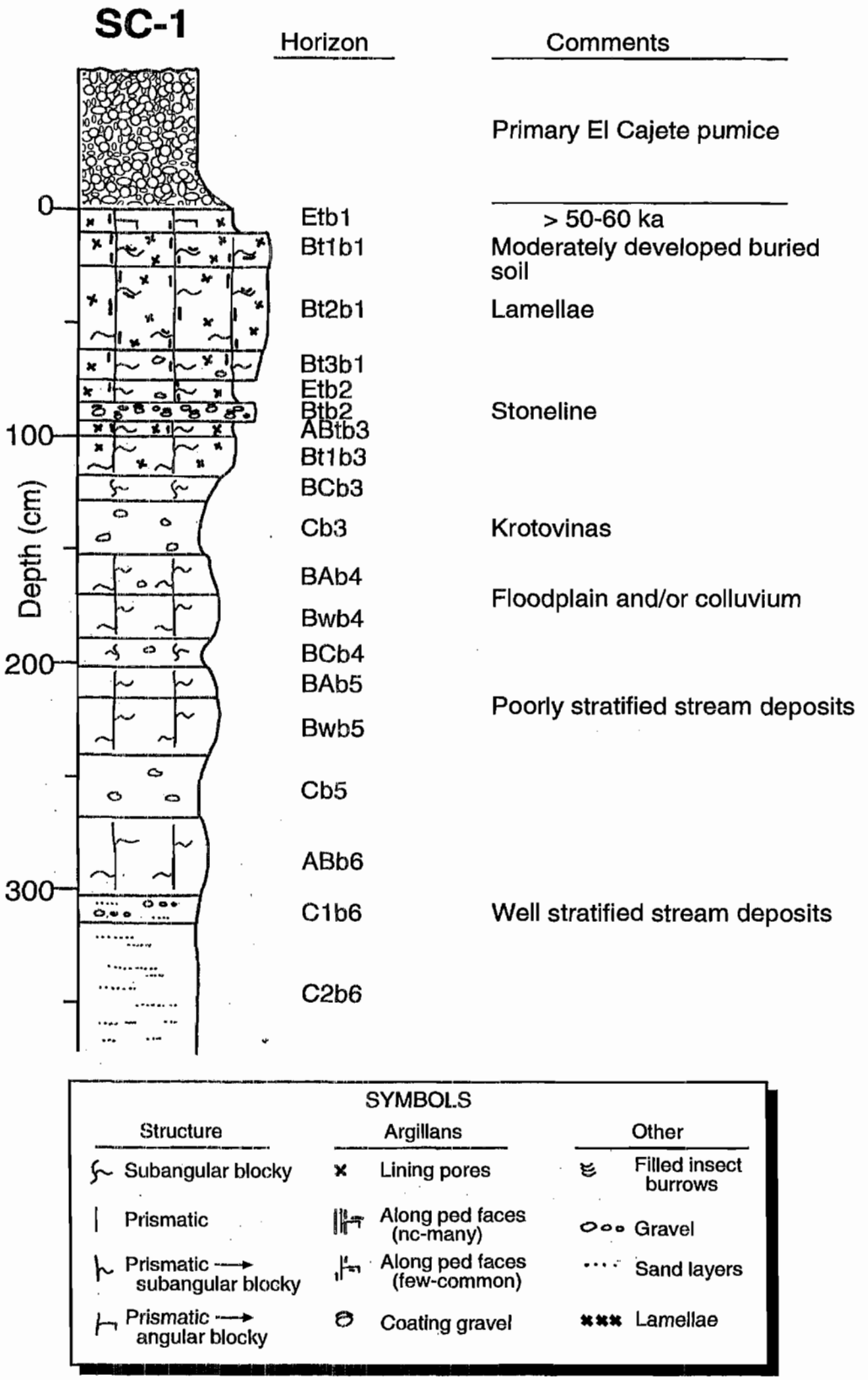

Fig. 1-9. Schematic diagram of soil-stratigraphy for soil profile SC-1, at Stop 1-2a. Number following"b" is refers to the number (stratigraphic position) of the buried soil. Symbols for soil features follow on next page. Extension of soil column to right indicates an overall greater degree of soil development. Symbols emphasize development of structure and argillans, two features that generally dominate temporal changes in soil morphology over time.

and Bw horizons. Furthermore, most hillslope soils across the Plateau (generally better developed on north facing slopes) are weakly developed, largely consisting of A and Bw horizons. Available ^{14}C dates indicate that in many places, present hillslope soils may be considerably less than 2 ka in age (Reneau and McDonald, unpublished data).

Buried Soils b4-b6: The remaining buried soils (b4-b6) largely consist of weakly developed soils formed in stratified stream deposits that are locally interbedded with colluvium. The primary feature of these soils is the development of BA and Bw horizons, with the strongest features consisting of weak to moderate prismatic and subangular structure and abundant tubular pores. We designate former, now buried, A horizons as either AB or BA horizons because buried A horizons now also display B horizon features (i.e. structure, color) due to overprinting of the overlying soil and loss of disseminated organic matter (presumably due to oxidation of the organic matter after burial). Former A horizons are recognized based on a combination of stratigraphic position, preservation of fine or medium subangular blocky and/or crumbly structures, and signs of abundant bioturbation. Krotovinas (animal burrows filled with soil) are also abundant throughout these buried soils. Many of the pores are vertically oriented and extend through the entire soil, suggesting that these buried soils originally had a thick cover of grass and/or shrubs. The lowest soil grades downward into well stratified stream sands and fine gravel.

- Walk upstream 75 m to a 4-m high south-facing stream bank.

Station 1-2a: Late Holocene alluvial fill

Holocene Alluvial Deposits. This stream bank exposes > 4 m of Holocene alluvium that is typical of the sediment present in many canyons on the Pajarito Plateau. Sandia Canyon heads on the Plateau, 6 km to the west, and stream sediments in this and other canyons are dominated by coarse sand derived from weathering of the Bandelier Tuff, consisting largely of quartz and sanidine crystals (note the bipyramidal quartz crystals and the blue, chatoyant sanidine crystals). Thin beds of black magnetite-rich sands are also common. The gravel fraction, often a small percentage, includes low density tuff clasts (relatively easily pulverized), resistant angular to sub-angular volcanic clasts that occur as lithic fragments within the tuff, and rare well-rounded dacite clasts reworked from early-post Bandelier fluvial deposits (derived from streams heading in the Sierra de Los Valles). Historic channel deposits can often be recognized by the presence of exotic clasts such as quartzites and granitic rocks, foreign to these watersheds and imported from quarries closer to the Rio Grande (presumably for use as road gravel, etc.). Floodplain deposits include variable percentages of coarse to fine sand, silt, and pumice fragments, and are often well-mixed due to bioturbation.

Stratigraphy and Age. The alluvium in this stream bank records at least 2 episodes of channel aggradation since 3 ka (Fig. 1-10). Radiocarbon dates of ca. 2.8 and 1.4 ka have been obtained from disseminated charcoal fragments within the two aggradational packages. An intervening bioturbated, sandy floodplain deposit (partially eroded) with distinct oxidized bands yielded a date of ca. 1.6 ^{14}C ka, supporting subsequent aggradation at ca. 1.4-1.6 ka. The genesis of the oxidized bands is presumed to be related to water infiltrating below the post-1.6 ka channel.

Although the presence or absence of general synchroneity between channel aggradation and degradation events in different canyons on the Pajarito Plateau is not certain, it is notable that the 2 channel sediment packages present here have ^{14}C dates similar to those obtained in other canyons. The age of specific Holocene aggradation events will be discussed further at other stops (Stops 1-5, 2-3).

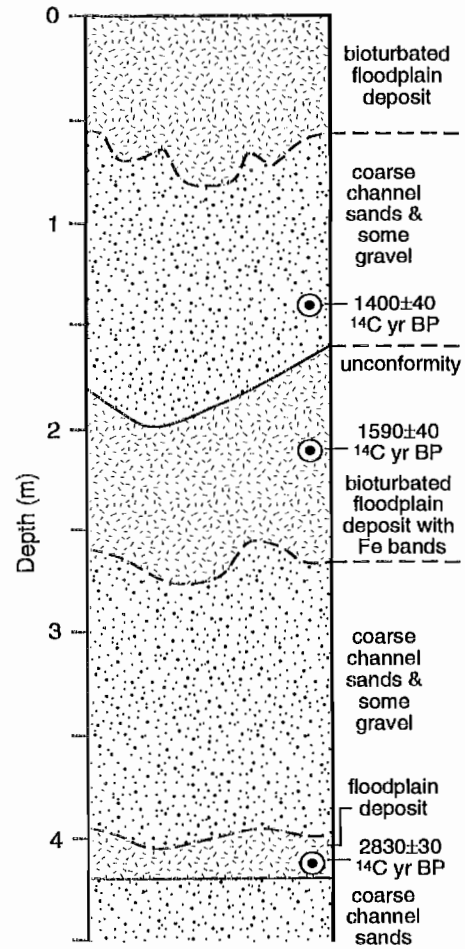

Fig. 1-10. Stratigraphic section of Holocene sediments in Sandia Canyon stream bank at Stop 1-2b, showing location of radiocarbon dates on disseminated charcoal fragments.

Soil-Stratigraphy of Profile SC-2. The SC-2 soil (Fig. 1-11; Table 1-1) is a good example of soils formed in late Holocene stream alluvium along canyon bottoms on the Plateau. The A horizons (A1, A2) extend down to 17 cm and have dark grayish brown colors indicating a weak accumulation of disseminated organic matter within the soil matrix. B horizon development largely consists of the formation of weak soil structure with little change in color relative to the soil parent material. The thin Bw horizon (17-30 cm in depth) has weak prismatic structure that parts to weak subangular blocky structure. The BC horizon has weak subangular blocky structure in places, but is largely single grain. Soil textures range from loam to sand and represent initial sedimentary textures. Abundant krotovinas and large soil-filled insect burrows indicate that thorough bioturbation has occurred throughout the horizon. Thin (2-8 cm) lenses or layers of oxidized soil or sediment with slightly higher chroma occur at 210-260 cm. These layers occur in a bioturbated zone that is interpreted to reflect a buried, partially scoured, floodplain deposit.

- Return to vehicles.

2.5 Continue 100 m to west and make a U-turn where west-bound lane divides. Watch for traffic. Retrace route to State Road 4.

4.9 **Stoplight, State Road 4.** Turn right.

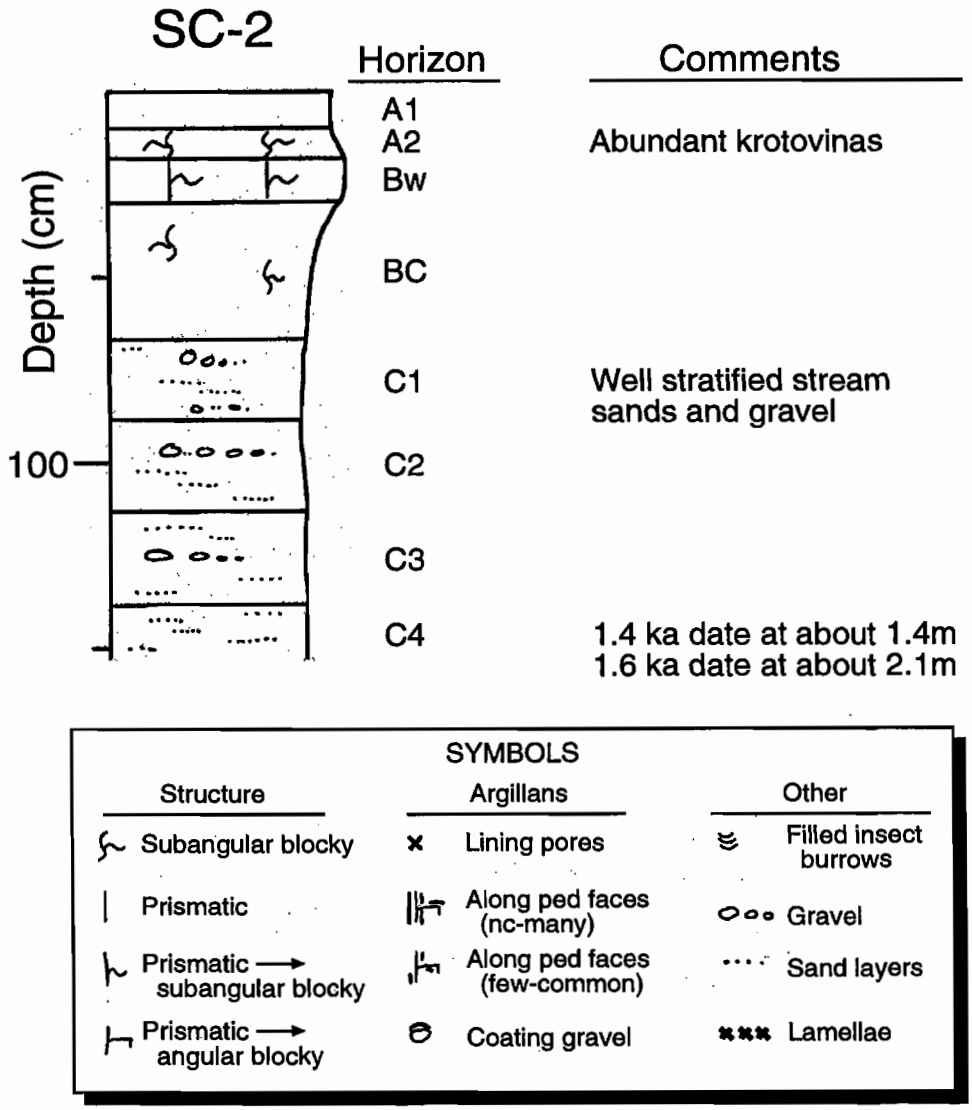

Fig. 1-11. Schematic diagram of soil-stratigraphy for profile SC-2, at Stop 1-2b. Symbols are same as in Fig. 1-9.

5.2 Channel of Sandia Canyon, 3 km upstream of knickpoint in basalt.

5.5 Roadcuts expose salmon-colored tuff of Qbt-1g, with glassy pumice protruding from the tuff. Bench is at base of Qbt-1v. For the next 2 miles State Road 4 is bordered by lands of San Ildefonso Pueblo, closed to the public.

5.6 Dirt road to right into Mortandad Canyon. San Ildefonso Pueblo land.

6.3 Mortandad Canyon channel. "Mortandad" means "massacre" in Spanish, and it is not recorded how this canyon came to be so named. In Adolf Bandelier's fictional account of prehistoric life on the Pajarito Plateau, "The Delight Makers" (1890), he has warriors from Puye ambushing and massacring a Frijoles Canyon (Tyuonyi) war party in a preemptive strike somewhere between the two pueblos, suggesting one possibility for the origin of this name. Upstream of San Ildefonso land, the Laboratory has discharged effluent from a liquid radioactive waste treatment facility since ~1960. The effluent soaks into an exceptionally thick section of alluvium (up to 21 m of

alluvium reported in one drill hole; Baltz et al., 1963), creating a perched alluvial aquifer that in turn allows infiltration into the underlying tuff. Tritium has been detected as deep as 60 m below the top of the tuff, although other radioactive contaminants have not been detected deeper than 3 m into the tuff (Stoker et al., 1991). Water contents near saturation have been reported in beds of the Cerro Toledo interval, between the Tshirege and Otowi Members and 19 m below the base of the alluvium, indicating the hydrologic significance of this unit.

7.2 Gap in low mesas at drainage divide between Mortandad Canyon and Cañada del Buey. The Bandelier Tuff is only ~25 m thick in this area, where the Tshirege ignimbrite was deposited on the flank of a pre-Bandelier paleotopographic high underlain by late Pliocene basalts.

7.7 **Rover Blvd., White Rock**. Turn left into metropolitan hub of White Rock. Street is named for Project Rover, which was active from 1955 to 1972 and at its peak was LANL's second largest program. Rover was a collaboration between the Laboratory and NASA that was initiated to launch large payloads into deep space. The technology involved passing hydrogen through a very high temperature nuclear reactor, where it expanded and blasted out of the reactor at high velocity (Los Alamos News Bulletin, 1995).

7.8 **Meadow Lane.** Turn left after fire station. 25 MPH speed limit (Note: Los Alamos police treat speed limits very seriously).

8.3 Chamisa Elementary School on right.

8.7 **Overlook Road**. Turn left into Overlook Park.

9.0 **Overlook Sports Complex, Concession Stand**, rest rooms. Turn right immediately after buildings into parking lot. Excellent examples of columnar tuff (Qbt-1v and Qbt-2) are visible across drainage of Cañada del Buey to north. **Lunch Stop.**

Stop 1-3. White Rock Canyon.

- Walk southeast between ball fields, following trails for ~350 m through piñon-juniper woodland to large open area adjacent to west rim of White Rock Canyon. Basal contact of non-welded Tshirege Member of Bandelier Tuff (Qbt-1g), overlying basalt, passed on route. Lunch on canyon rim.

Station 1-3a. Rim of White Rock Canyon (6260', 1910 m elev.)

Geologic Setting. The rim of White Rock Canyon is composed of basaltic rocks of the late Pliocene Cerros del Rio volcanic field. Vents of the Cerros del Rio visible from here include Montoso Peak, on the skyline to the south, and La Mesita on Buckman Mesa, a prominent cone to the northeast (Fig. 1-12). The Sangre de Cristo Mountains fill the eastern skyline, including the Santa Fe Range immediately to the east and the Taos Range to the northeast.

The canyon is 1.8-2.5 km wide in this area, and about 250 m deep. Most the canyon here is occupied by massive Pleistocene landslides, generally rotational slumps that have backtilted the capping basalts 30-70°. At this location, the highest rock unit is a vesicular tholeiitic flow (Tcb3 of Dethier, 1996) that was probably derived from a vent 1.4 km west, just west of White Rock. A K-Ar age of 1.8 ± 0.2 Ma was

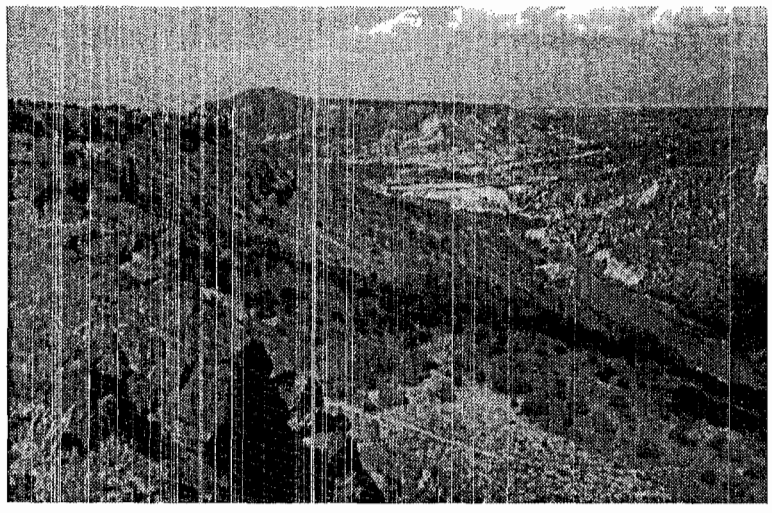

Fig. 1-12. Photograph of White Rock Canyon from Stop 1-3a. View upriver past mouth of Cañada Ancha to Buckman Mesa and cone of La Mesita. Low relief area to right of Buckman Mesa is underlain by Miocene sediments of the Santa Fe Group. Light-colored bluffs above river, in front of south (right) end of Buckman Mesa, display 30 m of late Pleistocene lacustrine sediments overlying Rio Grande gravels. Blue Dot Trail (see Day 0 log) is visible in foreground crossing sagebrush-covered flat on back edge of large slump block.

obtained from this flow to the north (Dethier, 1996), although a more recent $^{40}Ar/^{39}Ar$ analysis of 2.46 ± 0.02 Ma is considered more accurate, and is consistent with other ages of 2.3-2.5 Ma for tholeiitic basalts west of White Rock Canyon (Woldegabriel et al., 1996). The Cerros del Rio volcanic field includes rocks that range in composition from basalt to hawaiite to andesites, erupted from numerous vents. Of particular note are phreatomagmatic deposits associated with many separate maar volcanoes, generated from the interaction of magma and shallow groundwater near the late Pliocene Rio Grande (Aubele, 1978; Dethier, 1996; Heiken et al., 1996).

Rio Grande History. The elevation of the Rio Grande has fluctuated greatly in this area in the Pliocene and the Quaternary (Fig. 1-13; Reneau and Dethier, 1996b). After the peak of Miocene aggradation represented by the rift-filling Santa Fe Group, the Rio Grande incised at least 250 m. This was followed by at least 300 m of late Pliocene aggradation associated with eruptions of the Cerros del Rio lavas, which apparently effectively blocked the Rio Grande valley. The river subsequently incised a narrow canyon up to 180 m deep into the Cerros del Rio rocks, which was then filled by the Bandelier Tuff. To the south of this stop, downriver and across the canyon, a prominent outcrop of the Tshirege Member of the Bandelier Tuff, about 100 m thick, plugs an early Pleistocene Rio Grande meander bend, and the tuff is underlain by quartzite-rich cobbles like those present at this stop. The Rio Grande was dammed by the Tshirege Member about 9 km downriver near Chaquehui Canyon, and the highest level of the resultant lake would have been about 55 m higher than the rim at this stop (Fig. 8 in Introduction). Total lake length is estimated at about 75 km. The spillway for the lake was about 2 km east of the former channel, forcing the Rio Grande to cut through 200 m of basaltic rocks to reach its former grade and probably producing a major knickpoint on the river that controlled base level far upriver, including the part of the Pajarito Plateau visited on this field trip (Reneau and Dethier, 1996b).

The basalt at this stop is covered with quartzite-rich cobbles, similar to those transported by the modern Rio Grande, that were probably deposited when the river was slowly incising through the

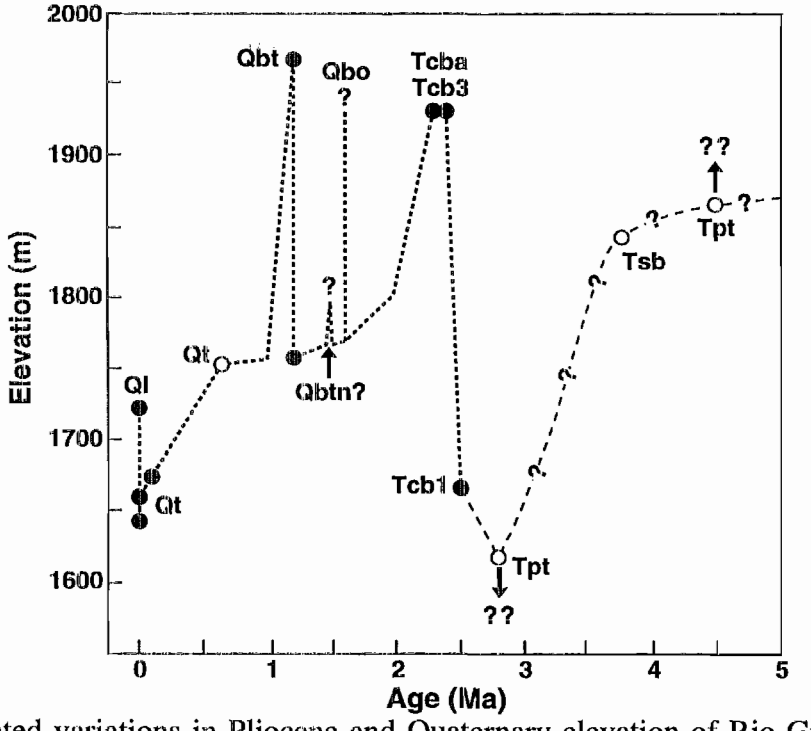

Fig. 1-13. Estimated variations in Pliocene and Quaternary elevation of Rio Grande in vicinity of White Rock Canyon, shown for the reach from Water Canyon to Chaquehui Canyon. Filled circles indicate age and/or elevation control in White Rock Canyon, and open circles indicate data from elsewhere in the vicinity. Qt indicates Rio Grande terraces, and Ql indicates highest late Pleistocene landslide-dammed lake. See Reneau and Dethier (1996b) for more details.

post-Tshirege basalt knickpoint (Reneau and Dethier, 1996b). These gravels have been previously referred to as "a stratigraphic enigma" by Gonzalez and Dethier (1991, p. 35), who were uncertain as to their age and significance. Later, Gonzalez (1993, p. 74-75) reported that they underlay the 1.61 Ma Guaje Pumice Bed. However, just north of here, at Station 1-3b, these Rio gravels overlie the lowermost Tshirege Member, demonstrating an age of ≤ 1.22 Ma.

Landslides and Landslide-Dammed Lakes. The slumps in White Rock Canyon have probably been active for about the last 0.5 Ma, and most of the large landslides are overlain by the El Cajete pumice, indicating an age of >50-60 ka (Reneau et al., 1995a). Periodic reactivation of these slumps has caused repeated damming of the Rio Grande during wetter periods in the late Pleistocene, recorded by widespread lacustrine deposits (Dethier and Reneau, 1996; Reneau and Dethier, 1996a). To the northeast, immediately downriver from the mouth of Cañada Ancha, the eroding bluffs expose 30 m of lacustrine sediment that overlie late Pleistocene Rio Grande deposits (Fig. 1-14). These lacustrine deposits have an estimated age of 40-70 ka, and the lake was probably about 25 km long, stretching upriver to the vicinity of Española.

Closer to the Rio Grande, within about 25 m of modern grade along this part of White Rock Canyon, are deposits of several smaller and younger lakes, 12.4-13.7 ka in age, that are overlain by late Pleistocene river terraces. The dama were produced by repeated failure of the toe of a large slump complex southwest of the mouth of Water Canyon, out of sight downriver. The slides were probably triggered by a combination of accelerated incision and lateral erosion by the Rio Grande during periods of higher flood discharges than today, and by higher water levels resulting from enhanced infiltration onto the slumps and higher discharge from the deep aquifer beneath the Pajarito Plateau. (See further discussion in Day 0 log.)

The abundant evidence for latest Pleistocene landscape change in White Rock Canyon, along a river that heads in distant glaciated mountains, is in striking contrast to the apparent scarcity of alluvial deposits from this period on the Pajarito Plateau. Similarly, available data indicate that the Rio Grande was relatively complacent in the Holocene (Fig. 0-10), at a time when streams of the Pajarito Plateau were experiencing major changes. These contrasts are discussed more at other stops on this field trip (particularly Stop 2-3).

- Walk ~200 m north on trails parallel to the canyon rim to dissected exposures of white tuff.

Station 1-3b. Early Pleistocene Rio Grande Terrace

The quartzite-rich gravels that cover the basalt at Stop 1-3a overlie the basal Tshirege Member of the Bandelier Tuff (Qbt-1g) in this area (Fig. 1-15), indicating that these gravels record remnants of a post-Bandelier Rio Grande terrace. The terrace is ~100 m above the pre-Tshirege river channel and ~55 m below the uppermost level of the tuff-dammed lake (Fig. 8, in Introduction), and was probably formed as the early Pleistocene Rio Grande slowly cut a new channel through Cerros del Rio basaltic rocks downriver at ≤ 1.22 Ma. Similar, possibly correlative deposits occur at the same elevation across White Rock Canyon at the northwest end of Sagebrush Flats, suggesting an early Pleistocene braid plain >2 km in width.

- Return to parking area, and retrace route to State Road 4.

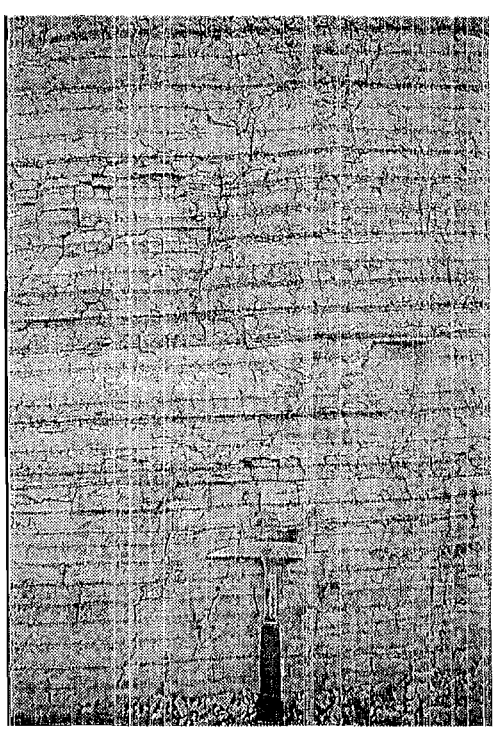

Fig. 1-14. Photograph of well-laminated silt and clay rich lacustrine sediments exposed in bluffs south of Cañada Ancha, 1.8 km northeast of Stop 1-3. Charcoal collected from basal sediments provided a possibly finite radiocarbon age of 43.2 ka.

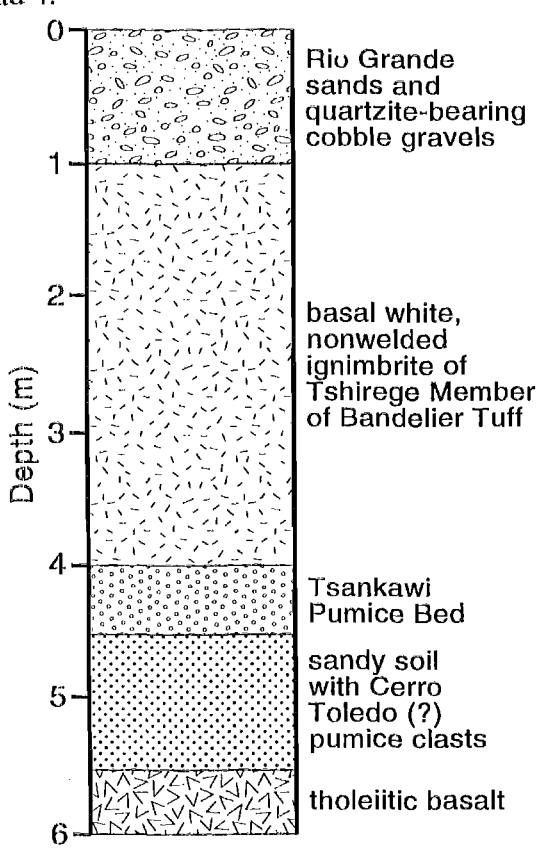

Fig. 1-15. Stratigraphic section near the White Rock Overlook at Stop 1-3b, showing early Pleistocene Rio Grande fluvial deposits overlying the Tshirege Member of the Bandelier Tuff.

9.4 **Meadow Lane**. Turn right at stop sign.

10.3 **Rover Blvd**. Turn right at stop sign.

10.4 **State Road 4**. Turn left at stop sign.

10.5 White Rock Visitor Center to right and Bandelier Inn to left. Cliffs behind Visitor Center expose Qbt-2 directly overlying Qbt-1g. Flow units comprising Qbt-1v pinch out immediately to the west on flank of pre-Bandelier basaltic high.

10.7 Sherwood Drive to left. Smith's grocery store and O'Henry's restaurant. Cañada del Buey channel to right, with stream gauge installed by USGS ~1994 (on land posted with DOE "No Trespassing" signs). Street is named for Project Sherwood, a national program in the 1950s to achieve magnetic fusion energy. The contribution of Los Alamos to this project included achieving the first controlled thermonuclear plasma in 1957. One device used at Los Alamos in Project Sherwood was called the Perhapsatron, which, according to local legend, got its name because "perhaps it would work and perhaps it wouldn't" (Los Alamos News Bulletin, 1995).

11.3 Stop light: go straight. Intersection of SR 4 and Pajarito Road to right and Grand Canyon to left. 7 mi to Los Alamos on Pajarito Road, through LANL. The Tshirege ruins, one of the largest ruins on the Pajarito Plateau, are located north of Pajarito Road for the next 0.6 miles, including both extensive cavate ruins along the base of the low cliff and a large pueblo ruin on the mesa top (a saltbush-covered mound visible a short distance east of the water tanks). (Note: these ruins are located on restricted DOE land). The Tshirege Member of the Bandelier Tuff was named after these ruins by Griggs (1964), and the Pajarito ("little bird") Plateau was also named after this site by the archaeologist Edgar Lee Hewett who conducted excavations here in 1916 (Hewett, 1938). "Tshirege" is a contraction of the Tewa word *Tsirege'onwikeji*, which means "pueblo ruin over at the bird place" (Hoard, 1981).

11.4 Pajarito Canyon stream channel, immediately past roadcut displaying scoriaceous tholeiitic basalt with abundant carbonate coatings. The basalt is related to those at Stop 1-3, and the vent area is exposed about 0.4 km to the southwest, where vertical dikes protrude through scoria (vent is on restricted DOE land). A $^{40}Ar/^{39}Ar$ date of 3.18 ± 0.38 Ma has been obtained from one of the dikes, although this date is older than dates for related flows and is suspect due to a large uncertainty that reflects low radiogenic yield (WoldeGabriel et al., 1996). Pajarito Canyon here is very shallow where the post-Tshirege channel was superimposed on a basalt high (Broxton and Reneau, 1996), although it is one of the main drainages across the Pajarito Plateau, heading 19 km west in the Sierra de los Valles. A perennial alluvial aquifer occurs upstream in Pajarito Canyon, where the alluvium is up to 9 m thick (Purtymun and Kennedy, 1971), although the channel is usually dry here where the alluvium pinches out on basalt. The absence of surface flow here suggests that the shallow groundwater has infiltrated into the bedrock upstream, perhaps into fractures in the basalt.

11.6 Karen Circle to left. For next 0.6 mi SR 4 bordered by "La Senda" and "Pajarito Acres" subdivisions to left and DOE land (marked by "No Trespassing" signs) to right.

12.2 Monte Rey S, on left. South end of Pajarito Acres residential area. For next 4 miles land to east of road is DOE land that is open to the public, and land to west is DOE land that is closed to provide buffer zones for firing sites farther west.

12.3 Roadcut at right exposes Tsankawi pumice bed (0-30 cm thick) at base of Tshirege Member, overlying a thin soil on late Pliocene basalt. The Tshirege Member is ~25 m thick in this area.

12.7 Potrillo Canyon channel. Upstream (on restricted DOE land) are firing sites with names such as "Lower Slobovia", where open-air (non-nuclear) weapons tests have been conducted since the mid-1940s. Depleted uranium (a byproduct of uranium enrichment processes that is depleted in the isotope ^{235}U) is one contaminant that has been widely dispersed near the firing sites. Becker (1991), in a study of uranium transport in this canyon, identified a broad unchanneled part of the canyon with high transmission losses where all surface flows infiltrated during her study (a "discharge sink"). Examination of airphotos dating back to 1935 showed that a channel existed through this reach at least until 1965, illustrating the dynamic nature of these canyon bottoms and documenting a historic aggradation event.

12.9 "Gate 9" to left, at dirt road down Fence Canyon.

13.1 **Stop 1-4: Fence Canyon**. Turn left into large parking area. Trail begins at "Gate 8A" at southeast end of parking lot (Fig. 1-16). This stop involves ~1.5 miles of hiking and a 100' climb, and we will be away from the vehicles for 2-3 hours. Bring water.

- Walk through gate and turn left on trail down Fence Canyon for 0.5 km. At dirt road along powerline, turn right and follow road 0.5 km to mesa top (Fig. 1-16). This powerline corridor was planned to be the route of a major 345 kV transmission line between Abiquiu Dam and Santa Fe (the Ojo Line Extension, or OLE). OLE received significant public opposition, particularly because it was to traverse a fairly wild part of the Jemez Mountains. After many attempts to proceed with this project over many years, it seems to have finally died. An extensive report on archaeological investigations conducted along the OLE corridor is presented in Acklen (1993), including sites on this part of the Pajarito Plateau.

- At junction with dirt road to right, leave road and head straight down slope to right into shallow mesa-top drainage basin. Stop 1-4a is in highly eroded and dissected area across drainage channel.

Station 1-4a. Historic erosion and vegetation changes on eastern Pajarito Plateau.

This stop is typical of many parts of the eastern Pajarito Plateau which are presently experiencing extremely rapid rates of erosion (Fig. 1-17). Vegetation cover is sparse and bare ground is widespread, including both dissected late Quaternary deposits and exposed tuff bedrock. Many juniper trees are perched on pedestals several decimeters in height, their roots exposed and subject to toppling.

The high erosion rates on the eastern Plateau are of particular concern to resource personnel at Bandelier National Monument because of ongoing damage to archaeological sites. For example, at a small monitored mesa-top drainage basin near the Frijolito ruins (Wilcox et al., 1996a, 1996b), about 1 liter of potsherds and lithic fragments such as chert and obsidian were collected from sediments deposited at a single 1 m^3 sediment trap during one summer runoff event in 1995. The historic erosion in the Frijolito area is believed to have been influenced by a major drought in the 1950s which resulted in

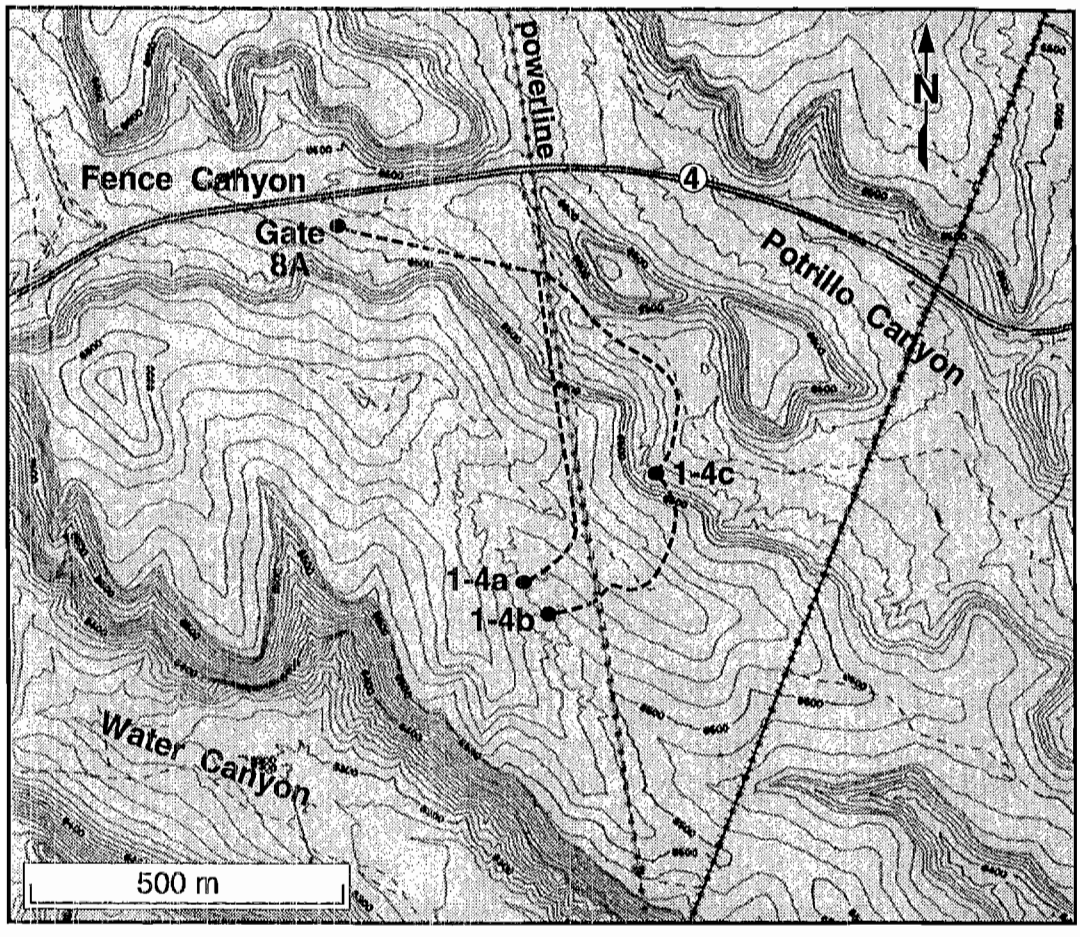

Fig. 1-16. Topographic map of Fence Canyon area, Stop 1-4. Base from FIMAD, with 10-ft contour interval.

dramatic vegetation changes. Ponderosa pine trees near their eastern mesa-top limit were stressed by the drought and suffered widespread die-off (associated with a bark beetle infestation), and the ponderosa ecotone almost instantaneously retreated as much as 2 km upslope to the west (Allen, 1989; Allen and Breshears, 1995). Erosion in the piñon-juniper woodlands of the Plateau is presently highest in intercanopy areas with minimal ground cover (Wilcox, 1994; Wilcox et al., 1996a, 1996b), and past decreases in groundcover resulting from variations in climate (e.g., the 1950s drought) or other causes are thus likely to have affected erosion rates.

Although the erosion presently occurring on the eastern Plateau may have been aided by the 1950s drought, the drought can not be entirely to blame because 1935 airphotos reveal that many sites, including this stop, were already deeply dissected at that time. The time that the present cycle of erosion was initiated is not known, but erosion may have been affected by land-use changes that began in the late 1800s associated with widespread and intensive sheep and cattle grazing (Allen, 1989). Evidence that grazing was very effective in reducing groundcover on the Pajarito Plateau is provided by a sharp drop in fire frequency that occurred at this time, indicating that fuel, particularly grass, was of insufficient density to allow lightning-caused fires to spread (Allen, 1989; Allen et al., 1995, 1996; see also discussion at Stop 2-1).

It is also worth noting that at least some of the thick, late Quaternary slopewash deposits on the eastern Plateau were also partly dissected and probably eroding prior to the 1600s. This is shown in part by prehistoric check dams visible in gullies in the Cañada del Buey drainage north of the Tshirege ruins.

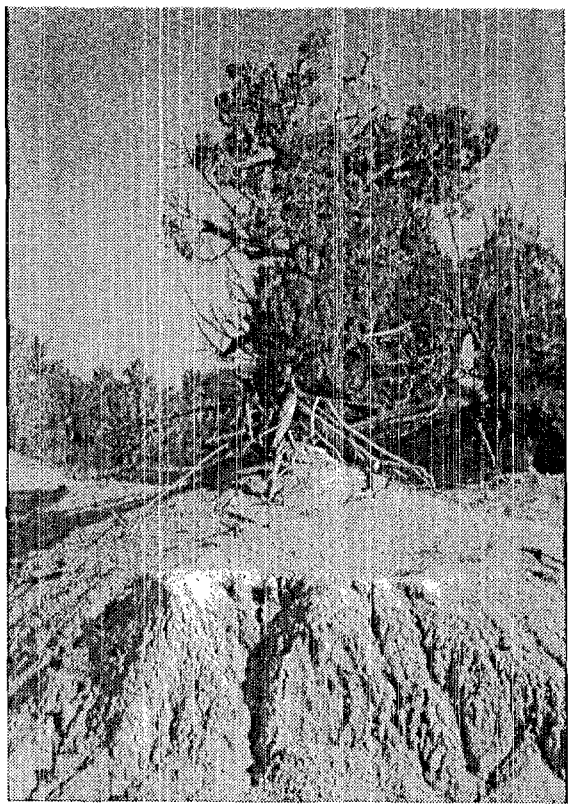

Fig. 1-17. Photographs of eroding late Quaternary deposits in shallow mesa-top basin, south of Fence Canyon at Stop 1-4a. Juniper tree in left photo was rooted in post-El Cajete slopewash deposits; prominent break in slope is top of buried pre-El Cajete soil, with light layer being a buried E horizon. In right photo, bench to left of Eric Von McDonald is a buried soil with an estimated age of ≥ 15 ^{14}C ka, and pre-El Cajete soil forms a lower bench to right.

The importance of land-use changes as opposed to climatic changes and other variables in causing periods of accelerated erosion is an intriguing problem, one that has long been and will continue to be debated throughout the Southwest. Although much remains uncertain, we hope that more detailed studies of historic vegetation changes, climatic variations, and contemporary erosion such as are being conducted on the Pajarito Plateau will allow improved insight into likely controls on prehistoric periods of accelerated erosion (as revealed in the geomorphic record), and also insight into likely future erosion.

- Walk ~60 m east to next low-order drainage channel in eroded terrain, the site of 1996 soil pits.

Station 1-4b. Late Quaternary soils and stratigraphy in mesa-top drainage basin.

The ongoing erosion in this area has provided excellent exposures of late Quaternary deposits similar to those seen at other mesa-top sites on the Pajarito Plateau. Stacked stratigraphic units and multiple buried soils reveal alternating periods of landscape stability and instability, although no evidence has yet been seen for prior episodes of deep dissection similar to what presently exists on this mesa. The thickness of the deposits (up to 4 m) is particularly striking considering the small upslope contributing area, which is only ~100 m long (Fig. 1-18). In addition to reworking of locally weathered tuff, the sediments include reworked El Cajete pumice and probably significant amounts of reworked eolian sediment, although their relative contributions have not yet been quantified.

Stratigraphy and Age. The deposits in this basin include: 1) pre-El Cajete slopewash deposits with a fairly well-developed buried soil; 2) the ca. 50-60 ka El Cajete pumice (largely stripped or heavily bioturbated in many areas); 3) a post-El Cajete, late Pleistocene slopewash deposit that includes 2 buried soils; and 4) Holocene slopewash deposits (Figs. 1-18, 1-19). The ages of these units are not

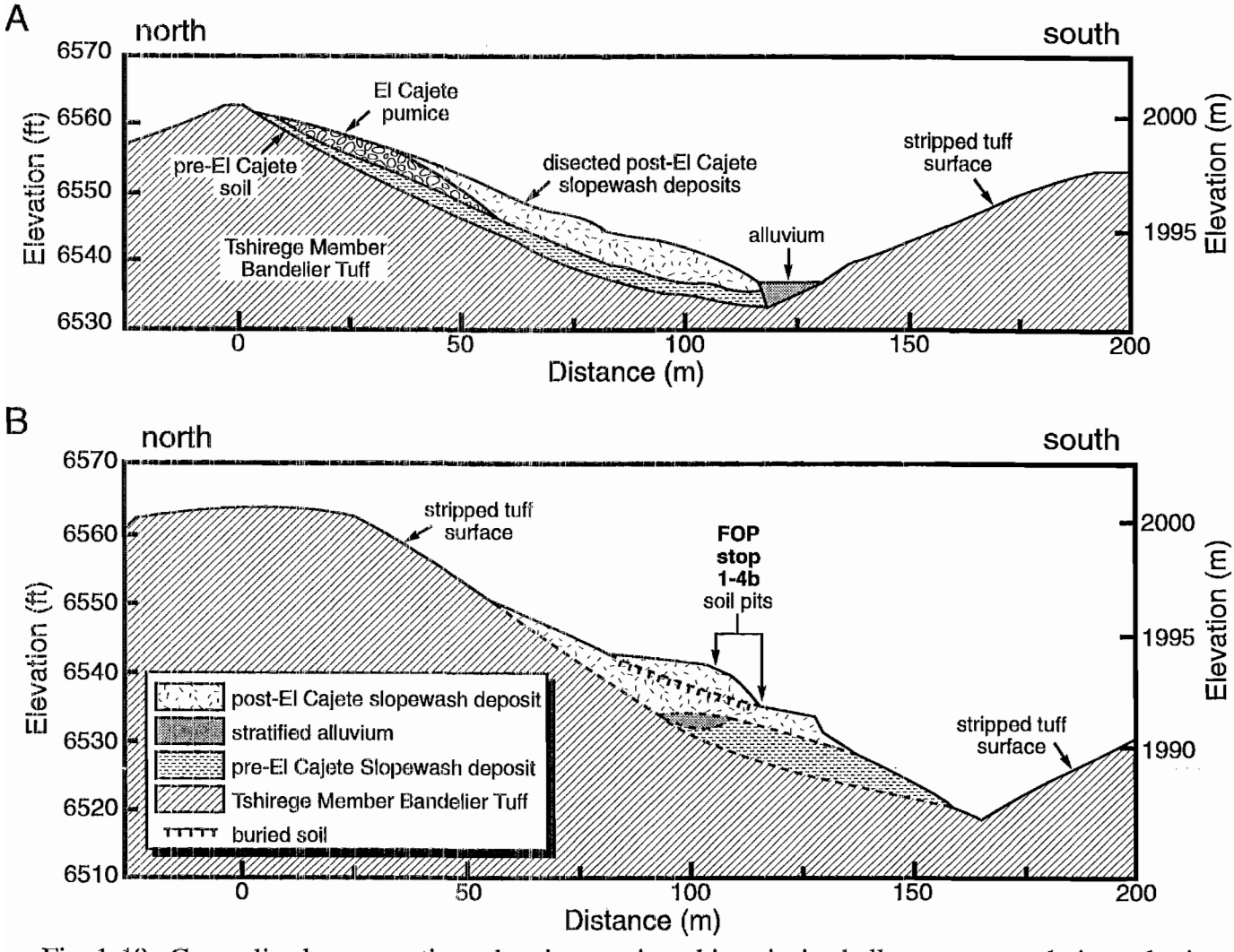

Fig. 1-18. Generalized cross sections showing stratigraphic units in shallow mesa-top drainage basin south of Fence Canyon. A) 100 m northwest of Stop 1-4b, where relatively thick deposits of pure El Cajete pumice are preserved in relatively shallow (local relief = 7.5 m) and gentle headwaters part of basin. B) Stop 1-4b, where more extensive stripping of late Quaternary deposits has occurred in a steeper part of the basin with greater relief (14 m).

well constrained, with the exception of the El Cajete pumice. The best age estimates are provided by the degree of soil development, discussed below, and by correlation with other dated deposits in the area.

Deposits in this basin were previously studied by McFaul and Doering (1993) as part of geoarchaeologic investigations for the OLE powerline. They recognized up to three buried soils in this area (site LA 6787A) and in similar deposits on a nearby mesa (site LA 82601), and used radiocarbon analyses on the humate fraction of buried soils to provide minimum-limiting age estimates for underlying units. A buried soil on this mesa at a depth of 1.55-2.07 m yielded a humate date of 15,960 ± 190 ^{14}C yr B.P., very similar to a humate date of 15,660 ± 170 ^{14}C yr B.P. from a correlative soil on the mesa south of Water Canyon. An overlying buried soil south of Water Canyon yielded a humate date of 9480 ± 80 ^{14}C yr B.P. Although these analyses do not provide precise age control for the mesa-top deposits in this area (discussed below), they do support a late Pleistocene age for the lower part of the post-El Cajete slopewash deposits.

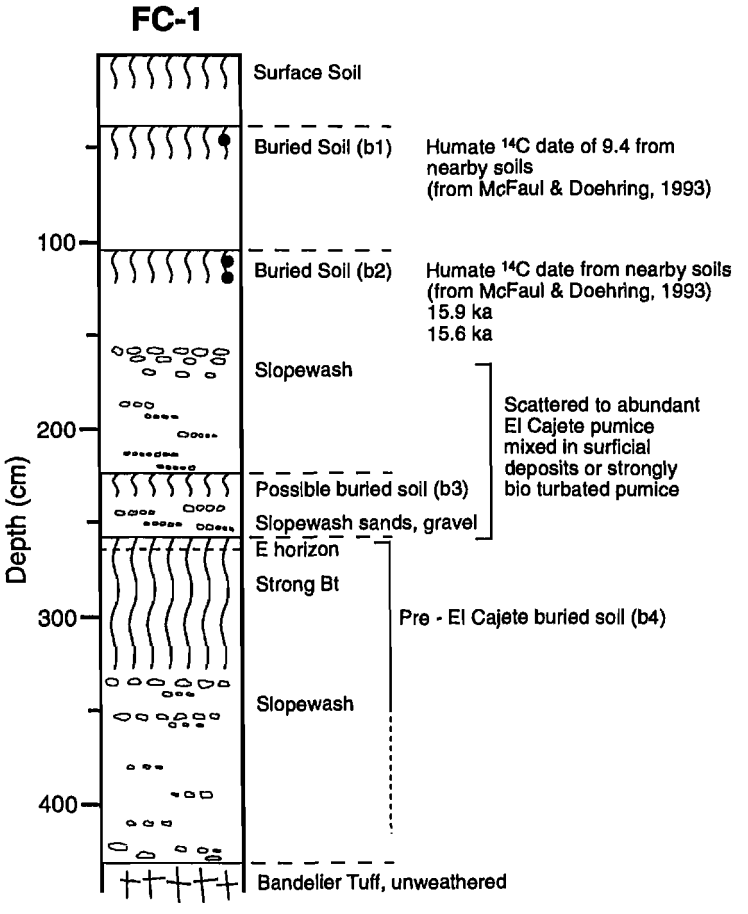

Fig. 1-19 . Composite diagram showing stratigraphy at profile FC-1 at Stop 1-4b, combining data from 3 soil pits.

Soil-Stratigraphy of Profile FC-1. The soil-stratigraphy at this stop consists of a 4.3 m thick complex of buried soils that pre- and post-date deposition of the ca. 50-60 ka El Cajete pumice (Figs. 1-18, 1-19, 1-20; Table 1-2). The soil-stratigraphy exposed here is generally similar to the typical soil-stratigraphy found at many localities on the Pajarito Plateau mesa tops, especially farther west and at slightly higher elevations.

Surface Soil. The surface soil consists of an A-BA-Bw horizon sequence. The A and BA horizons are light colored, indicating minimal accumulation of disseminated organic matter, and have weak to moderate crumbly to subangular blocky structure. The Bw horizon has prismatic structure that parts to subangular blocky structure and 7.5 YR color hues. Abundant evidence of bioturbation, including root channels, earthworm fecal pellets, and filled insect burrows are visible throughout this soil. A PDI value of 12.1 was calculated for this soil, suggesting an age of ca. 4.9 ka for the end of the most recent episode of slopewash deposition here.

Buried Soil (b1). The first buried soil sequence (b1) is a weakly developed soil consisting of a AB-Bw-BC horizon sequence. The top of the soil is denoted by a noticeable change in color (7.5YR 5.5/6 to 10YR 5/3) due to the weak accumulation of disseminated organic matter. Although the surface soil is partly superimposed over this buried soil, the increase in organic matter suggests that this weakly developed soil has been buried by younger slopewash colluvium, with likely contributions of primary or reworked eolian sediment. Soil structure largely consists of weak subangular blocky grading to

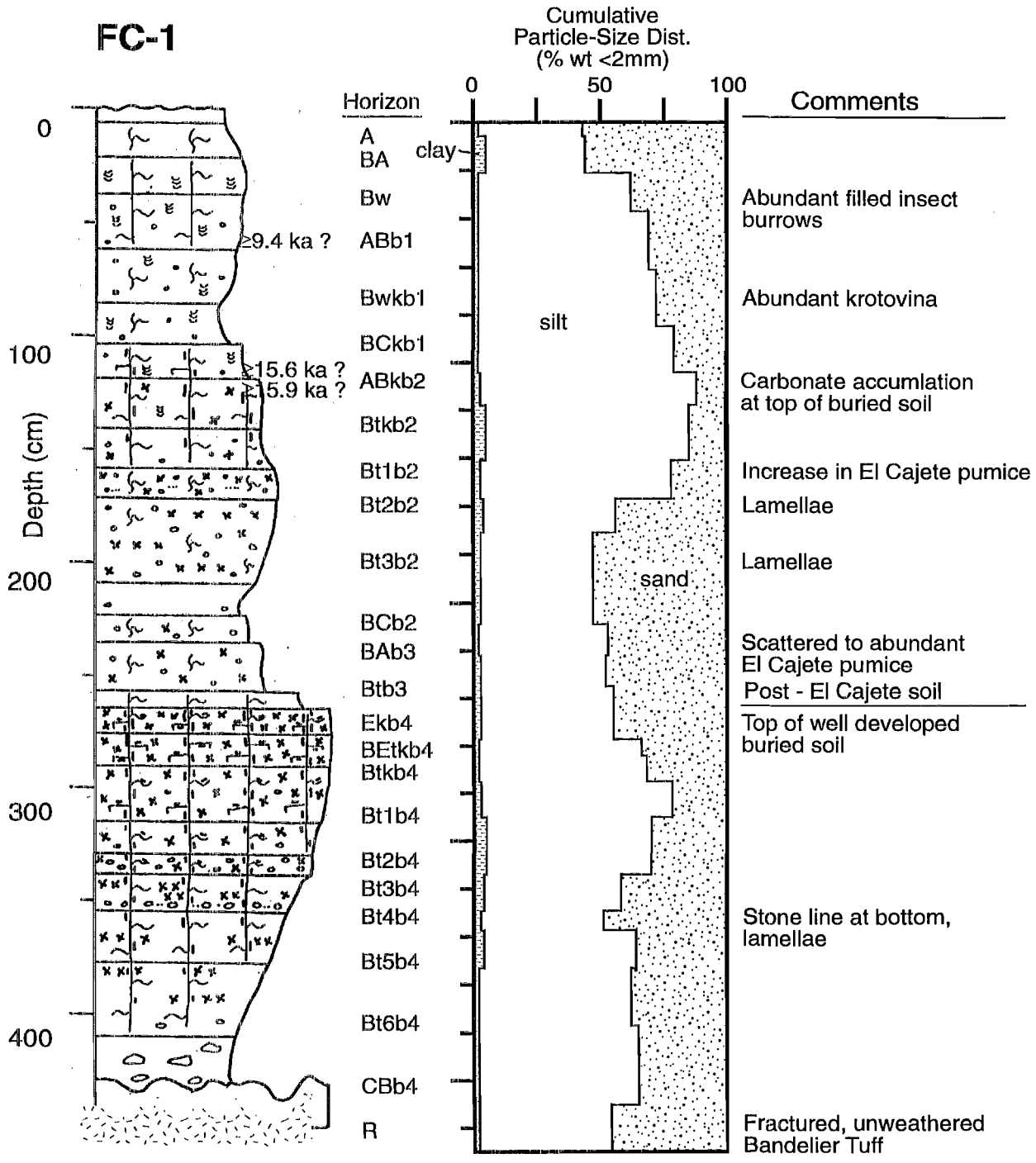

Fig. 1-20. Schematic diagram of soil-stratigraphy for profile FC-1 at Stop 1-4b. ^{14}C humate dates from McFaul and Doering (1993) are shown at approximate correlative depths.

massive in places. Development of structure is largely associated with abundant large (1-2 cm dia.) filled insect burrows. Abundant krotovinas also occur throughout this buried soil sequence. Stage I to II carbonates, consisting of thin, discontinuous coatings of carbonate and disseminated carbonate, occur in the Bwkb1 and BCkb1 horizons. Humate from a similar soil sequence 1.2 km to the south yielded a ^{14}C date of 9480 ± 80 yr B.P. (2Ab>Bkb horizon, LA 82601 - Profile 1 of McFaul and Doering, 1993), consistent with the mid-Holocene PDI-based age estimate for the overlying unit at this site. Although the horizon sampled by McFaul and Doehring (1993) is deeper than the horizon here (78-106 cm vs. 38-61 cm), the soil-stratigraphic position appears to be similar. However, any age correlation between these sites should be considered tentative.

Buried Soil (b2). The second buried soil (b2) consists of several moderately developed Bt horizons. This buried soil locally forms an intermediate bench (Fig. 1-17) and can also be recognized throughout the gullied landscape by a subtle increase in color (7.5 YR vs. 10 YR of overlying buried soil). This soil contains scattered El Cajete pumice clasts and in places overlies highly bioturbated deposits of this pumice.

The top of this buried soil is highly eroded and truncated due to bioturbation, evidenced by the abundant krotovinas and animal burrows seen throughout the local area. Where best preserved, the former top of this soil (ABkb2, Fig. 1-20) is seen as an increase in soil color hue to 7.5YR from 10 YR, an increase in strong to moderate, medium and fine, blocky structure, and Stage I-II carbonates that consist of filamentous coatings along ped faces. The accumulation of carbonates is greatest at the top of the horizon and systematically decreases downward, a relation that suggests that the accumulation of carbonates has been influenced by changes in texture and porosity associated with the top of this buried soil.

The dominant feature of this buried soil is a series of moderately developed Bt horizons. The Btkb2 and Bt1b2 have weak to moderate prismatic and subangular blocky structure, 7.5 YR color hues, and thin patchy argillans along ped faces and pores. A silt-loam texture and the limited amount of tuff fragments in the ABkb2, Btkb2, and Bt1b2 horizons suggests that eolian sediment may have also contributed to the soil parent material for these horizons. By comparison, the underlying Bt2b2, Bt3b2, and BCb2 horizons have formed in well sorted and stratified sandy-pebble slopewash, largely derived from eroded Bandelier Tuff and probably pre-existing soils upslope. The Bt2b2 and Bt3b2 horizons have weak subangular blocky structure. Argillans in the Bt2b2 horizon consist of nearly continuous to patchy coatings on gravel, clay bridges, and pore linings. Argillans in the Bt3b2 horizon are largely segregated into lamellae consisting of nearly continuous to patchy clay bridges and pore linings, whereas, argillans in the surrounding soil consist only of patchy clay bridges and pore linings. In all Bt horizons in this buried soil, clay accumulation is probably due to the illuviation of primary clay from either the original surficial sediments or eolian contributions of clay from dust rather than from *in situ* formation of secondary clay minerals.

A PDI value of 21.5 was calculated for the overlying soils, suggesting that soil b2 was buried at ca. 11.5 ka or earlier. Possible additional age control for burial of this soil can be extrapolated from the radiocarbon dating of buried soils reported in McFaul and Doering, (1993), although any age correlations between these sites should be considered tentative. Humate from a similar buried soil sequence 1.2 km to the south and from this gullied mesa top yielded two ^{14}C dates of 15,660 ± 170 and 15,960 ± 190 yr B.P. (3Ab horizon, LA 82601 - Profile 1, 3Acumb, LA 6787A - Profile 1 of McFaul and Doering, 1993). Although the depth of the dated horizons is deeper than the horizon here (143-161 and 155-207 cm vs. 104-118 cm), the soil-stratigraphic position appears to be similar. For example, at the two sites of McFaul and Doering, the dates came from the upper horizon of the uppermost buried soil sequence that consists of a moderately developed Bt horizon with 7.5 YR color hues, consistent with the soil descriptions here.

Buried Soil (b3). A third buried soil (BAb3, Btb3, Fig. 1-20) also contains scattered El Cajete pumice and appears to be a thin soil preserved at the base of the post-El Cajete pumice soil sequence. The BAb3 horizon has finer soil structure relative to overlying Bt horizons, consisting of weak to moderate, medium to fine subangular blocky structure and an increase in the abundance of fine and very fine pores. The underlying Btb3 has a sharp increase in argillans relative to the two overlying horizons, with argillans consisting of nearly continuous to patchy coatings along pores and forming clay bridges. Taken together, the above pedologic features suggest that this was a thin soil that post dates deposition of the pumice.

El Cajete Pumice. The ca. 50-60 ka El Cajete pumice stratigraphically lies between the b2 and the b4 buried soils (described below). Only scattered pumice is present within the b2 and b3 soils depicted in Figs. 1-19 and 1-20 and Table 1-2, with the soil parent material largely consisting of slopewash deposits derived from eroded tuff soils. Elsewhere within this gullied landscape, the Abkb2-Btib2 horizons overlie strongly bioturbated El Cajete that makes up the dominant fraction of the soil matrix between the b2 and b4 soils. Elsewhere across the Pajarito Plateau, primary El Cajete pumice conformably overlies soils similar to the underlying b4 soil that is exposed at this stop (e.g., Stops 1-6, 2-2). A PDI value of 65.0 was calculated for the overlying soil (surface to base of b3), yielding an estimated age of ca. 58.7 ka, that is similar to the age estimated for the El Cajete pumice by Toyoda et al. (1995) and Reneau et al. (1996a).

Buried Soil (b4). The buried soil that stratigraphically underlies the El Cajete consists of a sequence of well developed Bt horizons that systematically grade downward to a sharp contact with the underlying and truncated Bandelier Tuff. This buried soil forms a distinct bench within many of the local gullies (Fig. 1-17)..

The uppermost horizon is a light colored (10 YR 7/3) E horizon (Ebkb4) that forms a distinct upper boundary that is easily seen in the local gully exposures. The horizon has prismatic structure that parts to platy and subangular blocky structure and very patchy argillans along ped faces and pores, wwith the clay derived from the overlying soil.

The E horizon on initial observation looks like a thin loess layer (these light colored horizons have informally been attributed to this origin), and probably does contain a fair amount of eolian material. The E horizon at all sites where we have described pre-El Cajete soils on the Plateau, including the buried soil seen here, sharply overlies a silt- and clay-rich Bt horizon. This relation indicates that the formation of the E horizon cannot be solely due to deposition of a thin loess layer that has been serendipitously preserved by burial by the El Cajete pumice. It is highly improbable that a thin layer of loess would be deposited across the landscape and across well developed Bt horizons, which would require the A and other surface horizons to have been completely truncated, exposing the tops of the Bt horizons at the surface. There is no evidence (i.e. buried A horizons, or overlying slopewash deposits) that these Bt horizons have been widely exposed due to surface erosion. Further, if a thin loess layer was deposited, and unless it was soon buried by the overlying El Cajete, then surface bioturbation would have resulted in mixing the loess into the underlying soil. The lower boundary of the E horizon, however, is usually an abrupt or clear boundary that does not indicate active mixing due to bioturbation.

The Bt horizons (BEtk1b4, Btkb4, Bt1b4 - Bt6b4) have well developed structure consisting of strong to moderate prismatic structure that parts to moderate to weak angular and subangular blocky structure. Argillans within the Bt horizons range from nearly continuous to patchy coatings along ped faces, especially prismatic ped faces and pores. Mangans (coatings of MnO_2) also occur as patchy coatings along ped faces and pores in these horizons. Skeletans (bleached sand and silt grains) occur along the prismatic ped faces in the BEtkb4 and Btk1b4 horizons and reflect the strong eluvial pedogenic processes associated with the development of the E horizon. Argillans in the lower 3 Bt

horizons are largely segregated into weakly developed lamellae that are 1 to 3 cm thick. At least two discontinuous thin stone lines, consisting of subangular fragments of tuff 2-15 mm in diameter, can be traced through the Bt4b4 and Bt5b4 horizons. Increases in the development of argillans associated with the abundant coarse fragments in the layers indicate that the stone lines have enhanced the illuvial accumulation of clay in these horizons. Abundant large (1-2 cm) filled insect burrows can be found throughout this buried soil.

The noticeable increase in tuff fragments in the Bt3b4 horizon and below, especially in the two stone lines, indicates that the soil parent material largely consists of slopewash. The silt loam and silty-clay loam textures, the abundant argillans, and the low concentration of gravel (mostly < 5%) in the overlying Bt and E horizons, however, suggest that eolian contributions of silt and clay may have also strongly influenced development of this soil.

The base of the soil consists of largely unaltered surficial sediment that contains subangular fragments of tuff, and that abruptly overlies fractured and unweathered Bandelier Tuff. The top of the tuff has a continuous, thin coating of silt and clay. The nature of the soil contact indicates that the surface consisted of eroded, exposed tuff before subsequent burial by surficial sediment and the formation of the b4 soil, analogous to the tuff surfaces exposed nearby on slopes and in drainages. A PDI value of 63.2 was calculated for the pre-El Cajete soil, suggesting that this soil began forming ca. 56 ky before deposition of the pumice, or at >100 ka.

- Cross main drainage channel and walk up stripped tuff slope to southeast to drainage divide (Fig. 1-16). At divide, walk to right (east) for ~100 m and drop off slope to north into Fence Canyon (spot marked by small pile of concrete debris on left side of trail). Note the widespread exposures of tuff on the divide and on the slopes.

- Halfway into the canyon is a sloping bench developed at the transition between Tshirege Member units Qbt-3 and Qbt-2. At the back edge of this bench are isolated "islands" of El Cajete pumice overlying pre-El Cajete soils in an area dominated by thin and patchy soils over tuff. These "islands" suggest that similar deposits once covered much of this slope, and have been almost entirely removed by erosion.

- Veer left down bench, dropping over short Qbt-2 step and continuing down into large borrow pit in late Quaternary fill in bottom of Fence Canyon (Fig. 1-16). Stop 1-4c is at prominent 5-6 m high north-facing wall.

Station 1-4c. Fence Canyon borrow pit (6460', 1970 m elev.)

This borrow pit provides exceptional exposures of late Quaternary deposits at the base of a north-facing canyon wall (Fig. 1-21). The upper half of the 5.5-m thick section consists of early to mid Holocene slopewash deposits that have yielded dates of 4.5 to 7.8 ^{14}C ka, and the lower half consists of a late Pleistocene colluvial deposit that is ≥ 12.3 ^{14}C ka in age (Fig. 1-22).

A significant sedimentologic change is apparent at the contact between the late Pleistocene and the Holocene deposits. The base of the Holocene section is marked by stratified deposits of coarse sand and pumice that were probably deposited by shallow side-slope channels. Lenses of similar texture are present throughout the Holocene section, but apparently are absent in the underlying late Pleistocene colluvium, suggesting more vigorous surface runoff during deposition of the early to mid Holocene sediments. The relatively rapid deposition between ca. 4 and 8 ^{14}C ka is inferred to record a period of

Fig. 1-21. Photograph of exposure of late Quaternary sediments along south wall of Fence Canyon borrow pit at Stop 1-4c. Deposits had been incised ~4 m prior to excavation of borrow pit. Humboldt alumni for scale.

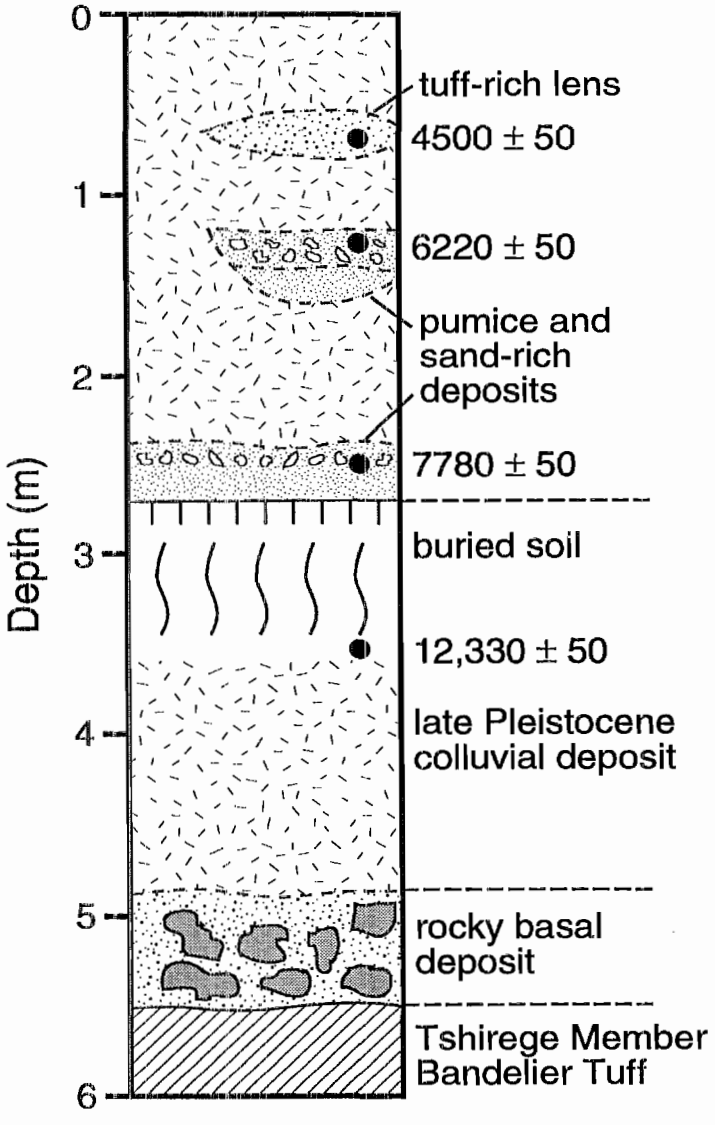

Fig. 1-22. Composite stratigraphic section showing late Quaternary units and radiocarbon dates in south part of Fence Canyon borrow pit at Stop 1-4c.

accelerated erosion on the slopes to the south, perhaps accompanying aggradation of the Fence Canyon channel. Evidence for contemporaneous aggradation of both master stream channels and low-order tributary drainages has been obtained from many other sites on the Pajarito Plateau, discussed by Reneau et al. (1996b) and at other stops on this field trip.

Aggradation ceased and initial dissection of this deposit occurred sometime after 4.5 ^{14}C ka, and side-slope channels had incised about 4 m prior to excavation of the borrow pit. Supporting evidence for the end of aggradation and subsequent incision in this setting is provided by a buried Archaic hearth exposed at another section in Fence Canyon and dated at 4660 ^{14}C yr B.P. (Fig. 1-23). The pre-hearth ground surface was buried by at least 0.65 m of slopewash prior to inception of gullying. Notably, the age estimate for the surface soil at FC-1 (Stop 1-4b) is very similar to the radiocarbon ages of the upper deposits in the borrow pit, suggesting roughly synchronous aggradation and subsequent incision at these two very different landscape positions.

The exact mechanisms responsible for the early to mid Holocene aggradation and the subsequent incision at this site are not certain, but are subjects ripe for speculation. One possible cause for the aggradation is accelerated erosion upslope triggered by an early Holocene increase in summer monsoonal rainfall, perhaps in combination with a decrease in vegetation density that accompanied the Pleistocene-Holocene climatic transition (Reneau et al., 1996b). Incision could have been related to external forces (i.e., Holocene climatic variations), or perhaps was an intrinsic response to changes in the upslope source area. Specifically, it is possible that the stripping of soils and pumice beds and the resultant increase in areal exposure of tuff resulted in both a decrease in sediment supply and an increase in the amount and flashiness of runoff, either of which could have lead to incision at this site (see further discussions of such process-response models for other arid and semi-arid areas by Bull,

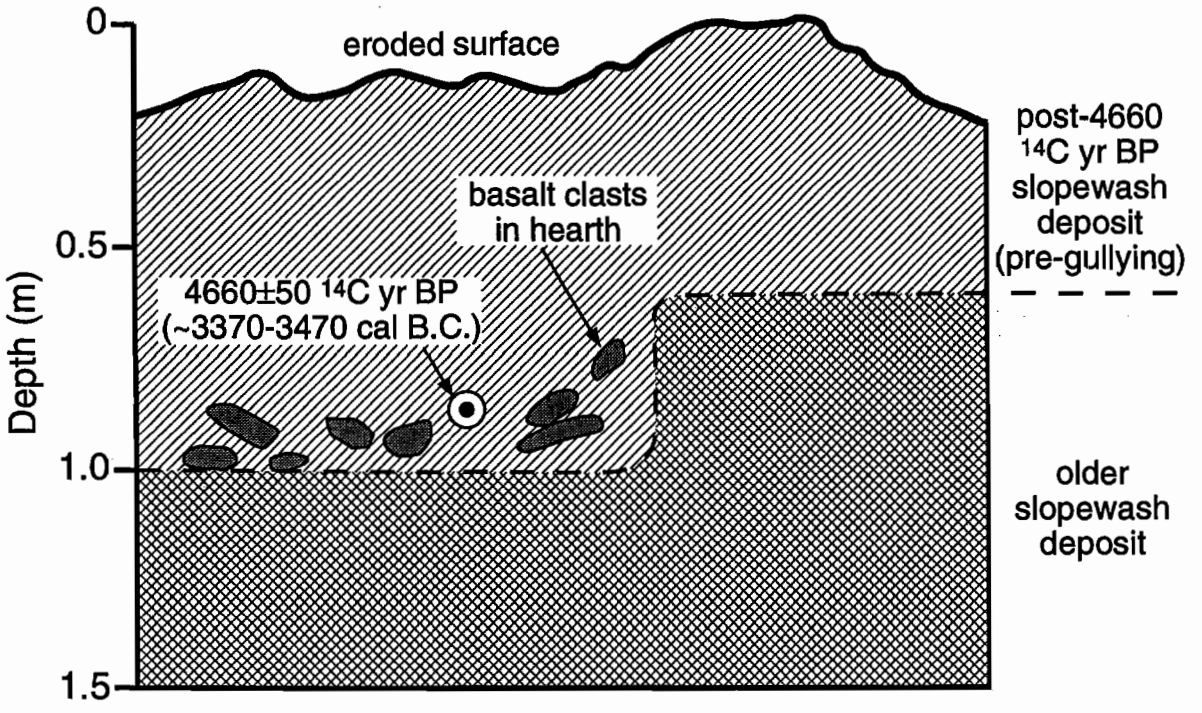

Fig. 1-23. Sketch of Archaic hearth exposed in Fence Canyon, defined by basalt slabs lining bottom of shallow pit, associated with blackened earth. The radiocarbon date is from charcoal fragments intermixed with the basalt clasts.

1991). We believe that incision here was probably not related to local base level changes (i.e., incision of the main Fence Canyon channel), because mid-Holocene terraces have not been recognized here or in other similar low-gradient canyons that head on the Plateau.

- Walk west up Fence Canyon through borrow pit (Fig. 1-16). Slope on left (south) side of pit is exhumed pre-El Cajete colluvial slope, overlain by isolated pockets of the pumice. The soil beneath the pumice appears to be similar to the pre-El Cajete soil seen at Stop 1-4b. To the west, in the center of the pit, the El Cajete pumice is also exposed near the center of the canyon. This indicates that the pre-El Cajete stream channel was located below the bottom of the pit, which is in turn ~2 m below the original pre-pit stream channel.

- Return to parking area, and continue south on SR 4.

13.5 The small drainage to the left follows the exhumed, north-facing margin of a pre-Tshirege canyon in basalt. This paleodrainage is inferred to originate in the modern Los Alamos Canyon headwaters, passing along the southwest side of White Rock basalt high. Dacite-rich gravels of the Cerro Toledo interval are exposed to the southeast within Water Canyon, overlying the Otowi Member, and confirm the location of a paleodrainage (Broxton and Reneau, 1996). The estimated orientation of this pre-Tshirege channel is roughly north-south at this location, contrasting with the roughly southeast orientations of the modern canyons. The tuff was originally at least 75 m thick over the axis of the paleocanyon, contrasting with a thickness of about 40 m over the basalt immediately to the south. "Gate 7" to left leads to a trail down the drainage (open to the public). Dirt road to right, heading up Water Canyon, leads into buffer zones for LANL firing sites and is closed to the public.

13.7 Water Canyon channel. Stream is incised 10 m into a tholeiitic basalt which was presumably derived from buried, yet unrecognized vents to west (Dethier, 1996). The basalt here is dated at 2.39 ± 0.08 $^{40}Ar/^{39}Ar$ Ma, similar to ages for other tholeiitic rocks on the eastern Pajarito Plateau (WoldeGabriel et al., 1996). Dacite gravels on the basalt immediately south of the channel are the remnants of a Water Canyon terrace of unknown age.

13.8 Pocket of El Cajete pumice to right.

14.0 Indio Canyon channel.

14.2 Roadcut to right exposes boundary between Qbt-1v and Qbt-1g ("vapor-phase notch": glassy tuff below; devitrified, vapor-phase altered tuff above).

14.9 Roadcut to right exposes pocket of El Cajete pumice at north end, overlying a thin pre-El Cajete soil, and the exhumed older soil to south (Fig. 1-24). The exhumed soil was sampled here as part of a LANL background soil geochemistry study (Longmire et al., 1996; McDonald et al., 1996a; McFadden et al., 1996; Watt, 1996). The base of the soil includes a $CaCO_3$-rich (Bkm) horizon overlying tuff, and $CaCO_3$ is also deposited along fractures in the uppermost, sub-horizontally sheeted tuff (Qbt-3).

15.1 View of Sandia Mountains, east of Albuquerque, straight ahead to south.

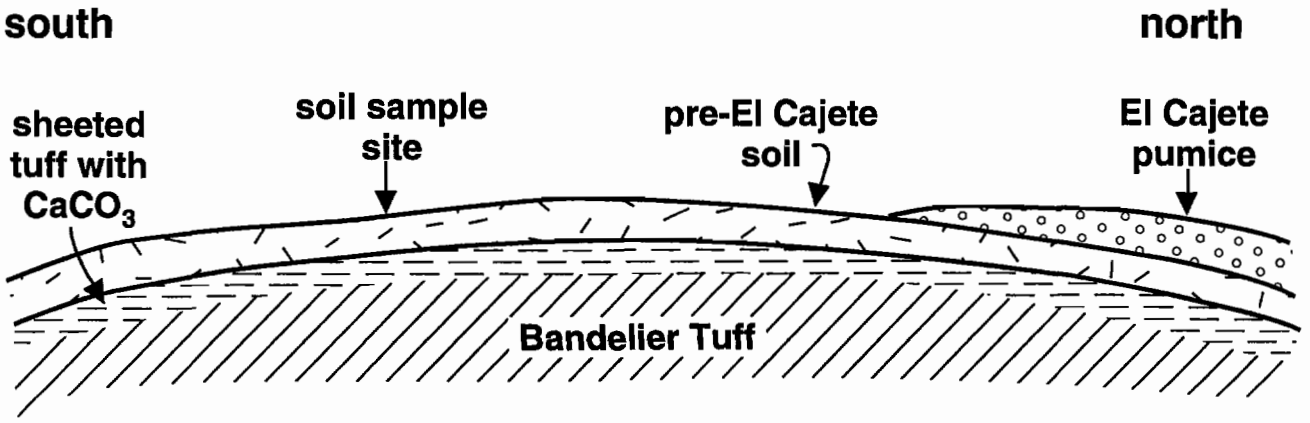

Fig. 1-24. Schematic sketch showing soil-stratigraphic relations on mesa top along State Road 4 at Mile 14.9, between tributaries to Ancho Canyon. Isolated patches of the ca. 50-60 ka El Cajete pumice overlie older, pre-El Cajete soils which have been exhumed after extensive erosion (from Longmire et al., 1996).

15.3 View of Montoso Peak, straight ahead to southeast, one of the larger late Pliocene basaltic vents of the Cerros del Rio volcanic field.

15.6 Begin descent into Ancho Canyon. Roadcut to right exposes contact between Qbt-2 and Qbt-1v, here marked by a pair of thin, crystal-rich volcanic surge beds separated by a thin ignimbrite. The boundary between these two tuff units on the eastern Pajarito Plateau is commonly marked by a series of relatively thin flow units, some pumice-rich, and surge beds, which provide excellent markers for recognizing relatively small-scale fault offsets. The surge beds in this area may represent ash-cloud deposits formed by elutriation from the underlying pyroclastic flows (Fisher, 1979). A small-scale depression between flow units in this roadcut has been interpreted as the product of minor explosive activity during a pause in the Tshirege eruptions (Self and Sykes, 1996, p. 51-52). An exceptionally thick section of the Tshirege Member, >150 m thick, is visible down Ancho Canyon where it fills the early Pleistocene paleocanyon of the Rio Grande 1.5 km northwest of the modern river (Reneau and Dethier, 1996b).

16.0 Entrance to LANL TA-39, to right, within unnamed north fork of Ancho Canyon (closed to public) (Fig. 1-25). This site was established in 1953, primarily for the open-air testing of high explosives for LANL's shock physics group. A variety of contaminants have been dispersed from the firing sites, including Be and U. Downstream within Ancho Canyon and upstream behind the security fence are exposed dacite-rich alluvial deposits between the Tshirege and Otowi Members of the Bandelier Tuff, indicating the location of a pre-Tshirege paleodrainage that headed in the Jemez Mountains, possibly in the headwaters of the modern Pajarito Canyon (Broxton and Reneau, 1996). 0.4 km upstream is a rare exposure revealing fluvial erosion of the lowermost Tshirege Member (Tsankawi Pumice Bed and basal Qbt-1g), prior to the pre-Tshirege stream being overwhelmed by subsequent ignimbrites. Core holes drilled 0.6 km upstream in 1994 near a landfill in the canyon bottom penetrated about 10 m of alluvium and revealed a complex stratigraphy; some holes penetrated layers of El Cajete pumice at depths of 3.5-7.5 m, whereas nearby holes lacked such pumice beds and yielded radiocarbon dates on charcoal of 10-11.5 ka at depths of ~4 m, indicating the thickness of Holocene sediment (Fig. 1-26, Reneau et al., 1996b).

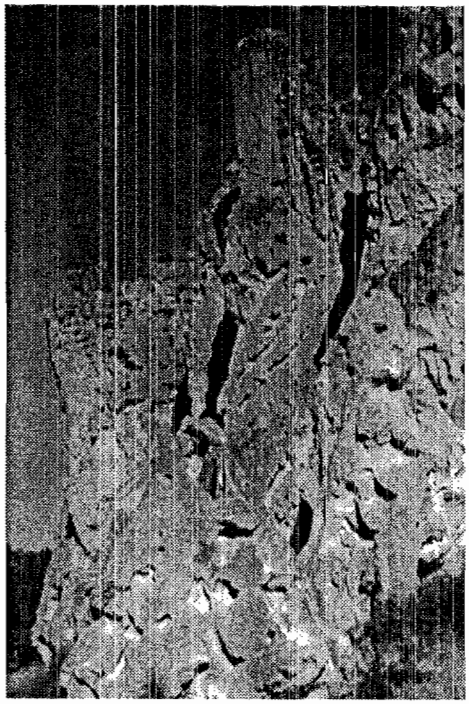

Fig. 1-25. Photograph of lower Tshirege Member of Bandelier Tuff (Qbt-1g) in Ancho Canyon at entrance to TA-39.

16.4 **Stop 1-5: Ancho Canyon** (optional). Pull off to left and right at high roadcut in white tuff.

Bandelier Tuff Stratigraphy and Zeolitized Zones. The roadcut here exposes, from bottom to top, nonwelded ignimbrite of the Otowi Member of the Bandelier Tuff, a thin colluvial soil, the 1-m thick Tsankawi Pumice Bed, nonwelded ignimbrite of the Tshirege Member (Qbt-1g), and bouldery colluvium (Fig. 1-27). Prominent, thin resistant layers in the lower Tshirege Member are zeolitized zones similar to those exposed in many canyons of the eastern Pajarito Plateau. Analyses of samples from this site indicate that the zeolites are clinoptilolite, which are believed to form in an open environment from hydrolysis of vitric ash by percolating water at or near the tops of saturated zones (Hay, 1978). K-Ar analysis of clinoptilolite (1-3 μm fraction) separated from one zone at this site yielded an apparent age of 1.0 ± 0.2 Ma (WoldeGabriel, 1993), suggesting they formed relatively soon after emplacement of the Tshirege Member; however, due to low radiogenic argon content (2%), this apparent age should be interpreted with caution (G. WoldeGabriel, pers. comm., 1996).

As this exposure was interpreted by Bailey and Smith (1978): "Near the crest of the Otowi mound, indurated zeolitized ground-water tables in the Tshirege ash-flow tuff curve downward forming cones of depression that mimic former piezometric surfaces drawn down by the more permeable Tsankawi Pumice Bed. Note that the cones of depression steepen in successively lower levels" (Bailey and Smith, 1978, p. 193). Bailey and Smith (1978) attributed the apparent successive lowering of the water table to the incision of

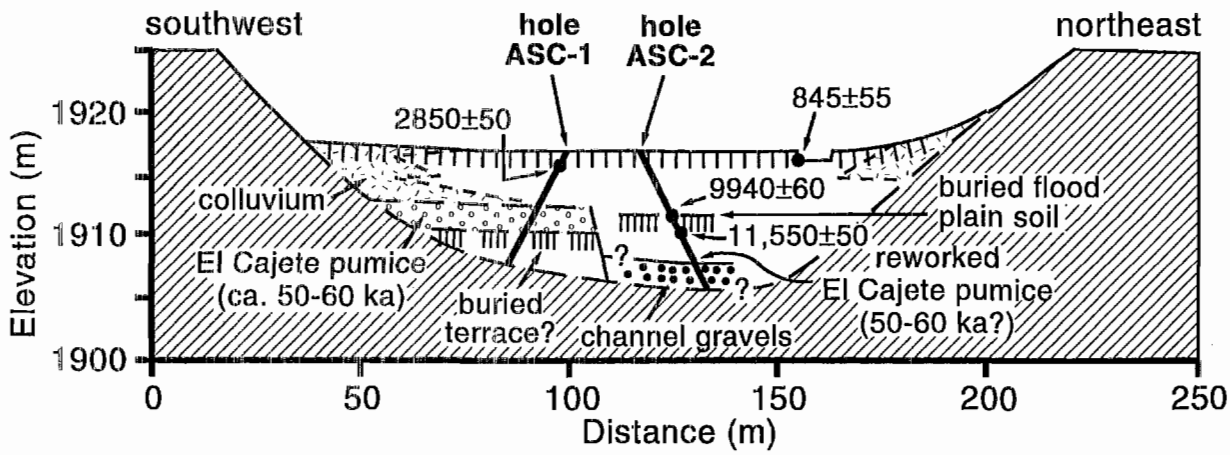

Fig. 1-26. Generalized cross section across north fork Ancho Canyon, 0.6 km northwest of Mile 16.0, showing radiocarbon dates and inferred stratigraphic context of units exposed in core holes (from Reneau et al., 1996b, modified from unpublished core logs of K. Shisler and others, 1994). Bedrock includes the Tshirege and Otowi Members of the Bandelier Tuff and alluvium of the intervening Cerro Toledo interval.

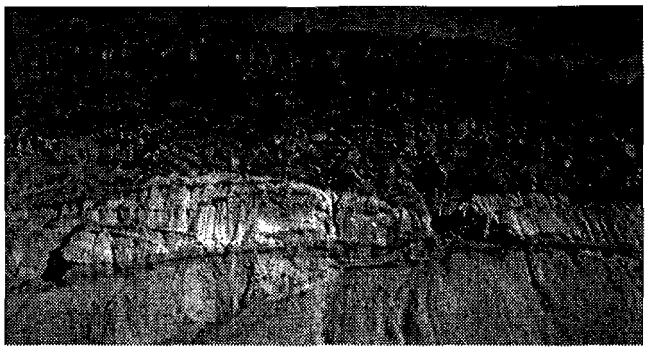

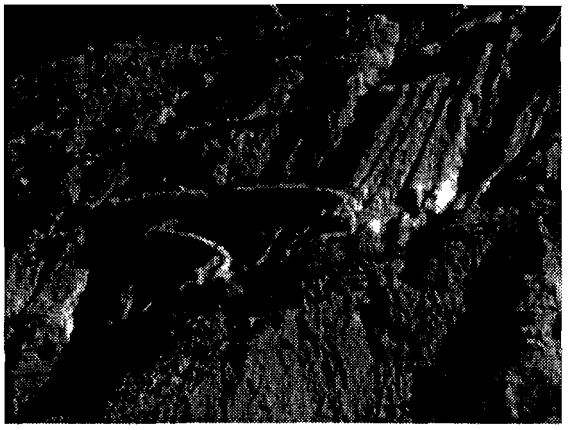

Fig. 1-27. Photographs of roadcut in Ancho Canyon at Stop 1-5. Roadcut exposes non-welded tuff of the basal Tshirege Member (Qbt-1g) with thin zeolitized zones, and the non-welded Otowi Member. The Cerro Toledo interval here is represented by a thin colluvial soil. Unit Qbt-2 of the Tshirege Member forms the upper cliffs. The right photo highlights the zeolitized zones, which are curving down to the Tsankawi Pumice Bed.

Ancho Canyon and the headward migration of a waterfall over a basalt flow that is exposed about 1 km downstream, implying that the zeolitized zones are local features related to shallow groundwater beneath the channel of Ancho Canyon.

Field observations suggest that the zeolitized zones are not local features related to specific canyons, but are instead widespread and project under the intervening mesas. For example, similar sets of zeolitized zones are exposed at similar elevations both to the north in the unnamed tributary of Ancho Canyon, and to the south in Frijoles Canyon (the upper ladders at Ceremonial Cave in Bandelier National Monument lead onto zeolitized ledges at the same elevation as these in Ancho Canyon). In addition, the zeolitized zones don't parallel either the Tshirege unit boundaries or the canyon profile, but are instead nearly horizontal, also suggesting that they are not related to groundwater associated with the modern canyons. An alternative hypothesis is that they record former levels of a regional aquifer that was adjusted to a much higher Rio Grande, perhaps when the river was slowly incising a new canyon through basalt following damming by the Tshirege Member and subsequent diversion of the channel eastward onto the Cerros del Rio volcanic field (see Reneau and Dethier, 1996b).

Early Pleistocene Paleotopography. At this site and at many other sites on the Pajarito Plateau, it is apparent that the modern canyons are not at the same locations as the pre-Tshirege drainages (Broxton and Reneau, 1996). The colluvial soil between the Tshirege and Otowi Members at this site contains clasts of basalt that were probably derived from a cinder cone that occurs to the south, and the modern Ancho Canyon has apparently incised into a north-facing paleocanyon wall here (Fig. 1-28). The axis of the pre-Tshirege paleocanyon is recorded by dacite-rich alluvial deposits that are exposed between the Tshirege and Otowi Members downstream near the entrance to TA-39 and also within the unnamed north fork of Ancho Canyon.

Holocene Alluvial Statigraphy. The sediments exposed within the stream bank immediately south of State Road 4 are typical of those found in many canyons on the Pajarito Plateau, particularly those that head on the Plateau and entirely drain areas underlian by Bandelier Tuff and younger deposits (e.g., Sandia Canyon, Stop 1-3). A stacked set of alternating channel deposits and floodplain deposits are present that have yielded radiocarbon dates from charcoal of about 1.2 to 4.9 ka (Fig. 1-29). Pumice clasts are abundant in these floodplain deposits, mainly derived from erosion of deposits of the El Cajete pumice upstream.

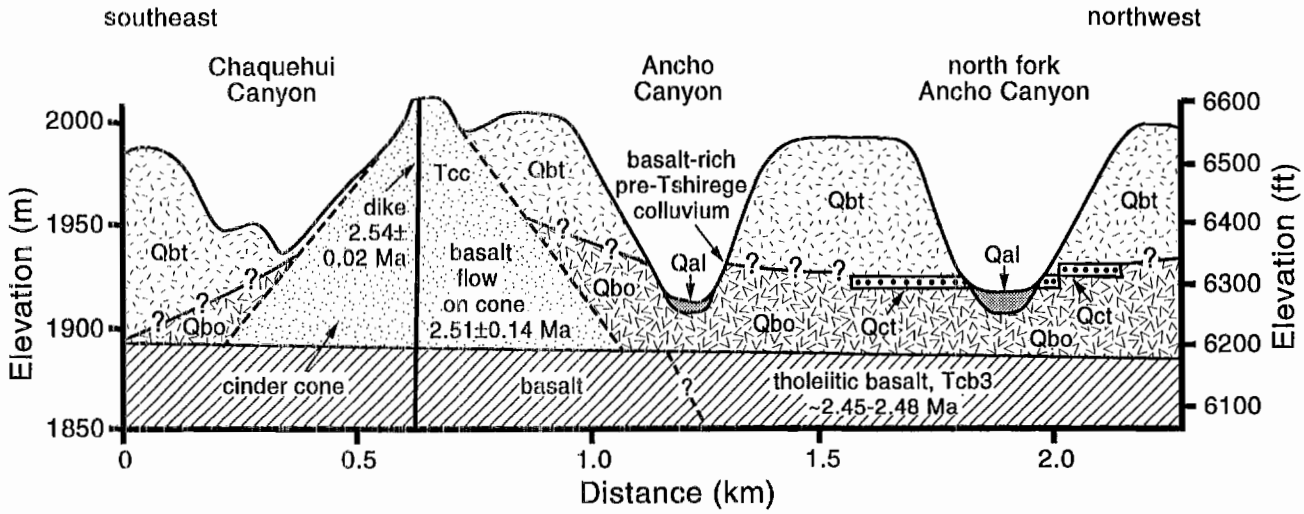

Fig. 1-28. Schematic geologic cross section through site of Stop 1-5, showing pre-Tshirege paleotopography and underlying units. Qal: late Quaternary alluvium; Qbt: Tshirege Member of Bandelier Tuff; Qct: fluvial deposits of Cerro Toledo interval; Qbo: Otowi Member of Bandelier Tuff; Tcc: Pliocene cinder cone; Tcb3: Pliocene tholeiitic basalt. Dates are preferred $^{40}Ar/^{39}Ar$ ages from WoldeGabriel et al. (1996). Geologic contacts from Reneau et al. (1995a) and Broxton and Reneau (1996).

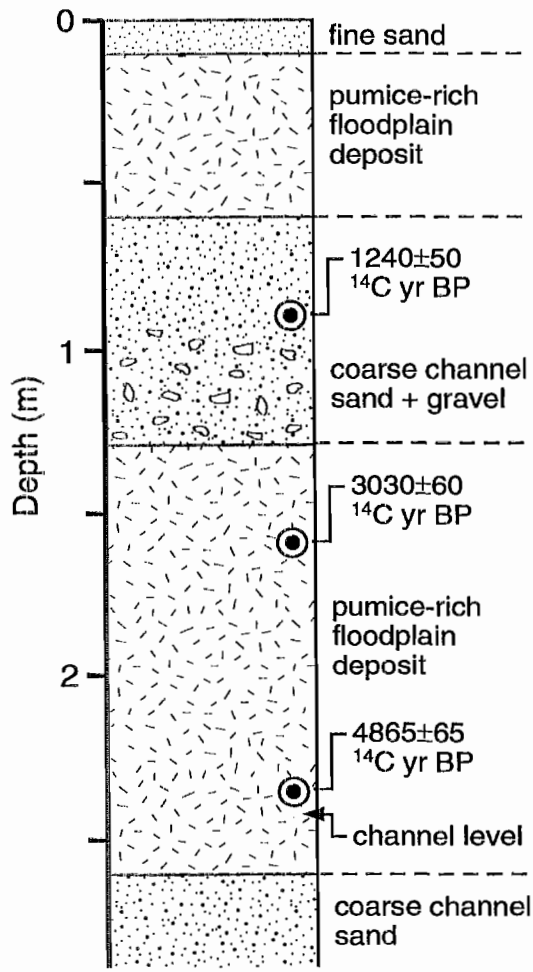

Fig. 1-29. Stratigraphic section through Holocene alluvium in Ancho Canyon at Stop 1-5, showing alternating channel and floodplain deposits and locations of radiocarbon dates on disseminated charcoal fragments.

The age control from this section indicates that the stream channel had aggraded to near its modern level by at least ca. 5 ^{14}C ka. The lack of recognized stratigraphic layers within the buried floodplain deposit and a ca. 3 ^{14}C ka age near its top suggest that aggradation over the next 2 ky or more was slow enough or discontinuous enough to allow thorough bioturbation of individual flood layers. In contrast, the sharp contact below the overlying channel deposit, dated at ca. 1.2 ^{14}C ka, indicates a significant late Holocene aggradational episode. Subsequently, the channel incised about 1.5-2 m to its present level.

A relatively small data set of dated channel deposits is available from the Ancho Canyon basin, mostly from the unnamed north fork upstream of the security fence. Two of the five dated deposits there are similar in age to this late Holocene channel deposit (Fig. 1-30), suggesting basin-wide aggradation at ca. 800-1300 cal BP. Similar clusters of ages from other canyons (e.g., Qt8 terrace in Rendija Canyon, Stop 2-3) suggests the possibility of Plateau-wide periods of aggradation, although the details of specific aggradational events in most canyons remain incompletely understood.

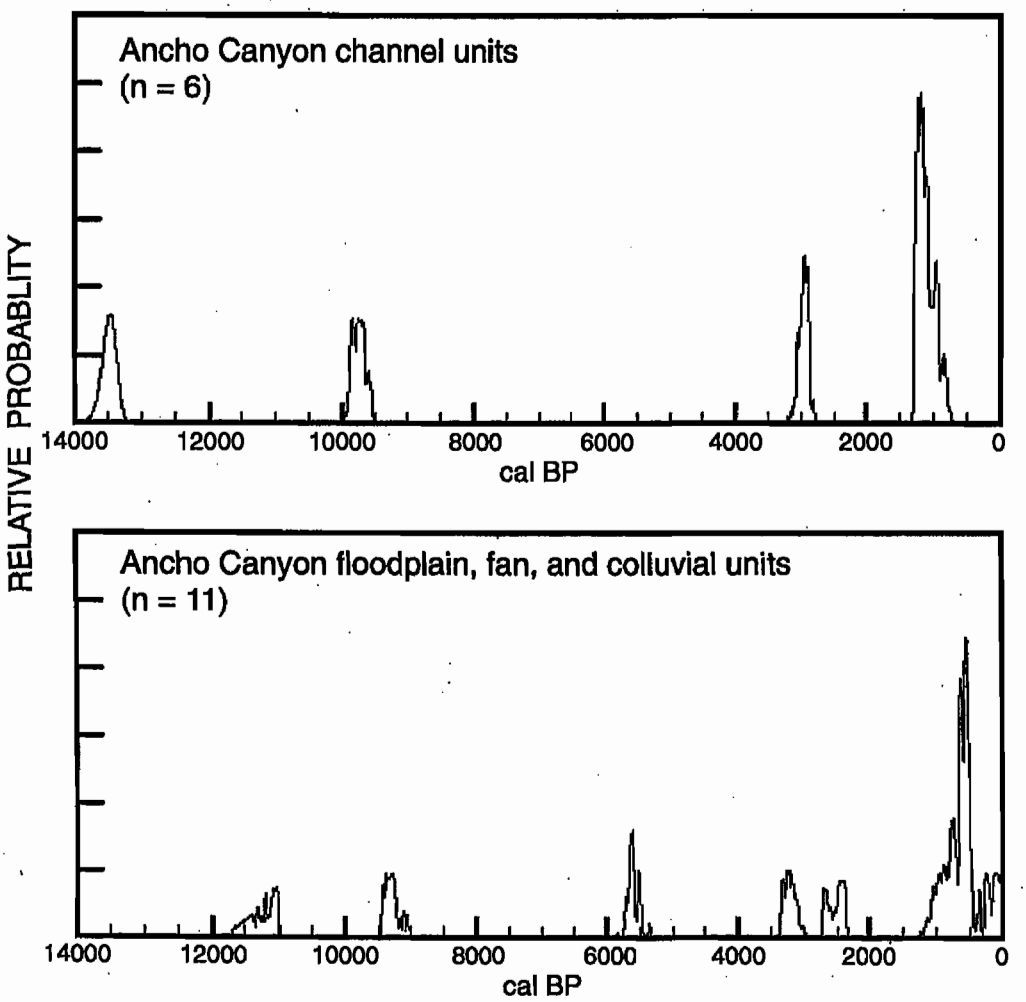

Fig. 1-30. Probability plots of calibrated radiocarbon ages showing dated Ancho Canyon stream channel units (n=6) and floodplain, fan, and colluvial units (n = 11). Probability plots were produced using CALIB 3.03 (Stuiver and Reimer, 1993), using 2-σ range and an error multiplier of 2.0 on the original analyses.

Soil-Stratigraphy of Profile AC-1. The surface soil in this exposure is typical of soils formed in young (< 2 ka) valley bottom stream sediments on the Pajarito Plateau. The soil contains weakly developed A and Bw horizons that overlie poorly altered and well-stratified stream channel deposits (Fig. 1-31). The A horizons have subangular and crumbly structure and a weak accumulation of disseminated organic matter resulting in a grayish brown color. The Bw horizons have prismatic and subangular blocky structure and patchy silans (coatings of silt) along some ped faces. Scattered El Cajete pumice occurs throughout the soil profile. Clay and silt content is considerably higher in the A and Bw horizons relative to the C horizons (Table 1-3), which probably reflects the predominance of finer-textured overbank deposits that overlie sand-rich stream channel deposits. Dithionite extractable Fe-oxyhydroxides range from about 0.26 % weight in the C horizon to 0.60 % weight in the Bw1 horizon; whereas, oxalate extractable Fe-oxyhydroxides range from about 0.17 % weight in the C horizon to 0.38 % weight in the Bw2 horizon (Longmire, McDonald, et al., unpub. draft report, 1996). The overall low concentrations of dithionite extractable Fe-oxyhydroxides and high oxalate to dithionite extractable Fe-oxyhydroxide concentrations reflects the young, late Holocene age for this soil. This soil is very similar in overall development to the SC-2 soil at Stop 1-2b that overlies sediment with an age of about 1.4 ^{14}C ka.

Buried soil b1. A weakly to moderately developed buried soil underlies the surface soil and well stratified stream sediments that yielded a 1.2 ^{14}C ka age (Fig. 1-31; Table 1-3). The soil contains two weakly developed Bt horizons that have weak subangular structure and patchy argillans along ped faces and pores. A lack of evidence for a buried A horizon suggests that the top of this buried soil has been removed by erosion, presumably in association with deposition of the overlying stream sediments. The lower soil contains BC and CB transitional horizons that overly unaltered coarse-grained stream sands. Abundant to scattered reworked El Cajete pumice clasts can be found throughout the profile. The generally massive character of the soil and the abundant silt and clay suggests that the soil parent material may have largely consisted of bioturbated overbank deposits. The overall degree of soil development suggests that the soil may be older than indicated by the two ^{14}C ages of about 4.9 and 3.0 ka. The dates could possibly reflect later emplacement of charcoal from bioturbation before burial.

16.6 Cavate ruins in cliffs to right.

16.8 Ancho Canyon channel. Hairpin turn.

17.3 Sangre de Cristo Range, east of Santa Fe, straight ahead to east.

17.5 Entrance to LANL TA-33, to left (closed to public). This area was once the site of LANL's tritium (^{3}H) production facility (tritium is an important component of "triggers" of nuclear weapons, but, due to its short half-life of 12.4 yrs, periodically needs replenishment). A variety of other weapons-related activities have been conducted here, including attempts to develop an "atomic cannon" in the 1950s. Many researchers in LANL's geoscience groups were housed here during the 1970s and the 1980s. TA-33 has some waste sites located near the rim of White Rock Canyon and tributary canyons, and a study of landslides within White Rock Canyon was conducted to evaluate potential mass wasting hazards that could affect these sites (Reneau et al., 1995a).

17.7 Late Pliocene cinder cone of the Cerros del Rio volcanic field is exposed 0.1 km to the southeast (on restricted DOE land), projecting a short distance above the top of the Tshirege Member (Fig. 1-28).

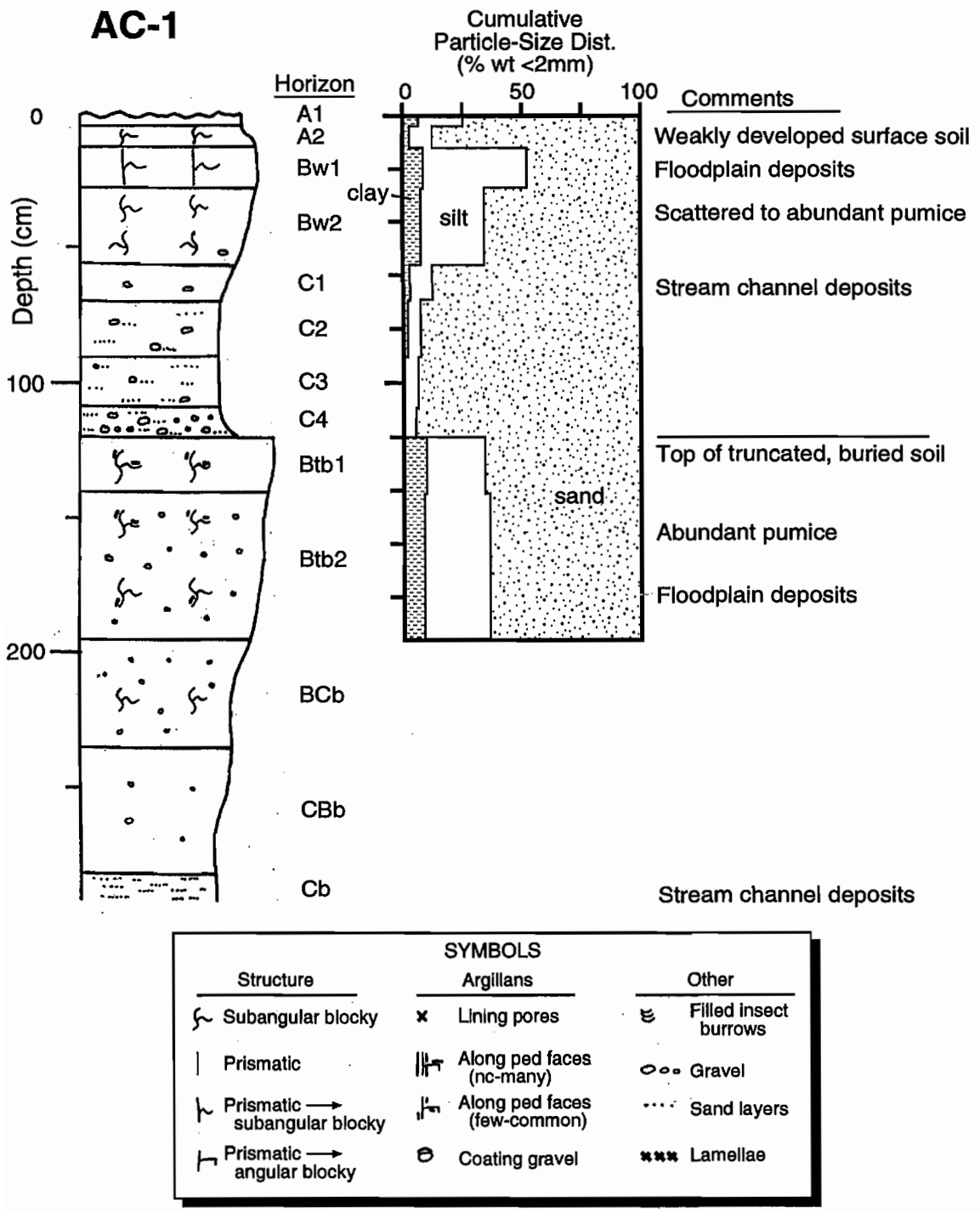

Fig. 1-31. Schematic diagram of soil-stratigraphy for profile AC-1 at Stop 1-5.

18.9 **Bandelier National Monument, main entrance,** to left. 3 mi to Visitor Center within Frijoles Canyon. A stop here to visit outstanding prehistoric Pueblo (Anasazi) ruins in a scenic canyon is highly recommended (Fig. 1-32).

19.9 **Stop 1-6: Frijoles Mesa** (optional). Park carefully on road shoulders. Note: stop is on DOE land posted with "No Trespassing" signs, so do not make this stop unescorted.

In a borrow pit on this mesa, north of the highway (on restricted DOE land) is exposed the thickest section of El Cajete pumice yet examined at the Laboratory, consisting of 2.2 m of primary fallout pumice. This is significantly greater than the <1 m thickness shown for this area on the El Cajete isopach maps of Self et al. (1991), suggesting that the isopach maps greatly underestimate the original thickness of the pumice bed. This underestimation is likely due to substantial erosion of the pumice over the past 50-60 ka. Notably, thin ash beds are locally interlayered with pumice at the top of the section, a feature that has only been observed at one other site on the Pajarito Plateau, and further indicate that this borrow pit displays an exceptionally complete section of the El Cajete.

The exceptional preservation of the pumice at this site, which would seem to indicate relative stability of the mesa top, is in sharp contrast to the overlying weakly-developed (late Holocene) soil, which would seem to indicate an eroding mesa. The soil beneath the El Cajete is relatively thin (0.6 m) but fairly well developed (discussed below), indicating a relatively stable mesa-top setting prior to deposition of the pumice but a site without significant aggradation. The contrast between the post-El Cajete soils present here and those seen at Stop 1-4, and to be seen at Stop 2-2, illustrate some of the as yet unresolved complexity of surface processes and soil development on the mesas of the Pajarito Plateau.

Soil-Stratigraphy of Profile FM-1. The soil stratigraphy at this stop (Fig. 1-33; Table 1-4) consists of a thin, weakly developed surface soil that overlies a thick, well-preserved (intact) section of El Cajete pumice, and an underlying buried soil and Bandelier Tuff.

Surface Soil. The surface soil contains a thin (4.5 cm) A horizon with subangular and crumbly structure. The Bw horizons are weakly developed, have weak subangular blocky structure and a weakly oxidized soil matrix. Scattered El Cajete clasts occur throughout the profile. The overall degree of soil development is generally similar, although somewhat weaker, than soils formed in ca. 1.2 to 1.4 ka stream sediments exposed at Stops 1-2b and 1-5. The soil unconformably overlies the El Cajete pumice.

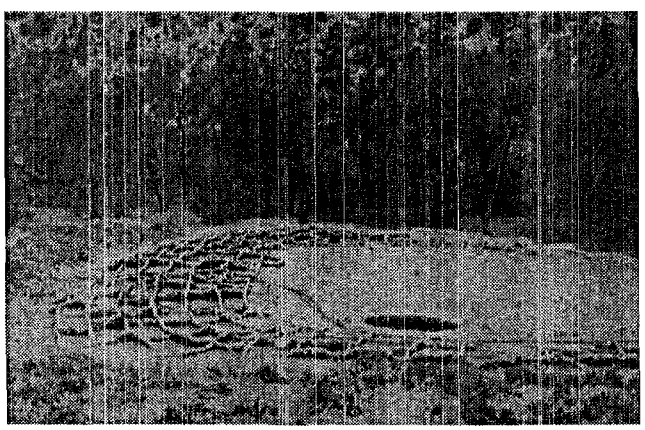

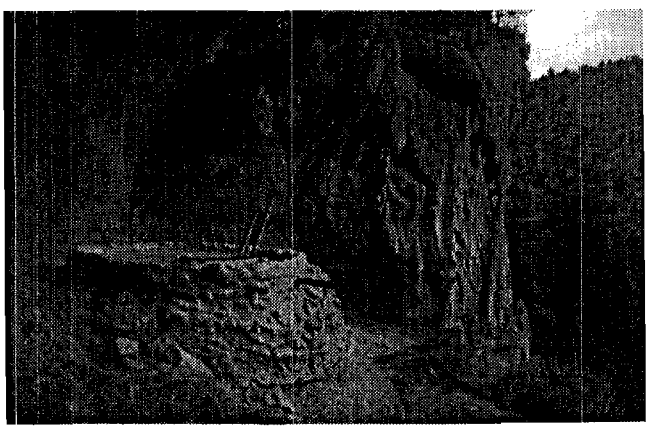

Fig. 1-32. Photographs of ruins in Frijoles Canyon. Tyuonyi (left) and Ceremonial Cave (right).

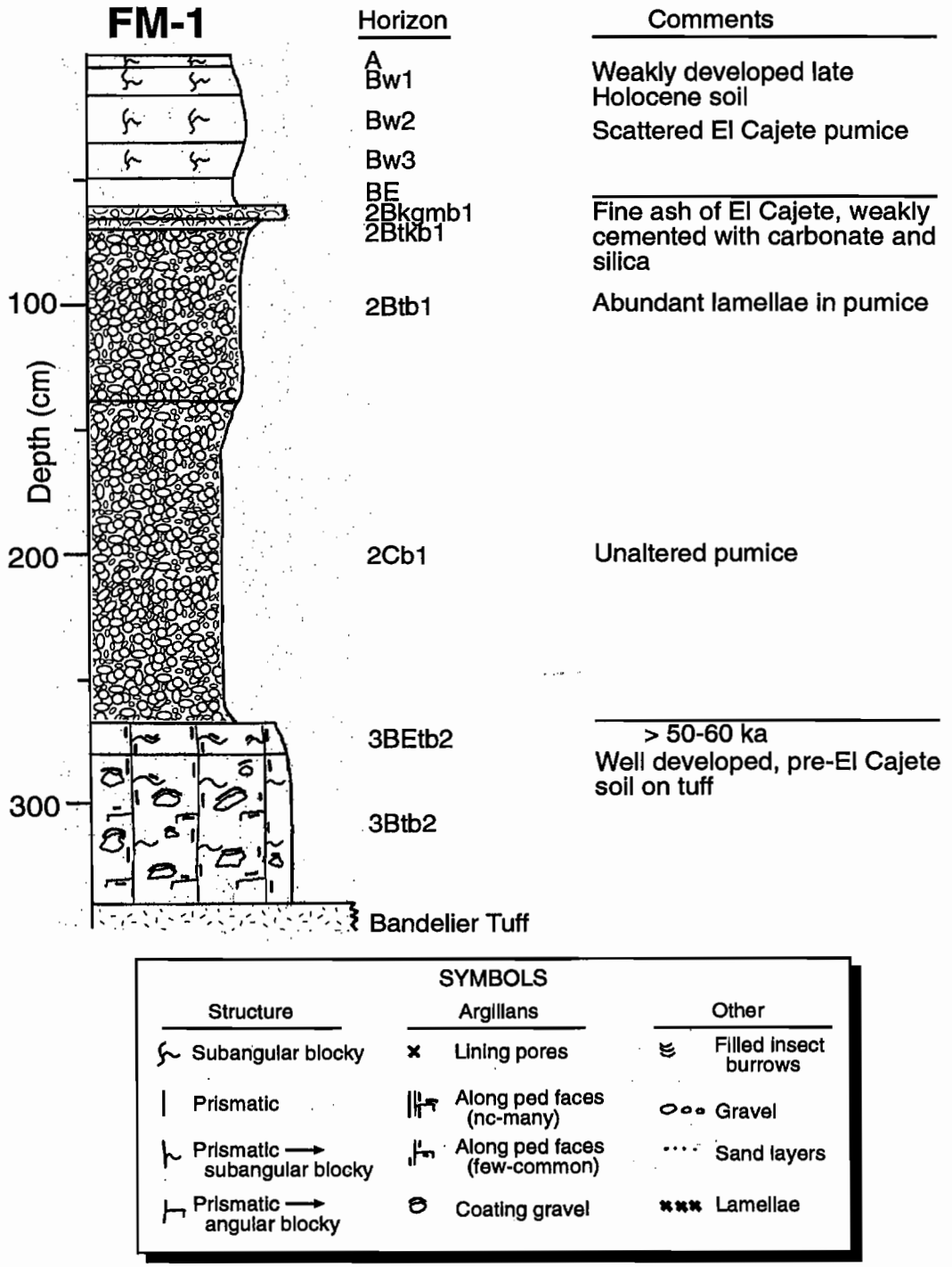

Fig. 1-33. Schematic diagram of soil-stratigraphy for profile FM-1 at Frijoles Mesa borrow pit, Stop 1-6. At other nearby exposures, a thin pumice bed is interlayered with the ash, indicating that the ash is associated with late stages of the El Cajete eruptions.

El Cajete Pumice. The pumice is capped by a 11 cm layer of volcanic ash (2Bkqmb1) that is weakly cemented with secondary carbonate and silica. Two weak Bt horizons have formed within the top of the pumice. The 2Btkb1 has single grain structure and stage I carbonate, including carbonate with needle-shaped morphology within some interstitial voids. Argillans in this horizon consist of coats and bridges formed on pumice, with accumulation of clay forming lamellae in places. The 2Btb1 is also single grain in structure and has argillans that coat and bridge pumice, forming abundant clay lamellae 0.5 to 1.5 cm thick throughout the horizon. The 2Cb1 contains a few scattered lamellae, but is largely unaltered.

The weakly developed surface soil, the preservation of a thick layer of pumice, the cemented ash layer, and lamellae formed in the pumice indicate that the pumice was previously overlain by a older, presumably better developed surface soil that has since been removed by erosion. For example, post-El Cajete soils at other sites on the Pajarito Plateau that overlie pumice and reworked pumice deposits, are up to 1-2 m thick and contain well developed Bw and Bt horizons.

Buried Soil b2. The El Cajete pumice conformably overlies a thin buried soil. The top of the soil has a transitional E horizon (3Ebtb2) with prismatic structure. The underlying 3Btb2 horizon has blocky structure and argillans along ped faces and bridging grains. The horizon also contains abundant tuff fragments. The Bt horizon overlies eroded and poorly weathered Bandelier Tuff (Qbt-4).

20.6 Area burned in 1977 La Mesa Fire to left. Beneath this part of Frijoles Mesa lies an exceptionally thick section of the Tshirege Member of the Bandelier Tuff, estimated at >200 m thick (Broxton and Reneau, 1996). The tuff here buried a southwest-draining early Pleistocene paleovalley that may have been a relict of a Tertiary graben which is believed to underlie much of the west-central Pajarito Plateau.

21.5 View of Sierra de los Valles (eastern Jemez Mountains) to west, San Miguel Mountains and St. Peters Dome (site of April 1996 Dome Fire) to southwest, and La Mesa Fire area.

22.1 Entrance to LANL TA-49, to right (closed to public). The heyday of TA-49 was from 1959 to 1961 when it was the site of hydronuclear and related experiments designed to test the safety of nuclear weapons. Limited quantities of "special nuclear materials" (Pu and ^{235}U) were used in combination with high explosives (HE) in shafts 9-43 m deep. This work proceeded by Presidential decree (recently de-classified), during an informal test ban, because these were deemed to be "laboratory" tests and not full-scale tests of nuclear weapons. The concept and science of "containmant" was pioneered here. This site was chosen partly due to its relatively remote location, and also after a USGS study confirmed a substantial depth to groundwater (~365 m) and other favorable hydrogeological conditions (Weir and Purtymun, 1962).

22.8 Burnt Mesa trailhead, Bandelier National Monument, to left.

23.7 High roadcut in upper units of Tshirege Member of Bandelier Tuff to right (Qbt-4 and Qbt-5), and large pullout to left. Exceptionally thick section of non-welded, vitric tuff is overlain by relatively thin, densely-welded flow unit with pronounced fiamme (squashed and welded pumice). Uppermost ignimbrite (Qbt-5) forms a prominent resistant cap rock on this part of the western Pajarito Plateau, but does not extend to the east.

24.0 View of 100+ m high Pajarito fault escarpment, straight ahead.

24.2 Bunkers visible on north rim of Water Canyon, to right. Bandelier Tuff units in this area are tilted gently to the west, towards the Pajarito fault zone, contrasting with the general 2-3° east dip on most of the Pajarito Plateau.

24.6 **Ponderosa Campground,** entrance to left. Group campground (reservations required), and trailhead for Bandelier backcountry. Trail to Upper Crossing in Frijoles Canyon parallels the Pajarito fault zone for 1.5 mi, and trail continues for 6 mi down Frijoles Canyon to Bandelier Visitor Center. This route makes an excellent one-way shuttle hike down a part of Frijoles Canyon that has experienced exceptional rates of Holocene incision through non-welded tuff, with a terrace dated at 5.3-6.2 ^{14}C ka stranded 20-25 m above the modern channel (Reneau et al., 1993, 1996b) (Fig. 1-34).

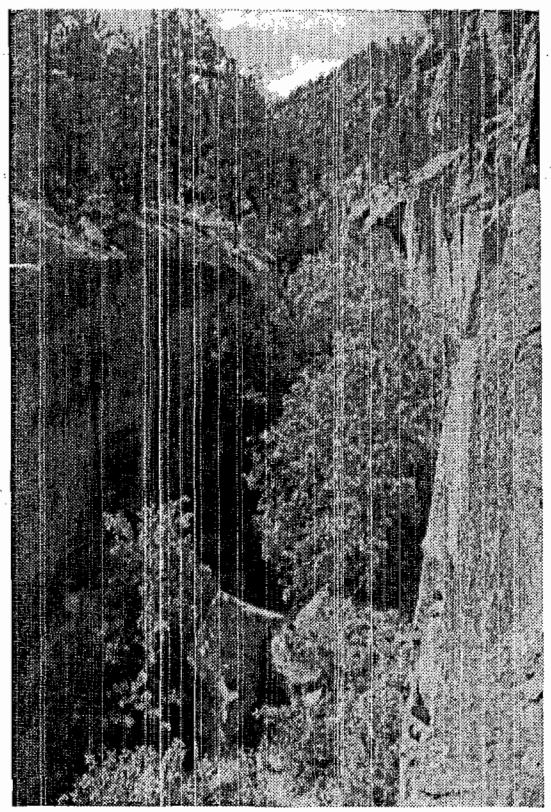

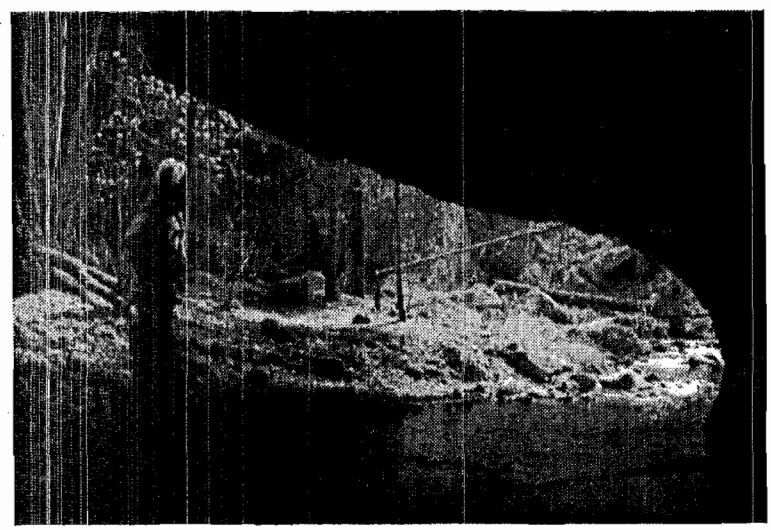

Fig. 1-34. Photographs of part of Frijoles Canyon between Bandelier Visitor Center and Upper Crossing. Left photo: stream has cut a narrow inner canyon >20 m deep into non-welded tuff (Qbt-1g) below a mid Holocene terrace level. Right photo: stream-side alcoves such as this one are produced by lateral erosion into non-welded tuff during periods of relative base level stability, such as at present; multiple Holocene paleo-alcoves are locally perched on the canyon walls, associated with Holocene stream terraces.

Day 2, Ponderosa Campground to Rendija Canyon

Leaders: Steven Reneau, Eric McDonald, Jamie Gardner, Bill Phillips, Dave Broxton, Craig Allen, Keith Kelson

Stop 2-1: Ponderosa Campground (7600', 2315 m elev.)

Day 2 of the field trip begins at the parking lot for Ponderosa Campground and Upper Crossing trailhead, 14 miles from White Rock, 5 miles from Los Alamos, and ~1 hr from Santa Fe. **Restrooms.**

- Walk ~50 m south into open area for views of the main escarpment of the Pajarito fault zone, into an area burned in the 1977 La Mesa Fire (Fig. 2-1).

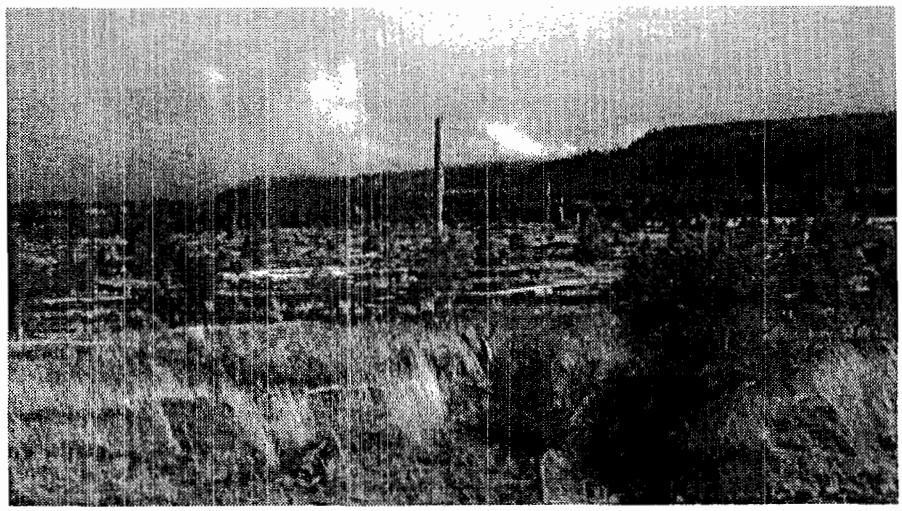

Fig. 2-1. Photograph of mesa near Ponderosa Campground, showing area of 1977 La Mesa Fire and Pajarito fault escarpment. Dome Fire is burning on top of escarpment (April 28, 1996 photo).

Fire History. Prior to 1977, this area was the site of a dense stand of ponderosa pines, the result of an apparently unprecedented absence of fires for ~100 yr. In a detailed study of local fire history, Allen (1989; see also Allen et al., 1996) found that prior to the 1890s small fires burned through the ponderosa forests of the Pajarito Plateau about every 5-15 yrs on average, probably creating an open parkland as was common throughout many parts of the Southwest. A sharp drop in fire frequency was apparently caused by the introduction of sheep and cattle to the area in the late 1800s, with the resultant loss of the grassy groundcover that had previously allowed lightning-caused fires to spread. Pine seedlings that would previously have burned in these ground fires instead flourished. The advent of organized fire-fighting efforts earlier in this century further helped suppress fires and allowed fuel to accumulate.

These conditions led to the La Mesa Fire of June 1977, an intense crown fire that started about 4 km southwest of here and quickly got out of control. A total of about 59.5 km^2 burned, including the southwest part of LANL (Foxx, 1984). Such a widespread crown fire was unprecedented in the ~300 yr long fire history developed by Allen (1989). Many parts of the burn, including this area, are still dominated by grass and shrubs almost 20 years later (Fig. 2-1). Note how the site of Ponderosa Campground escaped the intense burn. This was apparently due to the reduced fuel load in the former picnic area, where trees had been thinned and firewood collected.

Part of the Dome Fire area is also visible from here (Figs. 2-1, 2-2). The Dome Fire started at an incompletely extinguished campfire on April 25, 1996, after an exceptionally dry winter. It also got of control, turning into a firestorm on the afternoon of April 26, and burning about 66.5 km^2 before it was controlled in early May.

Fig. 2-2. Photographs of April 1996 Dome Fire area, San Miguel Mountains, Capulin Canyon basin. Extensive rilling occurred on burned slopes after the first summer thunderstorms, even on short convex slopes with thick deposits of the El Cajete pumice, contributing to rapid runoff and significant floods downstream. No true "hydrophobic" soils were present here, and instead extensive fine ash layers probably caused the reduced infiltration (July 3-4, 1996 photos).

Both fires have had major geomorphic effects. The effects of the La Mesa Fire were studied by White and Wells (1979, 1984), and included an increase in runoff and sediment supply from the burned slopes, associated with locally dense rill networks, which caused some temporary aggradation along channels and also a major increase in the height of flood peaks. The largest floods recorded in Frijoles Canyon, in the middle of the La Mesa Fire area, occurred in the summers of 1977 and 1978 (Purtymun and Adams, 1980).

Similarly, Capulin Canyon, in the middle of the Dome Fire area, has been experiencing repeated major floods since June 26, also generated by extremely rapid runoff from burned slopes (Fig. 2-2). These floods have incised the channel in many areas and scoured the banks. Significantly, the Capulin floods removed the cobble to boulder armor from the stream bed and exposed fairly easily erodible sandstone bedrock in several areas, which might be providing a modern analog for processes leading to channel incision and terrace formation in many Pajarito Plateau canyons. Reports from the burn area indicate that up to several meters of incision has already occurred in parts of Capulin Canyon this summer (Craig Allen, pers. comm., 9/4/96). Notably, true hydrophobic soils are apparently extremely rare in the Dome Fire area (S. Cannon, unpub.), and the rapid runoff may be due to the effectiveness of the ash cover in reducing infiltration rates, as previously proposed by White and Wells (1979, 1984) for the La Mesa Fire area.

Because the intensities and the widespread extent of both the La Mesa Fire and the Dome Fire were apparently unprecedented in the several-hundred year long fire record on the Pajarito Plateau, it is not known if the resultant geomorphic effects are also unlike that which would have occurred from fires prior to the late 1800s. In contrast to the ponderosa forests on the Plateau, the montane forests of the higher elevations of the Jemez Mountains were apparently subject to stand-replacing fires (recorded by the dense stands of aspen near Camp May and elsewhere), which in turn may have generated floods

capable of doing significant amounts of geomorphic work downstream. However, the existence and importance of such potential fire-flood relations in prehistoric times on the Plateau are presently unknown.

Pajarito Fault Escarpment. The prominent topographic break to the west (Fig. 2-1) is the main escarpment of the ~41 km long Pajarito fault zone, which is capped by welded units of the Tshirege Member of the Bandelier Tuff. Estimated offset in this area, based on topographic profiles, is about 110-130 m, yielding an average long-term vertical slip rate of ~0.1 mm/yr for the last 1.22 Ma (or ~0.12 mm/yr on a 60° fault plane) (Gardner and House, 1987; Wong et al., 1995; Olig et al., 1996). The amount of offset changes rapidly along strike, and the point of maximum offset, estimated at ~154 ± 5 m, is located only about 3 km to the north (Fig. 5, in Introduction).

This is probably as good a vantage point as any to discuss the paleoseismic history of the Pajarito fault, because its history doesn't get any clearer as one gets closer. Despite the obvious evidence for repeated Quaternary surface rupture events, the Pajarito lacks recognized fault scarps in alluvium as are commonly present along other major normal faults in the western United States. In addition, it does not consist of a single fault trace in most areas, but instead typically possess multiple traces in a zone up to 0.5-2 km wide (Fig. 2-3). It is also possible that much of the escarpment is mantled with landslides and other mass wasting features. For whatever reason, it has confounded attempts to obtain reliable paleoseismic information.

Woodward-Clyde Federal Services excavated trenches at 3 sites at the base of the main escarpment north of here in 1992 (Fig. 2-3), but the results were inconclusive. It was not clear that the "main trace" was ever crossed in a trench, leading to suspicions that it was always "a little bit farther west" (inconveniently on steep rocky slopes that limited the feasibility of excavation). The youngest evidence of faulting consisted of relatively small-magnitude offsets in a unit immediately below the El Cajete pumice, suggesting an event shortly before ca. 50-60 ka (Wong et al., 1995; Olig et al., 1996). In contrast, trenches across the shorter and presumably less active Rendija Canyon and Guaje Mountain faults to the north (Fig. 2-3) have both provided evidence of Holocene or latest Pleistocene events (Stops 2-3 and 2-4; Gardner et al., 1990; Wong et al., 1995; Kelson et al., 1996; Olig et al., 1996).

Because of the importance of the paleoseismic history of the Pajarito fault to an evaluation of seismic hazards at LANL, and because of questions about the validity of applying long-term slip rates to short-term hazard analysis, an alternative approach was developed to estimate possible short-term variations in slip rate on the Pajarito fault. McCalpin (1995) compiled all available data on short-term and long-term slip rates from normal faults throughout the Rio Grande rift and the Basin and Range province, and reached the conclusion that short-term rates could be significantly higher than long-term rates, related in part to temporal clustering of events. The work by McCalpin (1995) indicated that use of the long-term slip rate of ~0.12 mm/yr for the Pajarito fault could be extremely misleading, and that actual short-term rates could be as high as 0.92 mm/yr (at a 5% probability of exceedance).

- Return to parking lot.

Mileage from Ponderosa Campground

0.0 State Road 4 at entrance to Ponderosa Campground.

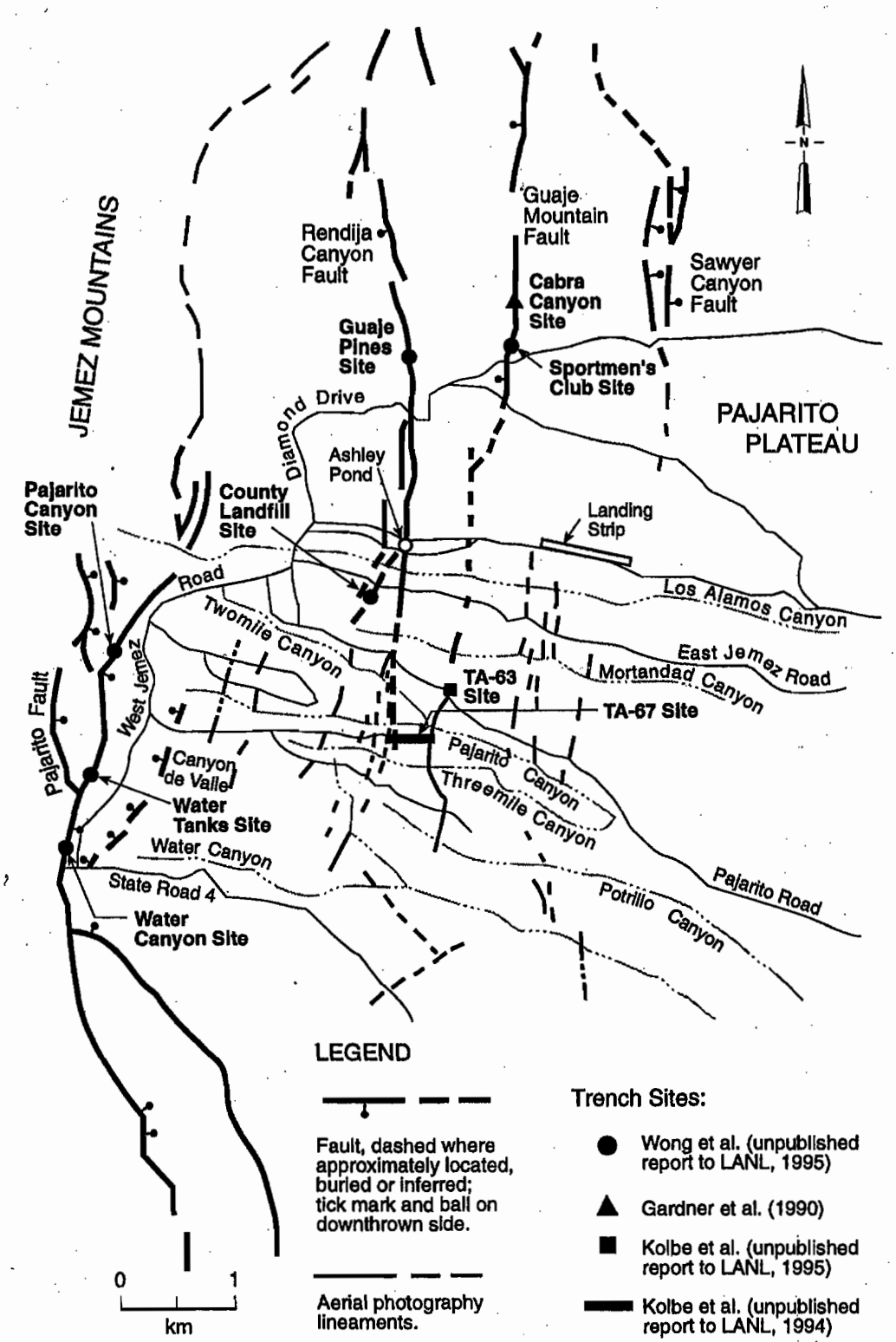

Fig. 2-3. Map of faults and lineaments in the Pajarito fault system near Los Alamos, and sites of paleoseismic investigations (from Olig et al., 1996).

0.2 NM **Highway 501** (West Jemez Road). Turn right towards Los Alamos. The small concrete building at the intersection is the "Back Gate", former site of a guard station dating from when Los Alamos was a closed community (November 1942 to February 1957).

Side-Note: SR 4 for the next 0.7 mi switchbacks up the Pajarito fault escarpment, and roadcuts expose extensive colluvial deposits that mantle the escarpment, plus a pocket of stratified, re-worked El Cajete pumice (+0.2 mi), and probably toppled and otherwise mass-wasted blocks of welded tuff. At the top of the escarpment (+0.7 mi) the roadcut exposes a filled fissure in densely welded tuff that separates horizontally-fractured tuff from a block where these fractures are tilted eastward (Fig. 2-4). We interpret the fissure to represent the back (west) margin of a toppling failure. Earlier workers have alternatively interpreted the fissure fill as representing gouge on a trace of the Pajarito fault zone (e.g., Bailey and Smith, 1978, p. 192), and these disparate interpretations illustrate some of the uncertainty in distinguishing tectonic from mass wasting features on a bedrock-dominated escarpment. 6 mi farther west SR 4 enters the Valles caldera, formed during eruption of the Tshirege Member of the Bandelier Tuff and site of subsequent eruptions that produced the El Cajete pumice and other, recently recognized, pumice beds associated with the Valles Rhyolite of Bailey et al. (1969) (see Stop 2-2c).

Fig. 2-4. Photograph of west edge of fissure fill along NM State Road 4 at the top of the Pajarito fault escarpment. Densely welded Bandelier Tuff with sub-horizontal fractures to left; to right of fissure fill (out of photo), these fractures are titled to the east, suggesting a toppling failure. Fissure fill includes both densely welded tuff from the adjacent walls and less-welded tuff from the overlying cooling unit.

For the next 4.5 mi NM Highway 501 is bordered to east by DOE land posted with "No Trespassing" signs, and to the west by a narrow strip of DOE land bordering the Santa Fe National Forest. The Pajarito fault escarpment is on National Forest land and is fully open to the public.

0.4 Roadcut on right exposes an old dacite-rich fan deposit derived from Water Canyon that predates initial incision of Water Canyon at this site east of the main Pajarito fault. The top of the fan gravels are ~20 m above the present channel. Gravels associated with this fan can be traced south past Ponderosa Campground, and also eastward down the mesas bordering Water Canyon. 0.1 km to east (on restricted DOE land) this fan deposit is apparently offset >15 m by a down-to-the-west antithetic fault which projects south into Bandelier National Monument. In the roadcut on the left the dacite-dominated deposit is overlain by a tuff-dominated fan deposit

derived from a smaller drainage off the escarpment, which is in turn overlain by the El Cajete pumice. As exposed in the roadcut to the right, a well developed soil has formed in these deposits. The upper 54 cm of the soil consist of an A-E-Bt horizon sequence developed in reworked and bioturbated El Cajete pumice. The pumice conformably overlies a well developed buried soil, formed in the dacite-rich alluvium, that has an E-BE-Bt horizon sequence, with total Bt horizon thickness extending to 260 cm below the surface. This soil is generally similar to a soil that will be seen at Stop 2-2b.

0.5 Water Canyon channel. Dirt road to west provides access onto National Forest land. A narrow 10-m high terrace above the dirt road, on the north side of the canyon, was the site of a paleoseismic trench excavated by Woodward-Clyde Federal Services in 1992 (Fig. 2-3; Wong et al., 1995; Olig et al., 1996). No faulting was exposed in the trench. The age of this terrace is not certain, but the gravelly fluvial deposit contained reworked El Cajete pumice, indicating an age of less than 50-60 ka. In a nearby soil pit the fluvial deposits were overlain by fine-textured slopewash colluvium which yielded ^{14}C ages of 8.06 and 9.49 ka (unfortunately in reversed stratigraphic order), with no intervening buried soil, suggesting a latest Pleistocene or earliest Holocene age for the terrace (Wong et al., 1995).

0.6 Abandoned road to right is old "Anchor Ranch Road", which traversed LANL Tech Areas now behind security fences. Roadcuts in this area expose a young, post-El Cajete fan to the west and an older, pre-El Cajete fan to the east.

0.8 **Stop 2-2: West Jemez Road (WJR) @ TA-16**. Park on shoulder. Note: this stop is on DOE land posted with "No Trespassing" signs, so do not visit area east of road unescorted.

- Climb up roadcut to east to site of reexcavated 1995 soil pit (Figs. 2-5, 2-6).

Geomorphology of the Pajarito Fault Zone. The Pajarito fault zone along the western boundary of LANL has a long, complex, and as of yet poorly understood geomorphic history. The escarpment itself is mainly covered with colluvium and other mass wasting deposits, including large-scale landslides. The base of the escarpment and the Pajarito Plateau to the east are mantled in most areas by colluvium, fans, and associated pumice beds that probably range in age from Holocene to ca. 1.2 Ma. No fault scarps in late Quaternary deposits have yet been confidently recognized, although degraded antithetic, west-facing scarps occur in early Pleistocene (?) fan deposits in some areas. Examples of some of the diverse Quaternary deposits present east of the escarpment will be examined at this stop, along with ongoing work on soils that may ultimately allow better resolution of the geomorphic and tectonic history of the Pajarito fault zone.

Station 2-2a, El Cajete pumice and post-El Cajete soil in soil pit WJR-5

Soil-Stratigraphy of WJR-5. The soil exposed in this pit (and along the adjacent roadcut) has formed in a ~1.3 m layer of surficial deposits that overlie a ~0.9 m layer of El Cajete pumice (WJR-5, Figs. 2-7, 2-8; Tables 2-1, 2-2). This soil is the thickest and best-developed soil we have found in post-El Cajete deposits. The pumice and surface soil, in turn, overlie a ca. 10+ m thick sequence of buried soils and surficial deposits. The underlying, and uppermost buried soil, will be discussed at Stop 2-2b.

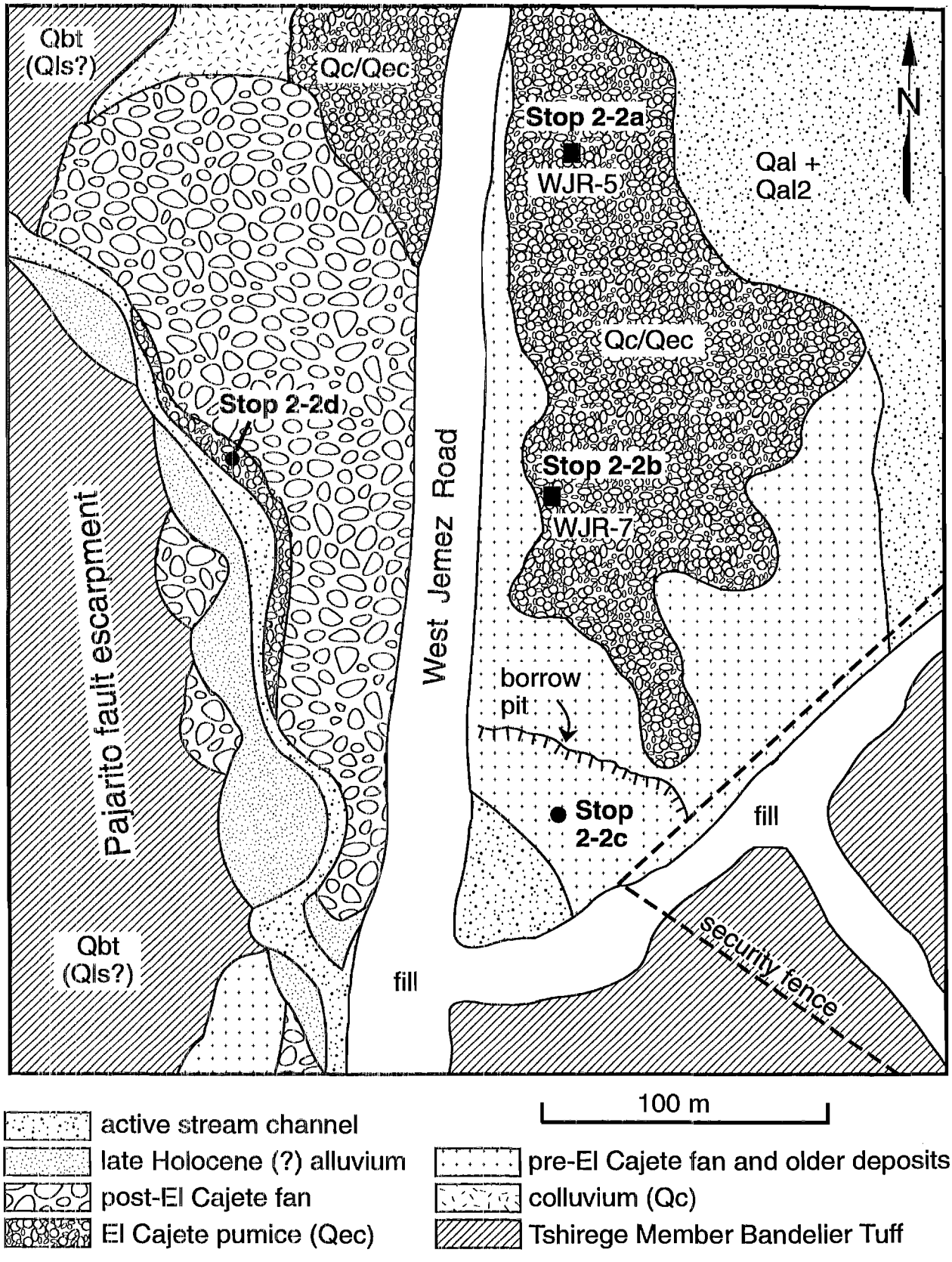

Fig. 2-5. Geomorphic map of area along West Jemez Road north of Water Canyon, at Stop 2-2. Label "Qc/Qec" indicates that colluvium buries the El Cajete pumice. Label "Qbt (Qls?)" indicates that the Bandelier Tuff may be involved in large-scale landslides along the Pajarito fault escarpment here.

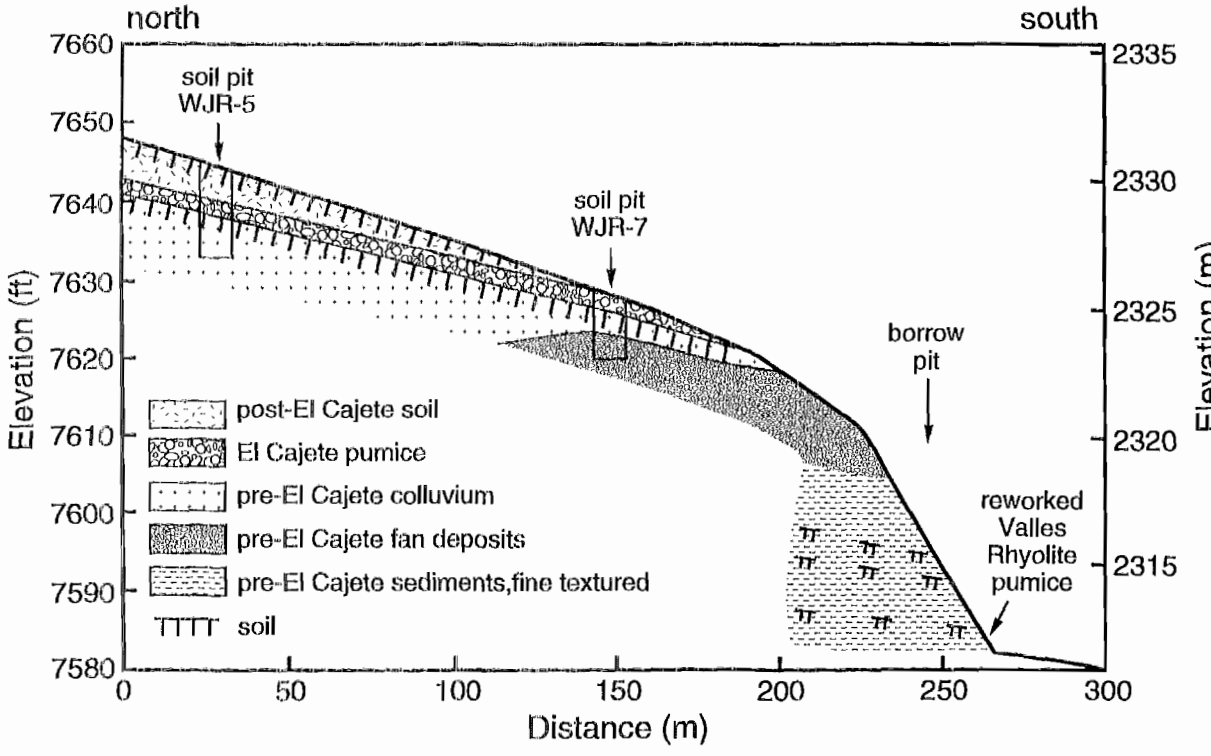

Fig. 2-6. Schematic cross section showing stratigraphic units exposed east of West Jemez Road at Stop 2-2.

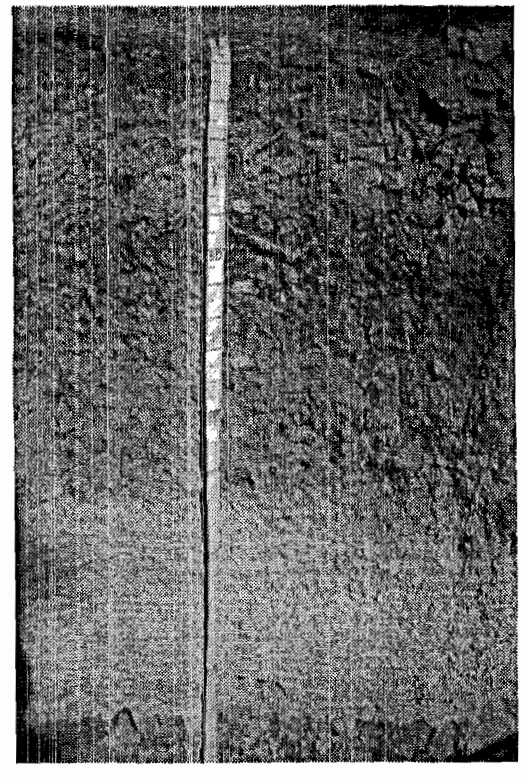

Fig. 2-7. Photograph of WJR-5 soil at Stop 2-2a. Change in color at ~40 cm is Bt1-Bt2 boundary. Light colored El Cajete pumice in lower 1/3 of photo displays pronounced lamellae (tiger-stripping). Top of 3EBtb horizon is dark grey zone at base of view.

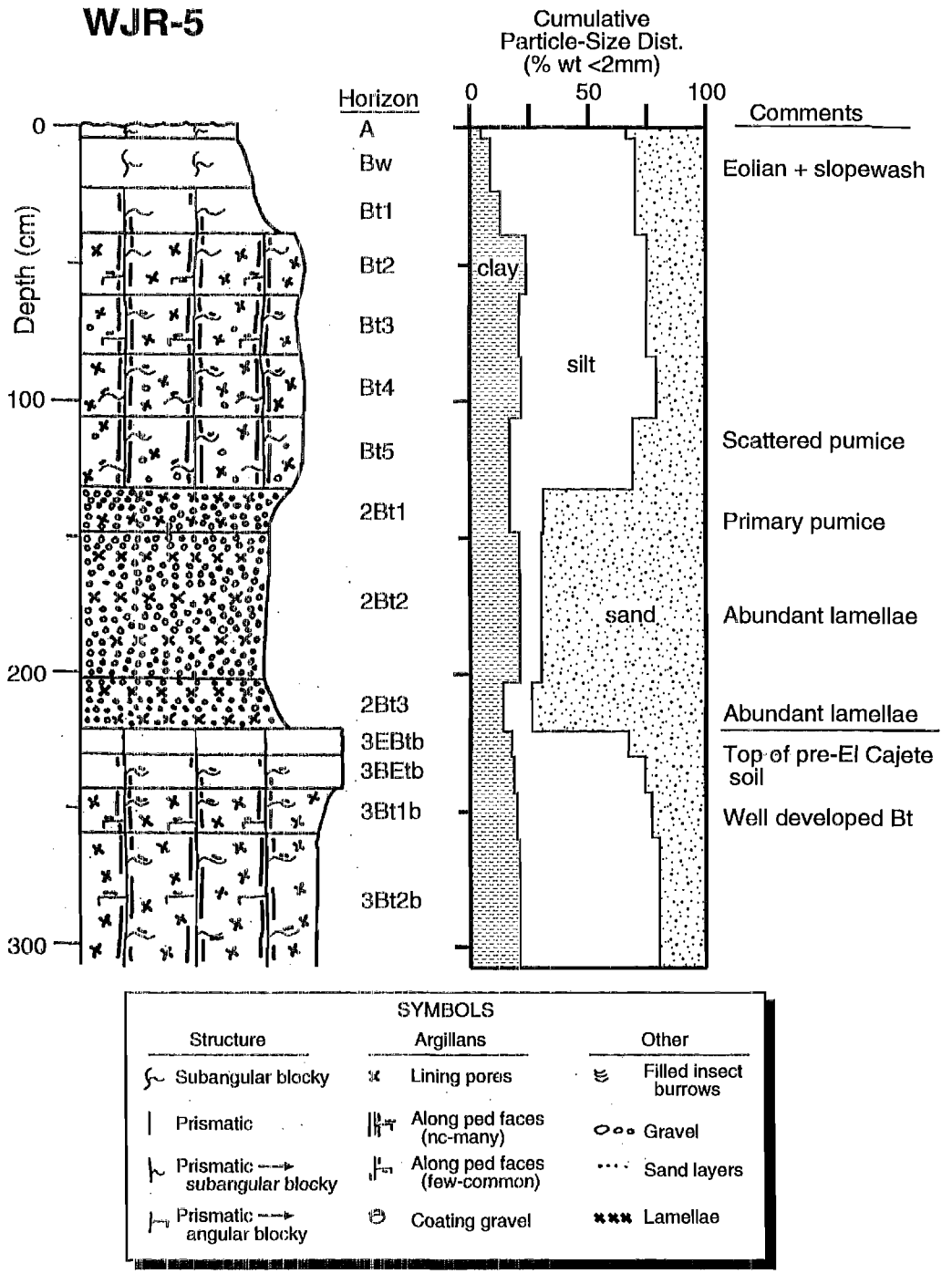

Fig. 2-8. Schematic diagram of soil-stratigraphy for profile WJR-5. Number following "b" refers to the number (stratigraphic position) of the buried soil. Extension of soil column to right indicates an overall greater degree of soil development.

Soil formed in sediments overlying the El Cajete pumice. The soil formed in the post-El Cajete deposits has an A-Bw-Bt-2Bt horizon sequence (Fig. 2-8; Table 2-1). The A horizon has platy and subangular blocky structure and only a weak accumulation of disseminated organic matter. The Bt horizons have prismatic and subangular blocky structure, 7.5YR to 10YR hues, moderately thick to thin argillans along ped faces and pores, and a total Bt thickness of nearly 200 cm (including 90 cm of pumice). Clay content in the Bt horizons ranges from 13 to 22 % wt. and is highest in the Bt2-Bt4 horizons (Table 2-2).

A nearly complete lack of gravel and predominantly silt loam texture in the A, Bw, and Bt1 horizons suggest that these horizons (A-Bt5; Fig. 2-8) were probably derived from both deposition of eolian materials and fine-textured slopewash from nearby hillslopes. Argillans in the Bt horizons are best developed along prismatic ped faces and large pores (>1-2 mm) indicating significant illuviation of clay from above. A considerable source of accumulated clay in the Bt horizons may be derived from the eolian influx of clay and fine-silt rather than the formation of secondary alluminosilicate clays from in-situ weathering (discussed in more detail below).

The 2Bt horizons that have formed in pumice are structureless (single-grain) and the pumice is, at best, only weakly weathered. Much of the pumice, however, is covered with moderately thick to thin argillans that coat and bridge pumice clasts. Most of the argillans form abundant lamellae 1-3 cm thick producing a tiger-stripped' appearance (Fig. 2-7). The pumice clasts in the 2Bt3 horizon are slightly more oxidized than overlying pumice and contain a noticeable increase in argillans at the base of the horizon. This increase in oxidation and illuvial clay may reflect the episodic blockage of percolating soil water, presumably due to the considerable increase in clay and silt and decrease in pore size in the underlying buried soil. Low silt and high sand contents and low bulk densities in the 2Bt horizons generally reflect the original coarse-grained texture of the pumice. High clay contents of 14 to 21 % wt. and abundant argillans in the 2Bt horizons, however, reflect a considerable illuviation of clay into these horizons.

The El Cajete pumice is largely restricted to depths below 132 cm and consists of a ca. 90 cm thick deposit of primary fallout pumice with minimal reworking. The lack of significant weathering of the pumice and the absence of extensive bioturbation of the pumice bed indicates that the pumice was probably buried soon after deposition of the overlying sediments. Based on the these relations, we interpret this soil as representing about 50-60 ky of soil formation. A date of 8420 ± 60 ^{14}C yr B.P. that was obtained from a depth 0.65 m in the adjacent roadcut is not consistent with the degree of soil development, and is considered, at best, to represent a minimum-limiting age for the soil; the anomalously young 14C date may be related to relatively recent bioturbation . A PDI value of 69.4 was calculated for total soil formation in both the sediment and underlying pumice (53.8 for the soil above the pumice bed). By comparison, PDI values generally range from about 14-23 for soils elsewhere on the Plateau that are about 6-12 ky old. The WJR-5 post-El Cajete soil is used as a key calibration point for developing a soil-chronofunction based on the PDI analysis of soil in Rendija Canyon, about 12 km to the northeast. The development of the soil-chronofunction and associated soils is discussed in more detail at Stop 2-4.

Buried Soil b1. The pumice conformably overlies a well developed buried soil that has an EB-BE-Bt horizon sequence. This soil is described in more detail at Stop 2-2b.

- Walk 100 m down slope to the south to a second reexcavated 1995 soil pit.

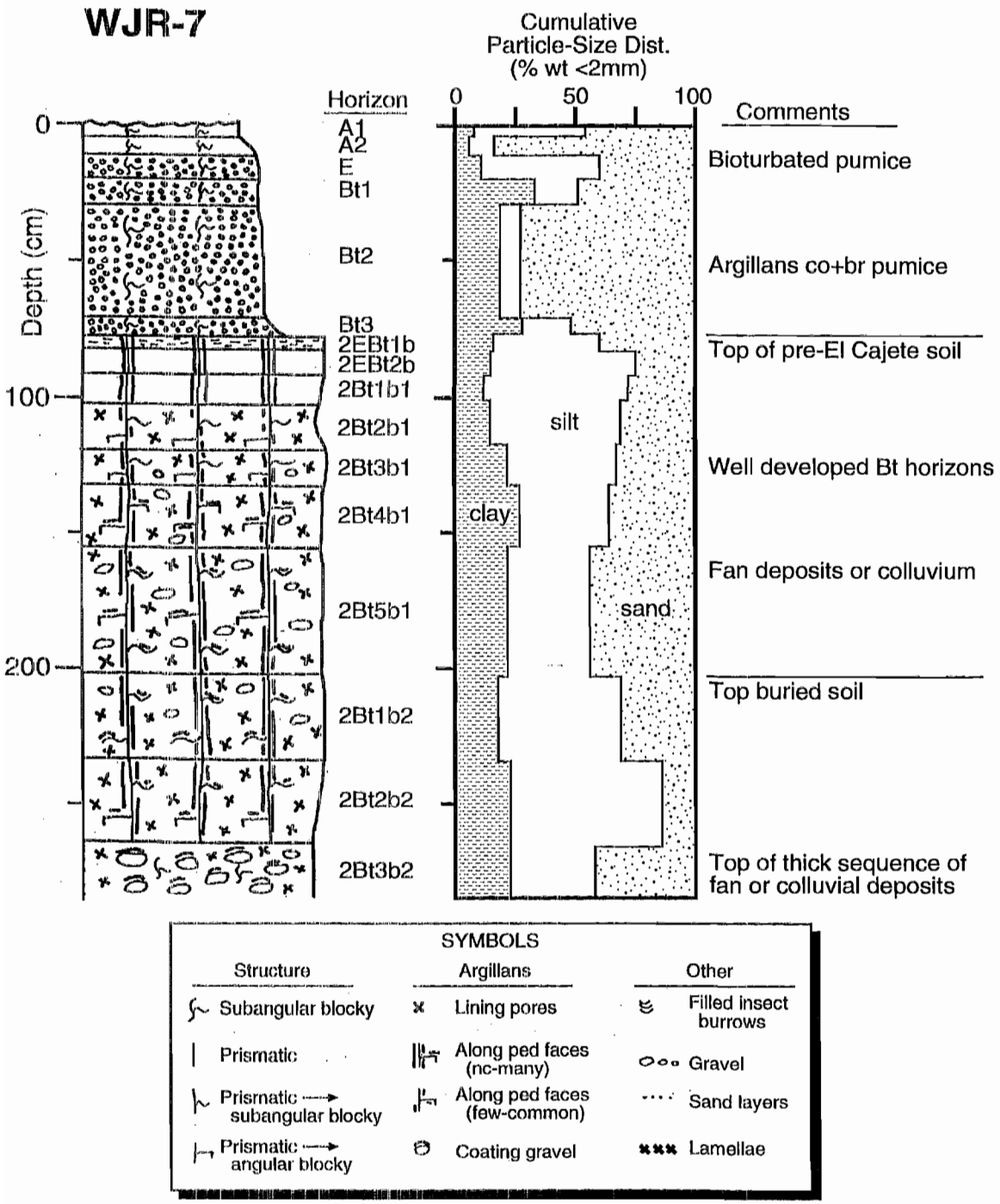

Fig. 2-9. Schematic diagram of soil-stratigraphy for profile WJR-7.

Station 2-2b, Pre-El Cajete soil in soil pit WJR-7

Soil-Stratigraphy of WJR-7. This soil pit exposes a thin surface soil that has largely formed in a truncated layer of the El Cajete pumice that, in turn, conformably overlies a well developed buried soil (Fig. 2-9, Table 2-2). The pre-El Cajete landscape at this site consisted of an old fan, derived from a small unnamed drainage off of the Pajarito fault escarpment, that is dominated by clasts of welded Bandelier Tuff.

Surface Soil. The surface soil consists of an A-E-Bt horizon sequence. The largely unbioturbated pumice that makes up this soil, and lack of the 1+ m thick layer of soil that overlies the pumice up slope at the WJR-5 site, suggests that the overlying soil at this location has been (recently?) stripped by surface erosion. The pumice-rich horizons in the current surface soil, therefore, were probably equivalent to the 2Bt horizons in the WJR-5 soil. Abundant evidence of surface erosion, including rills and small head-cuts, can be seen near the pit.

The A horizon has formed in bioturbated pumice that appears to be mixed with abundant silt. The light colored E horizon, also formed in bioturbated pumice, is weakly weathered and lacks argillans. Clay content in the E horizon is about 11 % wt., whereas clay in the underlying Bt1 horizon is about 33 % wt. This difference in clay content indicates that considerable clay has illuviated into Bt1 horizon from overlying soil horizons (and probably from overlying soil horizons before stripping). Considerable increases in extractable Al, Fe, and Si in the Bt1 horizon relative to the E horizon also indicate that significant illuviation of soil constituents into the Bt1 horizon has occurred (Table 2-3). Eluviation of soil-constituents from the E horizon in this soil is probably greatly enhanced because of the prior existence of abundant coatings of Fe-oxides and clay on pumice exteriors, which provides a ready source of eluvial materials. In addition, the coarse-texture of the pumice-rich soil will allow for rapid infiltration and percolation of soil water, enhancing leaching conditions within the E horizon.

Three Bt horizons have formed in deposits of pumice that are weakly bioturbated. These horizons have nearly continuous to patchy argillans bridging and coating pumice. The overall degree of argillans is greater than the development of argillans in the 2Bt horizons in the pumice bed in the WJR-5 soil. Increased accumulation of clay also appears to have covered pre-existing lamellae, which are only weakly preserved within these Bt horizons. An increase in illuvial clay probably reflects enhancement of clay accumulation as the pumice-rich soil becomes increasingly closer to the soil surface during stripping of the overlying soil. Accumulation of clay from *in situ* weathering is not considered a major source of clay because the pumice is only weakly weathered. A lack of considerable weathering is also supported in part by low concentrations of oxalate-extractable Si (Si_o) and dithionite-extractable Fe (Fe_d). The Bt3 horizon is a thin horizon that overlies a pre- El Cajete soil. Accumulation of illuvial clay has been enhanced at the base of the pumice (Table 2-2), presumably due to a decrease in soil permeability in the underlying soil. A 1 cm thick root mat has formed between the pumice and the underlying soil.

Pre-El Cajete Soil (Buried Soil b1). The dominant soil exposed in this pit (and along the adjacent roadcut) is a typical example of the well-developed buried soil that commonly underlies the El Cajete pumice at numerous localities across the Pajarito Plateau. As discussed earlier, this soil indicates that a considerable period of landscape stability and soil formation occurred before deposition of the pumice.

The top of the soil contains two EB horizons (2Ebt1b, 2Ebt2b) that have prismatic structure that parts to platy structure in places. The relatively light color of these horizons, especially within ped interiors, reflects the primary color of the parent material and original (i.e. pre-burial) color of the

horizon. Although not seen here, nearly continuous skeletans coating ped faces occur in the Eb horizons that underlie the pumice at the WJR-5 soil site. Extractable Al, Fe, and Si also do not show depletion, but rather enrichment of soil oxides, relative to underlying Bt horizons; however, nearly continuous argillans and coatings of Fe-oxyhydroxides along ped faces and pores reflects post-burial enrichment of illuviated materials in these E horizons from the overlying soil. High bulk densities (1.6 to 1.8 g/cm^3; WJR-5, WJR-7, Table 2-2) and very hard dry and firm moist consistence indicate that these horizons have undergone considerable transformation after burial. The abundant silt and the lack of gravel in these horizons suggests that much of the soil matrix may have been initially derived from eolian sediment.

A 100+ cm thick sequence of well developed Bt horizons underlies the EB horizons. These horizons have prismatic structure and subangular blocky structure, 7.5 YR hues, and nearly continuous to patchy argillans coating ped faces and pores. Clay content in the Bt horizons ranges from 12 to 27 % wt. Higher concentrations of Fe_d oxides relative to Fe_o oxides indicates a predominance of more crystalline forms of Fe oxides. Concentrations of Fe_d that are higher than Fe_d in s weak soil formed on nearby Holocene fan deposits (WJR-6, Table 2-3), also indicates considerable development of more crystalline pedogenic Fe oxides. A decrease in the ratio of dithionite-to-oxalate extractable Fe is thought to represent an increase in crystalline forms of Fe oxides relative to poorly crystalline forms (Schwertmann and Taylor, 1989). Fe_o is also lower in the buried soil relative to the overlying surface soil. The abundance of clasts and sand rich in quartz and sanidine increases systematically to a depth of about 200 cm (base of 2Bt5b1 horizon, Fig. 2-9). The parent material for this soil probably consists largely of alluvium and slopewash shed from the nearby scarp to the west.

Source of Accumulated Clay. Most of the argillans occur along better developed ped faces and pores, especially with diameters of about 1-2 mm or larger, indicating that most of the clay has probably accumulated by translocation from overlying horizons. The principle source of accumulated clay is most likely dust and additions of fine-textured slopewash to surface horizons rather than considerable chemical alteration of the soil matrix. A similar conclusion regarding the slight degree of chemical weathering for mesa top soils and importance of eolian sources of clay was also suggested by (McFadden et al, 1996; Eberly et al., 1996).

Given the abundance of easily weathered, silicic volcanic materials in these soils, the development of strong Bt horizons, and a semi-arid-to-sub-humid climate, we are interested in determining how, and to what degree, chemical alteration has occurred in these soils. Generally low concentrations of oxalate-extractable Al and Si suggests that minimal *in situ* formation of allophanic clays (allophane and imogolite) has occurred. The production of allophanic clays, however, in these soil may be limited due to lack of sufficient percolation of soil water. Production of allophanic clays appears to increase when there is sufficient precipitation and/or soil percolation rates that provide leaching >200 mm/year (Parfitt et al., 1984; Wada, 1989). Production of halloysite is favored in soils formed in silica-rich volcanic materials under semi-arid conditions (Parfitt et al., 1984; Dixon, 1989). Preliminary XRD (X-ray diffraction) results for a few of the horizons in the WJR-5 and WJR-7 soils indicate a strong peak at about 0.71-0.72 nm indicating that kaolinite may be the dominant clay mineral in these soils. Halloysite, which has a primary peak at about 0.74 nm (Dixon, 1989), may also be present but is difficult to determine based on our initial interpretation of preliminary XRD results. Available soil data strongly suggests that the major source of accumulated clay in the Bt horizons is clay-rich dust and perhaps additions of fine-grained slopewash.

Buried Soil b2. A noticeable decrease in tuff fragments and an increase in silt content suggest that a second buried soil begins at about 203 cm. This soil is largely preserved as three Bt horizons that are similar in development to the Bt horizons in the overlying soil. A lack of recognizable features

such as a buried A or E horizons suggest that the top of this buried soil has been stripped. Alternately, recognizable features associated with these horizons may have been obliterated from overprinting of soil features during the formation of the overlying soil. The base of this soil appears to have an uneven contact with a deposit that contains abundant boulders and large cobble of dacite and welded tuff.

- Walk 100 m down slope to the south into an old borrow pit.

Station 2-2c, Early to mid Pleistocene (?) sediments and Valles Rhyolite pumice

Stratigraphy. This borrow pit exposes a 10-m thick sequence of sediments and buried soils that underlie the fan gravels seen at soil pit WJR-7 (Figs. 2-5, 2-6, 2-9). This site has the potential for the longest post-Bandelier sedimentary record within the Pajarito fault zone, although we have just begun to examine the deposits here. The fine-grained nature of most of the section is in striking contrast to the overlying gravel-rich fan deposit, and presumably records some combination of eolian, overbank, and/ or distal colluvial deposition. The presence of multiple buried soils demonstrates episodic deposition of the section. Of particular significance is the occurrence of abundant reworked pumice clasts in a unit at the base of the section which are mineralogically distinct from Bandelier pumices, and which provide the potential for age control for the lower deposits.

Valles Rhyolite Pumice Beds. Pre-El Cajete, post-Bandelier pumice falls and reworked tuffaceous deposits have been recently recognized at a number of sites on the Pajarito Plateau, and may provide valuable early Pleistocene stratigraphic markers for units associated both with faulting and with drainage evolution on the Plateau. These pumice beds are believed to be associated with eruptions of the Deer Creek and Valle Grande Members of the Valles Rhyolite of Bailey et al. (1969) and Smith et al. (1970), the post-Valles caldera domes in the Jemez Mountains.

Mineralogic, geochemical, and stratigraphic examination of these pumices (unpublished work in progress by Dave Broxton) indicate that they record the products of multiple separate eruptions. Geochemical fingerprinting (Fig. 2-10) and petrographic characteristics indicate that the most common pumices are probably related to lavas erupted from the Cerro del Medio dome complex. Cerro del Medio lavas have yielded $^{39}Ar/^{40}Ar$ ages of 1.16 and 1.21 Ma (Izett and Obradovich, 1994), very close to the age of the Tshirege Member. Other stratigraphically lower pumices have petrographic characteristics similar to the older Deer Creek rhyolites which were erupted from the floor of the Valles caldera prior to uplift of the Redondo Peak resurgent dome (Smith and Bailey, 1968). Early Pleistocene pumice beds, probably from the Cerro del Medio eruptions, can also be examined in a mesa-top paleochannel at Stop 3-4.

- Cross West Jemez Road, walk across ditch and up onto and across late Quaternary fan surface, and drop into incised drainage. Walk up drainage ~50 m to 12-m high bank exposure.

Station 2-2d, Post-El Cajete fan

Stratigraphy, Age, and Geomorphic Significance. This site is along a minor unnamed tributary to Water Canyon near the base of the Pajarito fault escarpment (Fig. 2-5), which heads in Bandelier Tuff ~1.7 km to the west. The stream bank exposes, from top to bottom, 6 m of rocky fan deposits, 2 m of El Cajete pumice, and 1+ m of fan deposits (Fig. 2-11). Although poorly exposed, the upper fan deposits appear to record a single stratigraphic unit and a major late Quaternary aggradation event.

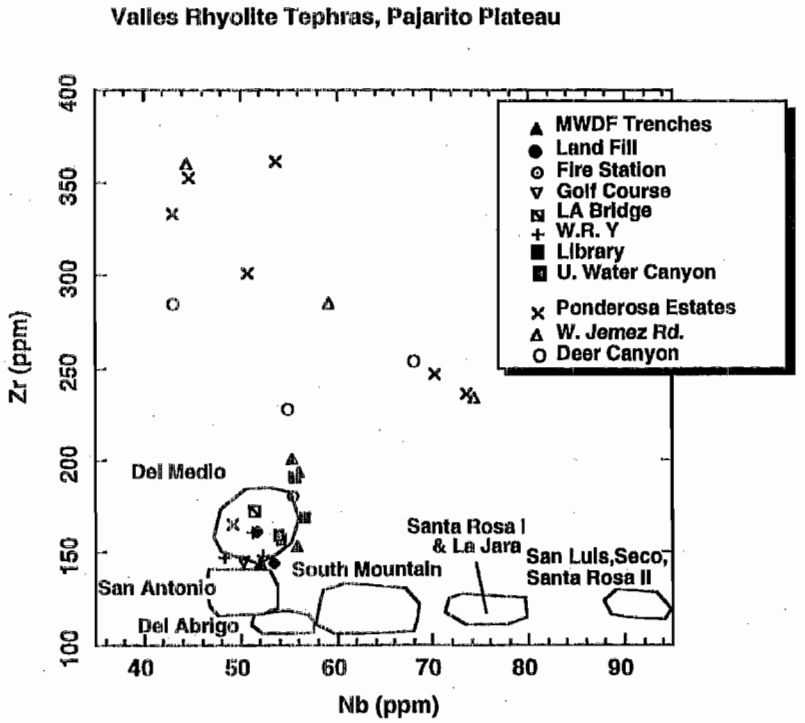

Fig. 2-10. Plot of Nb vs. Zr for samples of post-Bandelier pre-El Cajete pumice beds from the Pajarito Plateau, and chemical fields for Valles Rhyolite lavas (unpub. work by Dave Broxton, 1996). This plot indicates that most sampled pumices are associated with the early Pleistocene Cerro del Medio dome complex. Geochemically distinct, stratigraphically lower pumices may be associated with the Deer Creek Member of the Valles Rhyolite. Valles Rhyolite data from Spell (1987).

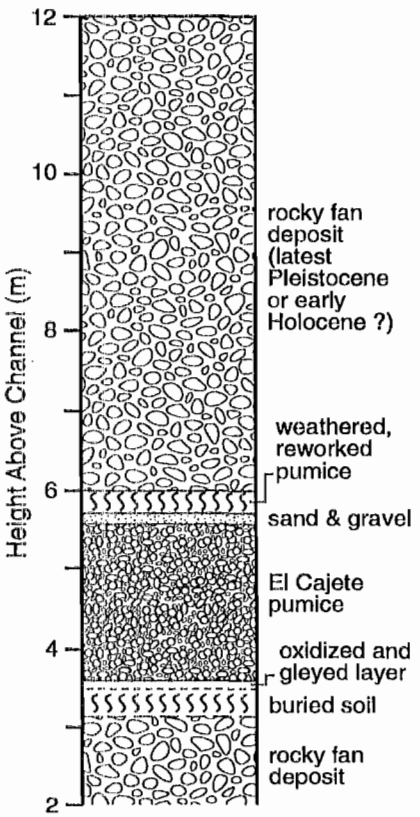

Fig. 2-11. Stratigraphic section showing units exposed in stream bank at Stop 2-2d, west of West Jemez Road.

As with most other late Quaternary units along the Pajarito fault, the upper fan deposit has not been cooperative in yielding reliable radiocarbon age control. Charcoal is rare, and a date of 1110 ± 40 ^{14}C yr BP that was obtained from the base of the fan gravels here is considered highly unlikely. We tentatively correlate this deposit with a terrace along Water Canyon 0.4 km to the south (see discussion at Mile 0.5 on the road log) and a large fan at Cañon de Valle 1 km to the northeast (see discussion at Mile 1.5 on the Log). Radiocarbon age control indicates an earliest Holocene or latest Pleistocene age for the Water Canyon terrace (Wong et al., 1995), and soil exposed in a pit at Cañon de Valle suggests a mid-Holocene to latest Pleistocene age for that deposit..

The post-El Cajete fan demonstrates the highly episodic nature of sediment delivery from the rugged forested terrain west of the Pajarito Plateau, and this supply of gravel-rich sediment has probably contributed to the late Quaternary aggradation experienced along canyons to the east. Although the deposits along the escarpment are not well dated, the sedimentary record in canyons to the east suggests that related aggradation downstream peaked in early or mid Holocene time. In particular, the absence of recognized latest Pleistocene terraces and the occurrence of early Holocene terraces along canyons that head in the Sierra de los Valles such as Frijoles Canyon (Reneau et al., 1993, 1996b) and Rendija Canyon (Stop 2-3), suggests that these deposits along West Jemez Road may also be early Holocene in age. It is also worth noting that the apparent existence of contemporaneous aggradation along lower elevation canyons that head on the Plateau (discussed at Stops 1-2, 1-4, 1-5) and canyons that head in the Jemez Mountains suggests a common climatic control, although age control is not yet sufficient to prove precise synchroneity.

Pre-El Cajete Buried Soil. A thin (<1 m) buried soil underlies the El Cajete pumice. We have not described this soil in detail, but casual observations indicate that this soil has a weak Bt horizon with weak to moderate prismatic and blocky structure, patchy argillans, and evidence of color reddening. The soil also has features associated with soil gleying (light bluish grey colors, mottles) that is probably a result of strongly reducing conditions when soil water is perched at the top of the buried soil. Similar features have been observed beneath the El Cajete pumice at other sites along West Jemez Road, including trenches at Mile 1.2 on the Log.

Surface Soil. We do not yet have detailed descriptions for the surface soil at this site. Initial observations of the soil indicate that it has an A-Bw-BC-C horizon sequence, with an abundance of fines within the upper A and Bw horizons. This soil appears to be very similar to the WJR-6 soil at the mouth of Cañon de Valle (discussed in detail at Mile 1.5 on the Log) which has also formed on rocky late Quaternary fan deposits. Additional soil study sites are planned for other soils formed in young fan deposits along the scarp, such as the one here, in part to refine the geomorphic mapping and to help evaluate possible synchroneity in depositional events between drainages.

- Return to vehicles, and head north on NM 501.

1.1 Road to right is entrance to LANL Tech Areas 11, 16, 28, and 37, all behind a security fence. TA-16 is also called "S-site", reportedly named after a large pile of sawdust left from the old Buckman sawmill which operated from 1897 to 1903. It is a large Technical Area which was an assembly area for the first atomic bombs during World War II, and continues to be the site of active weapons and high explosives (HE) research.

1.2 Large water tanks to left. Colluvial deposits at the base of the escarpment north of these tanks were the site of paleoseismic trenches excavated in 1992 by Woodward-Clyde Federal Ser-

vices (Fig. 2-3; Wong et al., 1995; Olig et al., 1996). This site was chosen partly due to the presence of El Cajete pumice exposed in excavations for the water tanks, and the resultant potential for age control. The pumice bed was not faulted, but small-scale (<0.2 m) offset of colluvial stratigraphy was present in the unit immediately beneath the pumice, providing evidence for faulting shortly before 50-60 ka. Some of the colluvial units underlying the El Cajete pumice could be traced upslope to apparent fissure fills in coarse gravelly colluvium, providing evidence for older faulting. Much of the escarpment here may be composed of large landslides, contributing to the difficulty of constraining the paleoseismic history of the Pajarito fault. These trenches were one of the sites where samples for TL dating of units immediately beneath the El Cajete pumice were collected by Steve Forman (Fig. 2-12; Wong et al., 1995; Reneau et al., 1996a), and soil samples were also collected here as part of a LANL background soil geochemistry study (Longmire et al., 1996; McDonald et al., 1996a; Watt, 1996).

1.3 Bandelier Tuff in roadcut on the left is the toe of a large landslide block.

1.5 Cañon de Valle channel, incised 7 m into a large alluvial fan. The age of the fan is not certain, but soils exposed in a pit excavated north of the channel in 1995 indicate a late Quaternary, possibly early to mid Holocene (?), age (see discussion of soil WJR-6, below), and a possible correlation with the Water Canyon terrace trenched by Woodward-Clyde. Cañon de Valle is intriguing because for 0.7 km east of the Pajarito fault escarpment it has not yet been incised into the Bandelier Tuff on the down-dropped block, and the western Pajarito Plateau in this area

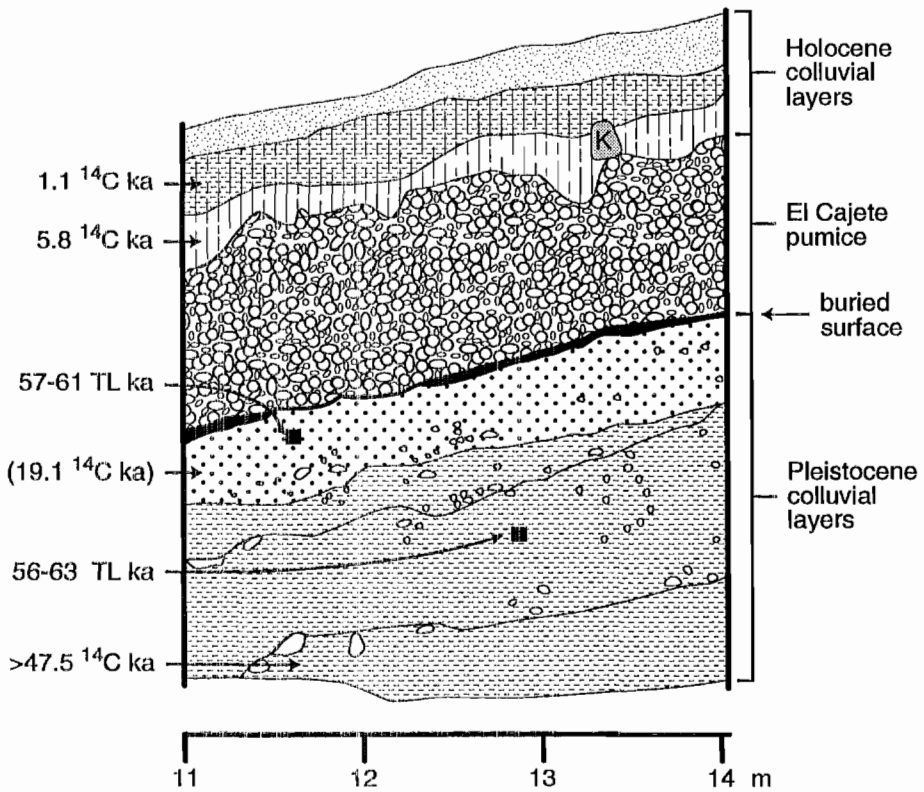

Fig. 2-12. Log of part of Water Tanks Trench 1, showing El Cajete pumice and associated colluvial units, and radiocarbon and TL analyses. 19.1 ^{14}C date below the El Cajete pumice is believed to erroneous. Black layer at the top of the buried pre-El Cajete ground surface is a gleyed and oxidized horizon similar to that exposed beneath the pumice at Stop 2-2d (from Reneau et al., 1996a, modified from Wong et al., 1995).

is mantled by a very extensive area of dacite-dominated alluvium that likely possesses a long and complex (although yet undefined) history. It is possible that the "mesa-top alluvium" that occurs discontinuously across much of the Pajarito Plateau in the Los Alamos area, particularly on the western Plateau, similarly possess a complex history related to varying times of incision and multiple fan-building events, although age control is poor. Cañon de Valle is near the point of maximum apparent offset along the Pajarito fault zone (Fig. 5 in Introduction; Wong et al., 1995; Olig et al., 1996), suggesting that the lack of incision in this area is in part related to the greater amount of down-dropping of the block to the east than at canyons to the north and south.

WJR-6 Soil-Stratigraphy. A weakly developed soil, consisting of an A-Bw-BC-C horizon sequence, has formed in the coarse, rocky fan deposits at the mouth of Cañon de Valle (Fig. 2-13). This soil appears to be very similar to the surface soil that has formed in the post-El Cajete fan deposits exposed at Stop 2-2d.

The soil at Cañon de Valle has a thin, 5 cm thick A horizon that has well developed crumbly structure and noticeable dark coloration due to the accumulation of disseminated organic matter. The Bw horizons have only weak subangular blocky structure, but development of structure is probably limited due to the abundant, large clasts. The texture of the A and Bw horizons appears to have been enhanced from additions of eolian and/or floodplain sediment, with silt contents noticeably higher in these horizons than in underlying horizons. Silans that form nearly continuous to patchy coatings along ped faces and on top of clasts also suggest that considerable contributions of additional silt have occurred. Low concentrations of extractable Al and Si and allophanic clays reflect the overall weak degree of soil formation (Table 2-4). A SDI value of 10.0 suggest that this fan was deposited before about 3.8 ka

2.0 Bandelier Tuff in roadcut to left, possibly the toe of a large landslide complex (?), is overlain by the El Cajete pumice.

2.2 Pond to right, below road, was part of the old Anchor Ranch, a homestead occupied until 1942 when the area was taken over by the government for the Manhattan Project.

2.4 Crest of alluvial fan emanating from an unnamed drainage in the Sierra de los Valles which, like Cañon de Valle, has not yet incised into tuff on this part of the Plateau. Soil pits excavated east of road in 1995 revealed a sequence of relatively thin depositional units at this site 0.3 km from the fan head. Although the history of this fan is poorly constrained, soil-stratigraphy exposed in these soil pits indicated that at least two periods of soil-formation, separated by dacite-rich alluvium, occurred prior-to and subsequent-to deposition of the El Cajete pumice (Fig. 2-14). The degree of development in the surface soil suggest that the last interval of deposition here occurred about 20-40 ka.

2.5 Crest of remnant of old dacite-bearing fan that probably emanated from Pajarito Canyon, 18 m above modern channel. Dirt road to left provides access onto National Forest land.

2.6 Pajarito Canyon channel. Stream is incised 12 m into tuff here, and is 10 m below a narrow terrace of uncertain age. A truncated, clay-rich soil (clay up to 40% by weight) exposed in a pit excavated in 1995 (WJR-2) indicates an age of >50-60 ka for this terrace, although the bouldery nature of the terrace deposit limited the depth of excavation and prevented full examination of the soil. A paleoseismic trench excavated in 1992 by Woodward-Clyde Federal Services on the

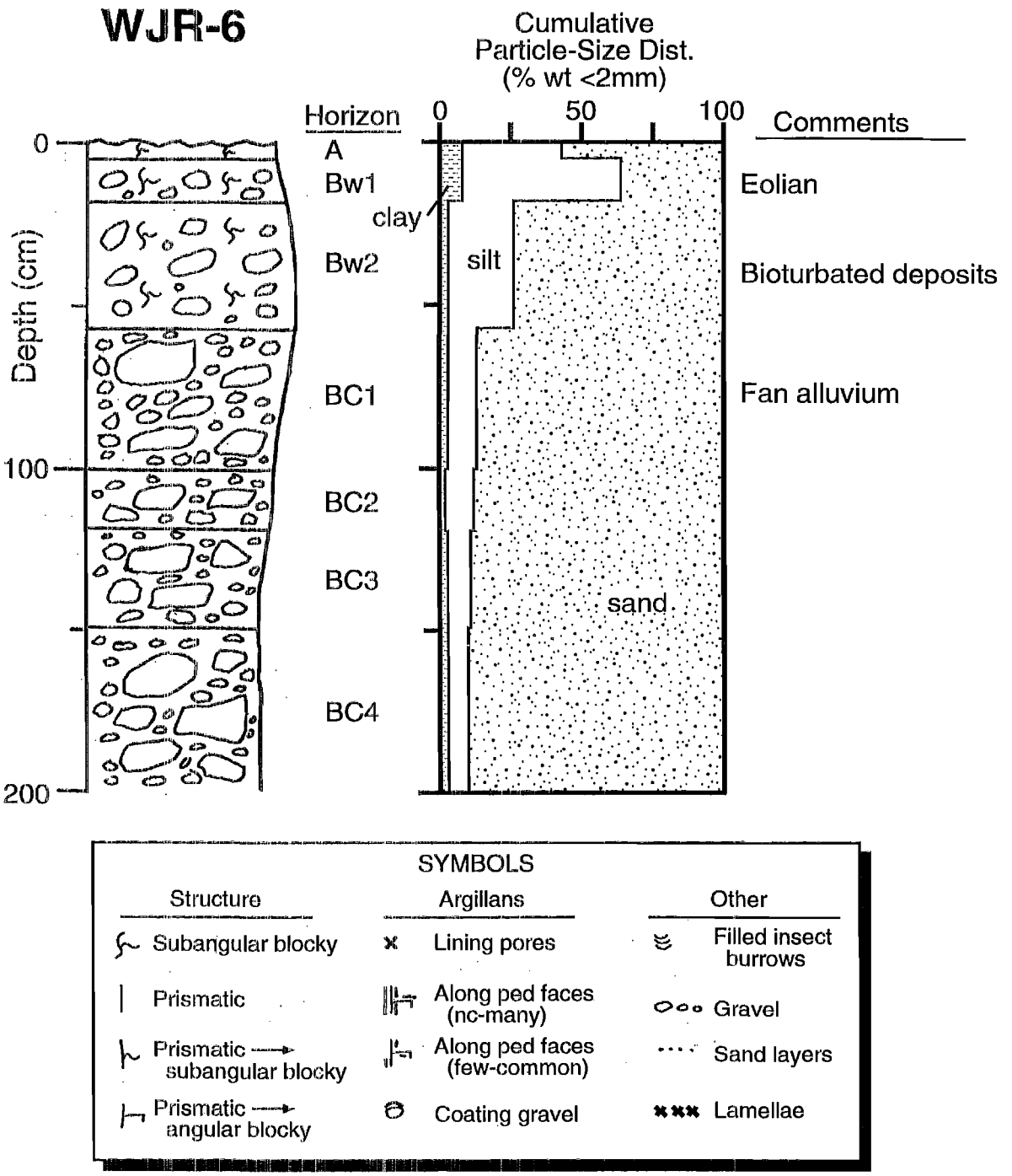

Fig. 2-13. Schematic diagram of soil-stratigraphy for profile WJR-6, Cañon de Valle.

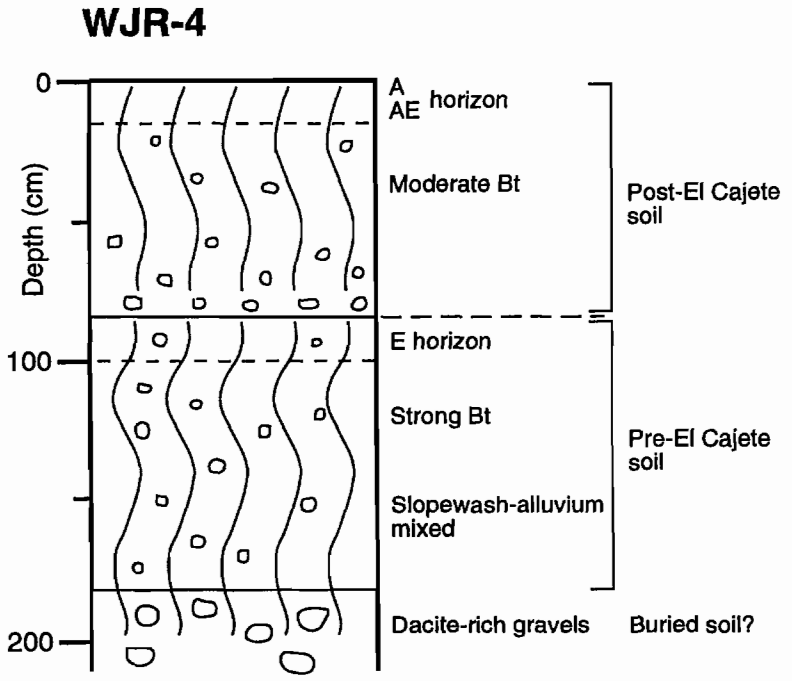

Fig. 2-14. Schematic diagram of soil-stratigraphy for profile WJR-4, on unnamed fan at Mile 2.4 on Day 2 log, showing pre- and post-El Cajete soils.

lower escarpment south of the stream, west of the terrace, revealed some obscure and confusing stratigraphy that was the subject of considerable amounts of debate (Fig. 2-3; Wong et al., 1995; Olig et al., 1996). Faulted dacite-bearing alluvium was overlain by a >4 m thick fine-grained unit that was cut by many small faults and was tilted west towards the escarpment. The origin of the fine-grained unit was particularly puzzling, considering its location at the base of a very rocky slope. A TL analysis by Steve Forman provided an age estimate of 137 ± 22 ka, although the sample was near saturation and the unit could actually be much older, exceeding the limits of the dating method. Dacite gravels eroding out of colluvium along the lower escarpment can be traced south to the area of the old fan at Mile 2.5 on the log, suggesting that these deposits are a faulted part of this fan. Similar dacite-rich gravels are exposed ~30 m higher, on top of the eastern escarpment. As at the other trench locations at the base of the Pajarito fault escarpment, interpreting the paleoseismic history is further complicated by the possible presence of large-scale mass wasting and the presence of additional fault traces to the west.

2.7 Roadcuts expose old pre-El Cajete post-Bandelier pumice beds that are probably derived from eruptions of Valles Rhyolite domes in the Valles caldera. This was one of the sample sites of Dave Broxton (Fig. 2-10). The pumice beds display small-scale faulting, and are overlain by dacite lag gravels that may represent the highest aggradation level of an early post-Bandelier Pajarito Canyon fan, 22 m above the modern stream channel. This fan is apparently cut by a west-facing antithetic fault 80 m to the east.

2.8 Road to right leads to LANL TAs 6, 8, 9, 14, 15, 22, 40, 67, and 69, behind security fences. A large variety of weapons-related research and testing has occurred in this area since LANL was established. At TA-67, on Pajarito Mesa, 1.3 km of trenches were excavated by Woodward-Clyde Federal Services in 1993 to evaluate the potential for faulting at a proposed new waste disposal facility near the southern projections of the Rendija Canyon and Guaje Mountain faults (Fig. 2-3; Kolbe et al., 1994). Although faulting of early post-Bandelier mesa-top alluvial de-

posits and associated pumice beds was recognized, the most recent events occurred prior to 50-60 ka. In addition to providing evidence of local fault history, these trenches provided an exceptional series of exposures of soils and stratigraphy on an undisturbed mesa and evidence for an early Holocene period of enhanced eolian deposition (Kolbe et al., 1994; Reneau et al., 1995b, 1996b).

3.0 Twomile Canyon channel.

3.1 **Camp May Road**, to Pajarito Mountain ski area. Turn left. Pajarito fault splays into many traces in an at least 2 km wide zone in this area, including prominent back-facing down-to-the-west scarps.

3.2 Road passes through eroded area of slopewash or fan deposits within a trough or graben. El Cajete pumice present to right. A soil pit excavated to the left in 1995 (WJR-1) exposed both a pre-El Cajete soil and a post-El Cajete soil sequence similar to that found at several other localities across the Plateau (e.g., Fig. 2-14). The degree of development in the surface soil suggests that the last major interval of deposition on this surface occurred about 20-40 ka.

3.3 Road turns to left, beginning climb up main Pajarito fault escarpment, ~45 m high here. Bend in road is within relatively wide and well-defined graben that extends north to and across Los Alamos Canyon.

3.5 Pocket of stratified, slope-reworked El Cajete pumice exposed in roadcut, beneath colluvium containing slabs of welded tuff in a reddened Bt horizon.

3.6 Volcanic surge beds exposed within densely welded tuff in roadcut to left. Contact of Tshirege units "E and F" of Rogers (1995) (inferred to be contact between Qbt-4 and Qbt-5).

3.8 Road crosses short west-facing step, part of a very dispersed Pajarito fault zone. Area south of road through here possesses relatively thin and patchy soils in a landscape of generally stripped, fractured, welded tuff, with many east-facing steps that are suggestive of relatively small (0-2 m) post-Bandelier fault offsets.

4.3 View into 170 m deep Los Alamos Canyon to right.

4.6 Road climbs hill, across east-facing fault step in welded Bandelier Tuff.

7.2 Pajarito Mountain ski lodge, owned and operated by the non-profit Los Alamos Ski Club. Ski area was originally established in the late 1950s, and now has 5 lifts and 34 runs.

7.6 **Camp May Community Park**, shelters, picnic tables, outhouses. **Lunch stop**. Road turns into 0.5-mi long one-way loop (keep left, parking at various places along the loop road). 9400' elev. in mountain meadows in the headwaters of Los Alamos Canyon, below 10,441' high Pajarito Mountain. Valley heads 1 km northwest on the topographic rim of the Valles caldera. This valley and the rest of the Sierra de los Valles have revealed no evidence of glaciation, and are apparently just below the lower elevational limit of glaciers at this southern latitude, although boulder fields that display transverse ridges and other flow features are present that

suggest periglacial conditions at various times in the Pleistocene (Fig. 2-15). Morphologically similar boulder deposits at similar or lower elevations farther south in New Mexico have been interpreted as fossil Wisconsin-age rock glaciers (Blagbrough and Farkas, 1968; Blagbrough and Brown, 1983; Blagbrough, 1984).

8.1 Camp May shelters. Retrace route to NM 501.

8.4 Pajarito Mountain ski lodge.

11.9 Pullout to right at top of Pajarito fault escarpment is locally called "The Ocean". Views eastward of Los Alamos, the northern Pajarito Plateau, and across the Española basin of the Rio Grande rift to 13,000' high peaks in the Sangre de Cristo Range.

12.5 **NM 501 (West Jemez Road).** Turn left. Roadcut on right side of NM 501 exposes dacite-dominated fluvial gravels deposited on top of the upper part of the Bandelier Tuff, part of a large, possibly early Pleistocene, fan that spread out over the western Pajarito Plateau from Twomile Canyon. Soils collected from a mesa-top trench 0.8 km to the southeast on a highly eroded remnant of this fan (identified by scattered well-rounded dacite lag gravels) possessed the most well-developed soil horizons examined in the LANL background soil geochemistry study (TA-69 site, Twomile Mesa; Longmire et al., 1996; McDonald et al., 1996a; McFadden et al., 1996; Watt, 1996), with a stripped Bt horizon that contained 53% clay. These clay and Fe-rich soils display the highest natural concentrations of trace elements such as As and Be that are of concern in evaluations of potential LANL-derived contamination. The soil sample site was at the location of a very well instrumented field experiment where precipitation, surface runoff, interflow, soil moisture, and isotopic composition of precipitation and soil water have been measured beneath a ponderosa pine forest (Newman, 1996; Wilcox et al., 1996a, submitted). One finding of this experiment was the occurrence of significant amounts of interflow (lateral flow within the soil) during spring snowmelt, apparently through macropores within the clay-rich Bt horizon.

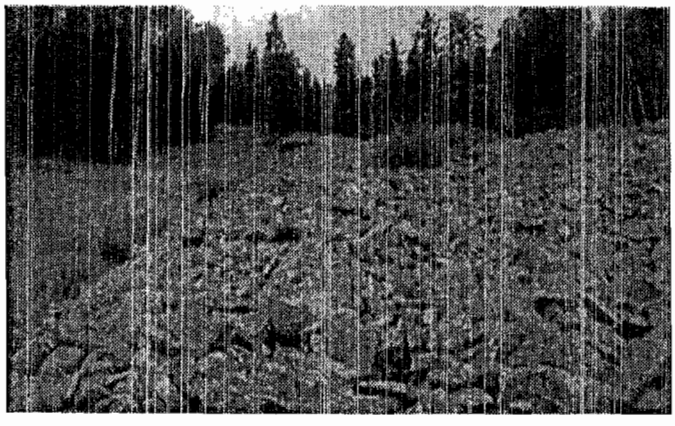

Fig. 2-15. Photographs of blockfield at "Three Fingers" ski run on northeast slope of Pajarito Mountain. This boulder deposit displays lateral and transverse ridges suggestive of flowage under periglacial conditions. Clasts are composed of mostly dacitic lavas of the Tschicoma Formation.

12.6 Upper welded Tshirege Member of Bandelier Tuff in roadcuts. Volcanic surge beds are well-displayed to the left, at the contact of Tshirege units "E and F" of Rogers (1995).

12.8 Road crosses east-facing step in tuff that represents ~10 m of offset of the Tshirege Member on an eastern strand of the Pajarito fault zone.

13.3 Roadcut on left exposes old, fluvially-reworked, pre-El Cajete post-Bandelier pumice beds that are probably associated with eruptions of the Valles Rhyolite. Above the pumice is a lag of scattered rounded dacite gravels that probably represents a remnant of an early Pleistocene (?) Los Alamos Canyon fan.

13.5 West Road to left, dropping into Los Alamos Canyon. Bikini Atoll Road to right leads into part of the main LANL Tech Area (TA-3, home of the Geology and Geochemistry Group). The road was named after the site of early post-war atmospheric testing of nuclear weapons in the South Pacific.

13.7 Stoplight. Continue straight. Pajarito Road to right, leading into LANL TA-3.

13.7+ Stoplight. Continue straight. Casa Grande Road to right leads to main LANL administration building. Stay in left lanes after light.

13.9 **Diamond Drive**. Turn left at stoplight at major 4-way intersection. Road to right joins Pajarito Road which leads to White Rock (6.5 mi), and road straight ahead is East Jemez Road ("Truck Route"), leading 6 mi to Tsankawi (Stop 1-1).

14.1 Center of Los Alamos Canyon bridge ("Omega Bridge"), built in 1951, 55 m above the stream channel. Note that the bridge slopes down to the north; the elevation difference between the mesa tops on opposite sides of the canyon has lead many to suspect the presence of an east-west oriented, down-to-the-north cross fault here (e.g., "Los Alamos Canyon fault" of Rogers, 1995), although no exposures of an east-west fault have yet been identified. 2.7 km down-canyon is the Omega West nuclear reactor at TA-2, a small research facility which began operations in 1956 and which was shut down in 1993 after discovery of a leak in the cooling lines. This leak may have been the major source of tritium which had been detected downstream in the alluvial aquifer. The reactor had been used for production of medical radioisotopes and a variety of scientific purposes (including Neutron Activation Analyses (NAA)). The Omega West reactor was built at the site of earlier experimental reactors, the first dating to 1943 and used by Enrico Fermi and colleagues, and the site is a designated National Historical Landmark. 5.8 km downstream from the bridge is the confluence with DP Canyon, Stop 3-3.

14.3 Stoplight. Continue straight. West Road to left (leading into Los Alamos Canyon) and Los Alamos Medical Center to right.

14.4 Stoplight. Continue straight. Trinity Drive to right (NM Highway 502), leads through the main Los Alamos townsite and "off the hill" towards Santa Fe. 1.0 mi down Trinity, on the left, is Ashley Pond, in the center of what was Project Y of the Manhattan Engineering District during World War II, devoted to developing the first atomic bombs. Ashley Pond is located within the Rendija Canyon fault zone, and may have originally been a sag pond. North of

Ashley Pond is Fuller Lodge, a log building that was part of the Los Alamos Ranch School, a private prep school for boys from 1917-1943. Trinity Drive is named after the Trinity test, the first explosion of an atomic bomb near Socorro, New Mexico, July 16, 1945, on what is now the White Sands Missile Range. Ashley Pond was named after the founder of the Ranch School, Ashley Pond.

14.5 Stoplight. Continue straight. Canyon Road to right.

14.7 Los Alamos High School on right. Los Alamos campus of University of New Mexico to left.

14.8 Stoplight. Continue straight. Orange Street to right. Sandia Drive to left.

15.0 Landfill over Pueblo Canyon channel. 1.5 km downstream is the confluence with Acid Canyon, where effluent containing Pu and other contaminants was discharged from ~1945-1964. Stops 3-1 and 3-2 are 8.5-10 km downstream, where investigations of the present distribution of contaminants are in progress.

15.2 Stoplight. Continue straight. Pueblo Complex to right.

15.6 First Baptist Church to right. Roadcut to left exposes exceptionally thick (up to 1 m) cross-bedded pyroclastic surge beds in upper welded part of Bandelier Tuff. Dune forms in this outcrop display wavelengths of ~2 m and amplitudes of ~0.4 m, with beds dipping up to 35° (Self and Sykes, 1996).

15.8 Stoplight at crest in hill. Continue straight. 38th Street to right. Arkansas Street to left. Good views of ex-government housing in this area, dating to the 1950s.

16.1 Beginning of Los Alamos Golf Course. Golf course built on part of wide alluvial fan complex that emanated from the upper part of Rendija Canyon, and which is preserved on the down-dropped block west of the Rendija Canyon fault zone. Fan deposits include well-rounded dacite-rich gravels and early Pleistocene pumice beds associated with the Valles Rhyolite, and are best exposed in roadcuts in a new subdivision to the north ("Ponderosa Estates", also called the "Cemetery Tracts").

16.5 Golf Course Clubhouse, to right.

16.7 Fire Station, to left.

16.8 Road to Guaje Pines Cemetery and "Ponderosa Estates", to left ("Range Road", unsigned).

16.9 Dip in road, along one trace of the down-to-west Rendija Canyon fault zone. Escarpment straight ahead bounds up-thrown block east of the fault zone.

17.0 **San Ildefonso Road**. Turn left at 4-way intersection. Roads to right and straight lead up west-facing Rendija Canyon fault escarpment onto North Mesa, a residential area of Los Alamos.

17.1 Road climbs to north across head of Bayo Canyon. This canyon was probably in part eroded by the streams that deposited the Golf Course fan, and abandoned after capture by a tributary of the

present Rendija Canyon. The coincidence of the head of the canyon with the Rendija Canyon fault zone suggests that stream capture may have been related to faulting, although many other canyons on the Plateau distant from the main faults also show evidence of capture, and a relation to fault events has not yet been demonstrated.

17.3 Road climbs onto Barranca Mesa, a residential area of Los Alamos. A small pocket of rounded dacite lag gravels in the soil in the roadcut to the left indicates a remnant of a mesa-top alluvial deposit that pre-dates incision of the canyons on this part of the Pajarito Plateau, and presumably pre-dates major displacement on the Rendija Canyon fault.

17.6 **Turn left as road bends right. Sign pointing left to Rendija Canyon and Sportsman's Club.** To the right is Barranca Road. To the left San Ildefonso Road continues east, on left side of "San Ildefonso Play Lot". The residential area to the left is on a narrow "finger mesa", and houses here experienced unusually high intensities from two pathetically small earthquakes in 1991 (Gardner and House, 1994). Local Mercalli intensities of ~V-VI were reported, including the stopping of a pendulum clock, despite moment magnitudes of only about 2 (yes, that's Mw ~2!). The epicenters are poorly defined, but apparently occurred ~6 km north and at a depth of only a few km. The shallow depth, possible funneling of seismic waves along fault zones, and possible topographic amplification may all have contributed to the remarkably high intensities. Because the events were so shallow, the velocity structure models for each station (built into the epicenter location routine) are not valid. Preliminary massaging of the data from each station suggest that both events were located on the Guaje Mountain fault zone.

17.7 Sign indicates Forest Road 57, as the road leaves the residential area. Begin descent down steep hill. Narrow, with sharp curves. Drive carefully.

17.8 Roadcuts in fractured Tshirege Member of Bandelier Tuff. Note red alteration along some of the fractures. Analyses of similar altered zones elsewhere on the Pajarito Plateau have indicated the presence of hematite, a mineral not normally associated with fracture fills in the tuff. This hematite is believed to have formed by early fumarolic or vapor phase alteration as the tuff originally cooled (Vaniman and Chipera, 1995). More typically, fracture filling minerals in Bandelier Tuff on the Plateau are dominated by smectite, with some calcite and kaolinite, and rare halite and gypsum, plus detrital minerals such as quartz derived directly from the tuff. Most of the fracture fills are believed to represent material translocated from surface soils, and not minerals formed *in situ* from weathering of the tuff (Davenport, 1993; Davenport et al., 1995; Vaniman and Chipera, 1995).

18.2 Drainage. Road dips across trace of down-to-west Guaje Mountain fault zone.

18.3 Roadcuts expose dacite-rich fluvial deposits associated with the Rendija Canyon Qt1 terrace, overlying early Pleistocene, pre-Tshirege pumice beds of the Cerro Toledo interval (1.22-1.61 Ma). Soil pits excavated in 1992 and 1995 above the roadcut to the south revealed a partially stripped, eroded soil, hampering attempts to derive soil-based age estimates for this terrace. (Note that the dacite-dominated terrace deposits in this canyon have been misinterpreted as part of the pre-Bandelier Puye Formation by various workers (e.g., Griggs, 1964; Self and Sykes, 1996).)

18.3+ Pavement ends, and road heads east down Qt2 terrace. Short dirt road to left leads to beginning of Pajarito Trail, which heads north for ~4 mi in or near the Guaje Mountain fault zone, and ends at Pine Springs in the Santa Fe National Forest. This is an alternative route into the bottom of Rendija Canyon when the Sportsman's Club firing ranges are active.

18.5 Pistol Range of the Los Alamos Sportsman's Club, to left.

18.6 **Stop 2-3: Rendija Canyon, at Sportsman's Club**. Park at clubhouse on Qt2 terrace. This stop involves an ~2 mi hike in Rendija Canyon with ~150' elevation change (Fig. 2-16). There are multiple points of interest, and we will plan to be out all afternoon. (Note: Firing ranges here are used frequently, so be aware of the limits of the range if this stop is made after the FOP. Thanks to the generosity of the Sportsman's Club, the firing ranges are closed for the day of this field trip.)

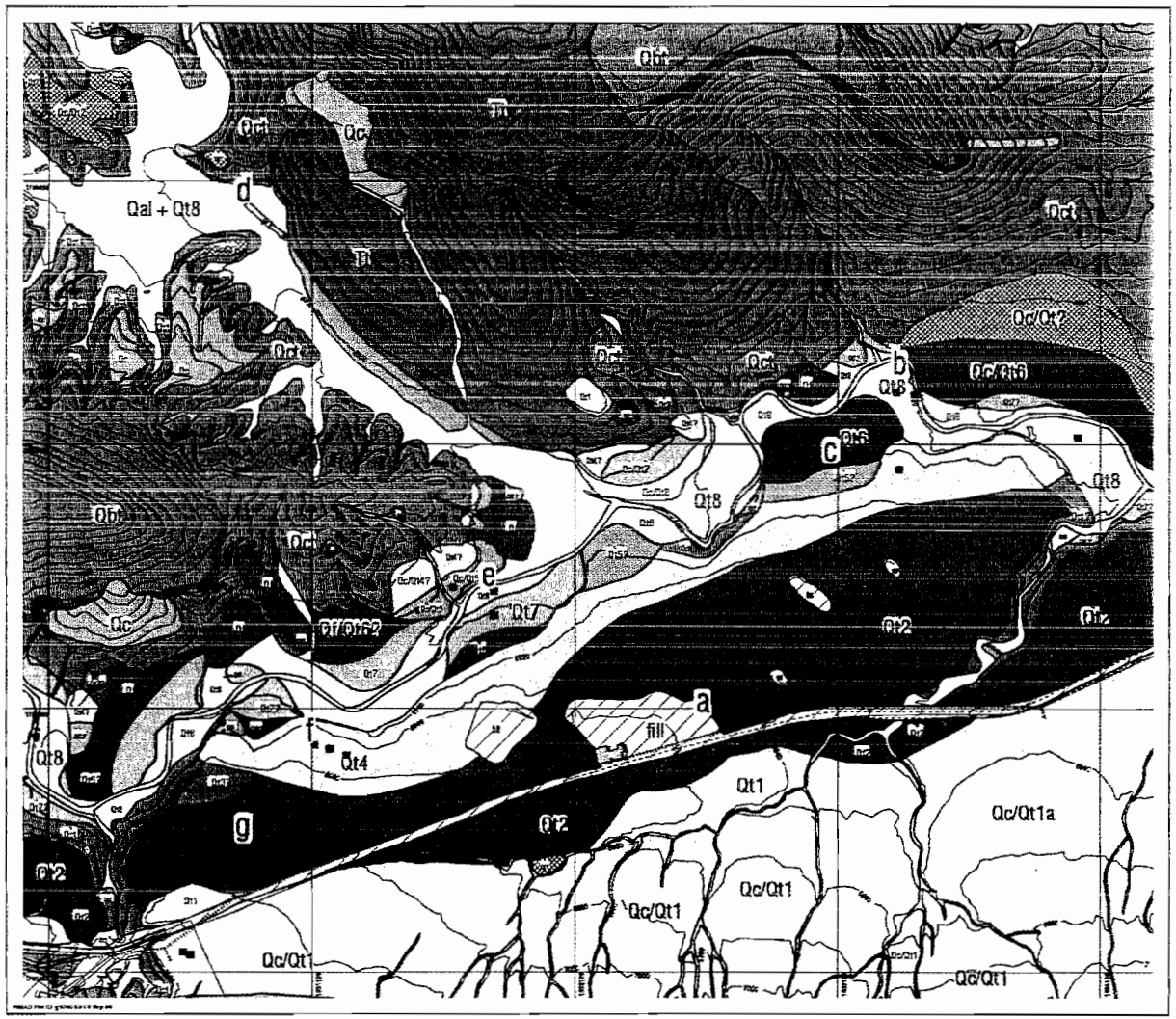

Rendija Canyon, Figure 2-16

LEGEND

- Contours, 2 foot
- Contours, 10 foot(indexed)
- Roads, Dirt
- Roads, Paved
- Water Lines
- Telephone Lines
- Power Lines > 13.2 kV
- Power Lines < 13.2 kV
- Qal
- Qct
- Qbo
- Qbt
- Qc
- Qg
- Qt
- Qc/Qt1
- Qt1
- Qt2
- Qt3
- Qt4
- Qt5
- Qt6
- Qt7
- Qt8
- Qf
- Tpf
- Tt
- fill
- Sites
- Pits

Mapping by S. Reneau. 1996

1996 Rocky Mountain Cell
Friends of the Pleistocene
Field Trip Stop 2-3

State Plane Coordinate System, New Mexico Central Zone, 1983 North American Datum

Grid provides NM State Plane coordinates in feet.
Grid interval, in feet: 1000
Feet per inch on map = 250

SCALE 1:3000

METERS

FEET

NOTICE: The information on this map is approximate. Feature location/extent depends on a single set of surveying field measurements and may not have been confirmed. Los Alamos National Laboratory is based on field information established in 1996. Topo data are from a Maple color 1997 aerial survey. All other data are from various unassessed sets part of the FIMAD repository.

University of California
Los Alamos National Laboratory
Earth and Environmental Sciences Division
FIMAD Facility for Information Management, Analysis, and Display
FIMAD is the electronic data repository for the Environmental Restoration Project at Los Alamos National Laboratory.

Produced by: Matt Rice, Jeff Blossom, Kerry Cummings

Date: September 09, 1996 FIMAD Plot ID: g105083

Station 2-3a: Sportsman's Club, Qt2 terrace (6950', 2120 m elev.)

Geologic Setting. This stop is in an area where several early Pleistocene and late Tertiary units are exposed in the vicinity of the Guaje Mountain fault zone. The rugged topography to the north is the south flank of Guaje Mountain, underlain by dacitic lavas of the Tschicoma Formation, which are dated at ~5 Ma by K-Ar to the north (Aldrich and Dethier, 1990). Guaje Mountain is bounded to the west by the Guaje Mountain fault zone, which has a maximum post-Bandelier offset of ~25-30 m farther north; post-Bandelier offset in this area is estimated at ~15-20 m (Fig. 5 in Introduction; Wong et al., 1995; Olig et al., 1996). The Bandelier Tuff has only partly buried the pre-Bandelier paleotopography in this area, and the Tshirege Member of the Bandelier Tuff is plastered onto the dacites on the south flank of Guaje Mountain (Fig. 2-17).

This stop is below the base of the Tshirege Member, and exposures within Rendija Canyon along our hike are of the Otowi Member of the Bandelier Tuff and of pumice beds of the Cerro Toledo Rhyolite. Both of these units and the overlying non-welded basal part of the Tshirege Member are very easily eroded, and extensive lateral stream erosion within these units has allowed development of relatively broad stream terraces that constitute the best flight of terraces in Los Alamos County. Downstream ~1 km from here, the channel begins incising into Pliocene fanglomerates of the Puye Formation (Fig. 2-18), corresponding to a significant increase in stream gradient and a narrowing of the Holocene terrace belt. In contrast to the basalt knickpoints that provide very persistent base level controls for other Plateau streams, the fanglomerates here apparently provide a "soft" base level control, one that allows maintenance of relatively gentle gradients upstream that in turn facilitates sediment deposition, but that also allows gradual incision and resultant abandonment of former floodplains. These terraces provide: 1) datum for constraining late Quaternary fault offset (rare elsewhere in the Pajarito fault system); 2) a relatively long and detailed record of late Quaternary fluvial history; and 3) a field laboratory for examining soil forming processes and soil development over time.

Stream Terrace Sequence. Rendija Canyon possesses the best flight of stream terraces on the Pajarito Plateau within Los Alamos County, both in terms of numbers and in terms of their preservation and exposure, locally including at least 5 Pleistocene surfaces and 4 Holocene surfaces (Fig. 2-19). These terraces were first examined by Gonzalez and Gardner (1990), and then later by Keith Kelson and colleagues (Wong et al., 1995). The terrace nomenclature we are using is based on that developed by Kelson, modified following more recent mapping and ^{14}C dating.

Tentative age estimates for these terraces were first made by Gonzalez and Gardner (1990), based on "height-above-grade" correlations with an Española basin terrace sequence (Dethier et al., 1988) and ^{14}C dates from Cabra Canyon (Gardner et al., 1990). Age estimates in Wong et al. (1995) were based on limited ^{14}C dating and initial field descriptions of soils exposed in pits, comparing these soils to soil chronosequences elsewhere in the region. These were revised by McDonald et al. (1996b) based on additional ^{14}C dating and on a preliminary Pajarito Plateau-specific soil chronofunction, and we have subsequently made a few additional revisions. Surface designations and age estimates made by these workers and those used in this guidebook are presented in Table 2-5. Note that the most recent soil-based age estimates of the Qt2 and Qt4 terraces are consistent with the initial estimates made by Kelson, providing support for the validity of general regional soil-based correlations (at least as an approximate dating tool). In contrast, the tentative "height-above-grade" method of Gonzalez and Gardner (1990) resulted in some age estimates that were too old (particularly for Qt5), illustrating the uncertainties that can result from assuming constant incison rates between drainage basins with variable geomorphic characteristics.

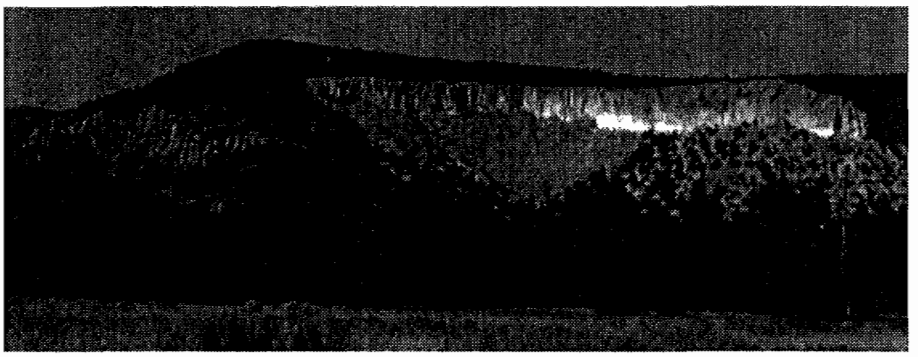

Fig. 2-17. Photograph from near Stop 2-3a in Rendija Canyon. Isolated outcrop of the Tshirege Member of the Bandelier Tuff is perched on dacitic lavas of the Tschicoma Formation on the south flank of Guaje Mountain. The pre-Bandelier topography was only partially buried in this area by the Bandelier Tuff ignimbrites. Guaje Mountain fault is to left (west) of escarpment.

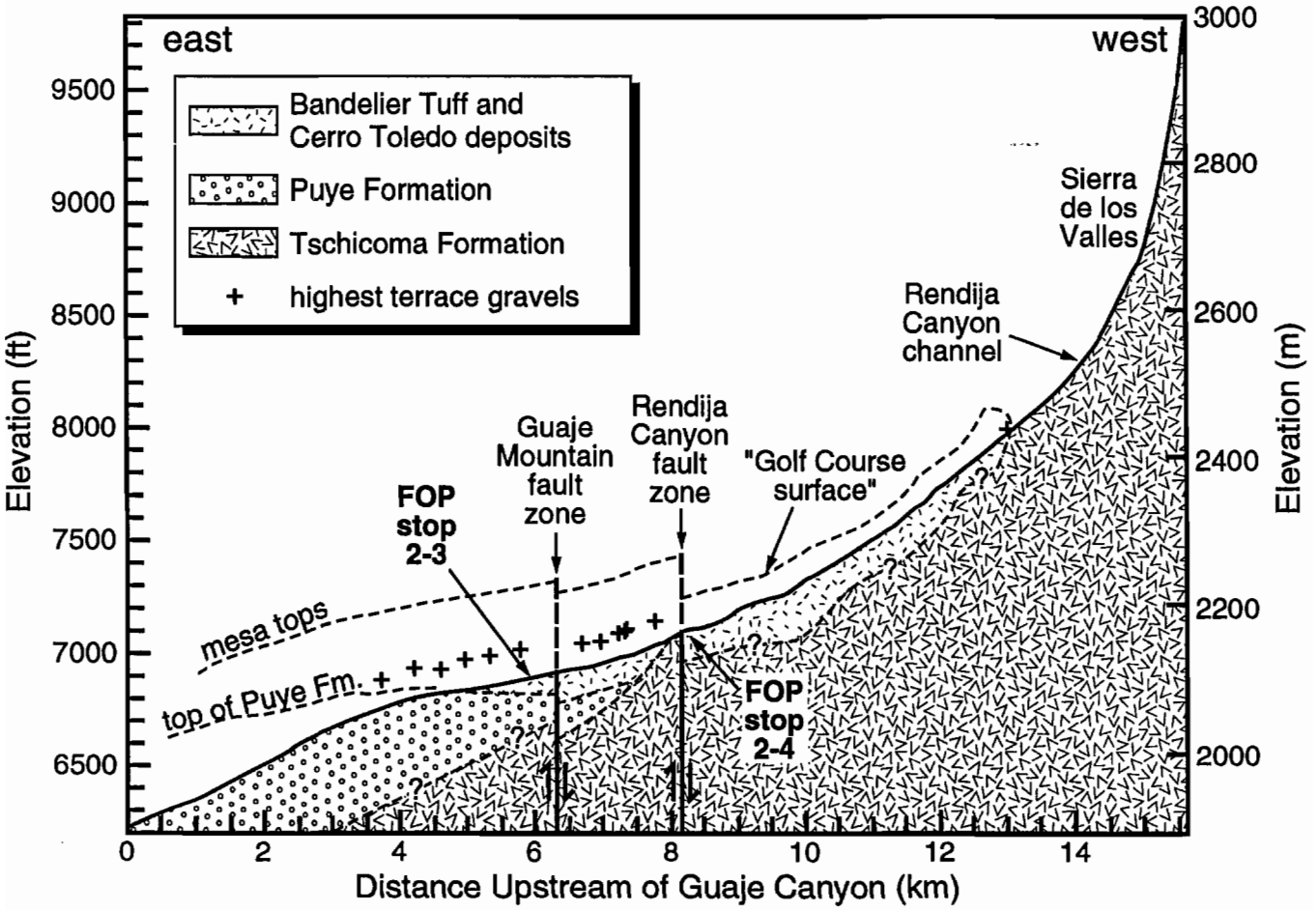

Fig. 2-18. Longitudinal profile of Rendija Canyon, showing generalized bedrock units, faults, and the upper limit of stream terrace gravels. The Bandelier Tuff is buried beneath an early Pleistocene (?) fan below the "Golf Course surface", east of the Rendija Canyon fault zone.

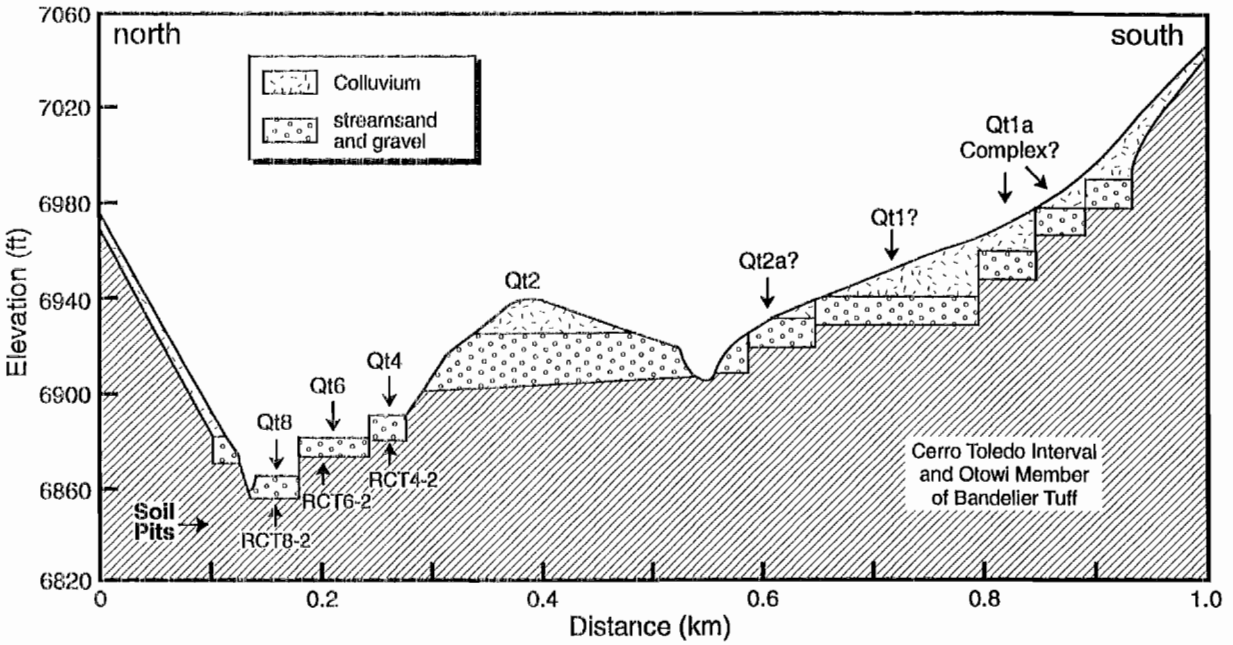

Fig. 2-19. Schematic cross section across Rendija Canyon east of the Sportsman's Club, showing stream terrace sequence. Highest, southern terraces are poorly defined due to burial by slopewash colluvium.

The Holocene terraces (Qt5-Qt8) primarily appear to be strath terraces overlain by 0.5-2 m of channel deposits and variable thicknesses of floodplain deposits and colluvium, although channel deposits occasionally reach up to 3 m in thickness and at least in part record minor aggradation. In contrast, the Pleistocene terraces (Qt1-Qt4) are typically overlain by 4-10 m of gravelly channel deposits, and record more significant aggradational episodes. Many or most of the mapping units may include multiple distinct terraces that have similar elevations relative to the modern channel and cannot be differentiated without precise geochronologic data. The ages of the Holocene alluvial deposits are well constrained by ~30 radiocarbon dates, but no firm radiometric ages are available for the Pleistocene terraces. The terraces converge downstream (Fig. 2-20), suggesting progressive reductions in stream gradient through the late Quaternary, although the possible influence of faulting on these stream gradients has not yet been evaluated.

Paleoseismic History. Work on the age and longitudinal profiles of the Rendija Canyon stream terraces (Wong et al., 1995; Olig et al., 1996), in combination with data from a trench excavated in Cabra Canyon (Gardner et al., 1990), have allowed estimates to be made of the amount and general timing of late Quaternary faulting on the Guaje Mountain fault zone. Vertical offset of the Qt1 terrace is estimated at 2.5-4 m, and of the Qt2 terrace at 1.8-2.5 m, suggesting as much as 2 m of offset in one or more events between Qt1 and Qt2 time, and one or more additional events after Qt2 time (Fig. 2-20). Data from Cabra Canyon indicate that the last event was between ca. 4 and 6 ^{14}C ka (to be discussed at Station 2-3e). Notably, approximate late Quaternary slip rates calculated from the offset terraces, ~0.008-0.027 mm/yr, are similar to the average long-term (post-1.22 Ma) slip rate of ~0.012-0.016 mm/yr calculated for this part of the fault.

- Follow dirt road to northeast across firing range, dropping into the bottom of Rendija Canyon (Fig. 2-16). Road passes by a Qt4 terrace to the east (site of a 1995 soil pit, RCT4-2), and a Qt6 terrace to the west (site of pit RCT6-2, Stop 2-3c'). At the canyon bottom, walk upstream (left) 50 m to a reexcavated 1995 soil pit.

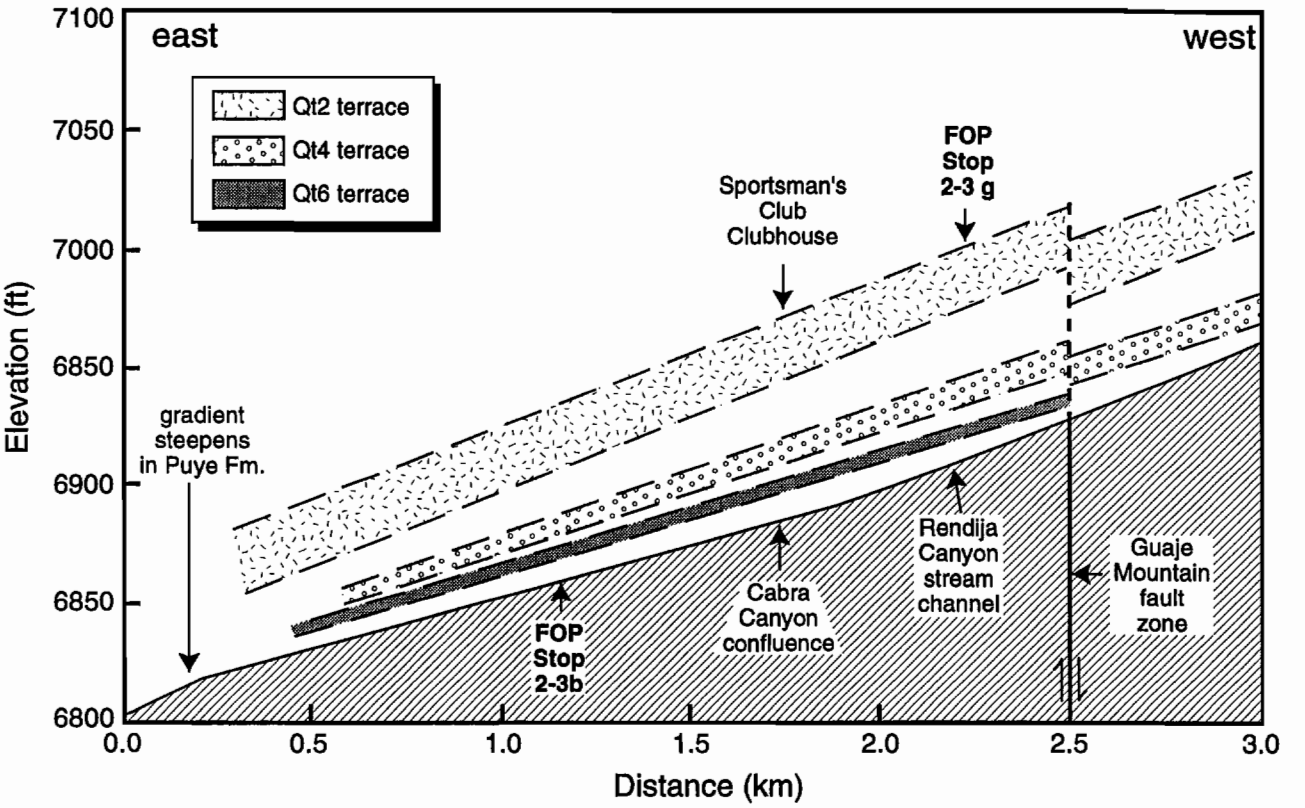

Fig. 2-20. Generalized longitudinal profile of Rendija Canyon near the Sportsman's Club, showing downstream convergence of stream terraces and approximate amount of fault offset. The amount of offset of the mid-Holocene Qt6 terrace is not yet defined.

Station 2-3b: Late Holocene Qt8 terrace; soil pit RCT8-2

Alluvial Stratigraphy and Age. A 2.2-m deep pit into a ~1.7 m high Qt8 surface exposed channel and floodplain deposits that are sedimentologically similar to Holocene deposits elsewhere in Rendija Canyon, although this section is thicker than many and provides evidence for an aggradational event at ca. 500 ^{14}C yr BP (~1430 cal A.D.; Fig. 2-21).

The stream channel deposits are dominated by coarse sand with variable amounts of pebble-to-cobble sized gravel, whereas "floodplain deposits" are typically finer-grained and poorly sorted, dominated by variable amounts of fine-to-coarse sand, pumice fragments, and gravel. Many sections through the latest Holocene floodplains show thin (5-20 cm) well-sorted sand layers of variable grain size (fine, medium, or coarse sand) that probably represent overbank deposition during floods of varying depth. The poorly sorted nature of the typical floodplain deposits probably represents bioturbation of the original flood stratigraphy.

This soil pit fortuitously exposed a paleo-stream bank that was completely buried at ca. 500 ^{14}C yr BP associated with >1.5 m of channel aggradation (Fig. 2-21). A date from the lower part of the buried floodplain deposit indicated an age of ≥1580 ^{14}C yr BP for the buried terrace, similar to a date obtained from another Qt8 terrace 2 km upstream. These relations demonstrate that at least some of the Holocene terraces in Rendija Canyon should be considered "fill terraces", although the thicknesses of associated channel deposits may not be great.

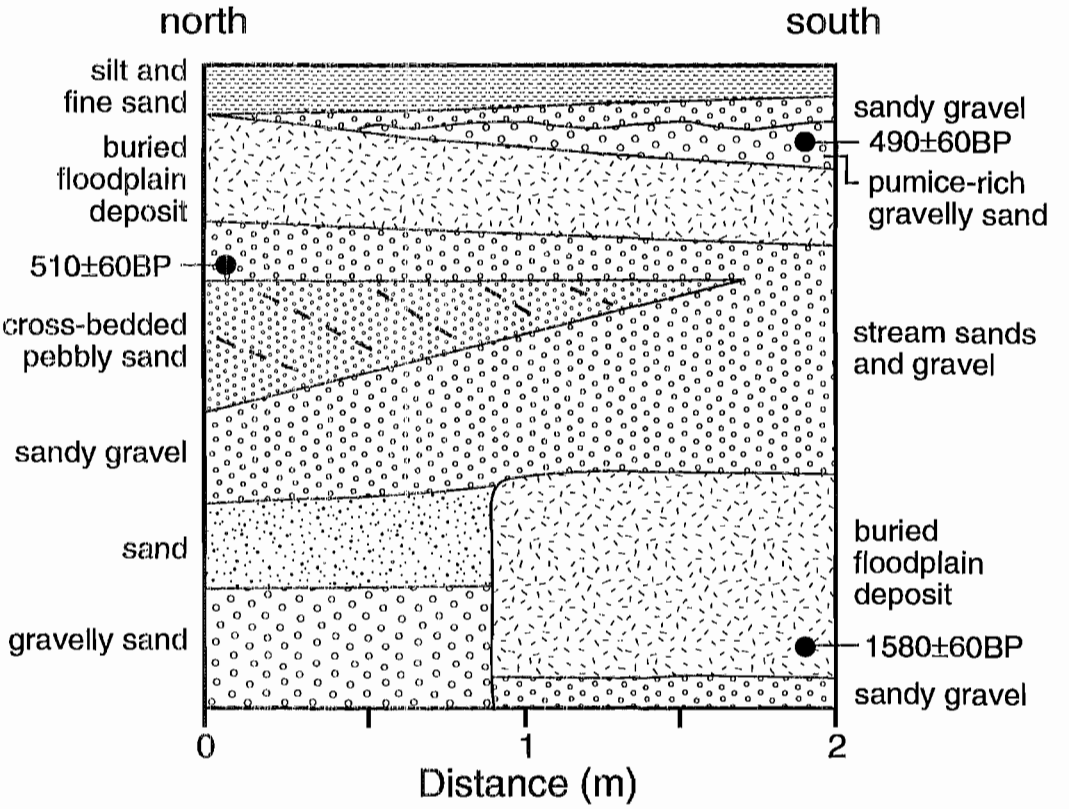

Fig. 2-21. Sketch of stratigraphy exposed in Rendija Canyon RCT8-2 soil pit, 6860' channel elevation, Stop 2-3b. A floodplain deposit that yielded an ~1.6 ^{14}C ka date is buried beneath deposits representing a channel aggradation event at ~0.5 ^{14}C ka. The Qt8 surface is thus at least in part a fill terrace, although the total thickness of the fill may be small.

Qt8 Soil Profile. The RCT8-2 profile (**R**endija **C**anyon **T**errace Qt**8**, Soil Profile **#2**) exposed in this soil pit is similar to those developed on other Qt8 surfaces in Rendija Canyon. The soil generally consists of a weakly developed A-Bw-C profile sequence. The thin (13 cm thick), incipient Bw horizon has weakly developed subangular blocky structure, no cutans, and a matrix color with 10 YR hues that is generally the same as the that of the parent material (Table 2-6). The soil texture within the upper 40 cm fines upward from loamy sand to sandy loam, has a clay content between about 3 to 8 % by weight, and a gravel content of less than about 10-20 % by volume (Fig. 2-22; Table 2-6). By comparison, the C horizons are generally loamy sand to sand and have a clay content less than about 3 % by weight and gravel content of greater than about 20 % by volume. The source of the finer texture within the upper profile is attributed to episodic deposition of fines associated with overbank deposition and local slopewash. Bioturbation (burrowing fauna, root activity) has probably enhanced mixing of the added silt and clay throughout the upper profile. Evidence for more recent deposition of sediment onto a pre-existing soil profile is seen in the A2 horizon, which has a slightly darker color than the overlying A1 horizon, suggesting that the A1 is younger than the A2 horizon.

A PDI value of 4.3 was calculated for this soil. PDI values for two other Qt8 soils of 3.9 and 4.4. These other Qt8 soils have formed in slightly older stream deposits that yielded indistinguishable calibrated ^{14}C ages of about 940 yr B.P. (Table 2-7).

Qt7 Soil Profile. A soil developed on a Qt7 surface (not shown here) generally has a A-Bw-C horizon sequence and displays a slightly greater degree of development relative to the Qt8 soils (Table 2-6).

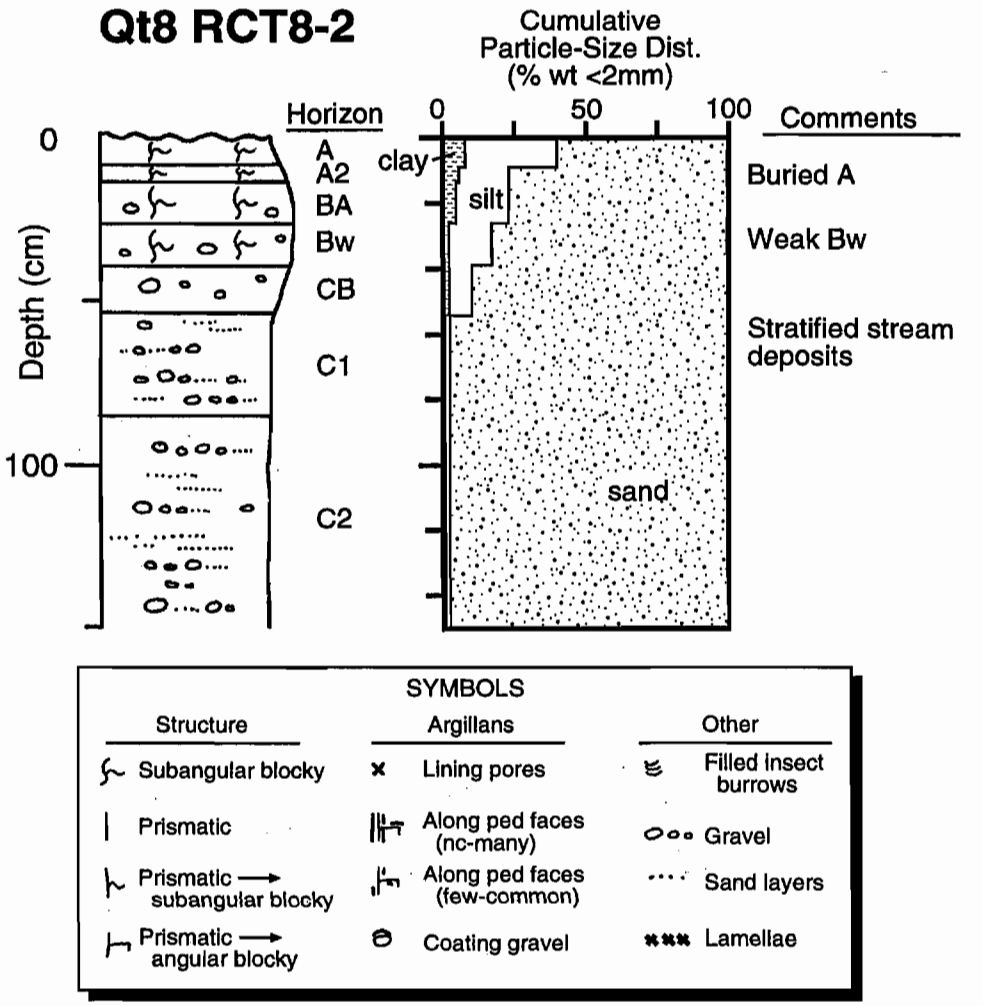

Fig. 2-22. Schematic diagram and particle-size distribution for the RCT8-2 soil profile. Upward fining in soil texture is largely due to episodic overbank sedimentation and subsequent mixing from bioturbation. Soil described along north wall of pit. A2 horizon is buried by more recent overbank deposits.

The soil morphology is generally similar to soils on the Qt8 except that total Bw horizon thickness has increased to 52 cm. Alluvium from a single Qt7 pit yielded a calibrated ^{14}C age of about 3.4 ka (Table 2-7). Mean PDI value for 3 Qt8 soils is 4.2 and a single Qt7 soil yielded a value of 7.6. The studied Qt7 soil has a 8 cm thick layer of colluvium (C horizon, Table 2-6), derived from nearby hillslopes. This layer of colluvium buries the base of young ponderosa pines rooted on the former soil surface defined by the top of the buried A horizon.

- Walk about 80 m upstream to a prominent north-facing stream bank exposure.

Station 3-3c: Mid Holocene Qt6 terrace; stream-bank exposure of strath surface

This stream bank displays a well-exposed cross section through a mid Holocene strath terrace (Figs. 2-23, 2-24). A relatively planar surface cut into tuff is overlain by ~1.1-2.5 m of coarse sands and gravels. This terrace, Qt6, is the widest and most continuous Holocene terrace in this part of Rendija Canyon, and has yielded 5 dates of 5.0-6.3 ^{14}C ka from 4 sample sites within 0.6 km of here (plus one anomalous date of 2.1 ^{14}C ka from this exposure). The available stratigraphic and chronologic evidence suggests that the stream channel elevation in this reach was relatively stable for >1000 years,

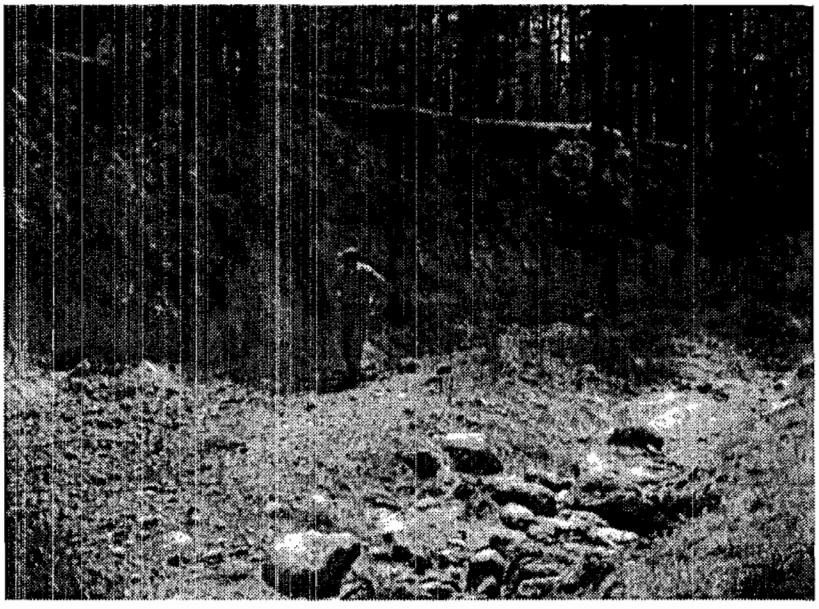

Fig. 2-23. Photograph of 5-m high mid-Holocene Qt6 strath terrace in Rendija Canyon, at Stop 2-3c. Strath surface carved into tuff is overlain by ~1-2.5 m of coarse sand and gravel and ~0.75 m of a sandy, pumice-rich floodplain deposit. Anomalous date of 2.1 ^{14}C ka was obtained from this exposure; all other ages for the Qt6 terrace in this part of Rendija Canyon are ~5-6 ^{14}C ka, including at a soil pit 35 m to the south.

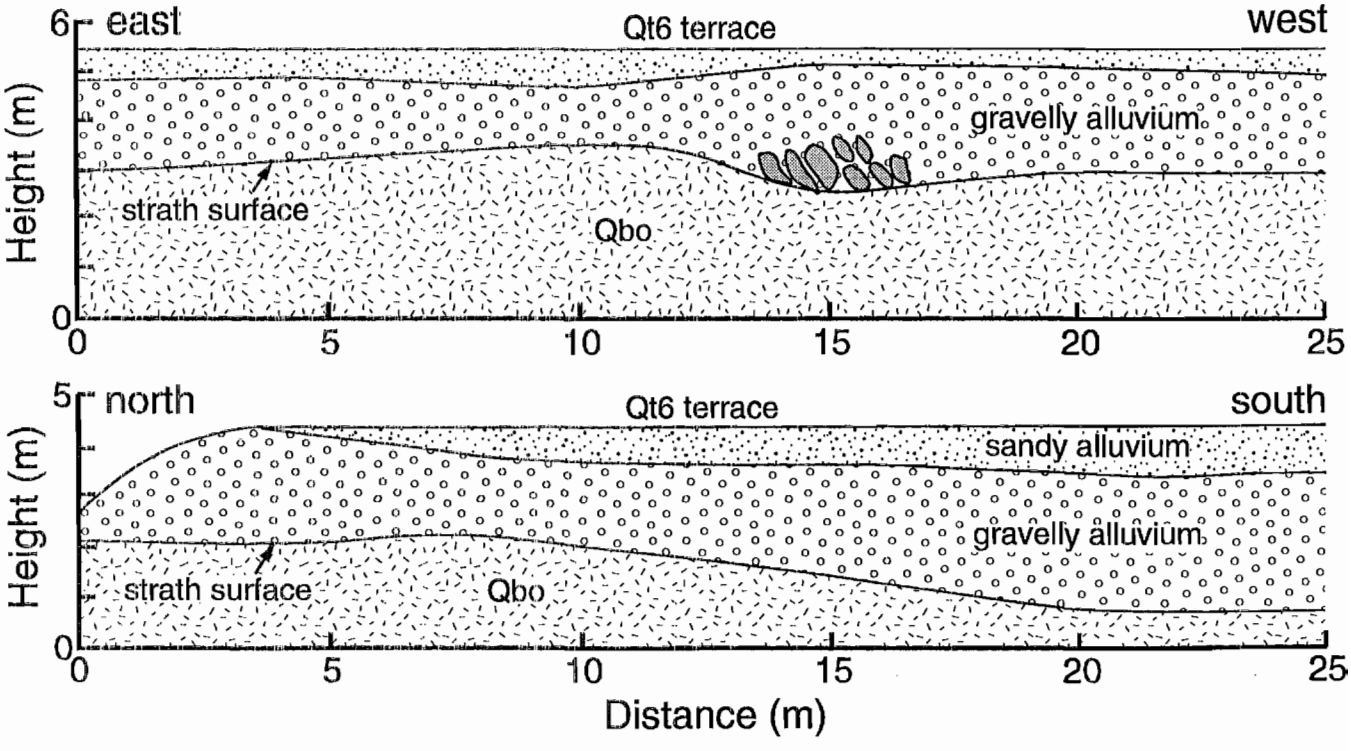

Fig. 2-24. Two cross sections through the mid Holocene Qt6 terrace. The east-west section is at Stop 2-3c, where the terrace is ~5.3 m high and the underlying strath is 2.5-3.5 m above the modern channel. The north-south section is 80 m to the southwest, where the terrace is ~4.4 m high and the strath is 0.6-2.2 m high. The height differences reflect local differences between terrace slope and channel slope. Gravelly stream channel alluvium at these sections ranges from 1.1-2.7 m thick, averaging about 2 m.

allowing planation of the relatively wide strath surface associated with this terrace. Measurements at 4 sites indicate thicknesses of associated channel deposits of ~1-2.7 m, consistent with little or no aggradation associated with formation of this terrace.

- Climb up stream bank, and walk to reexcavated soil pit 35 m to south.

Station 2-3c': Mid Holocene Qt6 terrace; soil pit RCT6-2

Alluvial Stratigraphy and Age. A 2.1-m deep soil pit into this ~5 m high Qt6 surface exposed 0.7 m of poorly sorted sandy floodplain deposits overlying >1.4 m of sands and gravels (Fig. 2-25). The uppermost channel deposits are the coarsest in this section, consisting of a poorly sorted bouldery layer that is similar to the modern stream bed and suggestive of a channel lag deposit. A date of ca. 5.92 ^{14}C ka was obtained from a pumice-rich sand layer at the bottom of the pit, and a second date of ca. 5.28 ^{14}C ka was obtained from a lens of silt, fine sand, and pumice near the top of the boulders at a depth of 0.95 m. The apparent age span between the lower and upper parts of this channel deposit is very similar to that obtained from another Qt6 terrace 0.6 km downstream, 5.98 ^{14}C ka from basal sandy gravels and 5.04 ^{14}C ka from the uppermost part of the channel deposit.

Qt6 Soil Profile. The RCT6-2 profile exposed in this soil pit is similar to those developed on other Qt6 surfaces in Rendija Canyon. The soil generally consists of an A-Bw-C horizon sequence. The Bw horizons have weakly developed subangular blocky structure, no cutans, and a matrix color with 10YR hues that has a slightly higher chroma than that of the parent material (Table 2-6). The Bw horizons in the Qt6 soils are only slightly thicker and have slightly better develop of rubification

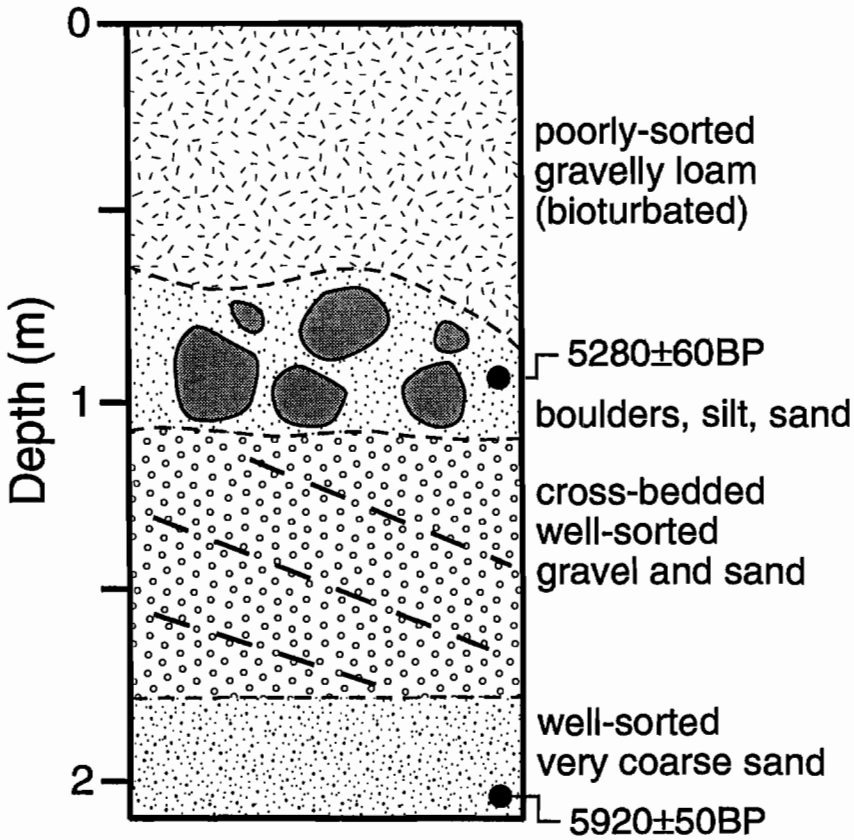

Fig. 2-25. Sketch of stratigraphy exposed in Rendija Canyon Qt6-2 soil pit, 6865' channel elevation.

and structure than the Bw horizons in the Qt7 soil. The soil texture within the upper 60 cm generally fines upward and varies between sandy loam to silt loam, has a clay content between about 9 to 16 % by weight, and a gravel content that decreases upward to less than about 20 % by volume. (Fig. 2-26; Table 2-6). By comparison, the C horizons are generally loamy sand to sand, have a clay content less than about 1 % by weight, and a gravel content of greater than 20-30 % by volume.

There is a considerable increase in clay and silt in the Qt6 soils relative to the younger Qt7 and Qt8 soils. The development of finer texture within the upper soil profile is probably due to additions of silt and clay from overbank and/or colluvial sediments during early stages of soil formation. Evidence for this is the distinct increase in silt content in the BA horizon that suggests that this horizon was a former surface A horizon that has been subsequently buried by a thin layer of overbank or colluvial sediment.

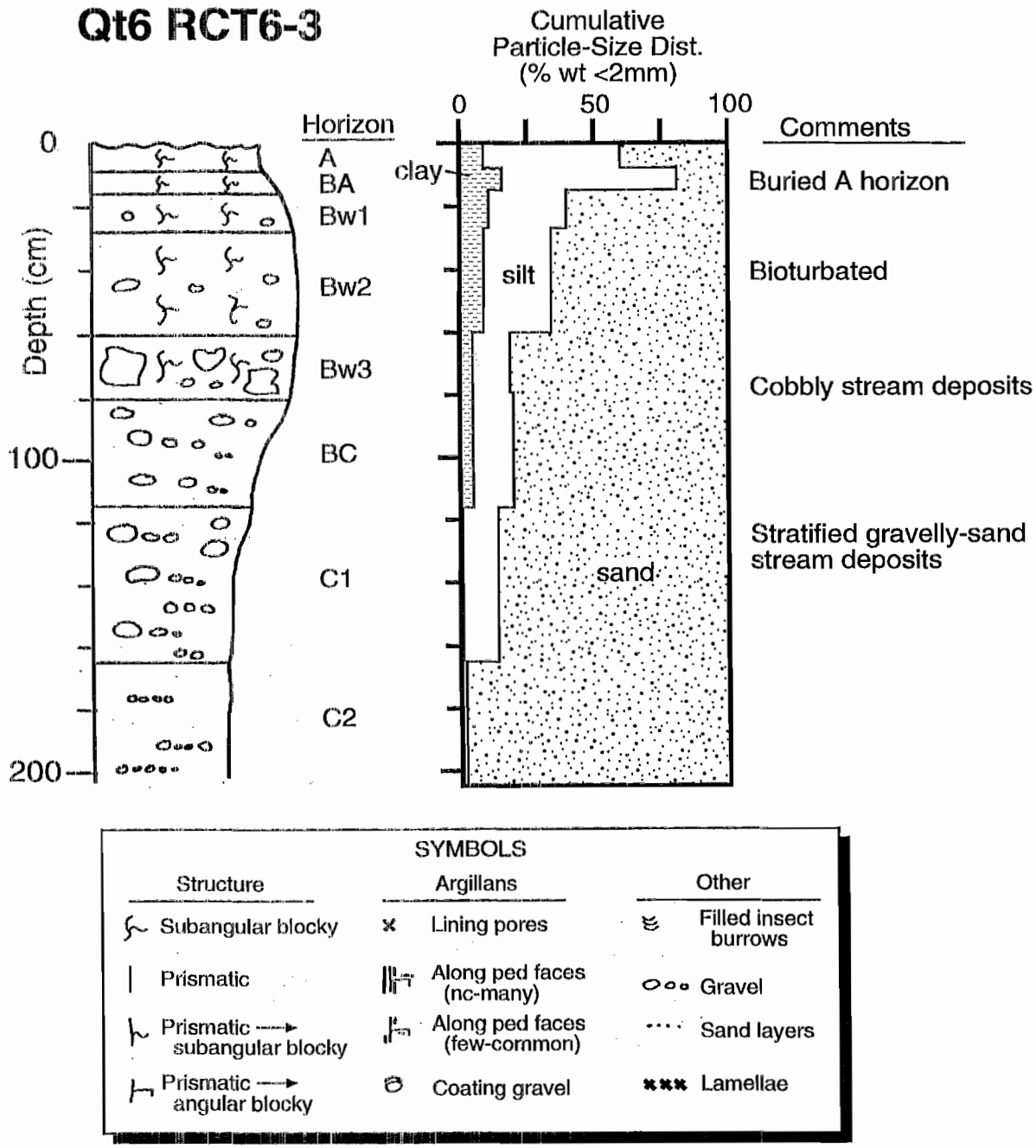

Fig. 2-26. Schematic diagram and particle-size distribution for the Qt6 RCT6-2 soil profile.

The downward decrease in silt and clay through the profile suggests that bioturbation has probably also enhanced mixing of the added fines throughout the upper soil profile.

Best age estimates for deposition of Qt6 stream deposits, based on calibrated radiocarbon ages, are about 5.7 to 7.9 cal ka (Tables 2-5 and 2-7). The younger part of this time period is probably more representative of the time of surface abandonment and initial soil development. A PDI value of 13.8 was calculated for the RCT6-2 soil, and two other Qt6 soils yielded values of 16.1 and 17.3.

- Return to stream channel and hike upstream. Note prominent 6 m high boulder-capped pedestal rock to right (north), formed in the Otowi Member of the Bandelier Tuff (Fig. 2-27). Similar pedestal rocks (also called "tent rocks", "hoodoos", or "precarious rocks") are common in parts of the Pajarito Plateau, developed both in tuff and in the Puye Formation (excellent examples in the Puye Fm. are visible from the road down Rendija Canyon to the east). These rocks have been cited by some as evidence for a lack of significant earthquakes in this area (e.g., Keller, 1968), seemingly contradictory to the more recent evidence for a mid-Holocene surface rupture event on the Guaje Mountain fault (Gardner et al., 1990). Rather than providing evidence for a lack of earthquakes, perhaps they instead provide more evidence for locally rapid rates of Holocene erosion on the Plateau. Another possibility is that ground motions associated with paleoseismic events may have been insufficient to cause many of the capping boulders to topple.

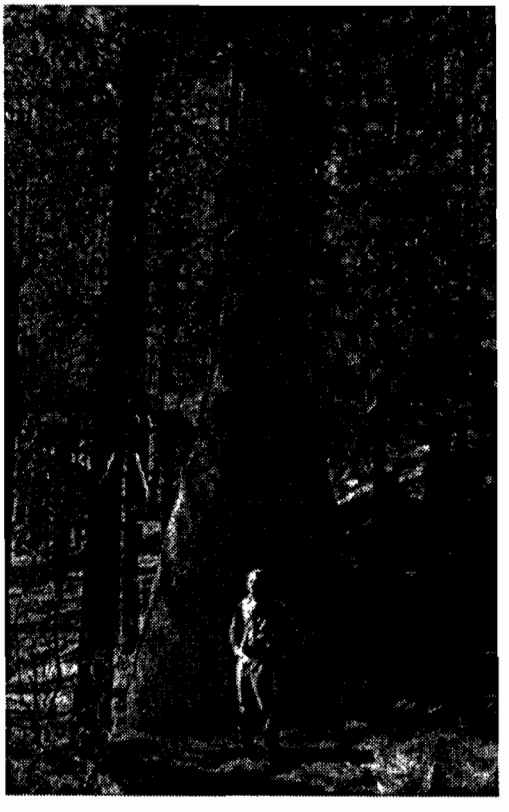

Fig. 2-27. Photograph of boulder-capped pedestal rock in Rendija Canyon west of Stop 2-3c. Otowi Member of Bandelier Tuff forms pedestal.

- ~130 m farther upstream to the left (south), at a sharp bend in the channel, is an exposure of a 5-m high strath surface beneath a Qt4 terrace remnant. ~4 m of channel deposits are present at this eroded exposure. Both the strath and the top of the terrace gravels are lower than for the Qt4 terrace upstream, providing some of the evidence for downstream convergence of terrace profiles (Fig. 2-20) and relatively little incision between Qt4 and Qt6 (discussed at Stop 2-3g).

- At a fork in the dirt road in a broad part of the canyon floor, turn right (north) up Cabra Canyon (Fig. 2-16). Note the lack of an incised channel in Cabra Canyon and the sandy floor, contrasting with Rendija Canyon where a bouldery channel is incised below banks.

- About 0.2 km upstream on the left (west) bank is a terrace remnant buried beneath slopewash. At the left side of the exposure ~0.7 m of coarse sands overlie a fluted tuff surface suggestive of a strath, whereas on the right side 1.6 m of sands and gravel fill a buried channel, suggesting that this terrace in part records an aggradation event (fill terrace). Charcoal from stream sands here yielded a date of 7.9 ^{14}C ka, intermediate between typical "Qt5" and "Qt6" ages.

- Continue walking up Cabra Canyon for about 0.4 km to a major bend to the left. The bend is in the Guaje Mountain fault zone, at the site of a paleoseismic trench excavated in 1987, the first such trench within the Pajarito fault system.

Station 2-3d: Cabra Canyon, site of SHT-1 trench (~6920', 2110 m elev.)

SHT-1. SHT-1 (Seismic Hazards Trench #1) was a 65-m long excavation largely through unconsolidated Holocene sediments that fill the bottom of Cabra Canyon (Gardner et al., 1990). The "trench" was typically about 4 m deep and 5 m wide, and was excavated with a front-end loader instead of the traditional backhoe in order to make it wide enough to meet safety concerns of the time (Fig. 2-28). This location was chosen in part because it is next to one of the few places where the Guaje Mountain fault can be observed in outcrop: tuff, presumably the Otowi Member, is juxtaposed against sheared Tschicoma dacite 100 m up the drainage to the north (Fig. 2-29).

Stratigraphy and Age. Units exposed in the trench were dominated by Holocene alluvium, both coarse channel sands and gravels and "matrix-supported" deposits that were originally interpreted to represent thin debris flows, but that may also represent bioturbated floodplain deposits. Ten radiocarbon dates, generally stratigraphically consistent, were obtained from SHT-1, and ranged from 0.3 to 5.69 ^{14}C ka (Figs. 2-30, 2-31). Underlying units included apparent lacustrine deposits with reversed magnetic polarity that are probably part of the Cerro Toledo interval (1.22-1.61 Ma), and several generations of colluvium that were apparently associated with faulting events.

Paleoseismic History. Evidence of at least 3 paleoseismic events were exposed in SHT-1, with net vertical displacement estimated at 1.5 to >2 m per event (Gardner et al., 1990). The most recent surface-rupture event apparently occurred between ~5690 ± 250 ^{14}C BP and ~3700 ^{14}C BP. The ca. 5.7 ka sediments were in fault contact with the presumed Cerro Toledo beds in the center of the trench, and the fault is overlain by the ca. 3.7 ka sedimentary package. Unfortunately, only one date was obtainable from the faulted unit, but we believe this date is reasonable because: 1) the unconsolidated nature of the faulted sediments indicates a Holocene age; 2) the general internal consistency of the dates from SHT-1 and also in Rendija Canyon indicates minimal problems with sample contamination or recycling of old charcoal in these sediments; and 3) the date corresponds with the well-documented period of deposition of the Rendija Canyon Qt6 terrace, a likely time of sediment deposition in Cabra Canyon as well. Evidence for the older events is provided by the faulted colluvial units near the southeast end of the trench (Figs. 2-30, 2-32), although these events are not dated.

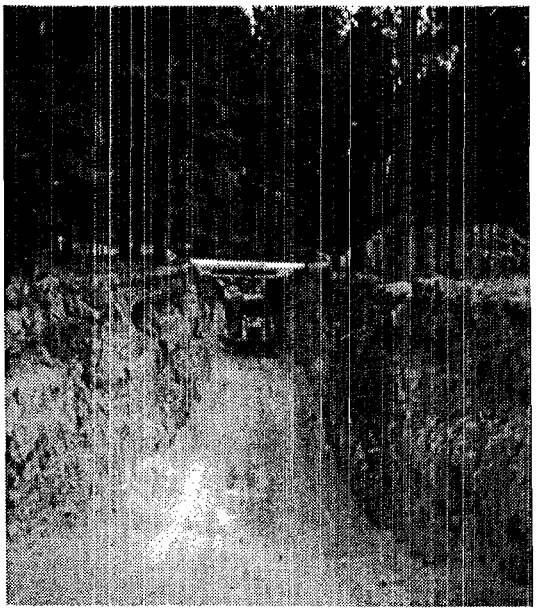

Fig. 2-28. Photograph of excavation of trench SHT-1 in Cabra Canyon, across Guaje Mountain fault zone (with front-end loader for scale) (photo by Jamie Gardner, 1987).

Fluvial History. The well-dated record of Holocene aggradation in Cabra Canyon at SHT-1 provides a strong contrast with the progressive Holocene incison in Rendija

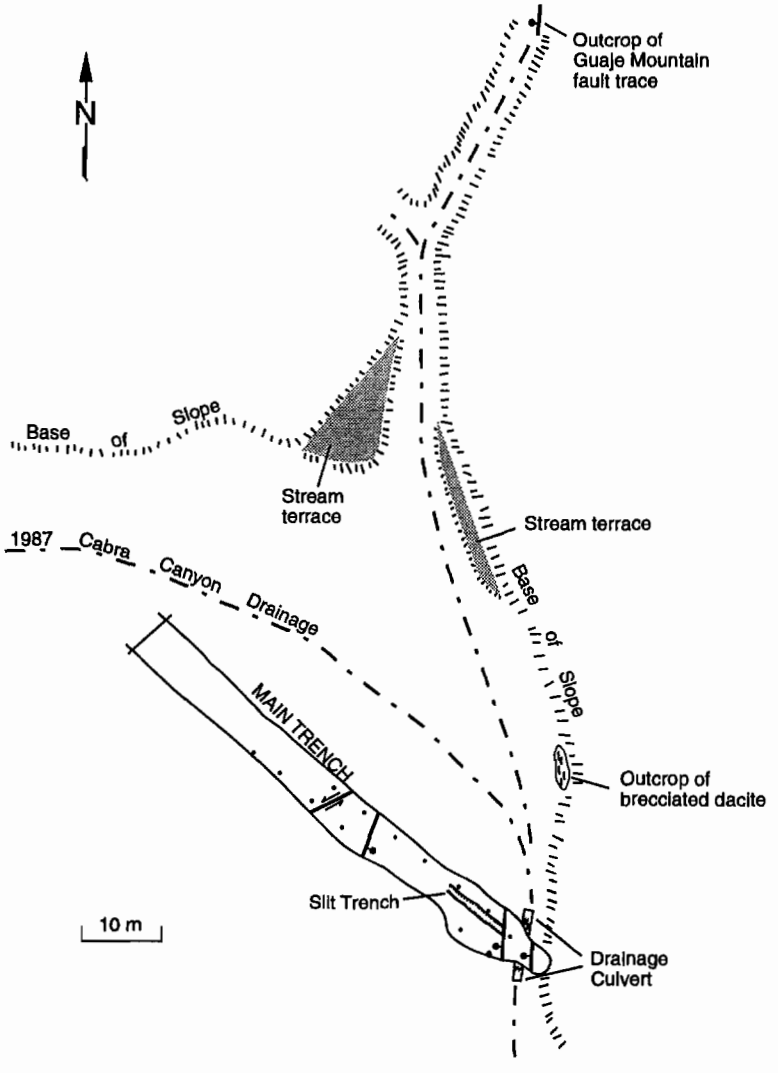

Fig. 2-29. Sketch map of SHT-1 area (from Gardner et al., 1990)

Canyon, only 0.6 km downstream (Fig. 2-33). This dichotomy provides an excellent illustration of the range in behavior of streams on the Pajarito Plateau during the Holocene, and provides some insight into underlying causes.

Cabra Canyon contains one of many streams on the Plateau which have been unable to transport all of the sediment supplied to it, resulting in progressive (albeit discontinuous) aggradation through the Holocene, with the late Pleistocene channel being buried meters below the modern channel. The general impression of Cabra Canyon upstream of SHT-1 is of a basin being literally flooded with sediment. Because Rendija Canyon has been incising during this same period, this upstream aggradation has caused a significant steepening of the channel gradient (Fig. 2-33). Although this steepening should help the stream transport sediment, the stream has apparently not yet reached a balance between sediment supply and transport capacity, and net aggradation continues (indicated by the lack of an incised channel along much of Cabra Canyon).

Basic drainage basin variables that should influence the tendency towards aggradation or incision along Pajarito Plateau streams include: 1) channel gradient; 2) basin area (influencing flood size); 3) mean basin elevation (higher elevation basins have the potential for more runoff per unit area because

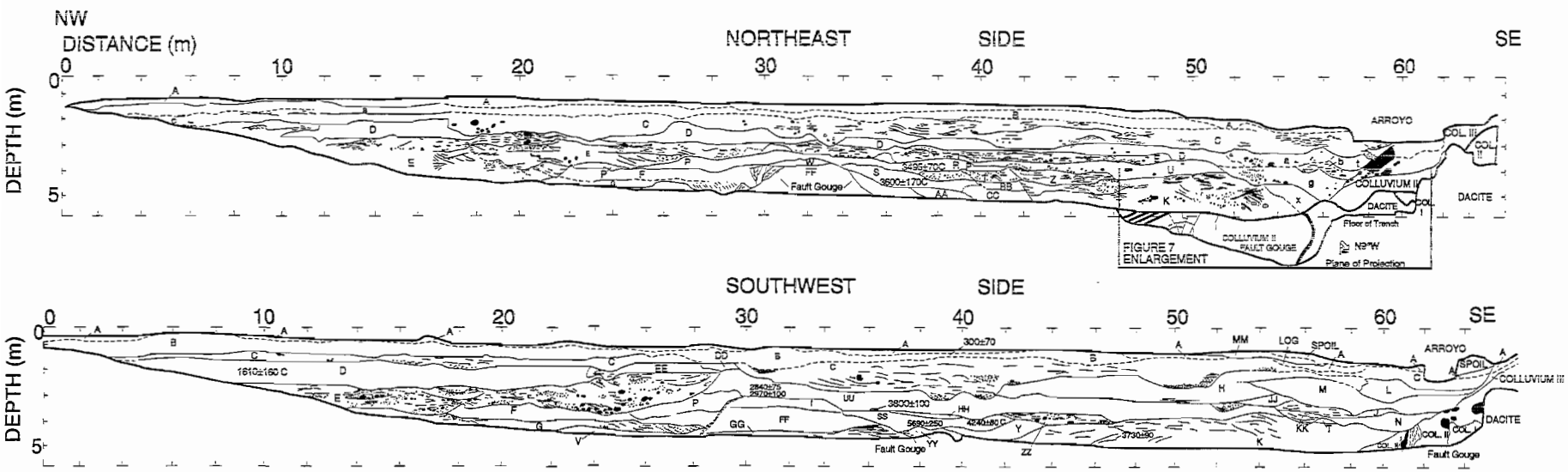

Fig. 2-30. Logs of northeast and southwest walls of trench SHT-1 in Cabra Canyon. Log of southwest wall is a "mirror image" to allow direct comparison of opposing sides (from Gardner et al., 1990).

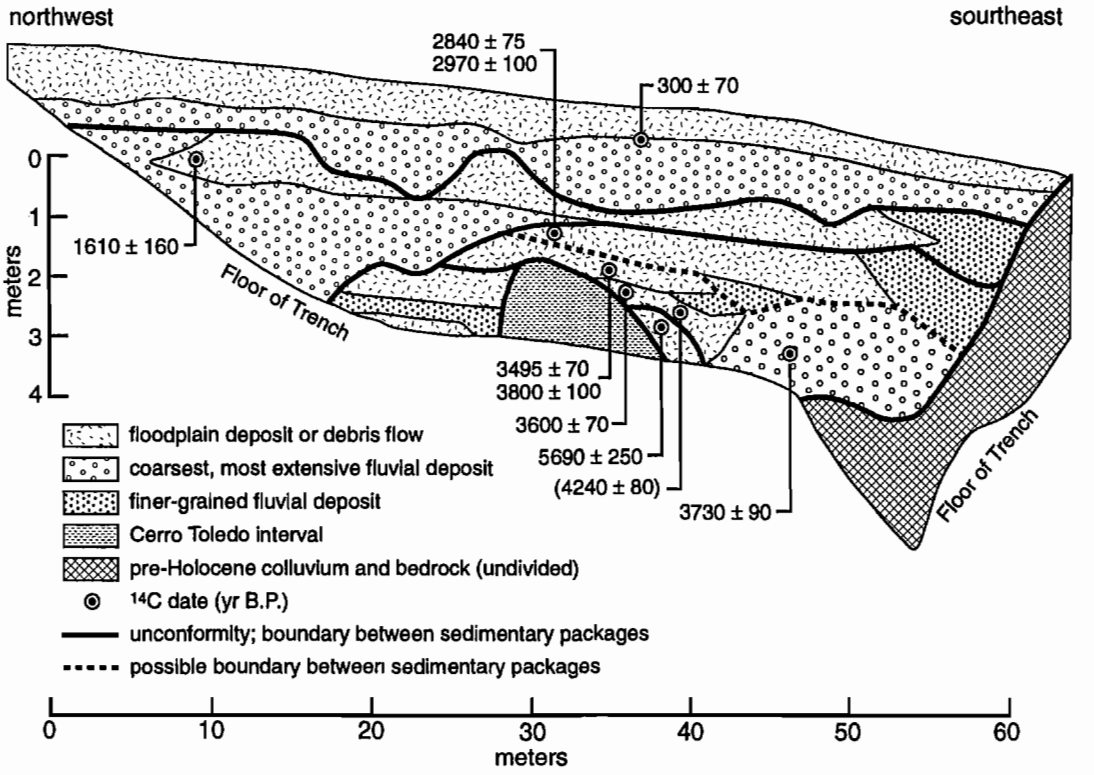

Fig. 2-31. Schematic log showing stratigraphic units exposed in SHT-1 and location of radiocarbon dates. Log is a composite of exposures on opposite trench walls, highlighting major stratigraphic breaks. Mid-to-late Holocene sedimentary packages are generally characterized by a basal gravelly channel deposit and an overlying finer-grained floodplain deposit. Suspect date shown in ( ). 3.6x vertical exaggeration. Prepared from original trench logs of Gardner et al. (1990).

of the strong local elevation-precipitation relation[Fig. 4 in Introduction], also influencing flood size); and 4) bedrock erodibility (influencing sediment supply, and also the potential for channel incision into bedrock). The variables (2) and (3), and in part (4), are often correlated on the Plateau, with larger basins tending to head in the higher elevation terrain underlain by the resistant Tschicoma Formation, limiting the ability to resolve their relative importance.

A comparison of basin variables between Cabra and Rendija Canyons (Table 2-8) indicates that the aggradation in Cabra Canyon could be related to some combination of: 1) a higher sediment supply per unit area (~74% of the Cabra basin is underlain by relatively erodible units such as the Bandelier Tuff and Cerro Toledo pumice beds, compared with only ~42% for the Rendija basin); and 2) smaller floods (the Cabra basin is much smaller than the Rendija basin, and its overall elevation is lower as well). The fact that the gradient of Cabra used to be less than Rendija's should have also aided the Holocene aggradation, although the progressive steepening of Cabra's channel should help diminish the tendency towards aggradation over time.

An examination of similar drainage basin variables for other streams on the Pajarito Plateau also indicate that canyons displaying pronounced aggradation tend to have most of their basin area underlain by tuff, generally (but not always) head on the Plateau at relatively low elevations and possess relatively small drainage areas, and have gradients similar to or less than canyons with apparently stable or incising channels.

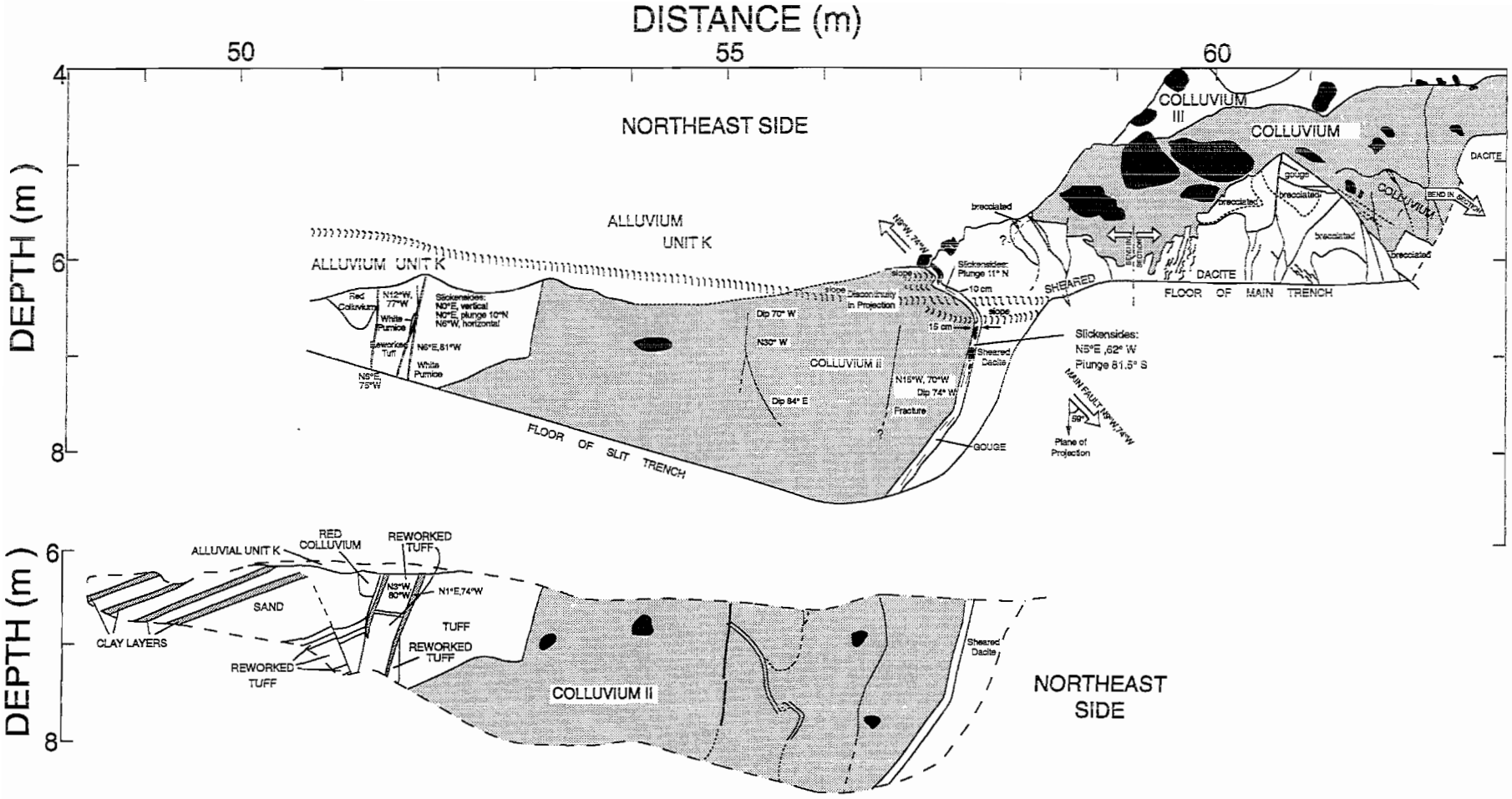

Fig. 2-32. Partial trench log showing details in main fault zone at southeast end of trench (from Gardner et al., 1990).

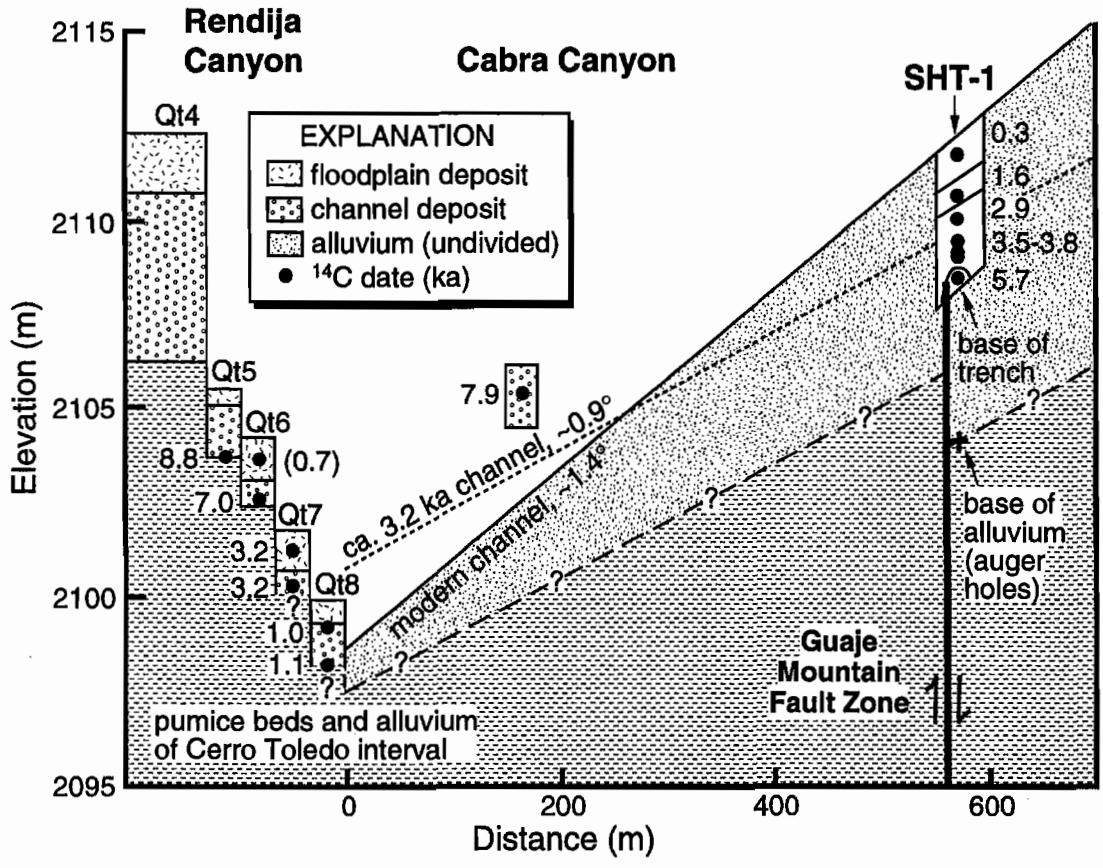

Fig. 2-33. Schematic longitudinal profile of lower Cabra Canyon and adjacent part of Rendija Canyon, showing sedimentary packages exposed in SHT-1, terraces in lower Cabra Canyon and in Rendija Canyon, and approximate profile of ca. 3.2 ^{14}C ka Cabra Canyon channel. The channel of lower Cabra Canyon has been steepening through the Holocene, associated with progressive aggradation upstream and progressive incision downstream at the confluence with Rendija Canyon.

- Retrace route south down Cabra Canyon, bearing right (west) up trail back into Rendija Canyon to point where a trail branches off of the dirt road and crosses the channel to the south.

Station 2-3e: Early to Late Holocene Terrace Sequence (Qt5, Qt6, Qt7, Qt8)

Holocene Terrace Sequence. Within Rendija Canyon here are 4 Holocene terraces, all yielding ^{14}C age control and 3 being sites of 1995 soil pits for the local soil chronofunction (Fig. 2-34). The north bank exposes a 5-m high Qt5 strath surface in tuff overlain by 1.5 m of sandy gravels, with the basal gravels dated at 8810 ± 50 ^{14}C yr BP. An almost identical date of 8940 ± 50 ^{14}C yr BP was obtained from another Qt5 terrace remnant 0.4 km upstream.

On the south side of the channel, dates of 1010 and 1070 ^{14}C yr BP were obtained from depths of 0.65 and 1.65 m below an ~1.3 m high Qt8 terrace, suggesting rapid deposition of this sedimentary section; >1 m of channel sands and gravels underlie this terrace, with the base not exposed. The next surface is an ~3.2 m high Qt7 terrace which yielded dates of 3220 and 3200 ^{14}C yr BP from depths of 0.55 and 1.45 m, also suggesting rapid deposition. The upper surface, an ~5.7 m high Qt6 terrace, has 0.5 m of channel sands and gravels above the 4-m high strath surface, and yielded an age of 6950 ^{14}C yr BP. The Qt6 terrace is overlain by ~1 m of fine-textured colluvium, and this input of fines has resulted in a better developed soil than on the Qt6 terraces downstream.

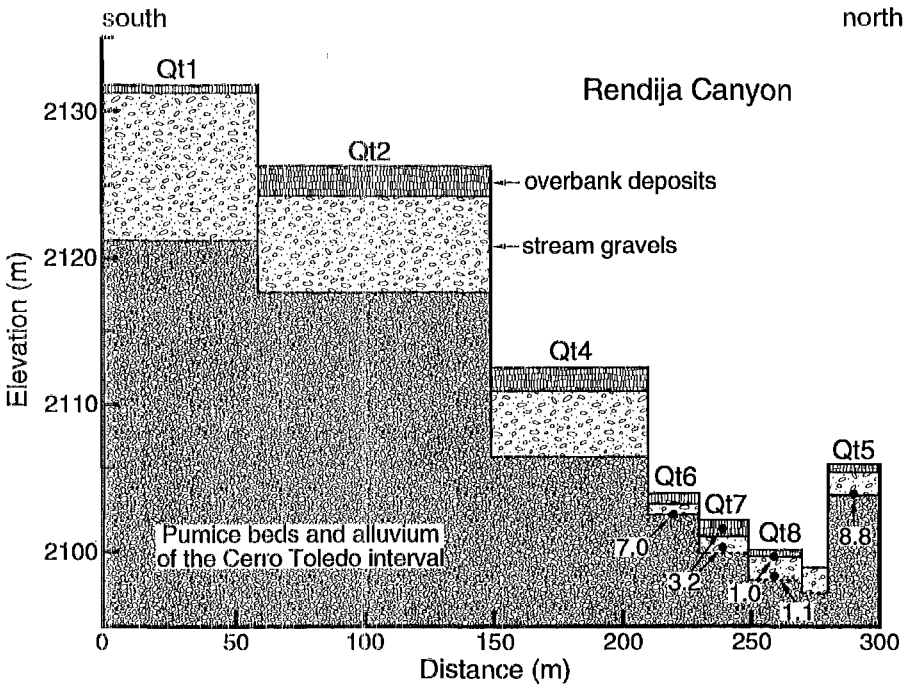

Fig. 2-34. Schematic cross section across Rendija Canyon near the Pistol Range, showing terrace sequence in area of Stop 2-3e. Radiocarbon ages (soild circles) shown for stream channel deposits (from McDonald et al., 1996b).

It is important to point out that although the ^{14}C age control from individual terrace sections can be tight and suggestive of brief periods of deposition, the ages commonly vary between sections (i.e., Qt8 and Qt6 = ~1.0 and 7.0 ^{14}C ka here, but ~0.5 and 5.0-6.0 at downstream soil pits). This may in part be due to time-transgressive terrace formation, but we believe that, more importantly, it is due to the terrace designations being in part artificial mapping constructs, lumping together multiple terrace forming events into single mapping units. Thus, instead of there being only 4 discrete Holocene terraces in Rendija Canyon, there may actually be several times that many.

Sportsman's Club Trenches. 0.35 km upstream of here was the site of paleoseismic investigations in 1992 as part of the Woodward-Clyde studies (Wong et al., 1995). Two trenches and 4 soil pits were excavated in unsuccessful attempts to obtain additional age control on faulting events on the Guaje Mountain fault. A promising west-facing step at trench SCT-1 was apparently a remnant of a Qt7 terrace at the site of a Qt8-age meander cut-off. Trench SCT-2, excavated nearby at the base of a steep slope, was largely in unconsolidated latest Holocene to historic slopewash deposits that continuously collapsed during excavation ("type C" material in OSHA excavation safety lingo) (Fig. 2-35). The fault zone itself was apparently just to the west on the steep slope, shown by offsets in Cerro Toledo beds that were exposed in a shallow drainage.

Despite the absence of paleoseismic data, these excavations provided excellent exposures of Holocene sediments that yielded valuable age control and insights into the mid to late Holocene history of Rendija Canyon (Fig. 2-36). In part, samples from these excavations provided the first age control on the Qt6 and Qt7 terraces, subsequently enhanced at many other sites. Additionally, they demonstrated that impressive amounts of sediment could be derived from relatively short slopes underlain by Cerro Toledo pumice deposits. The bases of young ponderosa pines exposed along the edge of SCT-2 were buried by up to 0.5 m of slopewash deposits (Fig. 2-35), and the oldest exposed sediments, 1.7 m deep,

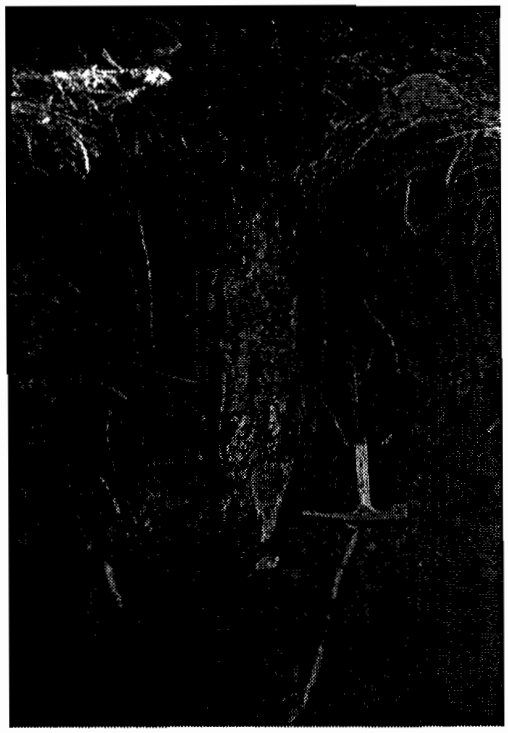

Fig. 2-35. Photographs of trench SCT-2, excavated in 1992 in unconsolidated latest Holocene slopewash deposits. Right photo shows 20 cm diameter ponderosa pine tree buried by 47 cm of sediment.

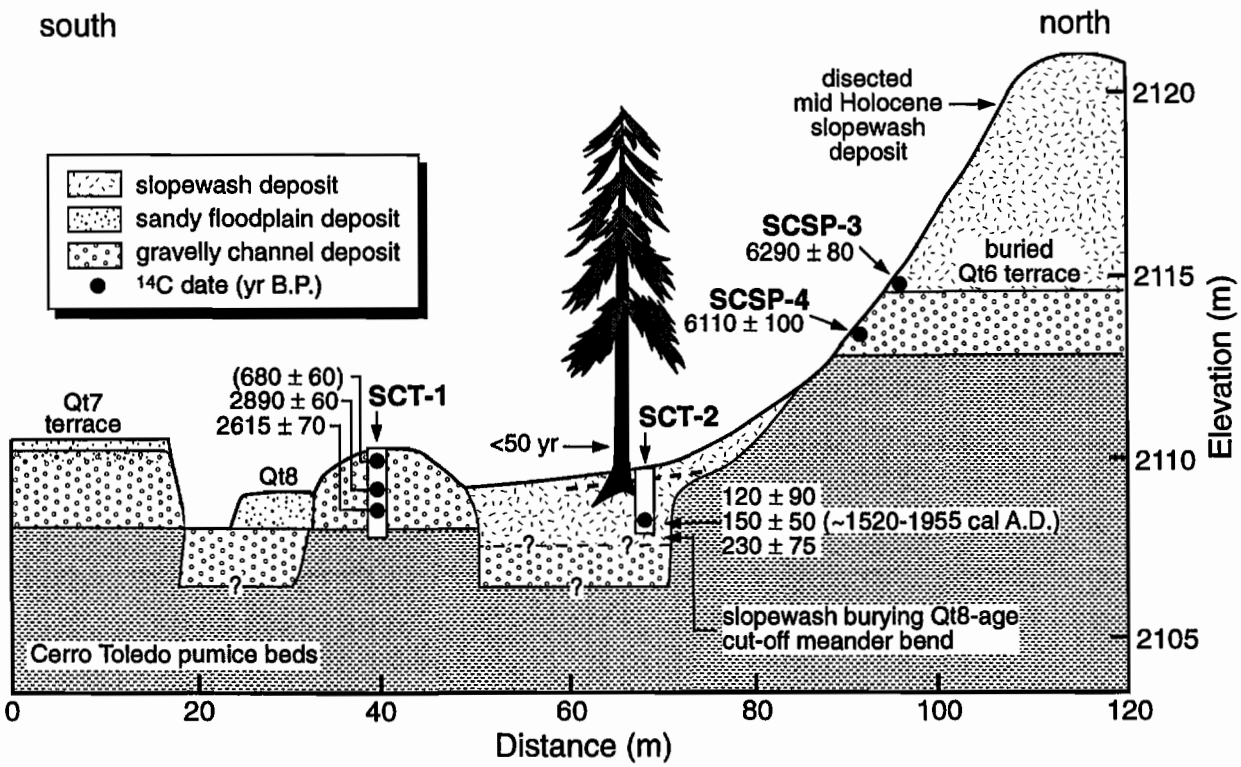

Fig. 2-36. Schematic cross section across Rendija Canyon at site of 1992 Sportsman's Club trenches (SCT-1, SCT-2) and soil pits (SCSP-3, SCSP-4) of Wong et al. (1995), near the Guaje Mountain fault zone. Inferred stratigraphic relations and ^{14}C dates are from Wong et al. (1995) and subsequent work. Suspect date shown in ( ). 4x vertical exaggeration.

were no older than 1520 A.D. in age (most probable age, based on 3 analyses, is 1680-1950 cal A.D.). In addition, the Qt6 terrace there is buried by >6 m of slopewash deposits, with inception of slopewash deposition apparently occurring contemporaneously with or soon after terrace formation.

Holocene Sedimentation on the Pajarito Plateau. Probability plots constructed using the ^{14}C analyses from stream channel deposits in Cabra Canyon and Rendija Canyon are shown in Fig. 2-37, and provide a basis for subdividing the Holocene terrace sequence and assigning average ages and age ranges to each mapping unit. These age estimates are shown in Table 2-5. It is notable that at least 3 of the 6 dated sedimentary units in Cabra Canyon have a matching dated unit in Rendija Canyon, suggesting that periods of sediment deposition between these two canyons are at least partially synchronous.

A similar probability plot constructed using all dated Holocene and latest Pleistocene stream channel deposits on the Pajarito Plateau is shown in Fig. 2-38. This more robust data set (55 dated units and 70 radiocarbon dates from 10 canyons) also shows apparent clusterings in the ages of sedimentary units. In the late Holocene, where the sedimentary record is likely to be most complete, apparent peaks in sediment deposition are indicated at ca. 500, 1000, 1300, and 2900 cal yr B.P. A scarcity of deposits dated to ~1800-2700 cal yr BP is particularly striking, suggesting net incision and/or decreased sediment supply during this period.

Fig. 2-38 shows a probability plot for all dated Holocene and latest Pleistocene fan and slopewash deposits on the Pajarito Plateau. Due to the relatively small sample size, the record is more likely to be incompletely documented than for the channel deposits, and less confidence is put in the "peaks and troughs" on this plot. However, at least a couple points are notable. First, no fan or slopewash deposits have been dated to the period from ~1500 to 2700 cal yr BP, supporting the possibility of relatively limited sediment supply at this time. Second, there is an apparent mid-Holocene peak in fan and slopewash deposition centered on ~6000-6500 cal yr BP. This coincides with formation of the Rendija Canyon Qt6 terrace and also a major fill terrace in Frijoles Canyon (Reneau et al., 1993, 1996b). In combination, these data suggest that pulses of sediment transported off the canyon walls and down minor tributary drainages are at least partially responsible for the periods of stream aggradation or strath terrace formation. Furthermore, they suggest that such periods of hillslope erosion and sediment deposition have been episodic through the Holocene and at least in part synchronous across the Plateau, suggesting that the erosional and depositional cycles have been influenced by Holocene climatic changes. These preliminary conclusions will continue to be tested as more data are collected.

- Follow trail to north across Holocene terraces, up the slope to the late Pleistocene Qt4 terrace. Berms of the Pistol Range are to the left. An excavation behind a trailer at the south edge of the Pistol Range provides an excellent exposure of the fill stratigraphy below the Qt2 surface (optional stop, when range is not being used). Keep right on Qt4 terrace to a reexcavated 1995 soil pit, near where pits were excavated in 1992 by Woodward-Clyde (Wong et al., 1995) and more recently in 1996 for additional soil descriptions and for collection of samples for cosmogenic nuclide analyses (discussed below).

Station 2-3f: Middle Wisconsin (?) Qt4 terrace; soil pit RCT4-1

Terrace Significance, Stratigraphy, and ^{14}C Age Control. The Qt4 terrace is presently the only significant terrace that has been recognized in Rendija Canyon between the Holocene suite and the

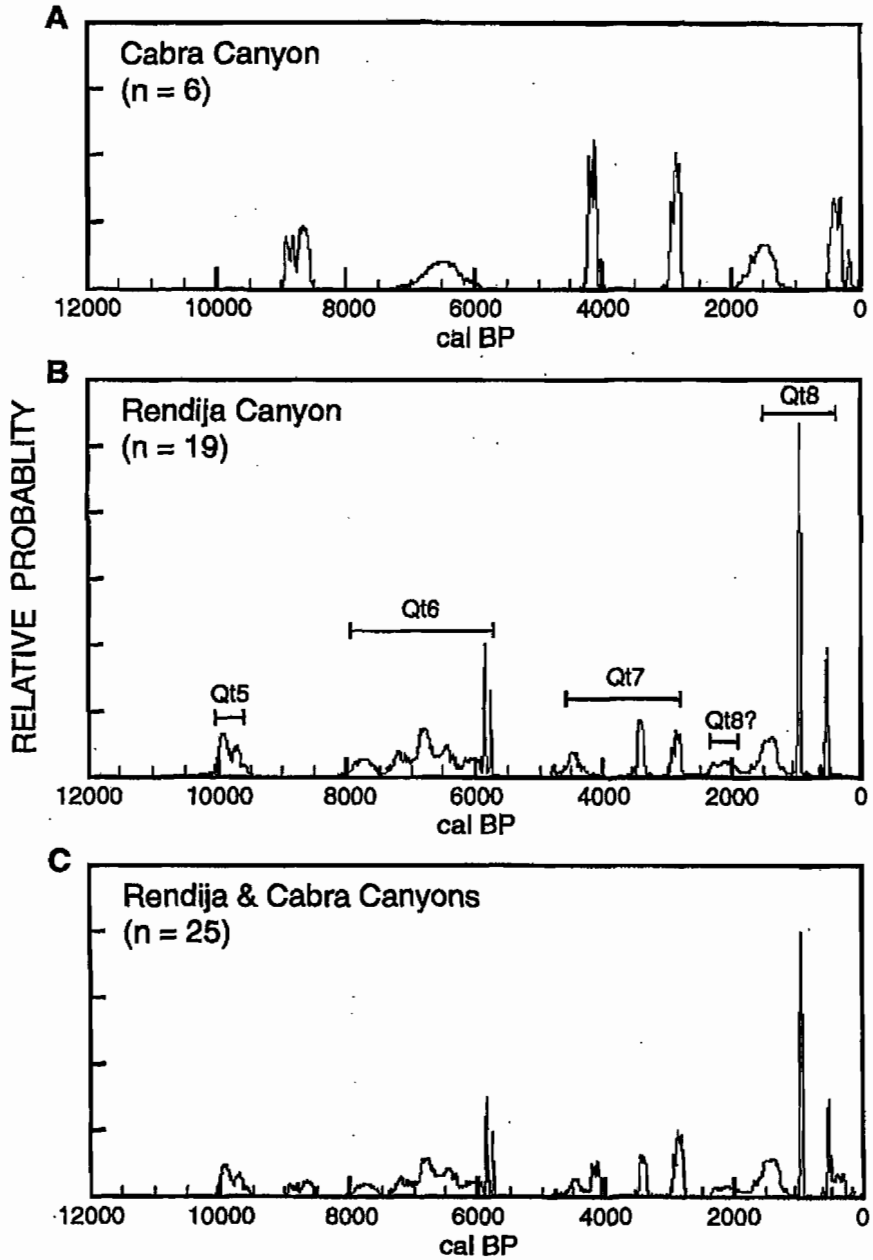

Fig. 2-37. Probability plots of calibrated radiocarbon ages showing: A) all Cabra Canyon stream units (using 11 dates from 6 units); B) all Rendija Canyon stream channel units (using 25 dates from 19 units); and C) all Cabra and Rendija Canyon stream units. Probability plots were produced using CALIB 3.03 (Stuiver and Reimer, 1993), using 2-σ range and an error multiplier of 2.0 on the original analyses. Averaged values of 2 or more dates were used for sedimentary units with multiple similar dates, resulting in a tighter probability distribution for those units. At some sites that span a significant time range (such as SHT-1), multiple dates are plotted from a single section. Note that half of the dated Cabra Canyon units have a corresponding dated unit in Rendija Canyon, suggesting that the periods of sediment deposition are at least partly synchronous between these canyons, despite their much different behaviors in the Holocene.

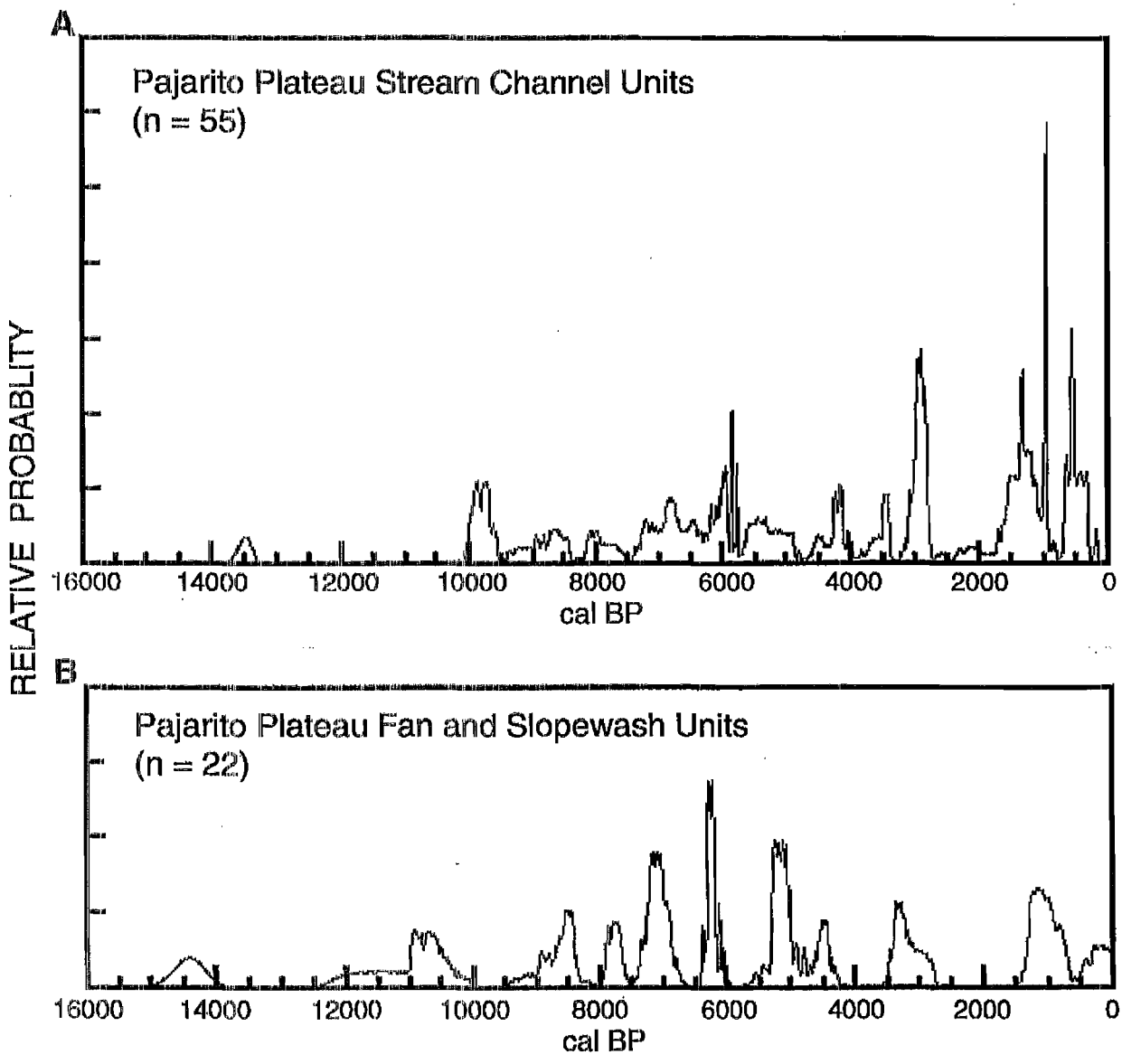

Fig. 2-38. Probability plots of calibrated radiocarbon ages showing: A) all dated Holocene and latest Pleistocene stream channel units on the Pajarito Plateau (using 70 dates from 55 units), combining data from 10 canyons; B) all dated slopewash and fan units on the Plateau (using 23 dates from 22 units), combining data from 9 canyons. Historic deposits are excluded from plots. Probability plots prepared as in Fig. 2-37. The similarity between many of the "peaks and troughs" suggests that periods of increased sediment supply from canyon walls and small tributary drainages correspond with periods of stream aggradation and/or strath terrace formation. The scarcity of deposits dated to ca. 2000 cal BP on both plots is particularly striking, and seems unlikely to be attributable to an incomplete record, as is possible for some of the older, lower magnitude "troughs".

broad Qt2 surface where we started our hike and which lies up the slope to the south. "Qt3" consists of relatively small and isolated mapping units between Qt2 and Qt4; its significance is unknown, and no sites for soil pits have been located on it. In contrast, Qt4 continues from here downstream for ~2 km, and soils examined in a pit at a downstream location were similar to those found here.

Qt4 represents a significant aggradational event, and the ~4 m of sandy gravels that comprise most of the section are thicker than found below any of the Holocene terraces. At this soil pit, a buried soil associated with the terrace is overlain by 0.6-0.75 m of colluvium, a feature seen at the other Qt4 (and Qt2) soil pits.

The Qt4 units have generally confounded attempts at ^{14}C dating. Charcoal is sparse, and the only "dateable" sample collected from within the fluvial section, from pit RCT4-4 (excavated in 1996 and located ~40 m east of here), yielded an improbable age of 3130 ^{14}C yr BP. A more reasonable date of 13,820 ^{14}C yr BP was obtained from the upper part of the buried soil at pit RCT4-2, providing a maximum-limiting date for the overlying colluvium, but only a weak minimum-limiting age for the fluvial sediments. An additional date of 780 ^{14}C yr BP was obtained from 0.6 m deep in the upper bioturbated colluvium in this pit, but is also suspect. Use of the 13.8 ka date and age control from Qt2 colluvium (discussed at the next station), indicates that deposition of the overlying colluvium began in the latest Pleistocene or early Holocene, which is consistent with other evidence for widespread erosion occurring on the Pajarito Plateau around this time.

RCT4-1 Soil Profile. The RCT4-1 profile exposed in this soil pit (Fig. 2-39; Table 2-9) is similar to those developed on other Qt4 surfaces in Rendija Canyon. The Qt4 soil profile generally consist of a surface soil with an A-Bw horizon sequence formed in a thin layer of colluvium, that, in turn, overlies a buried soil with a BA-Btk-Bt-CB horizon sequence that has formed in the Qt4 stream deposits.

Surface Soil. Soils formed on the Qt4 surfaces have been buried in places by a thin (<1 m) layer of colluvial sediment, generally associated with distal deposition from small alluvial fans or local slopewash, derived from nearby higher terraces or hillslopes (A and Bw horizons in Fig. 2-39; Table 2-9). High silt and clay contents for this layer also suggest accumulation of dust might be an important source of the fine-grained matrix (Table 2-9). The soil formed in this layer consist of well developed Bw horizons with prismatic and subangular blocky structure and hues from 10 YR to 8.75 YR. Clay content in the Bw horizons ranges from about 13 to 15 % by weight and is generally greater than that of soils formed on Holocene terraces. A lack of obvious evidence of illuviation or in-situ weathering suggests that these high clay contents may reflect the initial texture of the colluvium; however, abundant evidence of bioturbation from burrowing fauna (possibly cicadas and earthworms) may have resulted in enough mixing of the soil matrix to prevent accumulation of oriented clays and silt along pedologic features. Development of extensive argillans along pores and ped faces within the upper horizons of the underlying buried soil indicates that downward translocation of clay must be occurring within the overlying Bw horizons.

Soils that have formed in the thin layer of colluvium also overlie several of the studied Qt2 soils (Fig. 2-43; discussed in next station). The soils formed in colluvium on both the Qt4 and Qt2 surfaces are very similar in development. PDI values calculated for these surface soils range from 21.4 to 22.6. Strong similarities in profile morphology indicate that deposition of this colluvium was probably contemporaneous across both the Qt4 and Qt2 terrace surfaces. As discussed above, a maximum-limiting date of about 13.8 ^{14}C ka (calibrated date of 16.6 ka) was obtained from the top of the RCT4-2 buried soil. Analysis of charcoal collected from the base of the colluvial cap covering a Qt2 (RCT2-1) soil

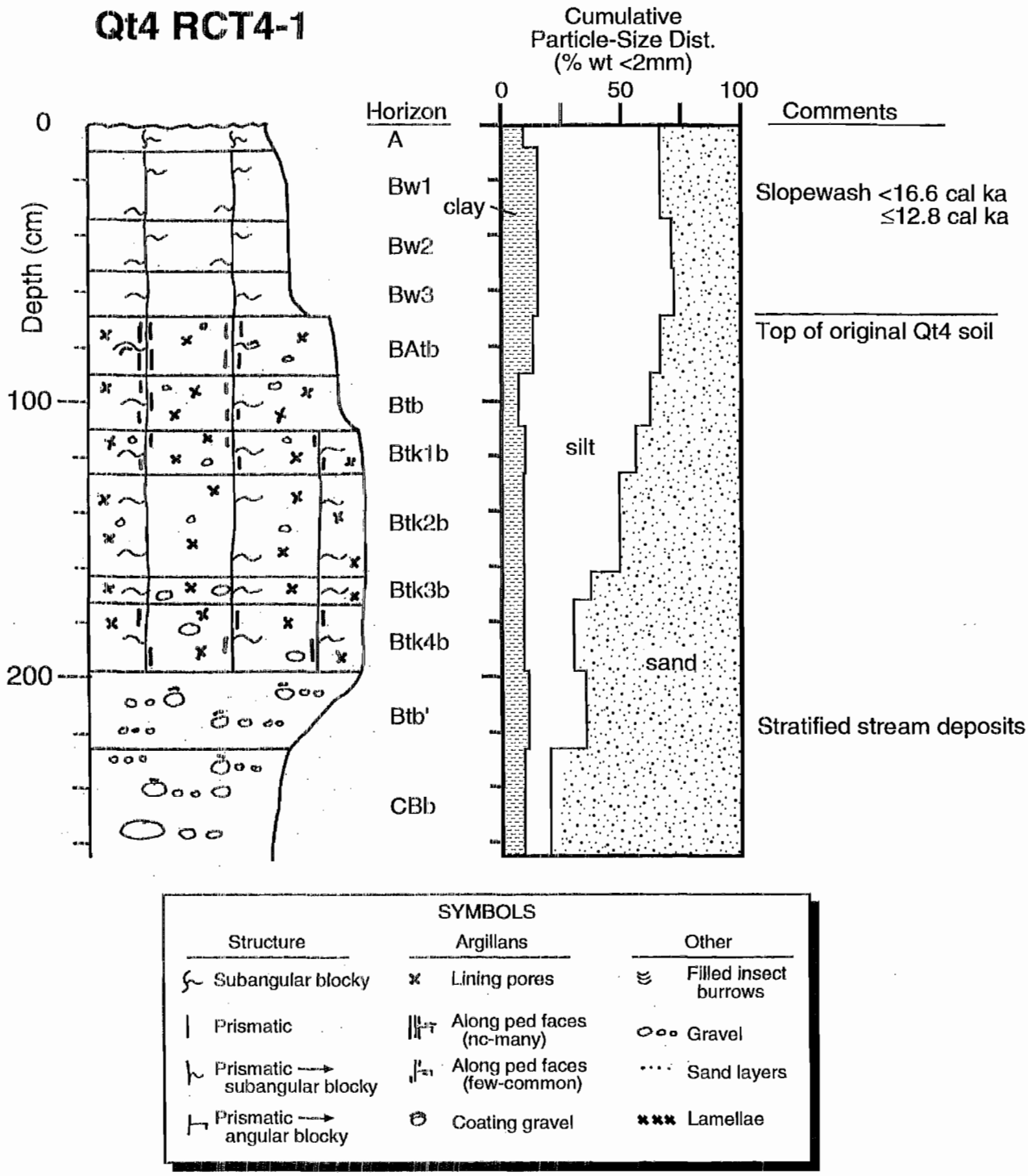

Fig. 2-39. Schematic diagram of soil morphology and particle-size distribution for the Qt4 RCT4-1 soil profile. The upper ~70 cm of the soil is a colluvial layer that buried the Qt4 surface at ca. 12.8 cal ka.

indicates that deposition of this layer began about 10.9 ^{14}C ka (12.8 cal ka; Table 2-7). A combination of greater PDI values and considerably stronger development of the Bw horizons for soils formed in the colluvial layer relative to soils formed on the Qt6 and younger terraces also indicates that deposition of the colluvium began before about 5.7 to 7.9 cal ka (Qt6 ages, Table 2-5).

Buried Qt4 Soil. Soils formed in the Qt4 deposits and that underlie the colluvial layer show considerably greater development than soils formed in Holocene deposits (Fig. 2-39, Table 2-9). The BAtb horizon is considered to be the A horizon of the pre-buried Qt4 soil; however, little remains of the original A horizon morphology. The original A horizon may have been eroded, or the features have simply been obliterated from overprinting by the surface soil. The Bt horizons have prismatic structure that parts to subangular blocky structure, 7.5 YR to 10 YR hues, discontinuous argillans along ped faces and pores, and a total Bt thickness of about 157 cm. Clay content in the Bt horizons averages from about 7 to 13 % by weight and is less than the overlying soils formed in the colluvial cap. Stage I to weak stage II secondary calcium carbonate has accumulated within some of the Bt horizons (Btk1b; Btk2B; Table 2-9). The carbonate appears to have been trapped within the uppermost Bt horizons of the pre-buried soil. This carbonate is largely superimposed over argillans along prismatic ped faces suggesting a more recent (Holocene?) increase in soil aridity or at least a decrease in the downward flux of soil water through the upper Bt horizons. A PDI value of 76.0 was calculated for this soil. Another Qt4 soil yielded a PDI value of 71.4 (Table 2-10).

An increase is clay content in the Bt horizons appears be largely due to illuviation of clay from overlying horizons rather than significant *in situ* formation of aluminosilicate clays. This is because most of the argillans occur along pores and vertical prismatic ped faces indicating that much of the clay has been transported along macropores by percolating soil water. Silt content also decreases downward below the BAtb horizon. At least part of the silt was probably derived from overbank deposits and dust, and subsequently mixed into the developing soil through bioturbation. Fining upward trends in the texture of soil formed on Holocene terraces suggests that bioturbation plays an important role in progressive increases of silt in soil B horizons.

Cosmogenic Nuclides (Bill Phillips). Cosmogenic nuclides are important new tools for estimating surface exposure ages and process rates. Here and at Stop 2-3g, we examine soil pits where cosmogenic ^{21}Ne depth profiles in sand-sized quartz grains have been measured. The purpose of this experimental work is to test new methods of applying cosmogenic techniques to depositional surfaces such as the Rendija Canyon terraces. Nuclide production prior to terrace formation make this kind of alluvial- and soil-based application difficult. Our goal is to document the effect of pedogenic processes such as bioturbation and changes in bulk density upon cosmogenic nuclide concentrations in soils. In addition, the feasibility of estimating terrace surface exposure ages and basin denudation rates is being evaluated.

Alluvial quartz in Rendija Canyon largely derives from the Bandelier Tuff, with older bedrock units contributing only trace amounts. After excavation and description of soil pits in terraces Qt2 and Qt4, each soil horizon was collected. Each analyzed sample represents a 10 cm depth interval and a 50 to 100 cm lateral extent. Quartz from the 2 to 0.425 mm (very coarse to coarse sand) size fraction was isolated using standard magnetic and heavy liquid techniques plus further cleaning by selective acid dissolution (Kohl and Nishiizumi, 1992). This treatment removes iron oxides, carbonates, clay minerals, and any feldspar or glass present as well as etching the outer few microns of the quartz. Quartz from 1 to 5 cm clasts in the Qt4 pit were also collected in order to evaluate bioturbation effects. The 0.25 to 0.425 mm size fraction from the crushed clasts was used in these samples.

Neon has three naturally occurring, stable isotopes, ^{20}Ne, ^{21}Ne, and ^{22}Ne. Secondary neutrons from the cosmic ray flux produce ^{21}Ne from Si in quartz. Since ^{21}Ne is otherwise very rare in nature, its buildup due to cosmogenic production can be used as a surface exposure geochronometer. Like other cosmogenic nuclides, ^{21}Ne has been successfully used to estimate exposure ages in bedrock geomorphic surfaces (Cerling et al., 1994). Unlike ^{3}He which leaks from quartz, ^{21}Ne is retained over the timeframes and temperatures experienced by surface rocks (Niedermann et al., 1994). By convention, ^{21}Ne greater than atmospheric levels is termed "excess ^{21}Ne" or $^{21}Ne^*$.

Neon isotopes were analyzed at Los Alamos National Laboratory by stable isotope ratio mass spectrometry (see W. M. Phillips, in preparation, for detailed description of mass spectrometric techniques). Neon was extracted by heating quartz at 800°C for 60 to 90 minutes under high vacuum. Procedural blanks for $^{21}Ne^*$ average $2x10^5$ atoms. For most samples, $^{21}Ne^*$ 2σ precision is 10% or better. Exposure ages and denudation rates were computed using a $^{21}Ne^*$ high latitude, sea-level production rate of 16.8 ± 3 atoms g^{-1} yr^{-1} for pure SiO_2 (Niederman et al., 1994; corrected following Clark et al., 1995). This rate was corrected for site latitude and elevation after Lal (1991).

In Rendija Canyon quartz, $^{21}Ne^*$ originates from three possible sources: (1) nucleogenic ^{21}Ne from the reaction $^{18}O(\alpha,n)^{21}Ne$; (2) inherited ^{21}Ne produced cosmogenically during denudation of bedrock hillslopes and subsequent sediment transport; and (3) cosmogenic production during residence on the sampled stream terrace. A basic task of our research is to estimate each of these components.

We tested for the presence of nucleogenic ^{21}Ne in a Bandelier Tuff sample from a nearby roadcut with 4.5 m of shielding from the cosmic ray flux. The shielded sample yields results similar to our $^{21}Ne^*$ analytical blank, demonstrating that the nucleogenic component is unimportant.

The inherited component is determined by measuring $^{21}Ne^*$ at the soil surface and at depth using the method of Anderson et al. (1996). Our application differs from Anderson et al. (1996) because we used sand-sized particles and terrace surfaces subject to burial. This technique is illustrated graphically in Fig. 2-40. After estimating the inherited component, both the exposure time since terrace stabilization and the basin denudation rate can be computed (Anderson et al., 1996; Granger et al., 1996; Bierman and Steig, 1996).

Such surface exposure ages and denudation rates are model-dependent and subject to a host of assumptions including uniform distribution of the inherited component throughout the terrace deposit, constant shielding for the sampled mineral grains, and constant ^{21}Ne production rate. All of these assumptions are violated to varying degrees in the soil-forming environment. Since the global cosmogenic ^{21}Ne production rate may vary as much as 20% over exposure times possible for the Rendija Canyon terraces (Gosse et al., 1996), a minimum experimental uncertainty of 20% is applied to exposure ages and denudation rates, even though our analytical uncertainty is much lower. We evaluated the importance of the other assumptions by measuring ^{21}Ne depth profiles in two soils with independent age control.

Our results are shown in Fig. 2-41. Concentrations of $^{21}Ne^*$ were expected to decrease exponentially with depth. However, three exceptions are apparent. First, $^{21}Ne^*$ within colluvium capping both terraces has nearly constant, but high concentrations. This is due to strong bioturbation of soil parent material derived from erosion of older terraces and soils. The bioturbation mixes the colluvium rapidly enough to prohibit development of a $^{21}Ne^*$ trend. Abundant evidence of bioturbation in the colluvium is apparent in both soil pits.

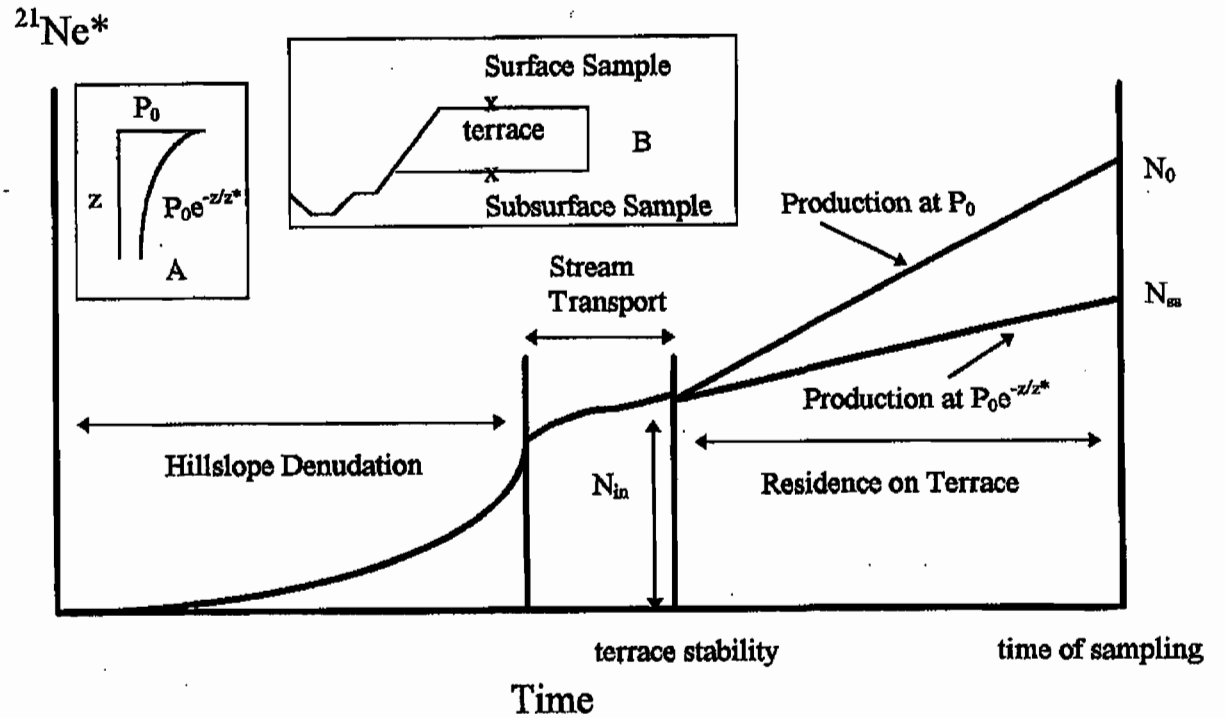

Fig. 2-40. Modeled history of ^{21}Ne* production in the Rendija Canyon basin (figure modified from Anderson et al., 1996). The production rate of ^{21}Ne* below the surface of a terrace decreases exponentially (insert A) as $P_0e^{-z/z*}$ where z is depth (cm), and z* is a neutron absorption coefficient (about 178 g cm^{-2} for Bandelier Tuff) divided by soil bulk density (range 1.2 to 1.7 g/cc). During hillslope denudation, ^{21}Ne* accumulates in quartz at a rate determined by the average basin erosion rate. Some ^{21}Ne* also forms during stream transport, but due to the small basin size, this is much less than during denudation and is neglected. At the time of terrace stabilization, quartz contains an average ^{21}Ne* concentration of N_{in}. This is the inherited cosmogenic component from which the basin denudation rate can be calculated as $d = (P_{eff}/N_{in})z*$ where P_{eff} is the effective nuclide production rate for the basin (Granger et al., 1996; Bierman and Steig, 1996). The inherited component is separated from the total ^{21}Ne* by measuring a nuclide depth profile (insert B): $N_{total} = N_{in} + t*P_0$ where t is exposure time = $(N_0 - N_{ss})/(P_0 - P_{ss})$. For this work, linear regression of multiple subsurface samples was used to estimate N_0 and N_{ss}, while measured soil bulk densities were used to calculate P_{ss}. P_0 is computed after Lal (1991) using the ^{21}Ne* production rate of Niedermann et al. (1994) as corrected by Clark et al. (1995).

Secondly, samples near the base of both pits yielded anomalously high ^{21}Ne* concentrations. Because soil development is minimal in these samples, they probably demonstrate inhomogeniety in inheritance, perhaps due to erosion of a local landslide containing much-exposed sediments.

Finally, while ^{21}Ne* in the older Qt2 profile follows an exponential profile closely, the profile in Qt4 is linear. Only bioturbation varying in intensity both spatially and temporally appears capable of creating this pattern. While an exponential function can be fit to the Qt4 profile, it requires unrealistic (<0.6 g/cm^3) bulk densities. U and Th concentrations in Pajarito Plateau soils (Longmire et al., 1996), while elevated relative to bedrock, are not high enough to create deviation from the exponential trend due to nucleogenic production in clay- and Fe-oxide-rich horizons. If this were true, the Qt2 profile would show a linear trend as soil development is much stronger in Qt2 than Qt4. Changes in global ^{21}Ne*

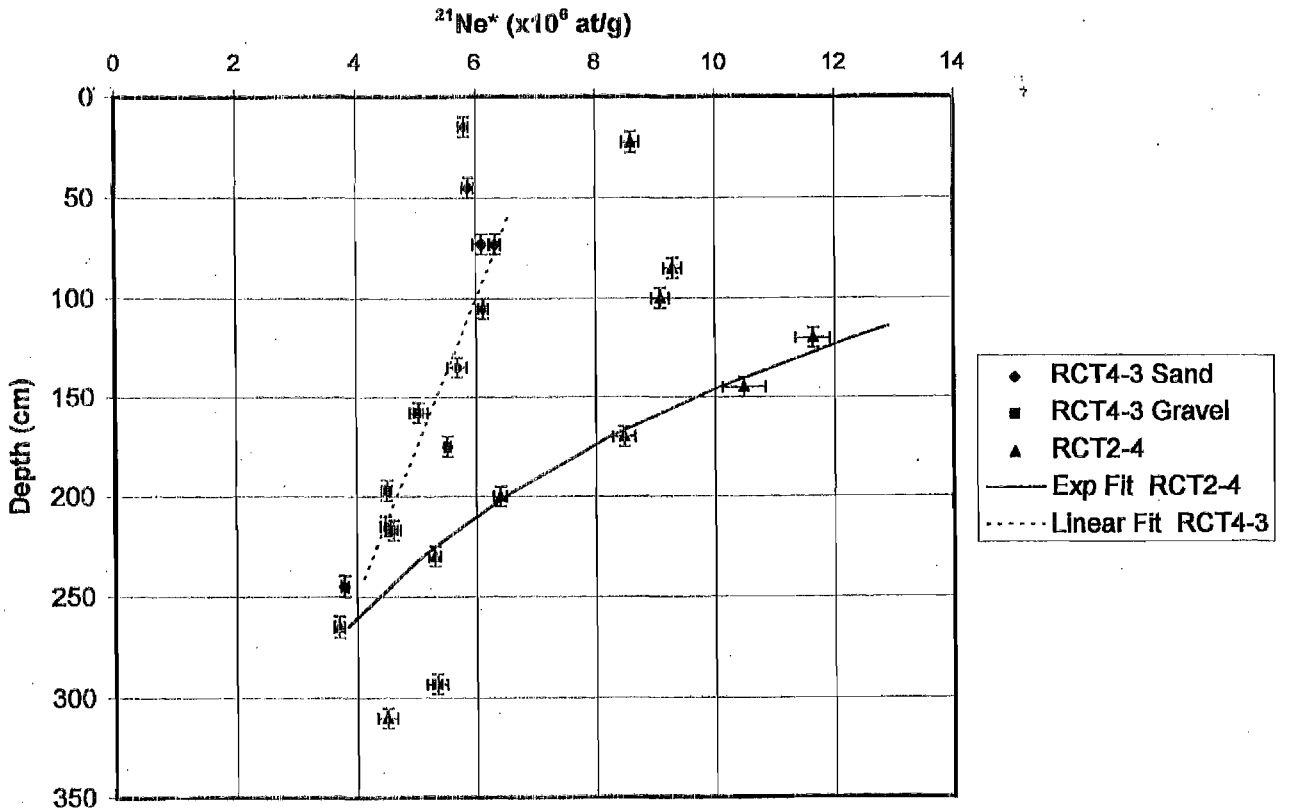

Fig. 2-41. Effect of bioturbation on ^{21}Ne* depth profiles. The solid line depicts the expected exponential decrease of ^{21}Ne* with depth. The dotted line illustrates how bioturbation could create the linear trend observed in soil pit RCT4-3 on Qt4 terrace. Near the soil surface, bioturbation destroys the exponential nuclide concentration profile, creating a uniform depth distribution that is less than expected. At depth, in-filling from above dominates and nuclide concentrations increase relative to expected exponential values.

production rates and shielding due to increases in soil bulk density also will not shift the profile away from an exponential pattern.

Bioturbation moving quartz vertically best explains the observed profile (Fig. 2-42), creating a pattern of lower-than-expected ^{21}Ne* at the soil surface, and higher-than-expected concentrations at depth. Bioturbation drops off in intensity with both depth and time. This may explain the exponential profile of the Qt2 pit. If true, the Qt2 profile may have had a stage of linear profile development, followed by exponential decreases with depth as bioturbation became unimportant. However, our confidence in bioturbation alone producing the linear trend is undermined by data from tuff clasts 1 to 5 cm in diameter in the pit in Qt4. They show the same linear trend as from sand-sized material, suggesting other factors may influence development of the linear trend.

For purposes of discussion, highly preliminary exposure ages and denudation rates can be calculated from our results. Given the need for simplifying assumptions, the terrace exposure ages agree surprisingly well with the independent age control. Terrace Qt2 yields a minimum ^{21}Ne* exposure age of 155 ± 30 ka. This age assumes that the buried soil exposed at a depth of 114 cm in the pit has always been at the terrace surface. Since the colluvium overlying this soil has an age of about 13 cal ka (Table 2-7),

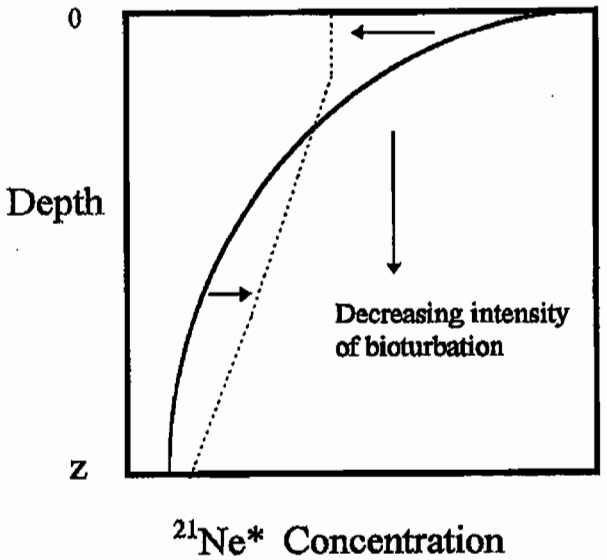

Fig. 2-42. $^{21}Ne^*$ depth profiles from soil pits in Qt2 (RCT2-4) and Qt4 (RCT4-3) terraces. $^{21}Ne^*$ displays an exponential decrease with depth below 114 cm in a buried soil in pit RCT2-4. Above 114 cm, strong bioturbation destroys the $^{21}Ne^*$ trend in the ~ 13 cal ka colluvium that caps the terrace. The source of colluvium is probably erosion of an older terrace as shown by the high $^{21}Ne^*$ concentration which cannot be produced in 13 ka of surface exposure. Soil pit RCT4-3 exhibits a puzzling linear trend in a buried soil below 60 cm which is tentatively attributed to bioturbation redistributing an exponential profile. Above 60 cm, RCT4-3 has a uniform $^{21}Ne^*$ distribution due to intense bioturbation. Near the base of both pits, anomalous $^{21}Ne^*$ concentrations are probably due to inhomogeneous inheritance.

the actual age of the terrace must be ~170 ka, in reasonable agreement with both the local soil chronofunction and amino acid age estimates on regional fan aggradation (Dethier and McCoy, 1993; see discussion at Stop 2-3g). The denudation rate computed for the Rendija Canyon basin during Qt2 time is 0.008 ± 0.002 cm/yr. This value uses the average elevation of the Rendija basin (Table 2-8) to estimate $^{21}Ne^*$ production during denudation.

Terrace Qt4 has a minimum $^{21}Ne^*$ exposure age of 42 ± 9 ka, assuming that the buried soil present at 60 cm depth has always been on the terrace surface, and that the linear trend of the profile does not invalidate the method of Anderson et al. (1996). Again, since colluvium over the soil has an age of about 13 cal ka, the true age of the terrace is at least 55 ka. This age is lower than the ca. 67-74 ka age estimate from the soil chronofunction (Table 2-5) and regional amino acid age estimates (see Stop 2-3g for discussions of soil- and amino acid-based age estimates), perhaps because bioturbation decreases nuclide concentration at the surface of soils and the model is sensitive to this process. The estimated denudation rate from the Qt4 data is 0.003 ± 0.001 cm/yr.

In summary, $^{21}Ne^*$ in sand-sized quartz from terrace Qt2 and Qt4 profiles show coherent trends with depth. The older Qt2 profile yields the expected exponential decrease of $^{21}Ne^*$ with depth. The younger Qt4 profile displays a puzzling linear trend that is attributed to bioturbation. Changes over time in soil bulk density and burial by colluvium render terrace exposure ages and basin denudation rates highly model-dependent. However, the reasonable agreement between preliminary cosmogenic exposure ages and independent age control encourages further work.

- Climb up the slope to the south, onto broad Qt2 terrace. Note the abundant evidence of tree-throw pits and mounds on the slope, indicating one process that has probably been responsible for generating the colluvium which buries the Qt4 terrace.

Station 2-3g: Pre-Wisconsin (?) Qt2 terrace; soil pit RCT2-2

Terrace Significance, Stratigraphy, and ^{14}C Age Control. The Qt2 terrace is the broadest and most continuous terrace in Rendija Canyon, extending at least 2.5 km east of here and also 0.7 km or more

to the west, across the Guaje Mountain fault (Fig. 2-20). It represents a major aggradational event, being underlain by 6-8 m of fluvial sands and gravels (Fig. 2-43). At least locally the fluvial section apparently includes buried soils, suggesting overtopping of older terraces. It apparently thins to the east where the underlying tuff pinches out onto the Puye Formation. This indicates that the Puye fanglomerates provided a local base level control for Rendija Canyon in Qt2 time, as it has in the Holocene, although the "knickpoint" or "knickzone" has apparently migrated to the west since Qt2 time.

As at the Qt4 terrace, the Qt2 terrace includes a buried soil which is overlain by fine-textured colluvium. At this pit, 2 colluvial deposits are recognized, an upper one that is 0.65 m thick and a lower 0.25 m thick deposit. The most reliable date for a Qt2 colluvial deposit was obtained at pit RCT2-1, 10,860 ^{14}C yr BP from a depth of 0.7 m near the base of the uppermost deposit (Table 2-7). A date of 880 ^{14}C yr BP from a depth of 0.35 m in this pit is suspect due to the extensive bioturbation present in these deposits.

Qt2 RCT2-2 Soil Profile. The RCT2-2 profile exposed in this soil pit (Fig. 2-44; Table 2-9) is similar to those developed at other Qt2 surfaces in Rendija Canyon. The Qt2 soil profile generally consists of a thin surface soil with an A-Bw horizon sequence formed in a thin layer of colluvium, that, in turn, overlies a buried soil with a BA-Btk-Bt-CB horizon sequence that has formed in the Qt2 alluvium. At this site, a second thin layer of colluvium that underlies the surface soil is also recognized.

Surface Soil. Soils formed on the Qt2 surfaces have been buried in places by a thin (<1 m) layer of colluvial sediment, generally associated with the distal parts of small alluvial fans or local slopewash, derived from nearby higher terraces or hillslopes (A and Bw horizons in Figs. 2-44, 2-45). The morphology of this soil is nearly identical to the soils formed in the colluvial cap the overlies the Qt4 surface.

Buried Soil b1. A second, thin (30 cm thick) layer of colluvium that overlies the top of the original Qt2 soil is also recognized at this site, but was not found at other Qt2 soil sites. Moderately developed Bt horizons that have formed in this colluvium have prismatic and subangular blocky structure and 10 YR to 8.75 YR hues. Argillans in these horizons are largely along prismatic ped faces and

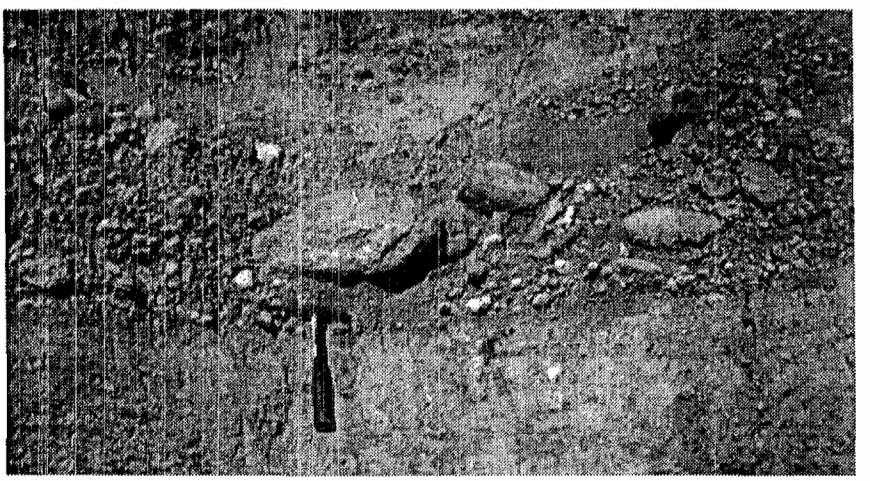

Fig. 2-43. Photograph of lower dacite-rich alluvium of Qt2 terrace, overlying strath surface cut in the Otowi Member of the Bandelier Tuff.

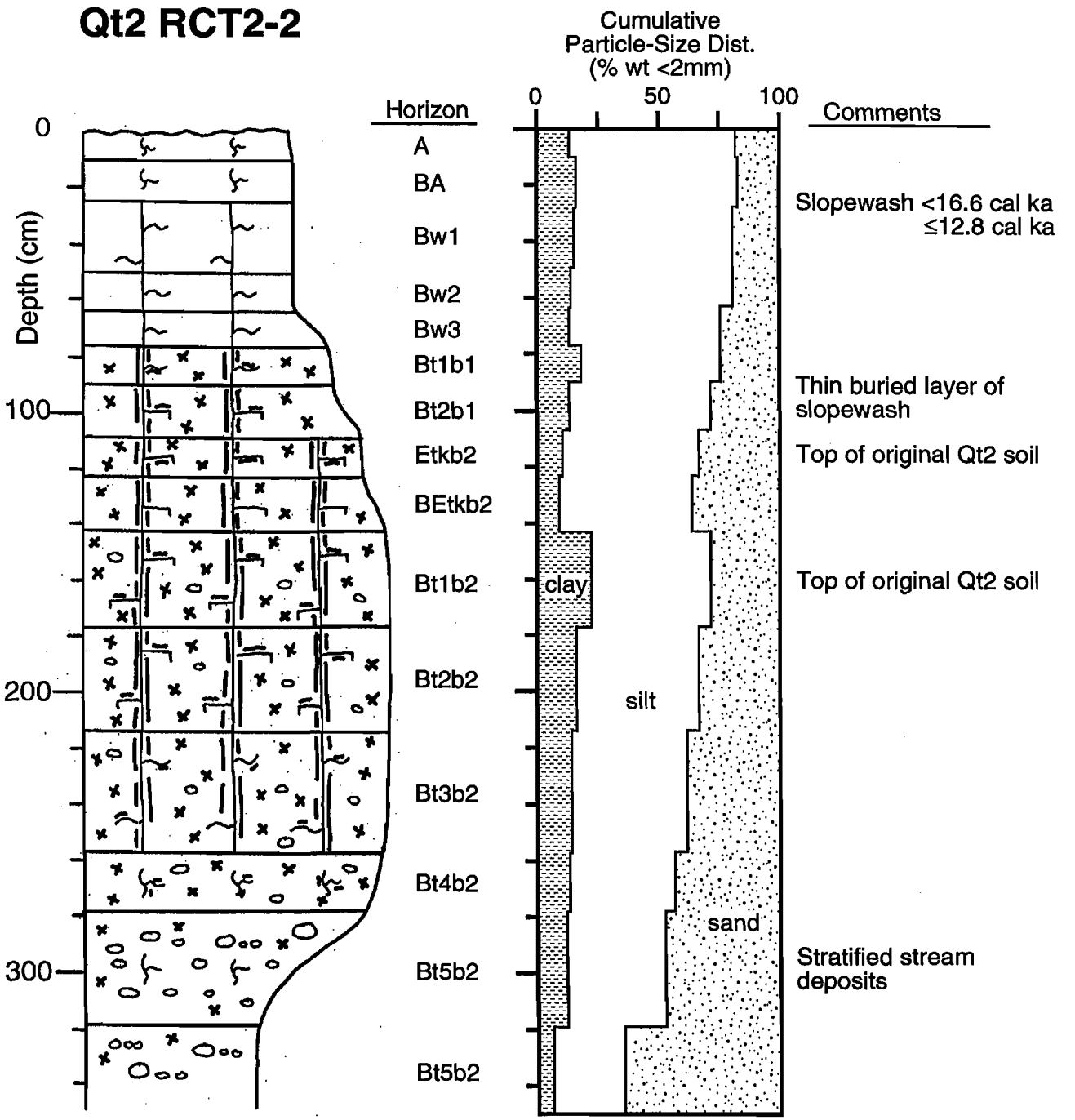

Fig. 2-44. Schematic diagram of soil morphology and particle-size distribution for the Qt2 RCT2-2 soil profile. The upper ~70 cm of the soil is a colluvial layer that buried the Qt2 surface at ca. 12.8 cal ka.

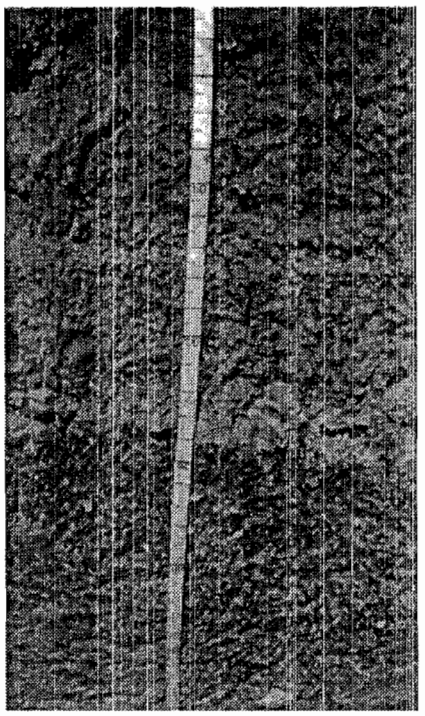

Fig. 2-45 Photograph of Qt2 (RCT2-4) soil showing base of uppermost layer of colluvium (~70 cm), and base of second colluvial layer and top of E horizon (~120 cm). Top of well developed Bt horizon is at ~140 cm.

pores indicating the most of the clay is from the overlying soil. A ^{14}C date from charcoal collected from the base of a similar colluvial layer at another Qt2 soil the indicates that deposition of this layer began about 10.9 ^{14}C ka (12.8 cal ka; Table 2-7).

Buried Soil b2. Soils formed in Qt2 stream deposits show significantly better development relative to soils formed in the Qt4 stream deposits. The top of the buried Qt2 soil is distinctly defined by an E horizon that has a pale brown color of 10 YR 6/3, prismatic and angular blocky structure, nearly continuous argillans along ped faces and large pores (Fig. 2-44). Stage I carbonates, consisting of filamentous coatings of carbonate, also line ped faces in the Etkb2 and BEtkb2 (Table 2-9). This carbonate is largely superimposed over argillans along prismatic ped faces suggesting a more recent (Holocene?) increase in soil aridity or at least a decrease in the downward flux of soil water through the upper Bt horizons.

The Qt2 soil has a thick (212 cm) sequence of well developed Bt horizons. The Bt horizons have prismatic structure that parts to angular and/or subangular blocky structure, 6.25 YR to 10 YR hues, moderately thick to thin argillans along ped faces and pores that are nearly continuous in the strongest Bt horizons. Clay content in Qt2 soil Bt horizons range from about 8 to 22 % weight, with the highest clay content in the Bt1b2 horizon. An increase is clay content in the Btb2 horizons may have been enhanced by additions of clay from eolian sources because most of the argillans occur along pores and vertical ped faces, indicating substantial illuviation of clay into the Bt horizons. The PDI value calculated for this soil is 128.3. Two other Qt2 soils yielded PDI values of 115.3 and 95.0.

Qt1 Soils. Soils formed on the Qt1 surface (not shown here) are spatially variable with laterally discontinuous B horizons, indicating that at least part of the original soil is missing due to truncation by surface erosion. Furthermore, most of the Qt1 surface has either been eroded or buried, leaving only scattered "terrace" remnants along the sidewalls of Rendija Canyon. Some of the preserved Bt horizons show an overall greater degree of development than Bt horizons in the Qt2 soils (Btkgm-Btk2, Table 2-9), although the total Bt horizon thickness is substantially less than in Qt2 soils. Soils formed in Qt1 deposits have prismatic structure that parts to subangular and angular blocky structure, 5 YR to 10 YR hues, moderately thick to thin argillans along ped faces and pores, and Bt horizon thickness of about 160 cm (Table 2-9). PDI values calculated for two Qt1 soils are 77.7 and 99.5. These values are lower than those for Qt2 soils, reflecting the decrease in profile thickness of the Qt1 soils and partial erosion of their well-developed Bt horizons.

Development of Soil Chronofunction for Rendija Canyon Soils. Soil ages can be estimated based on a systematic increase in soil profile morphology using simple linear regression analysis of logarithmic relationships between PDI values and ages of dated soils (Fig. 2-46). Several different methods of linear statistical analyses have been employed for evaluating rates of soil development based on SDI values and to account for poor age control of studied soil surfaces (Switzer et al., 1988; Harden 1990;

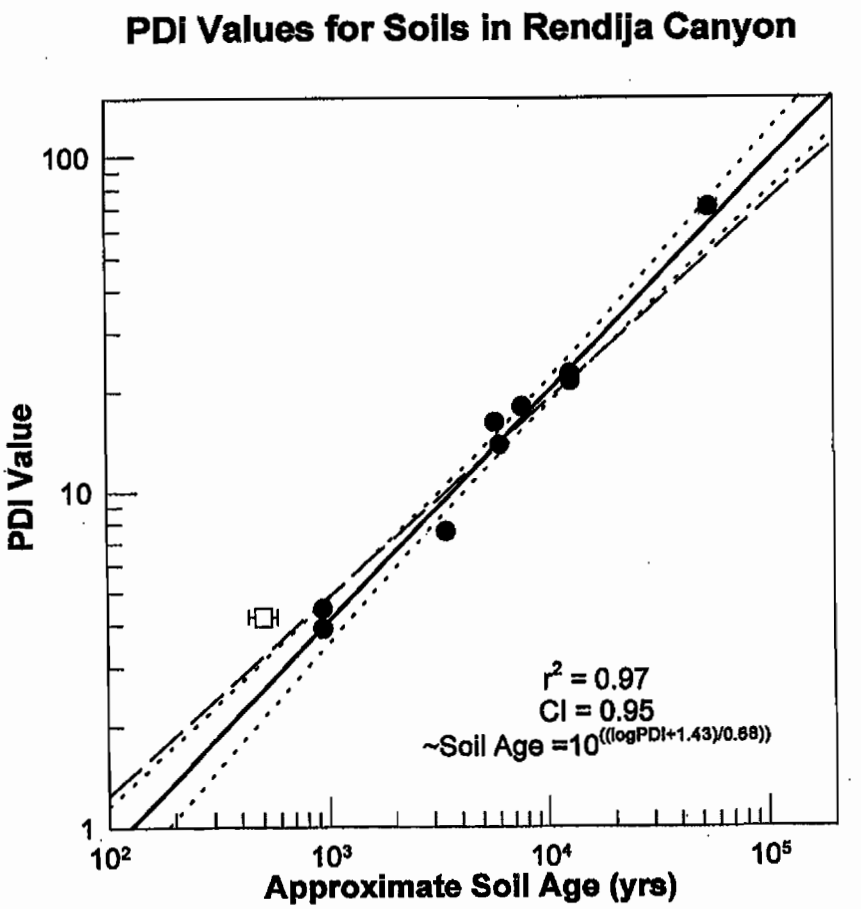

Fig. 2-46. Soil chronofunction (solid line) developed using linear regression of dated soils (solid circles) used in this study. Dotted line represents the 95 % confidence interval (CI) for regression line. The 0.5 ka RCT8-2 soil was excluded from this data set (open box) due to possible inconsistencies between PDI values and soil ages. A second chronofunction (dashed line) reflects the impact that inclusion of the RCT8-2 soil has on the slope of the line.

Harden et al., 1991). For the purpose of this study, simple linear regression was used to develop a soil chronofunction based on temporal increases in PDI values and to provide age estimates for non-dated surfaces.

The 11 best dated soils were used to develop the soil chronofunction shown in Fig. 2-46. The age used for each Qt8-Qt6 soil was based on calibrated ^{14}C analyses from that specific terrace, as ages may vary within a mapping unit. The RCT8-2 soil has a radiocarbon age of about half that of the other dated Qt8 soils, but a similar PDI value (Table 2-10). Inclusion of this soil within the data set resulted in a correspondingly large shift in the chronofunction because of the greater number of data points on the low end relative to only one PDI value for the upper end (WJR-5 soil; Fig. 2-46). We decided to omit the RCT8-2 soil from our best estimate of the soil chronofunction for Rendija Canyon because: (1) better linear agreement among all other soils results when the RCT8-2 soil is omitted; (2) a 500 year difference in dates for the Qt8 has such a large impact on the resulting soil chronofunction; and (3) because of the relatively low PDI values for very young, weakly developed soils that are insensitive to slight differences in soil age. PDI values from 4 soils developed in the colluvial cap that overlies the Qt4 and Qt2 soils were also included in the data set. Calculations of PDI values for these soils included pedogenic changes in the upper 2-3 Bt horizons of the underlying buried soil (extending to a maximum

depth of 107-109 cm). Pedogenic changes were considered for dry and moist consistence and argillans, and were based on differences between assumed morphology of the former A-BA horizons and the morphology of the current Btb horizons. Changes in these morphologic properties are a direct response to burial and overprinting by soil formation in the colluvial cap. A PDI value for the WJR-5 soil formed in deposits that overlie the ca. 50-60 ka El Cajete pumice was also used. Soil-stratigraphy of the WJR-5 soil indicates that this soil provides a reasonable approximation of 50-60 ky of soil formation.

Profile Development Index Estimates of Qt4-Qt1 Soil Ages. The soil chronofunction can be used to calculate approximate ages for each soil not directly dated by radiometric means by using the PDI-soil age equation derived from linear regression analysis (Fig 2-46; Table 2-10). However, given the uncertainties in both calculation of PDI numbers and in the slope of the soil chronofunction, these ages are, at best, general approximations. Best age estimates for the Qt4 soils range from about 67.5 to 74.0 ka and for the Qt2 soils range from about 102.7 to 159.7 ka. Soils formed on the Qt1 surface must be older than soils formed on the Qt2; however, because of profile loss from erosion, the approximate estimates are minimum-limiting ages of >67.8 to >109.9 ka.

Soil Chronosequence: Summary of Preliminary Results and Interpretations

Soil Morphology. The primary trend in soil development among the Holocene Qt8-Qt6 soils is the development of subangular blocky structure, slight increases in rubification, and the downward mixing of silt through the Bw horizons, largely through bioturbation (Fig. 2-47). The most significant temporal change is the thickening of the Bw horizons. Soils formed in a thin layer of colluvium, that in places covers the Qt4 and Qt2 soils, displays better development of rubification, structure, and stronger dry and moist consistence than the soils formed on the younger Holocene terraces. Available age control indicates that the soils may have been forming since about 12.8 cal ka.

Soil formed in stream deposits of the Qt4 and Qt2 terraces show considerably stronger B horizon development than the Holocene soils (Fig. 2-46). Depth profiles of horizon development index values also reflect temporal trends in increasing development of soil morphology (Fig. 2-48). Bt horizons in the Qt4 soils are thick (>1 m), have weak to moderate prismatic and subangular blocky structure, noticeable rubification, and patchy argillans along ped faces (especially prismatic faces) and pores. Abundant evidence of bioturbation within the strongest Bt horizons indicates that much of silt (and some clay) has been presumably added to these subsurface horizons by bioturbation. Bt horizons in the Qt2 soils show considerably better development than the Bt horizons in the Qt4 soils. These Bt horizons are very thick (>2 m), have moderate to strong prismatic and angular blocky structure in places, well developed rubification, and nearly continuous to patchy argillans along pedfaces, pores, and gravel exteriors. Evidence of bioturbation is not as well preserved in the Qt2 Bt horizons.

Extractable Fe Oxides. Mean concentrations of dithionite-extractable Fe (Fe_d) of 0.31 ± 0.15 % wt. Fe_2O_3 and oxalate-extractable Fe (Fe_o) of 0.38 ± 0.15 wt %. Fe_2O_3 for soils on the Qt8-Qt6 surfaces indicate that minimal pedogenic formation of Fe-oxides has occurred (Table 2-11; Fig. 2-49). In addition, generally high Fe_d/Fe_o ratios indicates a predominance of poorly crystalline forms of Fe oxides (Schwertmann and Taylor, 1989). Fe-oxides generally decrease with depth in the Qt8-Qt6 soil profiles, reflecting incipient development of pedogenic Fe-oxides in the A and Bw horizons. Some of the increases in Fe oxides may also be due to additions of colluvial deposits that contain material relatively high in Fe-oxides (as compared to stream deposits). For example, colluvial material in surface C horizons in some Qt8 and Qt7 soils has relatively higher levels of Fe oxides relative to underlying A and B horizons (Table 2-11).

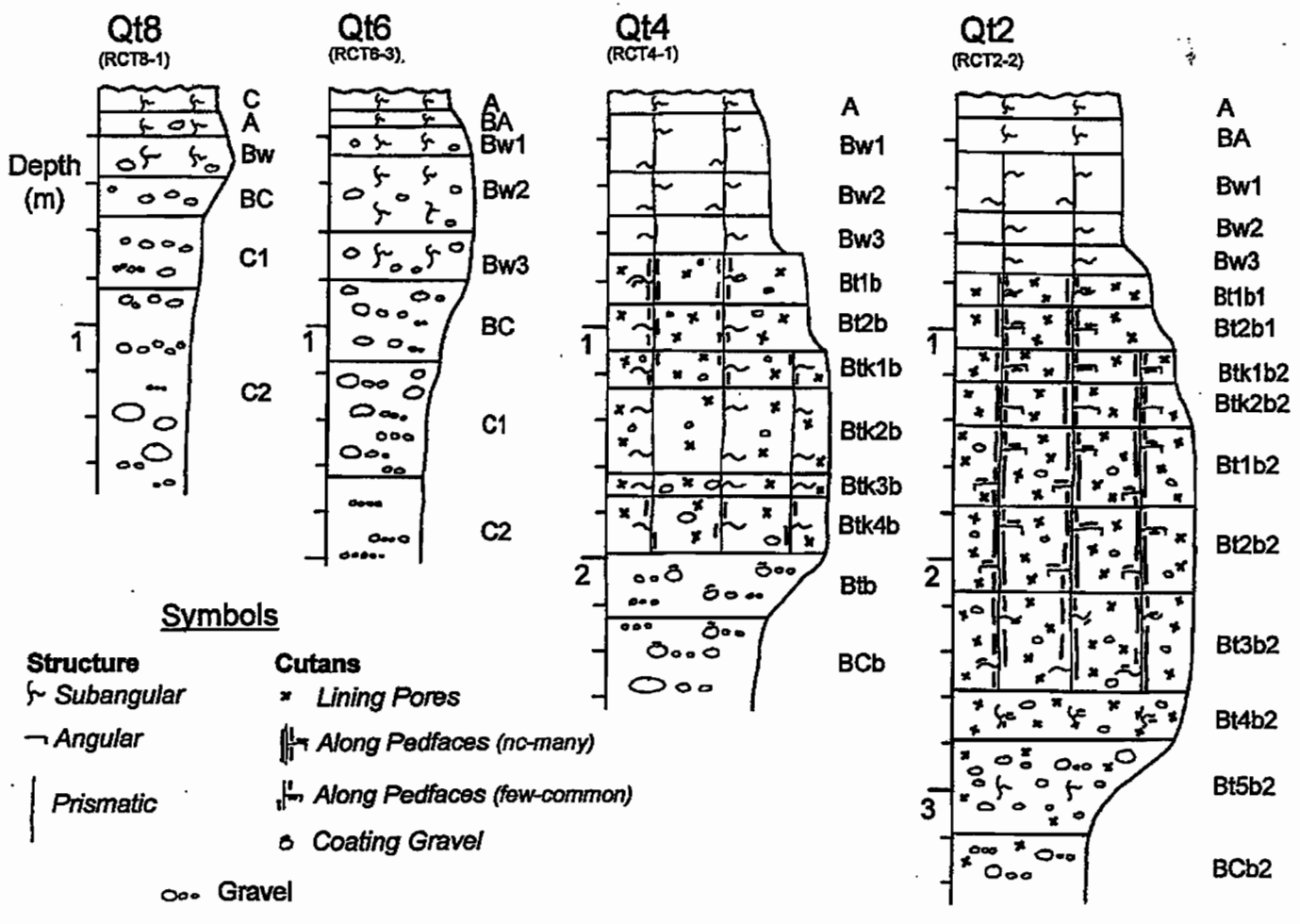

Fig. 2-47. Schematic diagram of dominant soil morphology of soil profiles formed on four of the terraces in Rendija Canyon. Sequence represents systematic increases in B horizon development and thickness, especially development of structure and argillans along pedfaces and pores. Note the difference in soil morphology between soils formed in alluvial cap and underlying buried soils on the Qt2 and Qt4 terraces. Symbols for abundance of cutans on pedfaces represent either nearly-continuous (nc) to many or few to common.

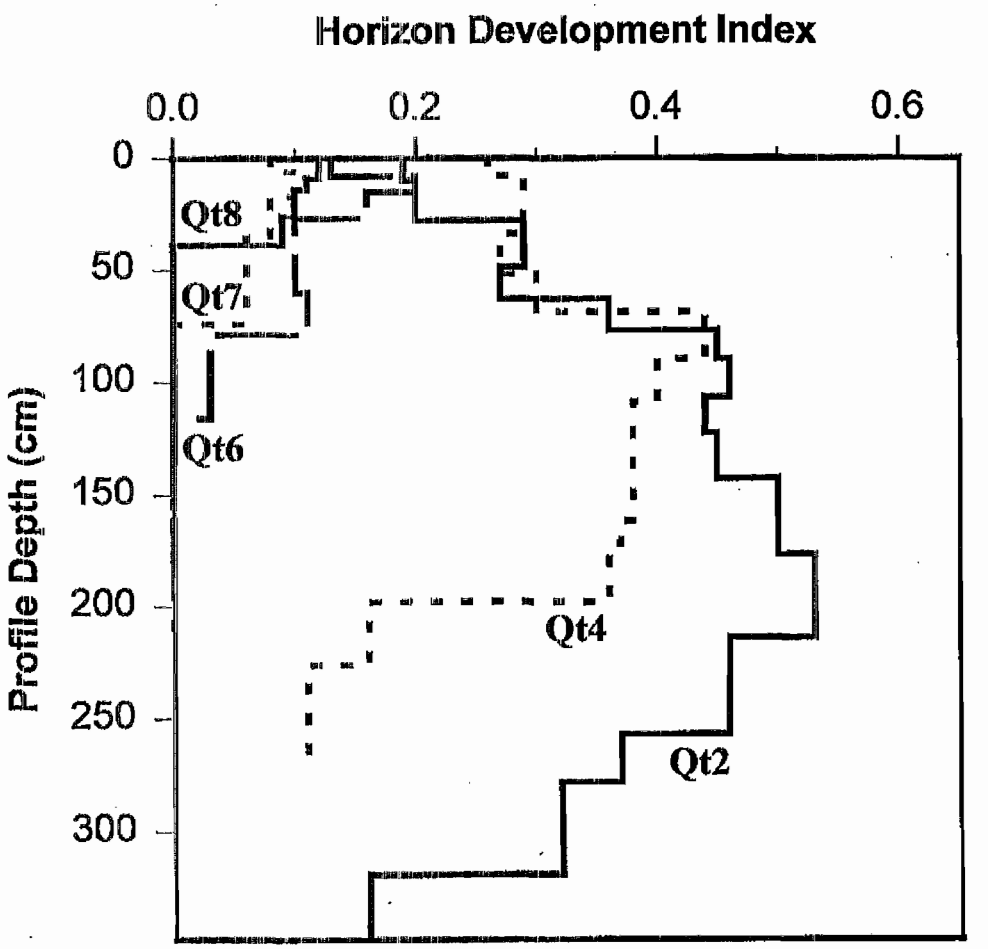

Fig. 2-48. Depth plot of HDI values for soils shown in Table 2 (except RCT8-1). HDI values are the average of normalized property values for each horizon and provide a relative indicator of horizon strength.

Mean concentrations of Fe_d of 0.21 ± 0.09 % wt. Fe_2O_3 and Fe_o of 0.63 ± 0.16 wt % for buried Qt4 and Qt2 soils formed in stream deposits (i.e. soils below the colluvial cap) indicate that considerably greater formation of pedogenic Fe oxides has occurred in the these soils relative to the soils formed in Holocene stream deposits. Low ratios of Fe_d/Fe_o indicate an increase in the crystallinity of pedogenic iron oxides. Concentrations of Fe oxides also decrease with profile depth (Fig. 2-49). Extractable Fe is higher in the overlying surface soil relative to the buried soils. In comparison, mean concentrations of Fe_d of 0.30 ± 0.04 % wt. Fe_2O_3 and oxalate-extractable Fe_o of 0.80 ± 0.10 wt % Fe_2O_3 for soils formed in the colluvial cap on the Qt4 and Qt 2 surfaces is slightly higher than that in the underlying, and considerably older, soils formed in stream deposits (Table 2-11; Fig. 2-49). The higher concentrations of Fe oxides are probably due to relatively high contents of Fe oxides in the colluvium. The primary source for much of the colluvium is eroding soils, alluvium, and colluvium from older soils upslope of the Qt2 and Qt4 surfaces.

Extractable Al and Si. Generally low concentrations of oxalate-extractable Al and Si and suggests that minimal *in situ* formation of allophanic clays (allophane and imogolite) has occurred (Table 2-11). The production of allophanic clays, however, in these soil is probably limited due to lack of sufficient percolation of soil water. Production of allophanic clays appears to increase when there is sufficient precipitation and/or soil percolation rates that provide leaching >200 mm/year (Parfitt et al.,

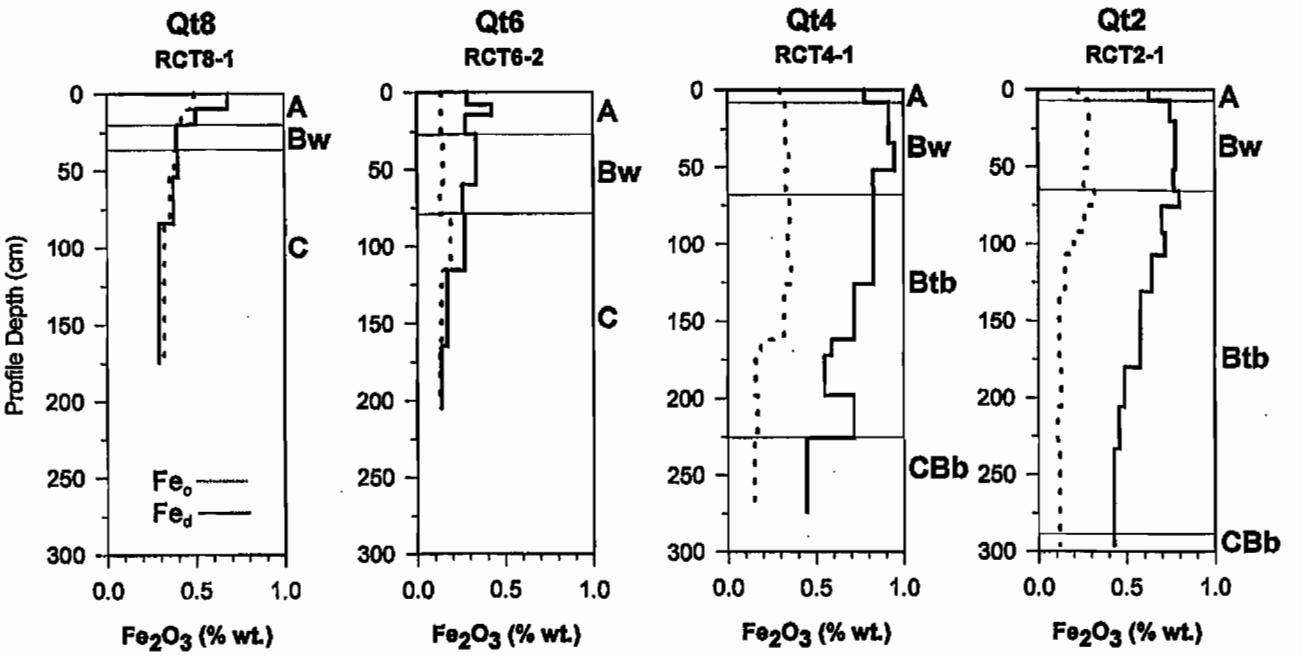

Fig. 2-49. Depth profiles of Fed and Feo for soils formed on Qt6, Qt4, and Qt2 surfaces.

1984; Wada, 1989). Available paleoclimate data, however, suggests that levels of precipitation may have been considerably higher at times during the late Pleistocene (see Introduction) suggesting that past, presumably wetter climates, could have enhanced the formation of allophanic clay in these soils. A lack of these clays in soils formed on either the Qt4 or Qt2 surfaces, however, indicates that either past conditions were not moist enough for formation of allophanic clays or that these clays were not preserved under current soil forming conditions. Production of halloysite is favored in soil formed in siliceous, volcanic-rich materials under semi-arid conditions (Parfitt et al., 1984; Dixon, 1989); however, preliminary XRD results (discussed below) indicate that halloysite may not be present.

XRD. Preliminary XRD (X-ray diffraction) results for a few horizons in Qt8-Qt2 soils indicates relatively slight changes in clay mineralogy between Holocene and Pleistocene soils. Diffractograms for a few A, B, and C horizons among the Qt8-Qt6 soils indicate a predominance of illite and kaolinite. Diffractograms for a few A, B, and BC horizons among the Qt4 and Qt2 soils also indicate a predominance of illite and kaolinite, but also indicate the possible presence of a mixed illite-smectite clay mineral. Kaolinite, illite, were also identified in several mesa top soils; however, smectite was also found to be a commonly occurring clay mineral, especially along bedrock fractures (Davenport, 1993; Davenport et al., 1995; Vaniman and Chipera, 1995).

Source of Accumulated Clay. An important question regarding the formation of the soils in Rendija Canyon, as well as across the Pajarito Plateau, is what are the primary sources of accumulated clay in moderately- to well-developed soils. Most argillans occur along better developed ped faces and pores, especially pores with diameters >1-2 mm, indicating substantial translocation of clay from overlying horizons. The principle source of accumulated clay is most likely derived from dust and additions of fine-textured slopewash to surface horizons rather than considerable chemical alteration of the soil matrix. A similar conclusion regarding the degree of weathering for mesa top soils and importance of eolian sources of clay was also suggested by (McFadden et al, 1996; Eberly et al., 1996). Development of smectite bearing clay minerals, increases in Fe oxides, and slight changes in high base/alumina

and base R_2O_3 molar ratios (where R_2O_3 signifies chemically conservative elements) for some well-developed soils on mesa tops (McFadden et al., 1996) indicates that at least some chemical weathering and the pedogenic formation of small amounts of aluminosilicate clay is probably occurring in the soils in Rendija Canyon. A lack of considerable chemical alteration of the largely silica-rich volcanic materials that make up the bulk of the soil parent material is surprising given that it is generally thought that these types of materials are conducive to weathering, even in semi-arid to subhumid environments. An overall lack of strong chemical alteration and strong accumulation of clay, that is most likely derived from accumulation of dust and slopewash, further illustrate the importance of geomorphic (i.e., external) contributions to soils forming in these environments.

Use of Soils for Addressing Geologic Problems on the Pajarito Plateau. An overall increase in development of several pedogenic properties (including structure, soil reddening, argillans, increases in the accumulation of clay, silt, and Fe oxides) and systematic increases in PDI values indicate that the formation of soils in Rendija Canyon, as well as across the Pajarito Plateau, are largely time dependent. Other factors, including the degree of landscape stability, geomorphic location, and climatic variability will also have an important control on the rates and processes of soil formation. Strongly temporal trends, combined with a careful analysis of soil-stratigraphy and geomorphic setting, indicate that the use of soils can provide important information for interpreting the ages and history of late Quaternary events across the Plateau.

Regional Correlations of Late Quaternary Fans and Terraces. The soil-based age estimates for the Qt2 and Qt4 terraces in Rendija Canyon are similar to age estimates for lower elevation fans in the Española basin (Dethier et al., 1988; Dethier and McCoy, 1993; Dethier, unpub., 1996), suggesting a similar climatic control on periods of aggradation. The Española basin work demonstrated that periods of floodplain widening along the Rio Chama and the Rio Grande, which head in glaciated terrain of northern New Mexico and southern Colorado, were out of phase with fan growth along streams that drain the northeastern Jemez Mountains. Floodplain widening along the axial rivers during glacial periods contrasts with fan aggradation and floodplain narrowing associated with the change to warmer interglacial climates. The model of Dethier and colleagues is consistent with the evidence for extensive aggradation and or episodic terrace formation on the Pajarito Plateau during the present interglacial climate, and the apparent scarcity of alluvial deposits dating to the last glaciation. Kelson and Wells (1987) similarly reported that a largely nonglaciated basin near Taos apparently experienced lateral erosion during interglacial periods and incision and resultant terrace formation during glacial periods, contrasting with opposing behavior in nearby glaciated basins.

Age estimates for periods of fan aggradation by Dethier and McCoy (1993) are based on a locally calibrated amino acid dating curve, applied to fossil gastropods, which somewhat revise previous age estimates presented in Dethier et al. (1988). The revised age estimates for the two youngest, pre-Holocene periods of major fan aggradation are 170 ± 40 and 95 ± 15 ka (Dethier and McCoy, 1993), subsequently revised to best estimates of ca. 150 and 70 ka (Dethier, unpub., 1996). The similarity with the age estimates for Qt2 and Qt4, presented in Table 2-5, is encouraging, providing further support for the validity of the soil-based age estimates and evidence for regional periods of aggradation along many non-glaciated drainages in northern New Mexico.

Late Quaternary Behavior of Rendija Canyon. The Rendija Canyon stream terraces record dramatic variations in late Quaternary fluvial processes. Based in part on the abundant evidence for widespread Holocene erosion across the Pajarito Plateau concurrent with the development of multiple terraces in Rendija Canyon, we infer that periods of floodplain widening (± aggradation) are at least in

part controlled by increases in sediment supply. Similarly, the apparent absence of latest Pleistocene terraces is consistent with reduced sediment supply, perhaps at a time when intense convective thunderstorms occurred less frequently and tree cover was denser than in the Holocene (although the paleoclimatic record is admittedly incomplete and subject to continual debate and revision).

Controls on periods of channel incision in Rendija Canyon are less certain. It is notable that the total amount of incision into tuff has been higher in the last 5-6 ka, following development of the Qt6 terrace (~3-5 m), than between Qt4 and Qt6 time (~2-3 m; Fig. 2-20). Average Holocene incision rates have thus apparently been an order of magnitude higher than average late Pleistocene incision rates, despite the evidence for high sediment supply and recurring floodplain stability in the Holocene. Although surface rupture on the Guaje Mountain fault might have affected these incision rates, with some of the post-Qt6 incision possibly related to the ca. 4-6 ^{14}C ka event identified at SHT-1 (Stop 2-3d), it can not entirely explain the discrepancy between Holocene and late Pleistocene rates.

We speculate that these apparent contrasts in the late Quaternary behavior of Rendija Canyon are due to significant differences in the magnitude of rare flood events between the late Pleistocene and the Holocene. Along much of the 4-km long study reach, the channel is apparently armored with dacite boulders, and nowhere is tuff exposed on the stream bed. Bull (1991) has pointed out how such armors can be very effective at impeding incision, although incision may proceed rapidly once such armors are removed. The evidence in Rendija Canyon for rapid, episodic incision in the Holocene suggests the recurrence of high magnitude flood events that can effectively strip the boulder armor and trigger incision into tuff. Conversely, the much lower rates of incision in the late Pleistocene suggests the absence of such events. Possible causes of such high magnitude Holocene floods could include unusually intense, basin-wide summer monsoonal rainfall, and rare extra-tropical storms (which typically occur in the fall in northern New Mexico). The channel scour and exposure of bedrock that has occurred this summer in Capulin Canyon, associated with floods that followed the Dome Fire (see discussion at Stop 2-1), suggests another possible contributing factor for rare, high magnitude, geomorphically effective floods in the Holocene.

The contrast between the relatively thick fills associated with the Qt2 and Qt4 terraces and the thinner Holocene deposits on Rendija Canyon terraces may also be related to variations in flood magnitude. One possibility is that Qt2 and Qt4 record extended periods with high sediment supply but lacking the rare floods required to strip channel-bed armors and trigger incision. Hopefully, future research on the fluvial systems of northern New Mexico and surrounding regions will be able to shed more light on these conjectures.

- Walk east down road to clubhouse. Retrace route to Golf Course.

19.6 **San Ildefonso Road, Barranca Road intersection**. Turn right.

20.0 **Diamond Drive**. Turn right.

20.2 **Road to Guaje Pines Cemetery**. ("Range Road", unsigned). Turn right for Stop 4 (optional).

20.3 Top of roadcut to left exposes basal alluvium of the "Golf Course surface", overlying Tshirege Member of Bandelier Tuff (Qbt-3?). These alluvial deposits are better exposed in roadcuts in the "Ponderosa Estates" subdivision.

20.4 Road into "Ponderosa Estates", on left ("Aspen Lane", not signed in 1996). Fresh roadcuts in this new subdivision (development began in 1993) expose: 1) excellent examples of fumarolic pipes in the uppermost, non-welded Tshirege Member; 2) faulted early Pleistocene, post-Tshirege pumice beds associated with the Valles Rhyolite; and 3) dacite-bearing alluvium of the "Golf Course surface", part of a presumed early Pleistocene Rendija Canyon fan that pre-dated major canyon incision and that is preserved on the down-dropped block west of the Rendija Canyon fault.

20.6 Entrance to Guaje Pines Cemetery. Turn right and drive east to end of cul-de-sac.

20.8 **Stop 4 (optional): Rendija Canyon Fault Zone at Guaje Pines Cemetery**

The Guaje Pines Cemetery is located on a late Quaternary alluvial surface within Rendija Canyon. The rugged topography to the north and west is mainly underlain by Miocene to Pliocene dacites of the Tschicoma Formation, and the escarpment to the southeast (the west end of Barranca Mesa) is underlain by the Tshirege Member of the Bandelier Tuff. The north-trending escarpment to the east parallels the Rendija Canyon fault, which displays about 30 m of post-Bandelier down-to-the-west offset in this area (Fig. 5 in Introduction; Wong et al., 1995; Kelson et al., 1996; Olig et al., 1996). To the east Rendija Canyon has incised a narrow slot through the southern slope of a pre-Bandelier paleohill (see Broxton and Reneau, 1996), and highly sheared Tschicoma dacite is exposed adjacent to the stream.

The low rise at the east end of the cemetery marks the trace of the Rendija Canyon fault. This is the only place within Los Alamos County where a fault scarp has been located across a late Quaternary alluvial surface, and a series of trenches were excavated here in 1992 to evaluate the paleoseismic history of the fault (Fig. 2-50; Wong et al., 1995; Kelson et al., 1996). As exposed in the trenches, the area east of the fault is underlain by dacite-rich late Quaternary fluvial deposits that in turn overlie a possible sag pond deposit, and the area to the west is underlain by a series of fault scarp derived colluvial layers that overlie faulted alluvium (Fig. 2-51). The most recent event produced an estimated 2 ± 0.5 m high scarp here, suggesting a magnitude 6-7 earthquake. The age of the most recent event is not certain due to discrepancies between different dating methods; radiocarbon dating of charcoal fragments indicates an age of ca. 8 ka, whereas thermoluminescence (TL) analysis of scarp-derived colluvium indicates an age of ca. 23 ± 4 ka. The age of the penultimate event is estimated at ca. 65 ± 9 TL ka, and the age of a prior event is estimated at $\geq 140 \pm 26$ TL ka (Wong et al., 1995; Kelson et al., 1996).

The seeming independence in age of the most recent surface rupture events here and on the Guaje Mountain fault at SHT-1 (Stop 2-3d) was surprising, considering their close proximity and similar styles of faulting. Similarly, the absence of recognized contemporaneous rupture on the Pajarito fault is also puzzling, as the down-to-the-west Rendija Canyon and Guaje Mountain faults appear to be antithetic to the down-to-the-east Pajarito fault. The Pajarito fault also has much higher long-term slip rates and would be expected to be more active, yet has not yielded evidence of events in the last 50-60 ka. Clearly, much remains uncertain about the kinematics and the paleoseismic history of the Pajarito fault system

- Retrace route to Los Alamos and Ponderosa Campground.

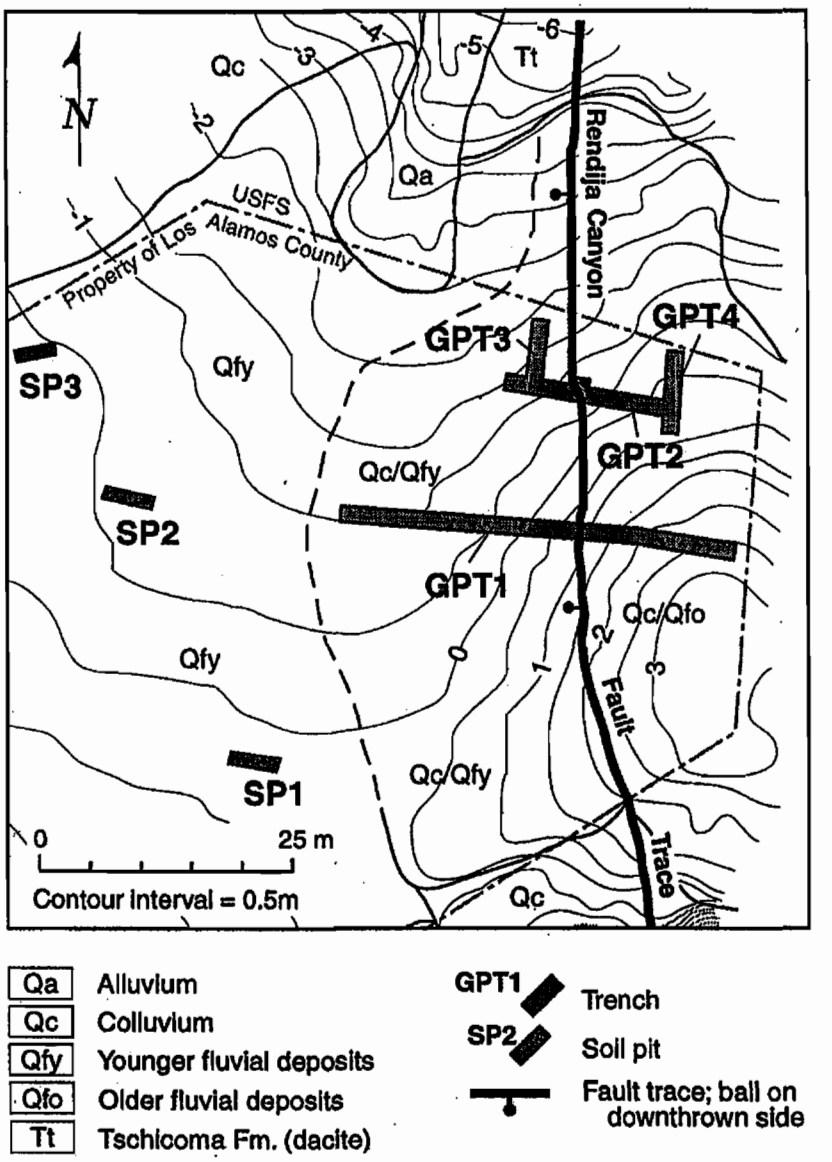

Fig. 2-50. Map showing paleoseismic trenches along the Rendija Canyon fault at the Guaje Pines Cemetery (from Kelson et al., 1996).

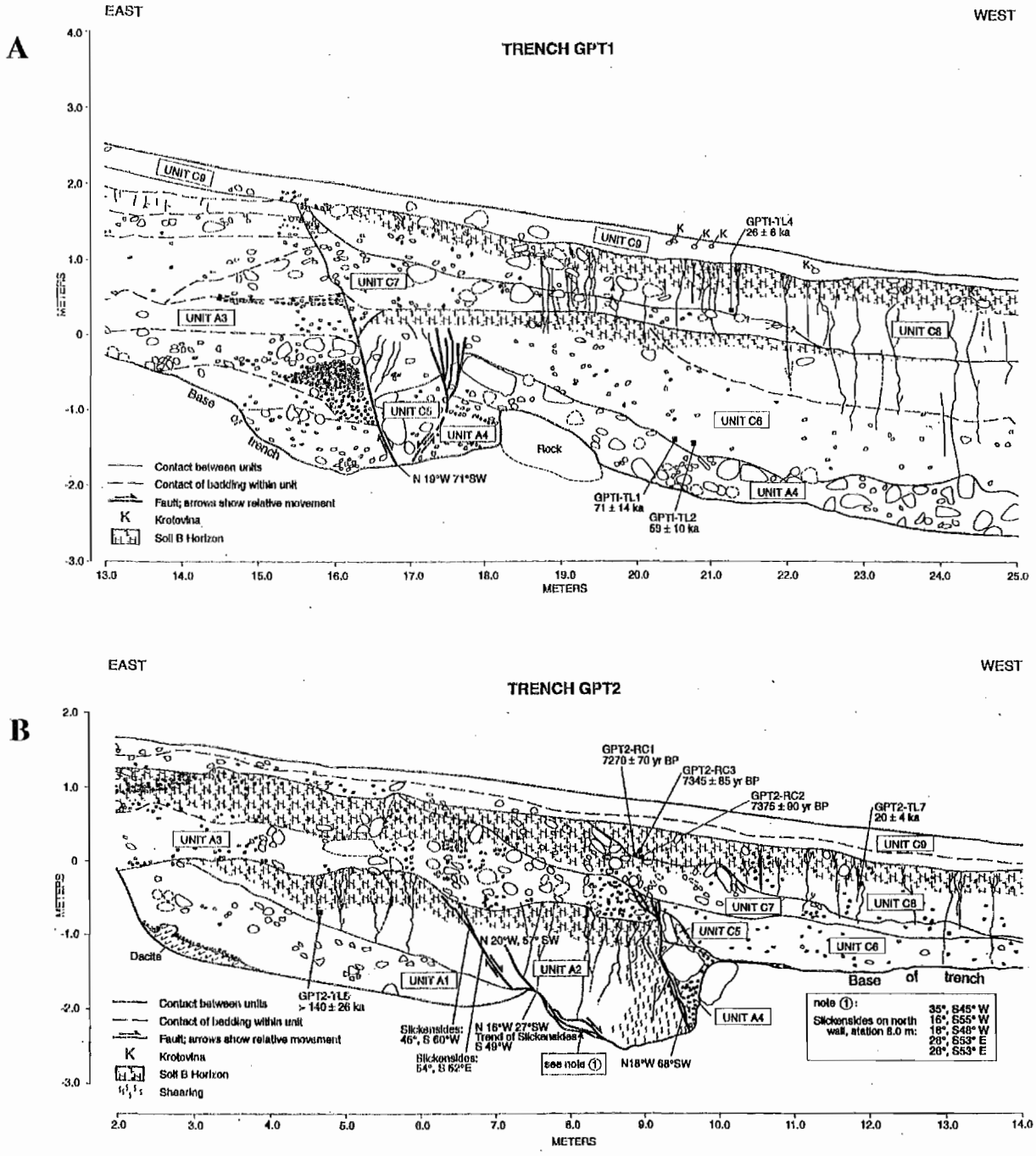

Fig. 2-51. Logs of parts of trenches GPT1 and GPT2. Units labeled "A" and "C" and alluvial and colluvial units, respectively. Units C7 and C8 represent scarp-derived colluvial layers that probably formed soon after the most recent surface rupture event, and units C5 and C6 similar deposits that formed after the penultimate event. Unit A2 is a possible sag pond deposit, >140 TL ka in age, that is buried by dacite-rich alluvium of unit A3. (from Kelson et al., 1996).

Day 3, Pueblo Canyon and Los Alamos Canyon

Leaders: Steven Reneau, Dave Broxton, Eric McDonald
(with many contributions to the sediment studies by Brad Wilcox, Will Graf, and LANL's "Canyons" investigation team)

The meeting area for Day 3 is on NM 502 at the interchange with NM State Road 4 (the "White Rock Wye"), at a dirt road to the north near the highway maintenance area. (From Ponderosa Campground, head north on Day 2 route [NM 501, West Jemez Road], heading straight through stoplight at intersection with Diamond Drive and down East Jemez Road to SR 4, north past Tsankawi to interchange, following sign to Los Alamos [left lane]; road is on right soon after joining NM 502. From Los Alamos, follow NM 502 towards Santa Fe, turning left at bottom of hill onto 1st and only road [opposite where road forks to White Rock]).

Mileage From NM 502

0.0 Gate at dirt road leading up Pueblo Canyon to Los Alamos County Sewage Treatment Plant (road unsigned; gate locked, but area open for recreational use). Highway maintenance area to right.

0.2 Gully to right exposes El Cajete pumice beneath colluvium. This is close to the northernmost recognized extent of the pumice bed (so far anyway).

1.3 Main dirt road bends to left, parallel to Pueblo Canyon channel, and dirt track heads right into woods. Park.

- Either walk down dirt track to east to where track ends at old corral, or walk down along stream channel (latter route can be overgrown and soggy).

Stop 3-1: Lower Pueblo Canyon

Station 3-1a, Pueblo Canyon near Monitoring Well PO-4 (6440', 1965 m elev.)

Geologic Setting. This stop is stratigraphically below the Bandelier Tuff, where the stream has incised into Pliocene fanglomerates of the Puye Formation (locally exposed in the stream banks) (Fig. 3-1). Basalts are exposed in the stream bed about 2 km downstream, immediately above the confluence with Los Alamos Canyon, providing a local base level control (Fig. 3-2). As discussed for other canyons, this part of Pueblo Canyon has experienced late Quaternary aggradation, and the canyon bottom near here at well PO-4 (Pueblo Observation Well 4, drilled in 1996) is underlain by 17 m of alluvium. The alluvium pinches out downstream on the basalt, and the present average channel gradient between here and the basalt of about ~0.019 m/m (1.1°) is steeper than the pre-aggradation gradient of ~0.014 (0.8°, assuming the same sinuosity as today). Alluvium exposed in the stream banks is largely or entirely latest Holocene to historic (post-1943 A.D.) in age.

Ongoing Environmental Investigations. Most of LANL's Environmental Restoration Project has been focused on characterizing and cleaning up sites at or near potential contaminant releases. The recently begun "Canyons" investigations are unique in that they examine present and potential future contaminant distributions on a watershed scale, evaluating contamination dispersed by surface water

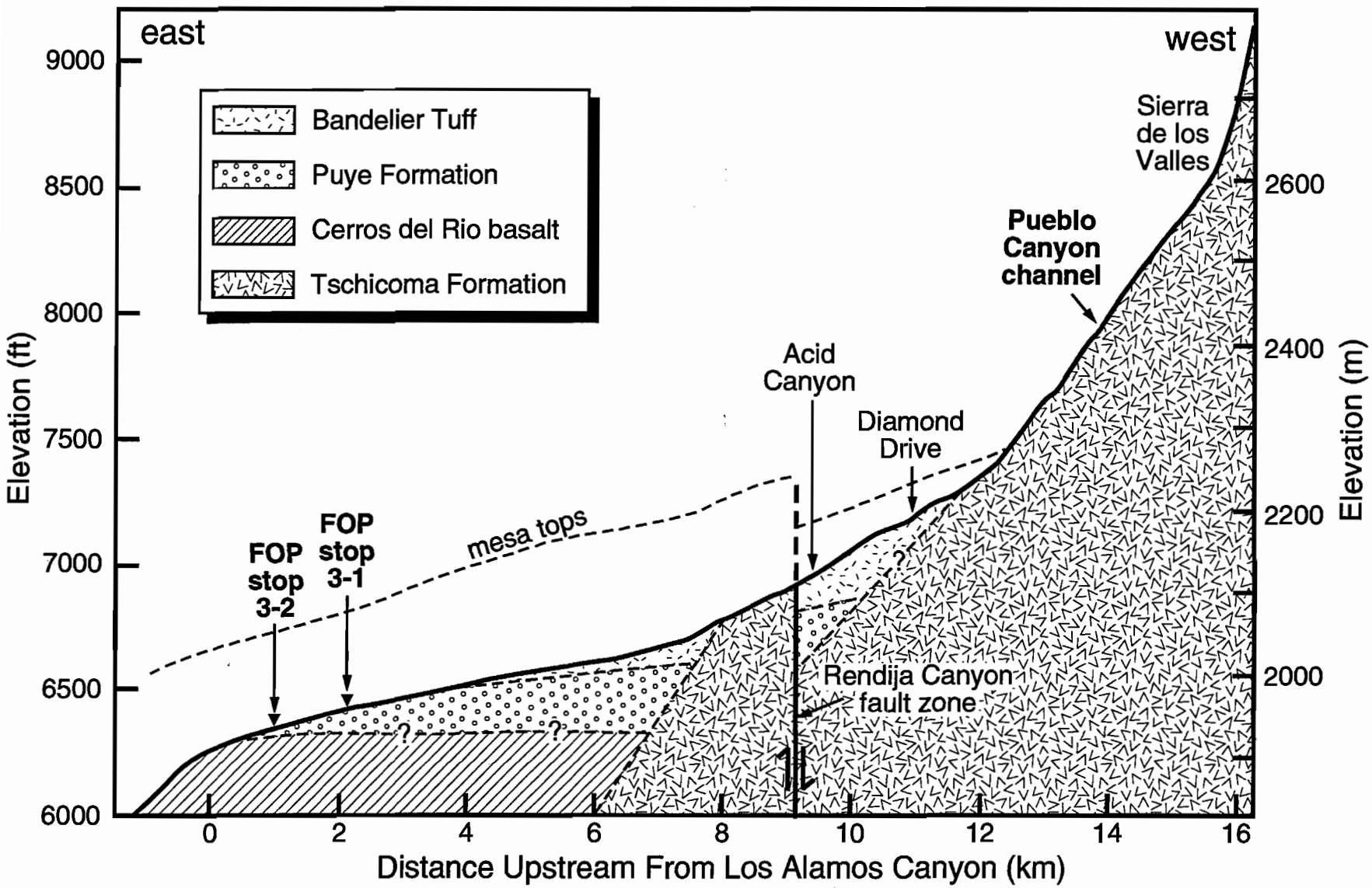

Fig. 3-1. Longitudinal profile of Pueblo Canyon, showing general distribution of bedrock units, location of Acid Canyon, and FOP stops.

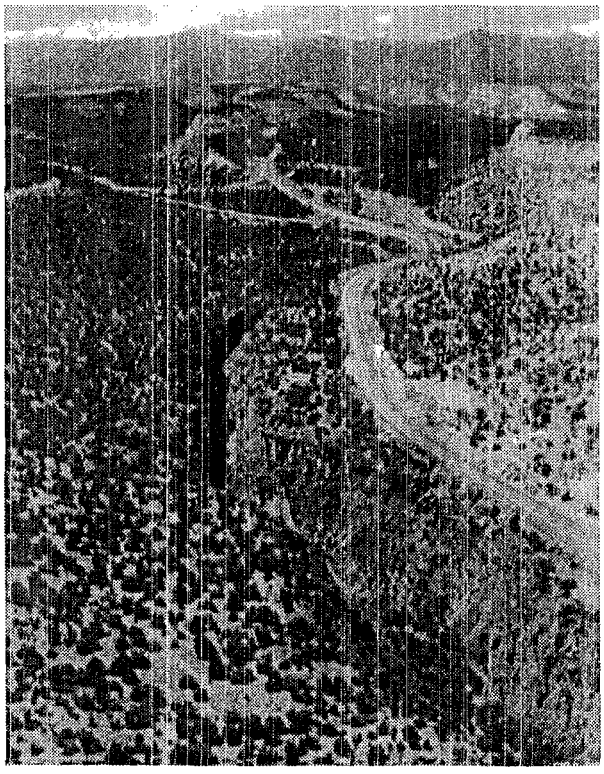

Fig. 3-2. Oblique airphoto of Los Alamos Canyon incised into basalt below NM 502, looking west past confluence of Pueblo Canyon (to right) and Los Alamos Canyon (to left). Knickpoints in both canyons occur immediately upstream of the confluence (LANL file photo).

(sediment) and ground water pathways between the release sites and the Rio Grande. These data will be used to evaluate the present and potential future risk (human and ecological) from such widely dispersed contaminants, which will in turn be used to make decisions on possible remediation alternatives (if necessary). The Los Alamos-Pueblo Canyon system was chosen for the first round of Canyons investigations, and field work began in February 1996. This morning's stops will highlight some of the initial results from the first season of field work on post-WW II sediments in Pueblo and Los Alamos Canyons, and the relationship of contaminant distribution to recent fluvial processes.

Plutonium in Pueblo Canyon. The sediments of Pueblo Canyon are believed to contain the largest amounts of plutonium released from early Laboratory operations. Effluent collected in "acid sewer lines" from the original Los Alamos Technical Area, including the present "downtown" area of Los Alamos, were released into Acid Canyon, a short tributary to Pueblo Canyon 7 km upstream from this stop. Discharge of effluent containing Pu probably began in 1945 and continued until 1964. The highest concentrations of Pu are believed to have been released prior to 1951, when a treatment plant began operation, although the amount of Pu discharged in the early years was not documented (Stoker et al., 1981; Graf, 1994).

Environmental sampling in Pueblo Canyon began in 1945, reflecting early recognition of potential health hazards from the Pu released into Acid Canyon. The most comprehensive sampling to date was conducted in 1976-1977, when a series of samples were collected along the entire length of Pueblo and lower Los Alamos Canyons between the effluent release site and the Rio Grande (Stoker et al., 1981). Findings of this study included a general downstream decrease in Pu concentration, and the storage of significant amounts of Pu in "inactive channels" and "banks", particularly in lower Pueblo Canyon.

More recently, Will Graf was contracted by LANL's Environmental Surveillance Group to provide an independent geomorphic evaluation of the distribution of Pu in the Los Alamos and Pueblo Canyon system (Graf, 1995, 1996). His work, based on a compilation of LANL surveillance data and field mapping, supported the earlier studies in showing a general (but irregular) downstream decrease in Pu concentration and in identifying this part of Pueblo Canyon as containing the highest inventory of Pu in the Los Alamos Canyon drainage basin (Fig. 3-3). Graf's work has formed the basis for subsequent (ongoing) investigations by LANL's Environmental Restoration Project, in particular by helping to articulate a conceptual model of contaminant distribution that can be tested and revised as additional data are collected.

A

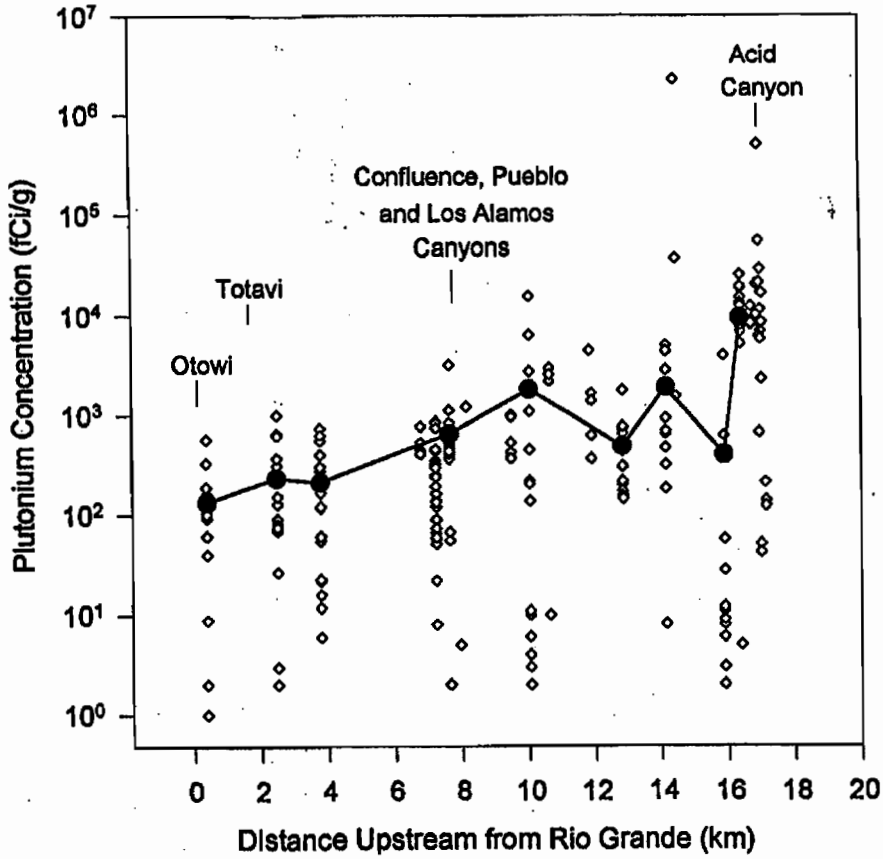

B

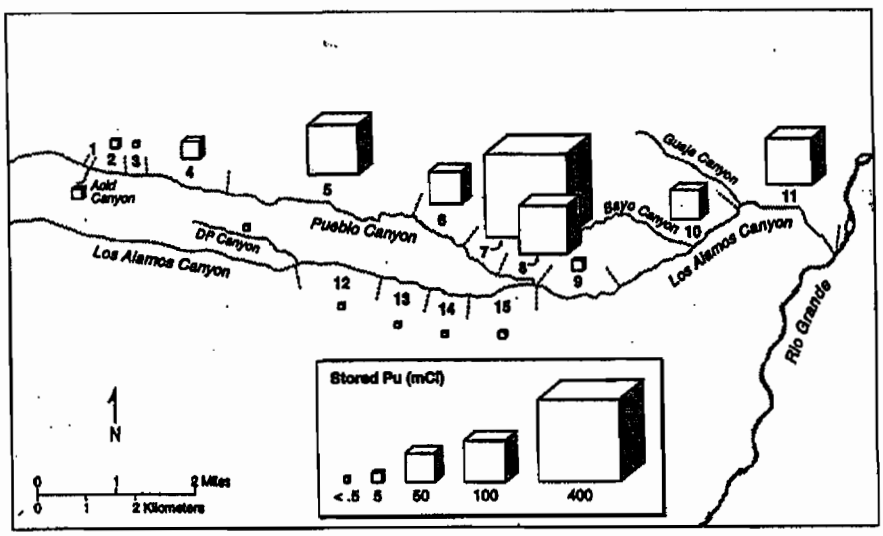

Fig. 3-3. A) Longitudinal variations in plutonium concentration in bedload sediments of Pueblo Canyon and lower Los Alamos Canyon as measured at environmental surveillance sampling stations. Based on 230 samples, generally collected from between 1977 and 1992. Open diamonds represent individual sample values. Filled circles connected by the line represent mean values at various locations, calculated using all the data available at each location except the highest and lowest values. "fCi" are femtocuries, or 10^{-15} curies. B) Map showing the estimated distribution of stored plutonium in sediments of the Los Alamos-Pueblo Canyon system. Proportional cubes represent the amount of plutonium stored within each reach. From Graf (1995).

Of particular geomorphic significance, Pu entering the environment in solution or as fallout tends to bind onto sediment particles, and is believed to remain geochemically immobile under typical near-surface environmental conditions (see summary in Graf, 1994). Understanding the transport and redistribution of Pu is thus primarily a sediment transport issue. This contrasts with some other radionuclides of concern at LANL, particularly ^{90}Sr, which has a relatively high solubility and is transported in the dissolved load of surface water and groundwater.

(**Note:** Although plutonium is present in this part of Pueblo Canyon above "background" concentrations, levels of contamination are low and have nowhere been found to exceed EPA "action levels" (24 pCi/g for ^{239}Pu). No health hazards for casual visitors have thus been identified, and this area is fully open to the public.)

Field Investigations of Contaminant Distribution. In the sediment investigations of Pueblo and Los Alamos Canyon, we have adopted an approach that is referred to as "Expedited Site Characterization". Instead of following a very detailed and specific "work plan", prepared in advance of field work (often standard practice in regulation-driven environmental work), we retain flexibility and rely on a multi-disciplinary team (earth scientists, risk assessors, statisticians, radiation technologists) to quickly assess new data and make decisions about what data to collect next, often on a daily basis.

A cornerstone of our approach is the posing of hypotheses about contaminant distribution based on prior knowledge (a "conceptual model"), and collecting data that is focused on continually testing and revising these hypotheses, building confidence in the model. The goal is a technically-defensible characterization that is focused on collecting data needed for the decision-making process, and that is both efficient and cost-effective. As part of this, we need to both understand the present distribution of contaminants in order to perform "present-day" risk assessments, and also sediment transport processes in order to allow forecasting of future changes in contaminant distribution.

Another important component of the sediment investigations is that we focus most of our work on "key reaches", allowing us to collect a higher density of data in relatively small areas and better test our hypotheses (similar to the "representative reach" concept in Graf, 1994). Specific reaches are chosen for a variety of reasons, including areas that are: 1) close to contaminant sources; 2) at significant geomorphic changes (e.g., where channels flatten and canyon bottoms widen, allowing more opportunity for sediment deposition); and 3) at major geographic or institutional boundaries. The area that we will visit a short distance downstream (reach P-4), was chosen in part to define the types and concentrations of contaminants at the Laboratory boundary, and thus what has been transported off DOE land and onto adjacent San Ildefonso Pueblo land.

Steps in our investigations include:

1) Review of prior knowledge.
2) Selection of reaches.
3) Geomorphic mapping of reaches, focused on units relevant to contaminant characterization.
4) Quick, low resolution field screening to thoroughly cover large areas, gathering general data on contaminant distribution and searching for "hot spots". Here we used a gross gamma radiation walkover survey (Fig. 3-4, left), with measurements made every 2 seconds and located using GPS, collecting up to 14,000 data points in a single day. These data were down-loaded, transferred to our GIS data base, and were ready for examination the next day.

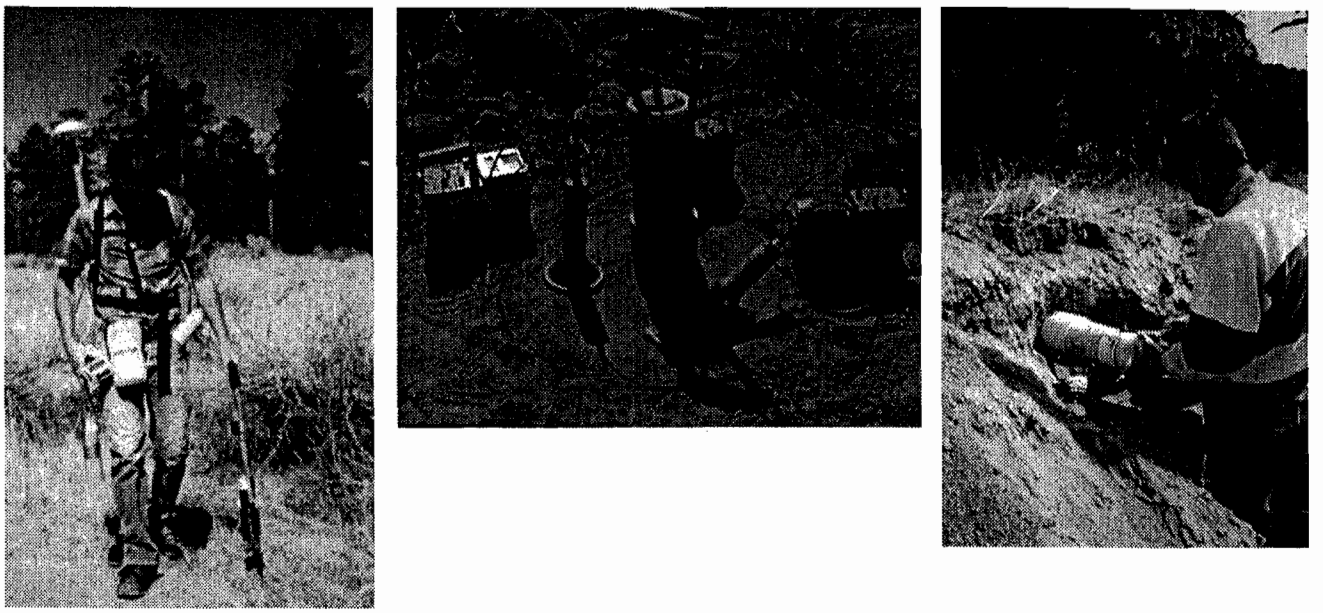

Fig. 3-4. Photographs of rad screening in lower Pueblo Canyon, reach P-4, in spring 1996. Left photo: Gross gamma walkover survey is being performed by ERG, out of Albuquerque, and the local gamma radiation is measured every 2 seconds. The surveyors location is recorded using GPS (GPS antenna is on backpack, and data recorder is in right hand). 2-inch gamma detector is hanging from right side, and a paint gun used to mark traverses is in left hand. Center photo: "Fixed point" measurement site of surface sediments, obtaining simultaneous readings of alpha (circular detector to left), beta (rectangular detector in front), and gamma radiation (2" detector is inside PVC holder which supports lead shielding), with 5 minute count times. Right photo: Fixed point measurements of sediments at depth, in bank exposure.

5) "Fixed point measurements", collecting higher resolution field data on alpha, beta, and gamma radiation at select spots (Fig. 3-4, center). In part, these data allowed testing the hypothesis of co-location of gamma emitters (e.g., ^{137}Cs, ^{235}U) and alpha emitters (e.g., ^{238}Pu, ^{239}Pu, ^{240}Pu). Fixed point measurements in bank exposures and hand-dug pits also allowed examination of depth variations in radionuclides (Fig. 3-4, right).

6) Collection of a small set of samples for "full suite" laboratory analyses. These are expensive analyses that look for a large range of possible contaminants (various radionuclides, metals, and organics), and we use them to confirm that we know which contaminants are present above "background", to further examine co-location of contaminants, and to narrow our list of analytes. Sample sites are selected based on the geomorphic mapping and the field rad measurements.

7) Collection of larger sets of samples for "limited suite" laboratory analyses, focused only on contaminants of concern to reduce the analytical costs. These analyses are intended in part to provide statistically defensible values for geomorphic units of concern. These analyses may also be of single "indicator" contaminants that are key for understanding sediment transport and testing components of the conceptual model.

At present, we have completed steps 1 through 6 for four reaches and are analyzing our "full suite" data, in combination with "background" data, as a prelude to the next round of sample collection.

- Walk 0.4 km downstream (east) either on trails in the trees or down the generally unincised, canyon bottom (Fig. 3-5), past a prominent knickpoint along the channel. Vegetation along this part of

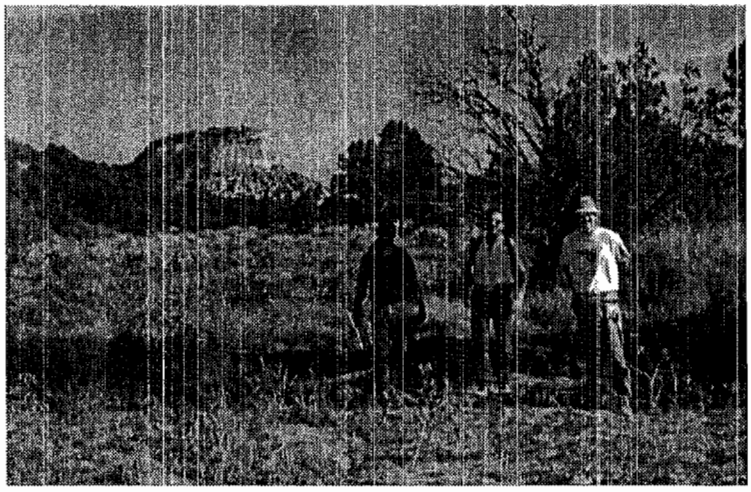

Fig. 3-5. Photograph of unincised part of lower Pueblo Canyon, above knickpoint. Based on exposures downstream, ~1.5 m of historic sediment probably underlie the canyon floor here.

Pueblo Canyon is uncommonly lush due to releases from the Los Alamos County Sewage Treatment Plant 1 km upstream.

Station 3-1b, Lower Pueblo Canyon, near knickpoint (6415', 1955 m elev.)

Historic Channel Changes. This part of Pueblo Canyon has experienced significant channel changes during this century, including at least ~1.5 m of aggradation and up to 3 m of subsequent incision (Fig. 3-6). These changes have been evaluated using both field mapping and examination of a sequence of airphotos that extend back to 1935, providing a relatively well documented example of a historic aggradation-degradation cycle. The historic channel changes have also had a strong influence on the present distribution of Pu in Pueblo Canyon, with the peak contaminant releases coinciding with a period of aggradation, resulting in an opportunity for extensive storage of Pu within this reach.

Pueblo Canyon through this reach was unincised in 1935 and had a relatively wide active channel (~15-35 m wide). The channel was locally braided, with side channels present through the adjacent mixed ponderosa pine-piñon-juniper woodland. Between 1935 and 1960 up to 30-40 m of channel migration had occurred (Fig. 3-7), accompanying channel aggradation, and local incision had also been initiated immediately downstream of the present knickpoint. The peak of aggradation at this site and subsequent incision probably occurred in the late 1950s, shown on a 1960 airphoto by a lightly vegetated sand lobe spreading over the flats to the southeast, above a slightly incised channel (chamisa or golden rabbit

Fig. 3-6. Photographs of lower Pueblo Canyon below knickpoint, where ~1.5-3 m of incision has occurred since the late 1950s. Left photo shows area a short distance downstream from 1996 knickpoint, where thick patches of chamisa have colonized terraces formed between the late 1950s and the mid 1980s. Right photo shows area downstream near location of 1969 intersection point, in a 1991 flood channel.

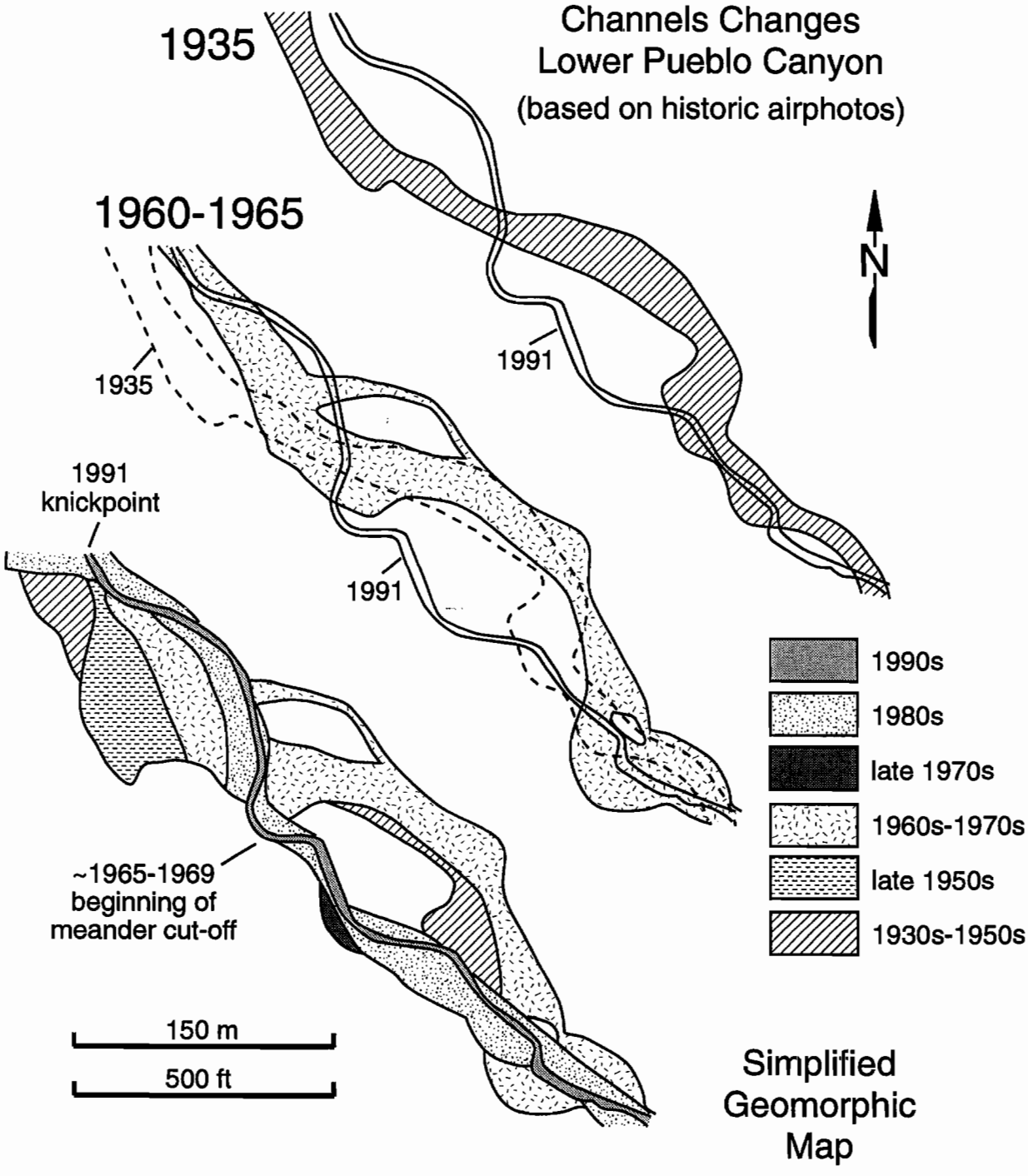

Fig. 3-7. Maps showing channel changes in lower Pueblo Canyon since 1935 (1935, ~1960-65, 1991), in area of Stop 3-1b.

brush, *Chrysothamnus nauseosus*, rapidly colonizes abandoned channels in this canyon, and 1991 sand bars can possess a relatively dense growth of chamisa). The thickness of the most recent aggradational deposit is estimated at about 1.5 m based on the maximum depth of exotic clasts such as quartzite and granite and on associated stratigraphic breaks.

The sequence of maximum channel aggradation followed by incision that began ~50 m downstream of the present (1996) knickpoint in the late 1950s was repeated at downstream sites over the following 20-30 years as an intersection point migrated ~1.5 km downstream (Fig. 3-8). As aggradation at each site proceeded, lobes of coarse sand and some gravel spread out onto the adjacent floodplains or terraces, followed by incision and surface abandonment, creating a diachronous fill terrace. A flight of inset "fill-cut" terraces has formed during incision, generally underlain by <0.5 m of contemporaneous sediment over older historic or prehistoric deposits (Fig. 3-9).

The present knickpoint is formed where the incising channel encountered a resistant unit of partially cemented alluvium, impeding upstream incision, and this feature does not appear to be typical of channel erosion processes. The initial channel incision near here and subsequent incision at downstream sites appears to have been largely by vertical incision into the stream bed, and not caused by migrating knickpoints.

Plutonium Distribution. The historic channel changes that have occurred in this reach have substantial implications for the distribution of plutonium in the stream sediments. The time transgressive channel aggradation and incision that occurred following the initial releases resulted in the storage of large volumes of contaminated sediment and its subsequent partial remobilization by channel and bank erosion. Because contaminant concentrations in both the suspended load and the bed load are likely to

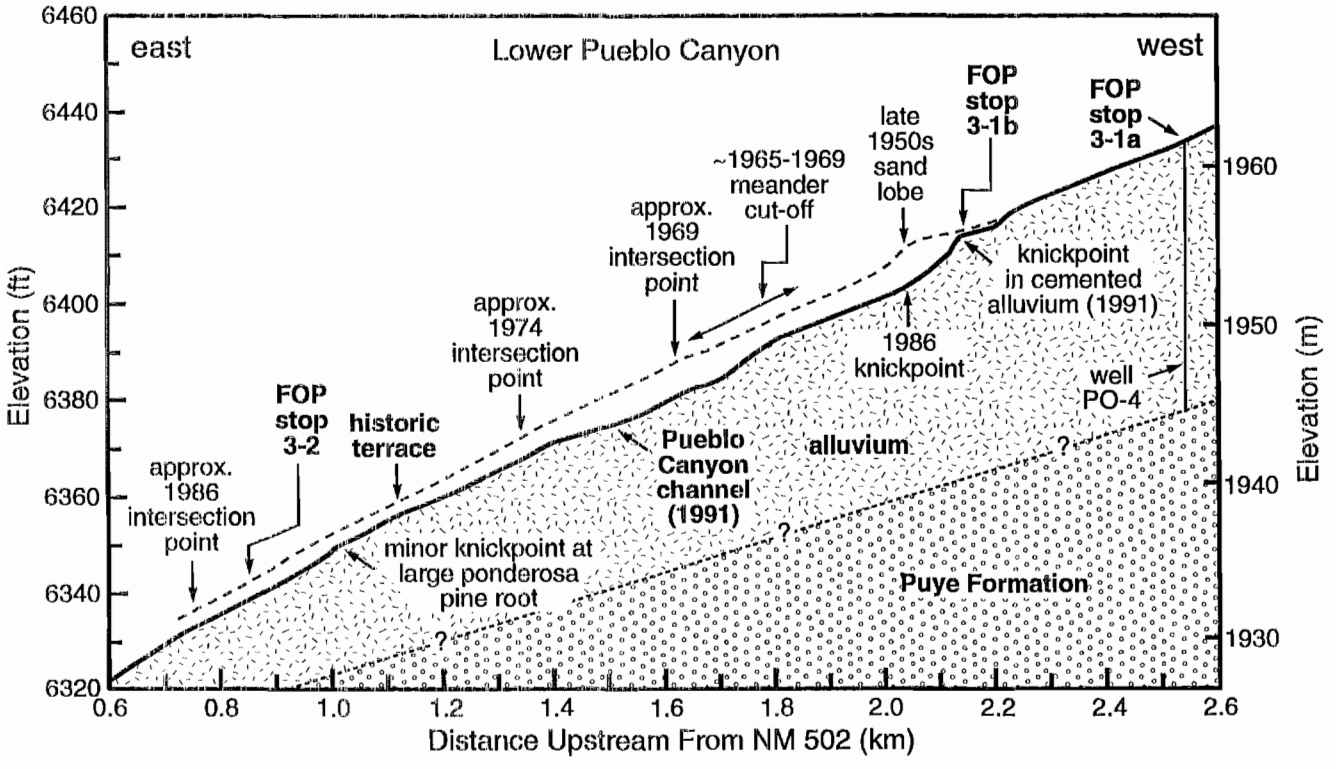

Fig. 3-8. Longitudinal profile of lower Pueblo Canyon, showing historic terrace and location of intersection point at different times, as inferred from airphotos.

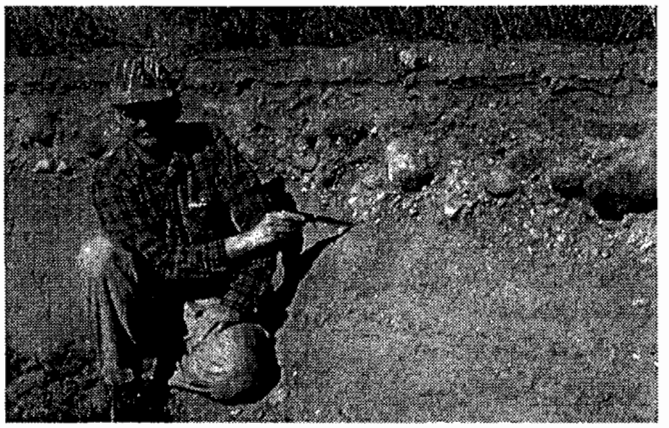

Fig. 3-9. Photograph of exposure below ca. 1986 inset terrace, near site of ca. 1965-1969 meander cut-off. Deposit associated with historic fill-cut terrace is apparently only about 10 cm thick here (line at hat level). Gravel layer apparently contains no "exotic" material, and may have been deposited during an earlier pre-1943 aggradation-degradation cycle, perhaps representing a channel lag at the base of an earlier fill-cut terrace. Lowermost unit is a partially cemented alluvium of unknown age, similar to that present at the 1996 knickpoint (photo by Brad Wilcox).

have decreased over time, associated with progressive dilution by "clean" sediment, we expect that Pu concentrations vary longitudinally along the historic fill terrace. Limited data obtained in 1996 seem to support this hypothesis: one sample of the coarse channel sands deposited in the late 1950s yielded a $^{239+240}$Pu concentration of 4.75 pCi/g, whereas sands deposited in the early 1980s and in a 1991 flood yielded values of 0.76 and 0.54 pCi/g, respectively. These data are consistent with samples of "active channels" collected during the 1976-77 investigations, 0.27-1.00 pCi/g from this reach (av. = 0.69 ± 0.29 pCi/g, n = 7) (Stoker et al., 1981). We plan to further evaluate these possible age-Pu relations in our next round of sampling.

The historic channel changes have also probably resulted in spatial distributions in Pu carried as suspended load and deposited from overbank floodwaters. The widest dispersal of floodwaters over the prehistoric terraces or floodplains likely accompanied the peak of aggradation in each part of lower Pueblo Canyon, with subsequent channel incision decreasing the opportunity for overbank flooding. Relatively old overbank deposits with higher Pu concentrations may thus occur at the surface near areas abandoned by the channel in the middle of this century, and deposits with the highest concentrations may be buried beneath later channel or overbank deposits in other areas. Consistent with this hypothesis, the highest value of Pu obtained this field season from this part of Pueblo Canyon, 11.3 pCi/g, was from an overbank deposit (silt loam) at a site abandoned by the active channel between 1935 and 1960. This is similar to, but slightly lower than, the highest value obtained from this reach in the 1976-1977 investigation, 15.3 pCi/g from a "bank" deposit downstream (Stoker et al., 1981). The highest value of Pu we have found so far in Pueblo Canyon sediments, ~500 pCi/g, is at depth of 70 cm a short distance downstream from Acid Canyon (Fig. 3-10), buried by less contaminated sediment and thus also supporting a decrease in Pu concentration over time.

Plutonium Remobilization. The potential remobilization of stored Pu is of concern to "stakeholders" such as the downstream landowners, San Ildefonso Pueblo. Part of our goals include determining how much Pu is stored in Pueblo Canyon, and where, and forecasting trends of future contaminant transport.

Plutonium is remobilized from this reach largely by lateral bank erosion during floods. As many of the eroding banks consist of prehistoric sediments, resulting Pu concentrations will be less than that stored in the historic deposits due to dilution with "clean" sediment. Since incision began at this point ~1960, there has been relatively little lateral bank erosion (in comparison to the width of the historic canyon bottom), with channel change instead dominated by incision. Thus, we expect that much of the stored Pu will remain here for decades or longer if these trends continue. In contrast, Los Alamos Canyon at

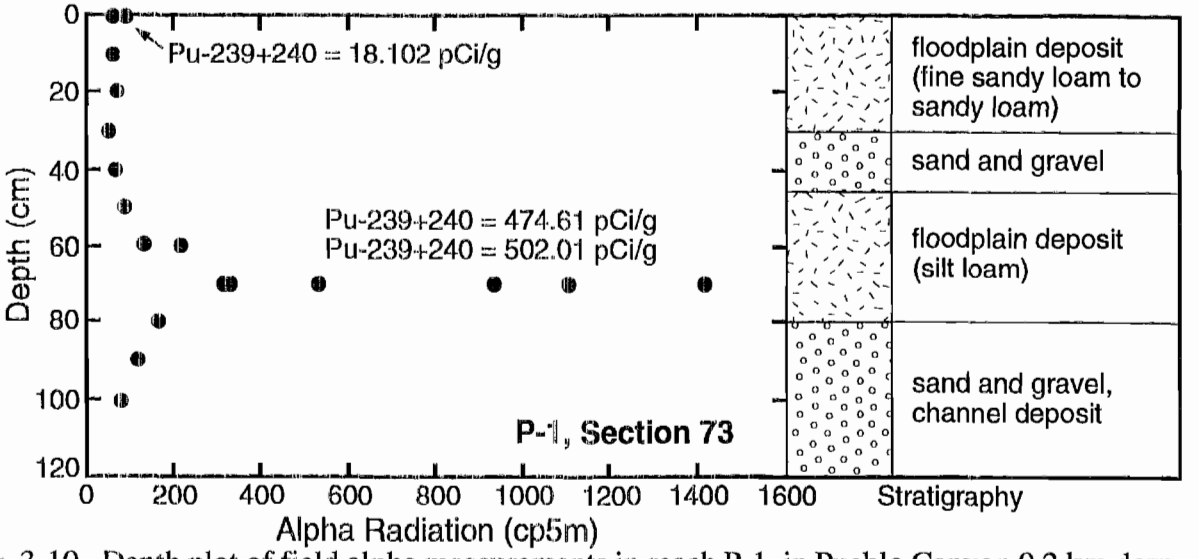

Fig. 3-10. Depth plot of field alpha measurements in reach P-1, in Pueblo Canyon 0.2 km downstream of Acid Canyon, and available laboratory values of $^{239+240}$Pu. The highest level of alpha radiation occurs about 0.7 m deep in a silt-rich floodplain deposit which is buried by "cleaner" sediment. The variability in alpha at each depth reflects multiple measurements on same sample, with the large variability likely due to some combination of small-scale heterogeneity in the distribution of Pu and poor counting statistics related to the small number of counts.

Stop 3-3 displays evidence for relatively rapid flushing of sediment and a greater potential for remobilization of stored contaminants.

Remobilization of stored Pu in Pueblo Canyon could also occur by headward erosion of the knickpoint and enlargement of the incised channel system to the west (Graf, 1995). Although the knickpoint has only migrated ~80 m since 1986, with channel erosion currently impeded by a bed of partially cemented alluvium, rapid erosion could presumably occur during and following a large flood if the channel relocated the loose, unconsolidated historic alluvium. If sufficient Pu is stored upstream to be of concern (planned to be investigated in 1997), stabilization of the knickpoint might be one remediation alternative.

- Return to vehicles, and head upcanyon to turnaround point.

1.6 Junction with dirt road up Pueblo Canyon to left. Turn around and drive back on road to gate near NM 502.

3.2 Gate. Park near highway maintenance station.

- From gate, walk north to right of highway maintenance station buildings, down old dirt road to incised canyon bottom. Fence to right encloses test well TW-1, completed in 1950; basalt, underlying the Puye Formation, was encountered at a depth of 15 m, or about 5 m below the present channel (Purtymun, 1995).

Stop 3-2: Lower Pueblo Canyon near "White Rock Wye" (6340', 1935 m elev.)

Historic Channel Changes. This part of Pueblo Canyon, about 0.8 km upstream from the first outcrop of basalt in the stream bed, has experienced at least ~1.6 m of aggradation and subsequent inci-

sion this century. Many ponderosa pine snags are partially buried (Fig. 3-11), and sawn stumps are also emerging from the eroding banks. The aggradation that apparently peaked upstream in the late 1950s continued here until the early 1980s, with incision having occurred along most of lower Pueblo Canyon below the knickpoint by 1986 (Fig. 3-8). The historic fill terrace is about 1.7 m above the present (1996) channel, and the snags and stumps are rooted about 0.9-1.1 m deep, presumably on a prehistoric floodplain or low terrace.

Bank exposures and surface mapping reveal some aspects of the stratigraphy produced by the historic aggradation event. Most of the section in the banks is composed of coarse channel sands and gravels, although up to 50% of the section along the north margin includes fine-textured overbank layers, apparently deposited at slackwater sites along the edge of the floodplain.

This part of Pueblo Canyon had a braided channel through the trees from 1935 until at least 1981, and an abandoned channel occurs ~40 to the north (Figs. 3-12, 3-13). As aggradation proceeded, coarse sand lobes spread out over the former floodplain surfaces, widening the "active channel". Analogous layers of coarse channel sands that overlie floodplain deposits at many sites on the Pajarito Plateau (e.g., Ancho Canyon, Stop 1-5; Rendija Canyon, Stop 2-3) may similarly record brief aggradation events associated with migrating intersection points.

Airphotos taken in October 1991, following a major flood in August 1991, revealed a relatively broad sandy flat along the channel at this site. Between 1991 and 1996 an additional 0.3 m of incision occurred, stranding the 1991 sand deposits as a low inset terrace, which has been colonized by chamisa. A series of similar inset terraces, mostly dating to the 1980s, were formed upstream as incision progressed. This post-1991 incision heads ~100 m upstream where the degrading channel encountered large ponderosa pine roots. Except at such sites of unusual resistant bed material (including the cemented alluvium near Stop 3-1b), there is no evidence of sharp knickpoints along lower Pueblo Canyon, and we thus infer that incision through the predominantly loose sandy fill is dominated by channel bed erosion and not the progressive headward migration of knickpoints.

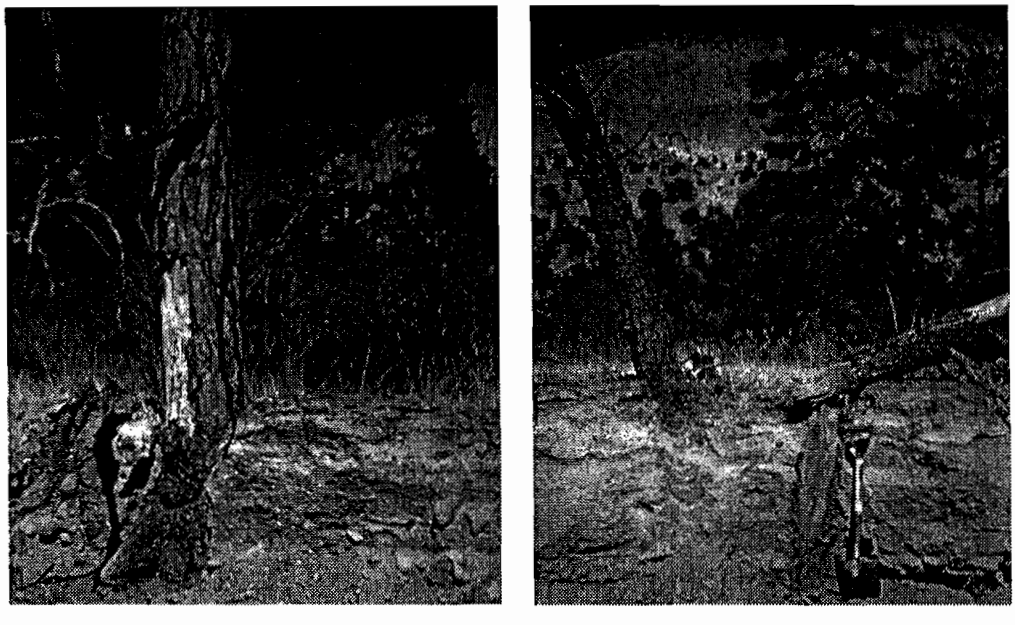

Fig. 3-11. Photographs of ponderosa pine snags at Stop 3-2, rooted about 1 m below the surface of a historic terrace, probably on a "prehistoric" (pre-1943) floodplain or terrace. Trees were living in 1974 (photo by Brad Wilcox).

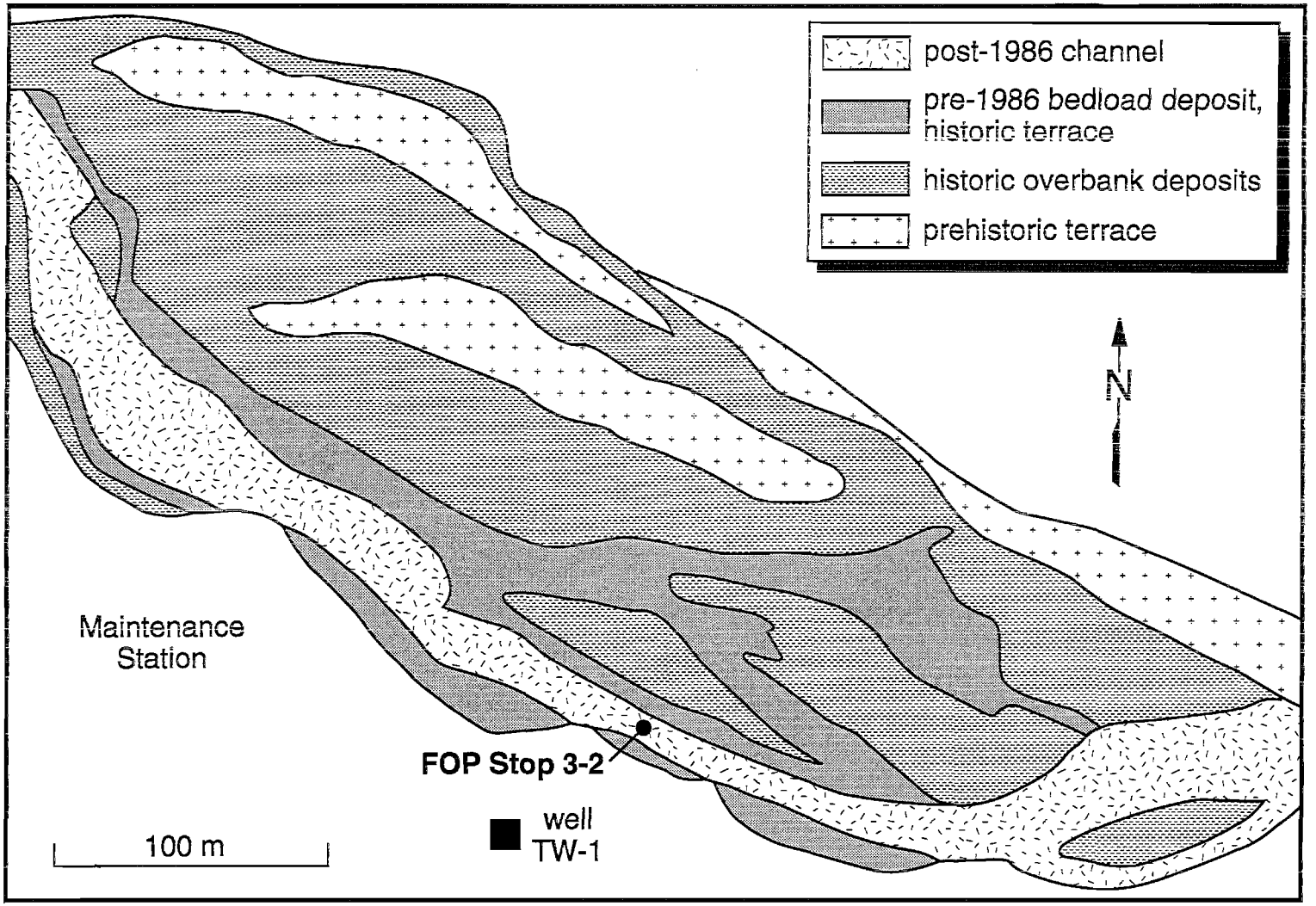

Fig. 3-12. Simplified geomorphic map of lower Pueblo Canyon near Stop 3-2, showing areas that experienced channel aggradation in the mid-1970s to early 1980s and parts of the canyon bottom inferred to have been overtopped by historic floodwaters. Historic overbank layers can be interbedded with or underlie the historic bedload deposits, and lobes of coarse sand and gravel were deposited on some of the areas mapped as "floodplains". Extent of historic overbank deposition may be revised following additional plutonium analyses.

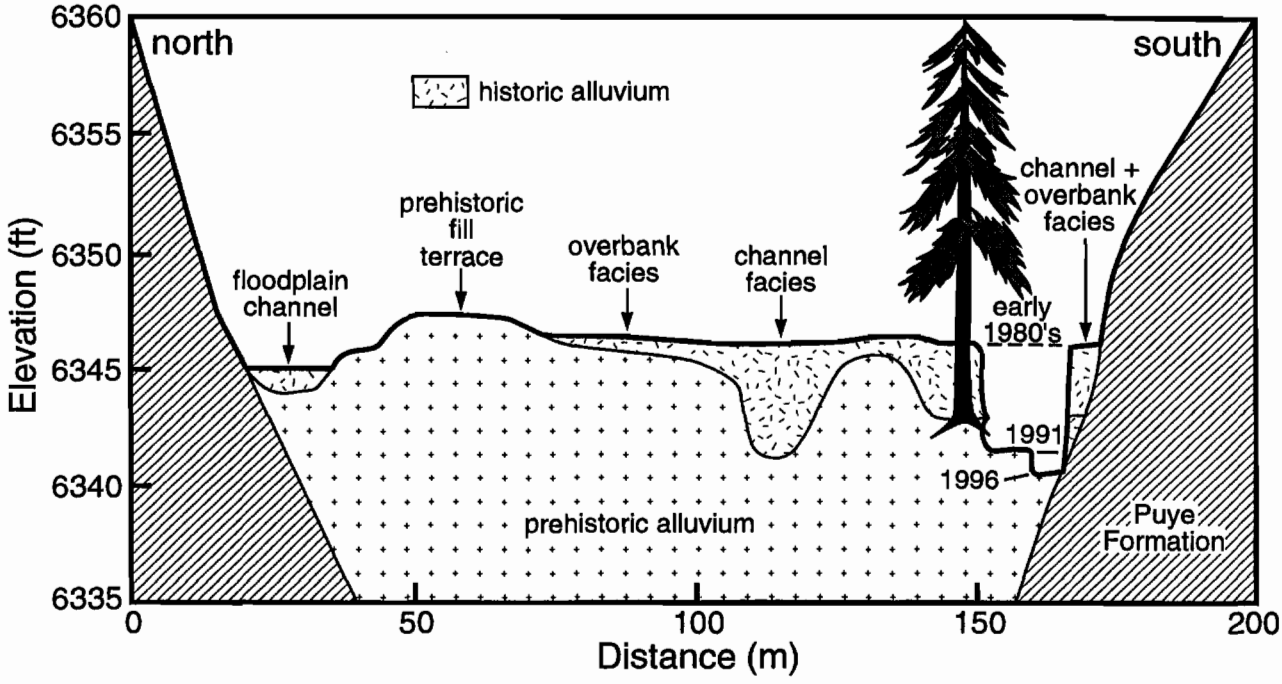

Fig. 3-13. Schematic cross section across lower Pueblo Canyon at Stop 3-2, showing inferred extent of historic alluvium.

- Return to vehicles.

3.2 From turnoff, head CAREFULLY straight across NM 502 to south, taking turnoff to State Road 4 towards White Rock.

3.4 Up the Los Alamos Canyon channel 70 m to the west was a sample site for the LANL background soil geochemistry study (Longmire et al., 1996; McDonald et al., 1996a; Watt, 1996). In a stream bank exposure, 2 m of pumice-rich slopewash sediments overlie Los Alamos Canyon stream gravels, the latter within 0.5 m of the present channel. Charcoal from the basal slopewash deposit yielded a ca. 2.8 ^{14}C ka date, and a burned stump rooted in the stream gravels yielded a date of ca. 2.5 ^{14}C ka (Fig. 3-14). These analyses indicate that the channel was very near its present level about 2.5-3 ka at this location close to the local basalt base level, and also helps document locally rapid late Holocene erosion on slopes underlain by non-welded tuff and pumice.

3.5 **Gate to right.** Dirt road leads up Los Alamos Canyon. This is DOE land that is open to the public. Drive through gate and up road (note: gate usually locked). Many cavate ruins occur along the base of south-facing cliffs upstream (Fig. 3-15) and in most other canyons at this elevation on the Pajarito Plateau.

3.8 Old borrow pit to left, in Los Alamos Canyon stream terraces of unknown age (Qt2 and Qt1 of Rogers, 1995). Upper terrace, ~30 m above the channel, grades to a broad saddle to the east, immediately north of Tsankawi Mesa, and this saddle marks the former course of Los Alamos Canyon prior to capture by a stream to the north. The lower terrace may mark the stream level after adjustment to the new post-capture base level.

4.2 Near the base of the cliffs to the north are excellent exposures of pumice beds and associated buried soils of the early Pleistocene Cerro Toledo interval.

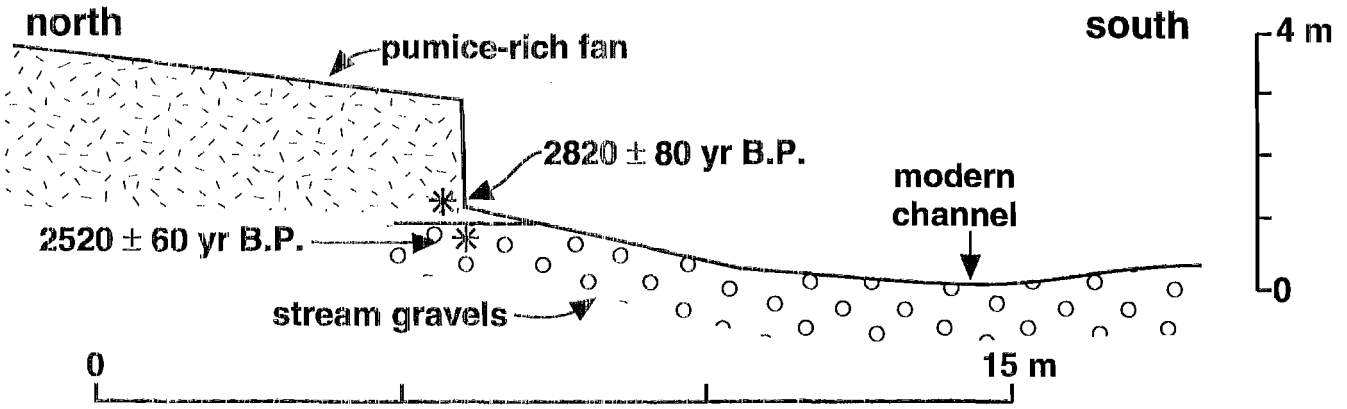

Fig. 3-14. Cross section of radiocarbon sample site in lower Los Alamos Canyon, showing pumice-rich fan overlying Los Alamos Canyon stream gravels. Fan sediments are largely derived from the Guaje Pumice Bed, non-welded Otowi ignimbrites, and non-welded basal Tshirege ignimbrites. Background soil sample site is located 15 m to southeast (from Longmire et al., 1996).

Fig. 3-15. Photographs of cavate ruins and petroglyphs in Los Alamos Canyon.

5.2 Canyon bottom to left is filled by a broad boulder deposit. Similar boulder deposits occur along at least 9 km of Los Alamos Canyon, and may record a single extreme flood event. Charcoal collected from sediments and soils buried by this deposit upstream (near Stop 3-3) indicate an age of ca. 290-610 ^{14}C yr B.P.

5.4 Powerline. East end of "reach LA-2". A lone alligator juniper tree (*Juniperus deppeana*) next to the road may be the northernmost individual in New Mexico (its nearest known relatives are 9 km south, between Frijoles Canyon and State Road 4; Craig Allen, pers. comm., 1996). Near here is the axis of a pre-Tshirege paleodrainage that headed in the modern Rendija Canyon basin and flowed southeast across the present Bayo, Pueblo, Los Alamos, and Sandia drainages, emptying into the ancestral Rio Grande north of the White Rock basalt high (Broxton and Reneau, 1996). The axis itself is not exposed, but a pre-Tshirege stream terrace, buried by Cerro Toledo Rhyolite pumice beds, can be viewed at the base of the cliffs west of the powerlines.

5.7 Test well TW-3 to right, drilled in 1949. Base of Bandelier Tuff is 53 m deep here, overlying Puye Formation fanglomerates (Purtymun, 1995). Immediately to west, road crosses DP Canyon.

5.8 Well house for water-supply well Otowi 4. Park.

Stop 3-3: Los Alamos Canyon at DP Canyon (6610', 2015 m elev.)

(**Note:** Our investigations in spring 1996 identified one area a short distance downstream of DP Canyon with relatively high levels of ^{137}Cs and ^{90}Sr in the sediments, exceeding EPA "action levels", and this area is posted. Please respect these signs. This site is one candidate for remedial action, although risk assessments have not yet been completed and the possible need for cleanup has not yet been evaluated.)

Setting. This stop is at the confluence of Los Alamos Canyon and a short side canyon from the north, "DP Canyon", which drains "DP Site" (TA-21) and part of the Los Alamos townsite. (Variations that have been heard on the origin of the name "DP" include "Delta Prime", "Deuterium-Plutonium", and "Dump Plutonium"). Los Alamos Canyon is about 130 m deep here, incised into the Otowi Member of the Bandelier Tuff. Excellent exposures of both dacite-rich alluvial deposits and pumice-rich beds of the early Pleistocene Cerro Toledo interval occur up DP Canyon (Broxton et al., 1995a; Goff, 1995).

Alluvial Units. Alluvium is about 5 m thick in this part of Los Alamos Canyon (e.g., Purtymun, 1995), containing abundant dacitic clasts that often impede drilling operations. Several Holocene units are exposed in this reach (Figs. 3-16, 3-17). Unit Qt1 includes cobble-rich terrace deposits, dated at ca. 2.9-4.8 ^{14}C ka in this reach and extending up to 3 m above the active channel, that may record the timing and maximum height of Holocene aggradation here. Qt1 is generally buried by slopewash deposits (Qc), and likely includes several distinct terrace units (equivalent to Q1 of Drakos and Inoue, 1994, and Drakos et al., 1996, upstream at TA-2).

Qt2 typically occupies much of the canyon bottom and is notable for its large boulder bars that may record a single rare high-magnitude flood event (Fig. 3-18). The underlying gravel-rich alluvium is ~1 m thick and sedimentologically distinctive, unlike that seen in other exposures on the Pajarito Plateau and resting in sharp contact on older alluvium or soils. Analyses of charcoal from underlying deposits at 2 sites in this reach indicate an age of 290-610 ^{14}C yr B.P (ca. 1300-1650 cal A.D.) for this deposit. The dominance of dacite clasts in the deposit indicates a source for the sediment in the upper Los Alamos Canyon watershed in the Sierra de los Valles. (This unit is in part equivalent to the Q2 of Drakos and Inoue, 1994, and Drakos et al., 1996, although some of their Q2 unit appears to be younger.)

Historic alluvial units are inset into Qt2 and often are restricted to a narrow strip ~5 m in width, although they locally broaden to 20 m in combined width (Figs. 3-16, 3-17). "c1" is the active channel, typically about 1.5 m wide and composed of coarse sand and gravel. "c2" are adjacent surfaces, ~0.5-1.0 m high, that typically include 0.3-1.0 m of overbank deposits (often dominated by fine sands) above historic channel deposits (containing "exotic" quartzite and granitic clasts, pieces of metal, etc.). "c3" is a relatively high (1.3 m) historic surface downstream of DP Canyon with the highest levels of contamination in this reach (discussed below). "f1" refers to those portions of prehistoric terraces that have been overtopped by contaminant-bearing floodwaters.

Contaminant Sources. Several LANL sites upstream have released contaminants into the Los Alamos Canyon watershed over an ~50 year period, probably including a variety of radionuclides, metals, and organics. TA-21, an industrial site located on DP Mesa to the west, has housed a plutonium processing facility, a tritium facility, and other weapons-related operations dating back to the early post-war years. The main source for contaminants that have entered the stream channel is believed to be an outfall into DP Canyon ("21-011(k)"), where a variety of radionuclides were discharged in effluent water, including ^{241}Am, ^{137}Cs, ^{238}Pu, ^{239}Pu, ^{240}Pu, and ^{90}Sr. Other outfalls from TA-21 discharged effluent over the

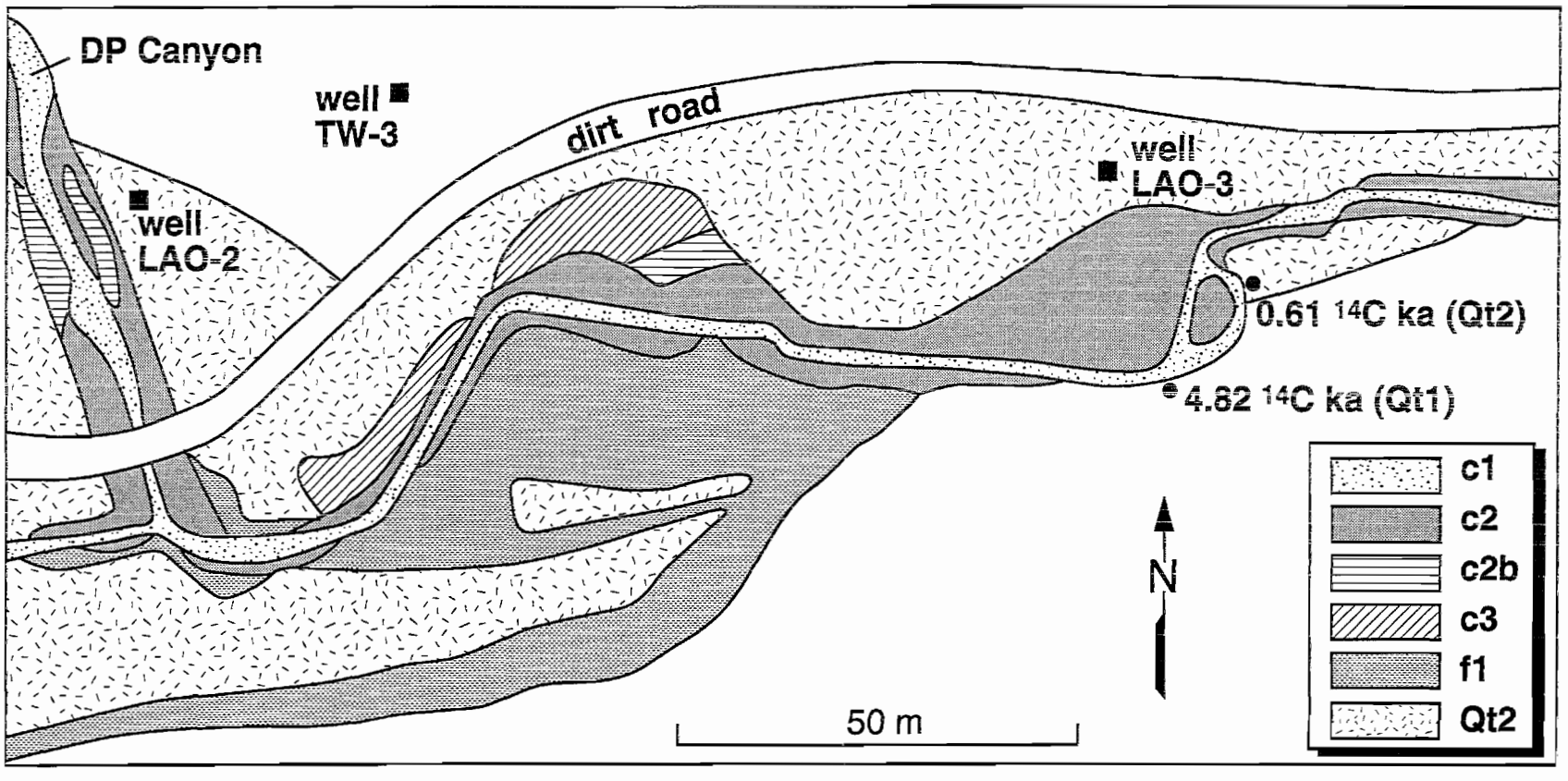

Fig. 3-16. Simplified geomorphic map of Los Alamos Canyon at confluence with DP Canyon, Stop 3-3, showing distribution of historic sedimentary units, late Holocene Qt2 terrace, and radiocarbon sample locations.

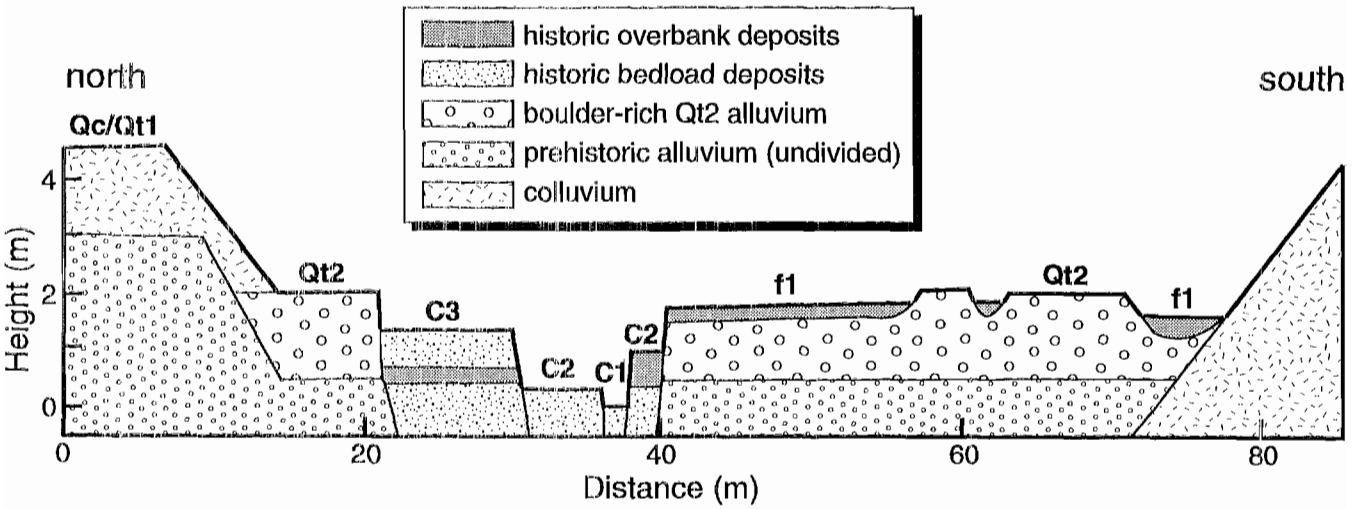

Fig. 3-17. Schematic cross section across Los Alamos Canyon floor at Stop 3-3, showing inferred relationships of geomorphic units.

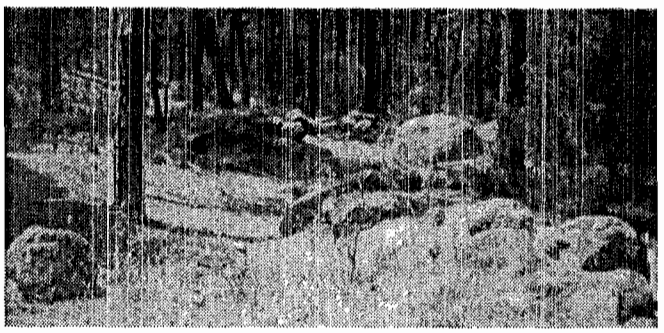

Fig. 3-18. Photograph of bouldery Qt2 terrace surface in reach LA-2, dated at ca. 1300-1650 A.D. and possibly recording a single extreme flood event.

cliffs to the north, directly into Los Alamos Canyon. 3 km upstream from DP Canyon is the Omega West nuclear reactor at TA-2 (off-line since 1993, after discovery of a leak in the cooling lines). Radionuclides released from TA-2 include ^{3}H (tritium) and ^{90}Sr. Farther up Los Alamos Canyon, various outfalls from TA-1, the original WW II-age Technical Area, also discharged effluent over the cliffs.

Contaminant Distribution. Due to the release of relatively large amounts of ^{137}Cs, a strong gamma emitter, from TA-21, we have been able to fairly quickly and precisely define the extent of radionuclide contamination in this part of Los Alamos Canyon using field instruments (Fig. 3-19), and to also define variations in the relative abundance of ^{137}Cs between geomorphic units. We are continuing to evaluate whether other contaminants in the sediments are co-located with ^{137}Cs, which would allow defensible use of the gross gamma walk-over survey to bias sampling, but the initial results are encouraging; the highest concentration of ^{241}Am and $^{239+240}Pu$ (alpha emitters) and ^{90}Sr (a beta emitter) have all been measured in units with high field gamma measurements.

Gamma radiation above "background" (upstream) levels is measurable in all historic channel units downstream from DP Canyon. Values in the "c2" unit are consistently higher than in "c1" (Fig. 3-20), consistent with the expected higher contaminant concentrations in the finer sediment sizes that are carried in suspension and deposited by overbank floodwaters. Variations in gamma radiation in c2 may reflect a combination of particle size variations, age variations, and variable contributions of sediment from Los Alamos Canyon vs. DP Canyon. The highest gamma measurements in each vertical section through c2 correspond with relatively fine-textured layers, and the sections with the highest gamma values ("c2b") appear to represent relatively old deposits that have been scoured from most of the reach (Fig. 3-21a, b).

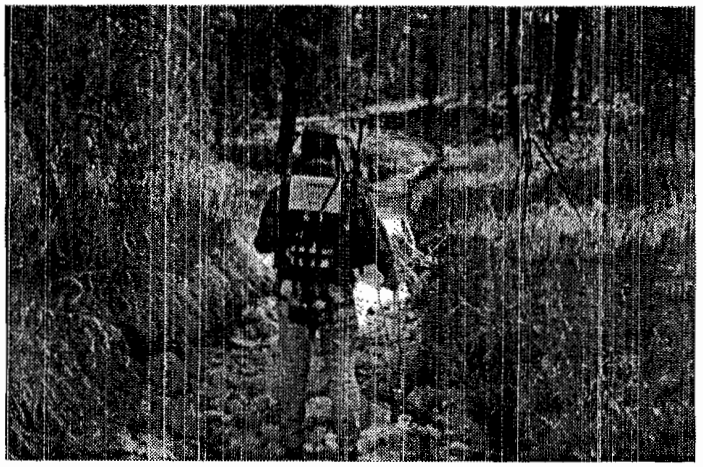

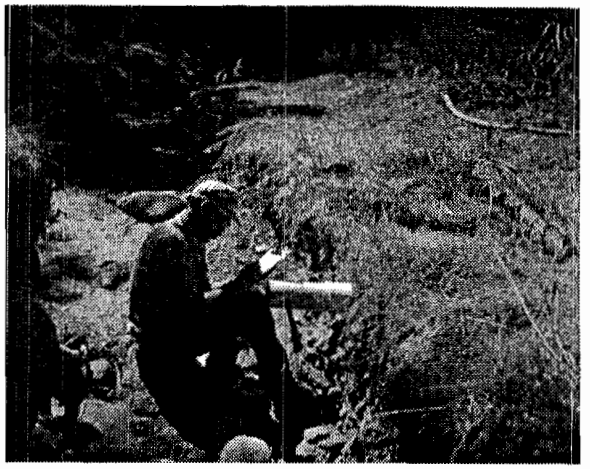

Fig. 3-19. Left photograph shows field screening for gross gamma radiation in reach LA-2, near observation well LAO-3, in spring 1996. Survey was performed by Chemrad, out of Oak Ridge, Tennessee, utilizing the USRADS positioning system (the surveyor carries an ultrasonic transmitter, and a computer locates the surveyor every second by triangulating from a local network of receivers; one receiver is visible on tripod to right). Measurements were made every 1 second using a 1-inch detector (dangling from right hand). Right photograph shows "fixed point" measurements for gross gamma radiation every 10 cm in bank exposure, using a shielded 2-inch detector. In both photographs, the narrow "c1" channel is bordered by grassy "c2" surfaces.

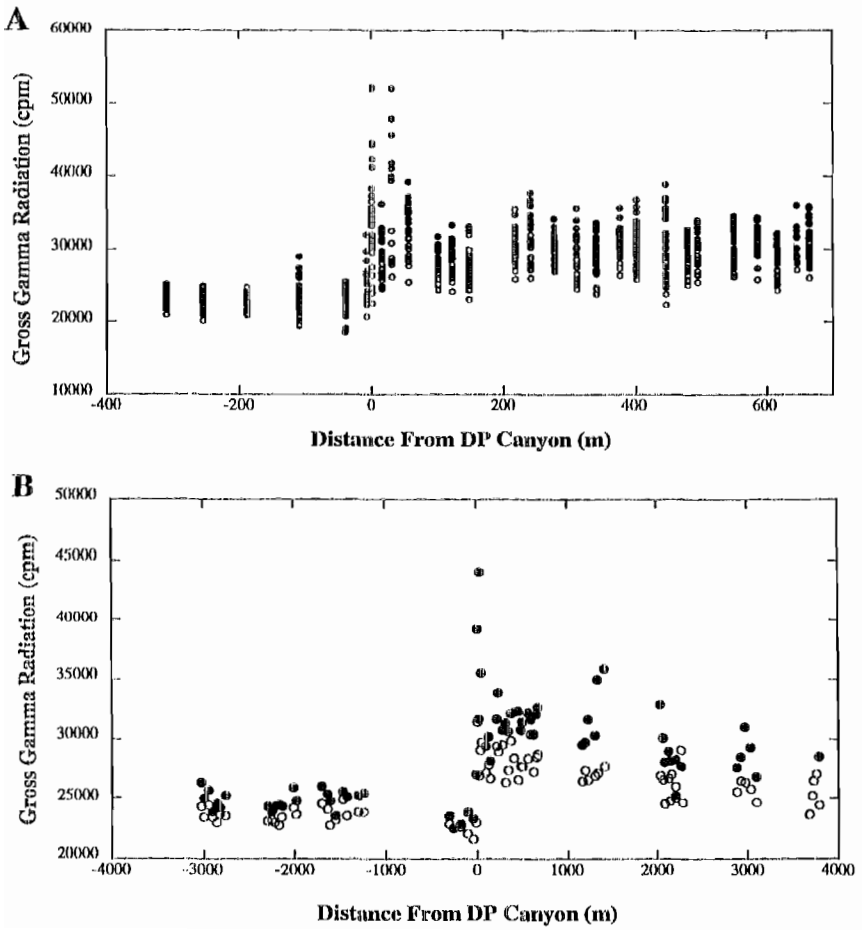

Fig. 3-20. Plots of variations in gross gamma radiation along Los Alamos Canyon. Active channels ("c1") are shown by open circles, and "c2" surfaces, generally underlain by historic overbank deposits, by filled circles. A) Data from reach LA-2, immediately upstream and downstream of DP Canyon, showing all 2-second measurements in "mini-reaches". B) Data from 7-km long stretch between TA-2 and State Road 4, showing averages of channel and "floodplain" ("c2") measurements for each "mini-reach". Mini-reaches are typically about 20 m long. Gamma readings clearly increase at confluence with DP Canyon, and generally decrease down canyon. Locally high values downstream may record the locations of either relatively old sediments or possibly relatively pure DP Canyon sediments.

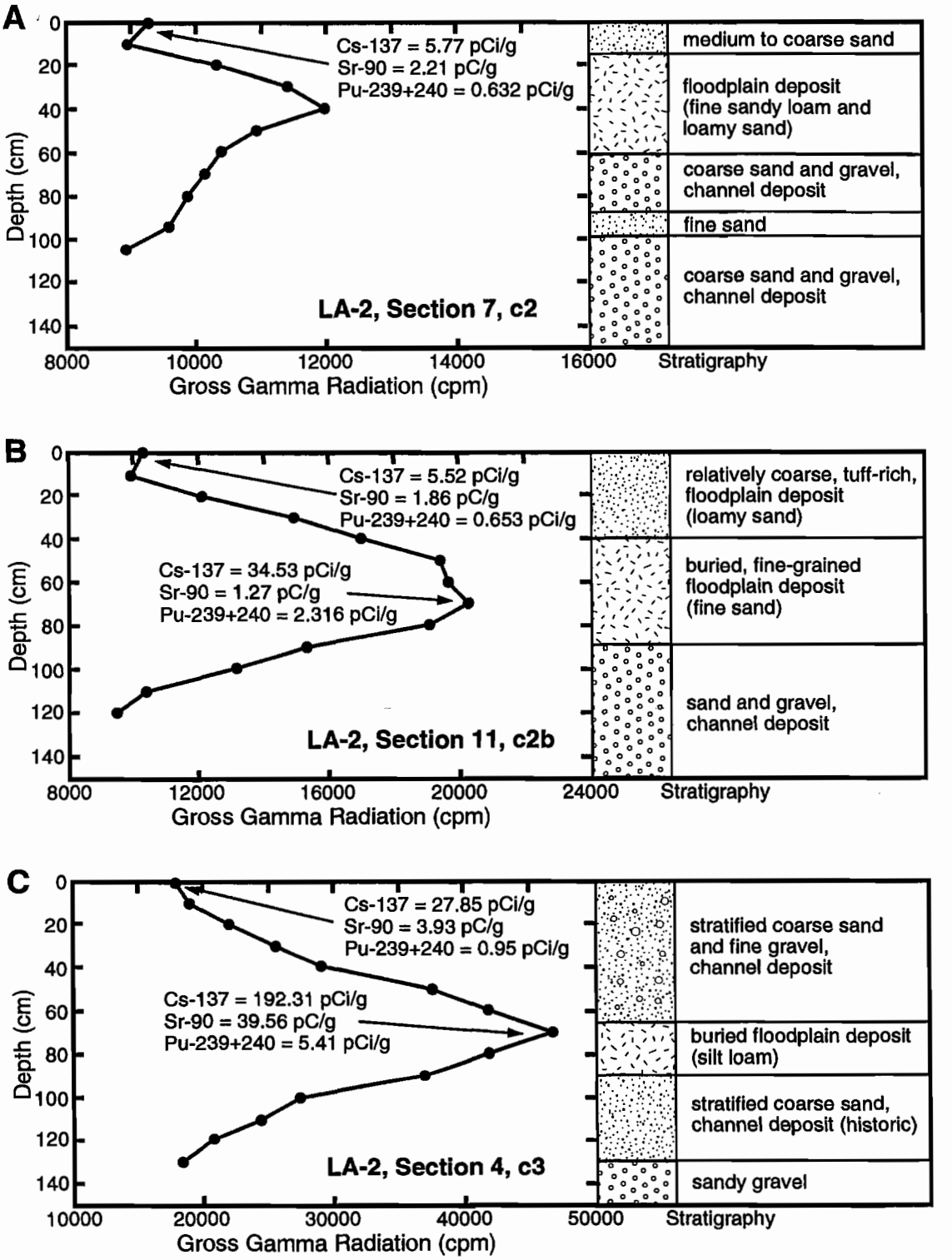

Fig. 3-21. Depth profiles of gross gamma radiation through historic sediment deposits in Los Alamos Canyon, reach LA-2, obtained using 1 minute count times and shielded 2-inch detector. Simplified stratigraphy shown to right, and concentrations of select radionuclides at "full suite" sample sites shown to left. Note that gamma scales vary between plots. A) Typical "c2" unit, ~100 m downstream of DP Canyon. B) Relatively high-gamma part of c2, "c2b", ~220 m downstream of DP Canyon. C) Site with highest field gamma readings, "c3", ~70 m downstream of DP Canyon.

Except for relatively high local values within ~100 m of DP Canyon, gamma values in the "c1" and "c2" units show no systematic variations in the 700 m long study reach downstream of DP Canyon (Fig. 3-20a). In contrast, data collected from a series of "mini-reaches" in the 4 km between DP Canyon and State Road 4 indicate a general downstream decline in gamma radiation in both the c1 and c2 units (Fig. 3-20b), consistent with the progressive dilution of ^{137}Cs by the addition of sediment from uncontaminated sources (tributary drainages and banks in prehistoric deposits).

The highest values of gamma radiation measured in reach LA-2 are in the "c3" unit a short distance downstream of DP Canyon. These exceed values measured in the lower part of DP Canyon, and we believe that c3 records sediments from DP Canyon floods that were deposited in Los Alamos Canyon as the gradient abruptly dropped. Notably, recent observations indicate that DP Canyon often floods in response to localized precipitation events that do not generate floods upstream in Los Alamos Canyon (Brad Wilcox and others, unpub. data, 1995), which should aid in the deposition of DP Canyon sediments close to the confluence. As in c2, the highest values in c3 are measured in a relatively fine-grained floodplain deposit at depth (Fig. 3-21c).

Contaminant Remobilization. The contaminants deposited in Los Alamos Canyon downstream from DP Canyon are largely located within several m of the active channel, and are thus susceptible to remobilization by bank erosion during floods. This includes the area of highest radionuclide concentrations, c3. The largest inventory of ^{137}Cs appears to be in overbank deposits in the c2 unit, whose characteristics suggest relatively short residence times (narrow deposits underlain by historic channel sands and gravels, produced during channel migration within a narrow belt). The scarcity of relatively high gamma readings downstream (<10% of the total area of c2 deposits) also suggests low residence times for most historic deposits in this canyon. The c2 and c3 deposits are thus acting as active "line sources" for contaminants, continuing to contribute radionuclides to the channel but probably at progressively lower concentrations as these contaminants become diluted with sediment from other sources.

- **End of "official" field trip.** After lunch, interested individuals can take a hike up a prehistoric Pueblo ("Anasazi") trail to an excellent example of an early Pleistocene mesa-top paleochannel.

5.8 Well house for water-supply well Otowi 4. Retrace route to NM State Route 4.

8.1 Gate at SR 4. Turn left, keeping in right lane towards Santa Fe.

8.4 Turn-off to Santa Fe.

8.9 Narrow slot of Los Alamos Canyon to right, incised into basalt (Fig. 3-2). This is a popular rock climbing area.

9.2 Roadcuts to left expose the basal layer of the Bandelier Tuff, the Guaje Pumice Bed, overlying basalt.

9.7 "Twin Tanks" at bend in road. Ahead to north are large landslides in Bandelier Tuff overlying late Pliocene lacustrine deposits (Smith et al., 1970).

10.4 Divider ends. Make U-turn and head back up-hill towards Los Alamos. Pliocene fanglomerates of Puye Formation well exposed in road cuts.

10.9 During road reconstruction in 1992, there were temporarily excellent exposures of basalts overlying lacustrine sediments in the roadcuts here, with nice examples of soft sediment deformation. This lake was formed by blockage of the Rio Grande valley by other Cerros del Rio basalt flows to the south, possibly in the vicinity of the present Water Canyon. Prior to road reconstruction, this was a popular field trip stop to examine pillow lavas and associated palagonitic breccias (the mineral palagonite gives the basalt rubble in the roadcut the yellowish color) (e.g., Bailey and Smith, 1978, p. 194-195).

11.2 The roadcut has excellent exposures of the ca. 1.61 Ma Guaje Pumice bed overlying the late Pliocene tholeiitic basalt (Fig. 3-22). The Guaje Pumice Bed here is about 7 m thick and includes a series of fall units and surge beds that can be correlated between outcrops (e.g., Self and Sykes, 1996, p. 18-19). Depressions in the top of the lava flow are filled with lacustrine sediments, which locally display buried soils.

11.5 Park on shoulder at west end of exposure of Guaje Pumice Bed. Hike leaves from here.

Stop 3-4 (optional): Unnamed mesa north of Pueblo Canyon-Los Alamos Canyon confluence

This hike climbs 360' in <1 km to visit an excellent example of an early Pleistocene mesa-top paleochannel, part of a widespread drainage system that pre-dated incision of the present canyons (examples on other mesas discussed in Reneau, 1995a, and Reneau et al., 1995b) (Fig. 3-23). The paleochannel contains dacite cobbles and boulders transported from the Sierra de los Valles, and also tuffaceous sediments and pumice that are associated with Valles Rhyolite eruptions (see discussion at Stop 2-3c). This paleochannel was originally mapped by M. A. Rogers in the mid-1970s (Rogers, 1995), but to our knowledge no further examination of this site or other mesa-top alluvial deposits on the Pajarito Plateau was conducted until the 1990s.

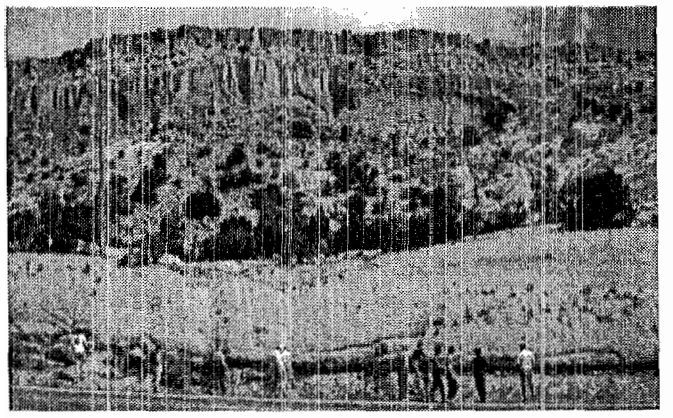

Fig. 3-22. Photograph of NM 502 roadcut near Stop 3-4, taken in 1992 before road reconstruction. Contact between Guaje pumice bed and underlying late Pliocene tholeiitic basalt is ~ 1m above road. Slopes are underlain by non-welded Otowi ignimbrites, and cliffs by Tshirege ignimbrites. Unit Qbt-2 forms the cap rock.

- From NM 502, cross the barbed-wire fence and head on poor, unmaintained trails towards the northwest part of the broad embayment in the mesa. The lower slopes are covered by slopewash and bouldery colluvium that mantles non-welded ignimbrites of the Otowi Member. Cerro Toledo beds are not exposed on this route, being covered by colluvium as is typical in many canyons. On the upper slopes, the route traverses across vapor-phase altered tuff of Tshirege unit Qbt-1v, and then climbs up through the short Qbt-2 cliffs at the head of the embayment. The presence of prehistoric steps in the tuff indicates long usage of this route.

- The cliff at the head of the embayment intersects the south edge of the paleochannel,

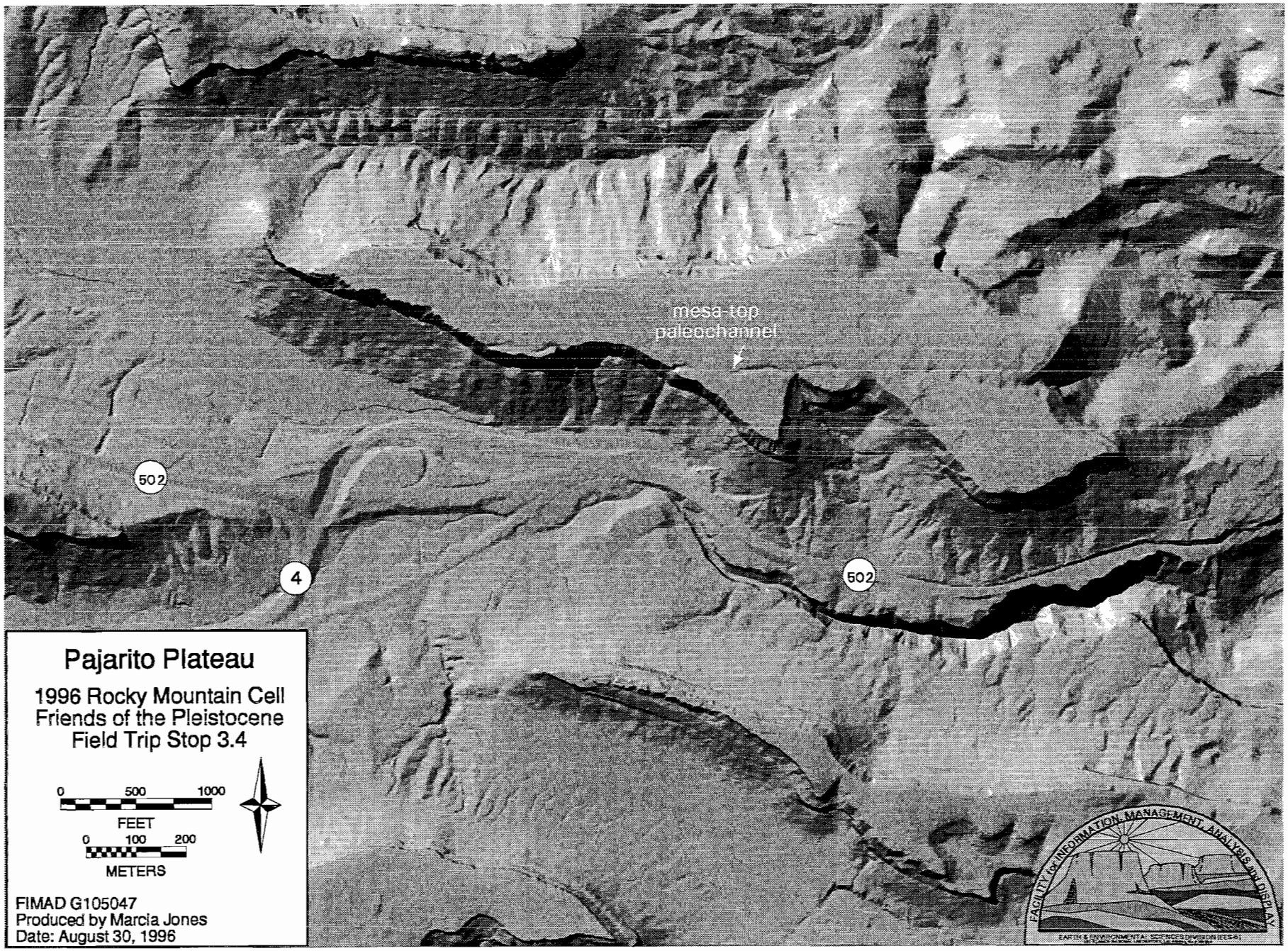
mesa-top
paleochannel
502
4
502
Pajarito Plateau
1996 Rocky Mountain Cell
Friends of the Pleistocene
Field Trip Stop 3.4
0 500 1000
FEET
0 100 200
METERS
FIMAD G105047
Produced by Marcia Jones
Date: August 30, 1996
FACILITY for INFORMATION MANAGEMENT ANALYSIS and DISPLAY

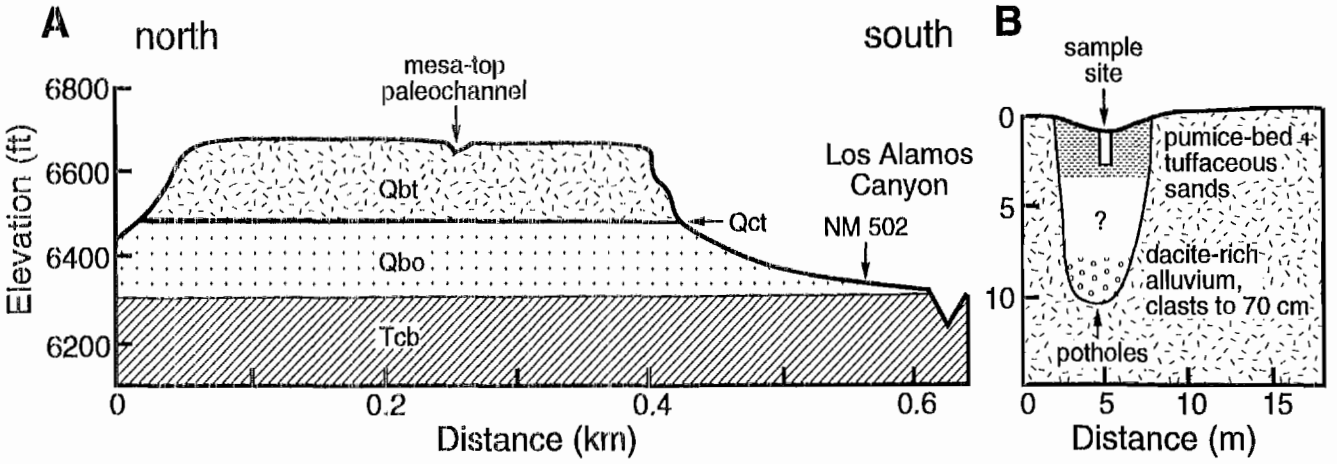

Fig. 3-23. A) Schematic cross section at Stop 3-4, showing location of early Pleistocene mesa-top paleochannel and geologic units. Schematic sketch of ~11 m deep paleochannel, showing sample site for Valles Rhyolite pumice in uppermost part of deposit, and dacite-dominated gravels exposed in base of channel at mesa edges.

expressed as an east-west oriented trough in the mesa-top. Head west up the trough to a low divide. A 1.65 m deep pit excavated here in 1994 exposed an early Pleistocene alluvial deposit and associated pumice beds. The lower 0.78 m of section consisted of well-sorted, well-stratified white tuffaceous sand. Above this is a 2-cm thick pumice-rich layer, 12 cm of coarse tuffaceous sands, and an upper pumice bed that is at least 78 cm thick (top likely eroded). The upper pumice bed is pure, clast-supported, and contains angular to sub-angular clasts up to 8 cm in diameter. Pervasive clay coatings reflect translocation through the upper section. The pumice bed is not obviously stratified, and may represent a primary fallout deposit or very local reworking. Analyses of the pumice (Fig. 2-10) suggests an association with the Cerro del Medio dome complex, and thus an age of ca. 1.16-1.21 Ma. This in turn suggests that the paleochannel at this site was carved and abandoned within ~10-60 ky of eruption of the Tshirege Member.

- Continue west down the trough to the mesa edge, where the paleochannel projects into space (it intersects the cliff again about 200 m west). The base of the paleochannel is exposed here, displaying well-preserved early Pleistocene potholes scoured into the tuff. Dacite boulders up to 70 cm in diameter (intermediate axis) occur in this area, demonstrating a source >12 km to the west in the Sierra de los Valles, presumably in the headwaters of the modern Los Alamos or Pueblo Canyons. Scattered well-rounded dacite clasts also occur on this mesa to the north, probably representing lag gravels similar to those occurring on many other mesa tops (e.g., Reneau et al., 1995b) and indicating a much wider extent for the original alluvial deposit.

End of field trip. Retrace route to NM 502, or continue exploring this mesa. Scattered patches of El Cajete pumice represent the northernmost recognized extent of the fallout plume. From the east end of the mesa are excellent views of a large dissected landslide complex composed of rotated Bandelier Tuff blocks overlying late Pliocene lacustrine deposits, and also views across the Española basin to the Sangre de Cristo Mountains. From the west end of the mesa are views up Pueblo Canyon past Stop 3-1. A route off the west end of the mesa can be followed into a deep gap reflecting stream capture and abandonment of a former course of Pueblo Canyon, and then down into Pueblo Canyon between Stops 3-1 and 3-2 (Fig. 3-24). The gap was called *Tse'ewi'i* ("gap of the eagle") by the local Tewas, and the bordering mesas *Tse'ewikwaje* ("height above the gap of the eagle") (Hoard, 1981).

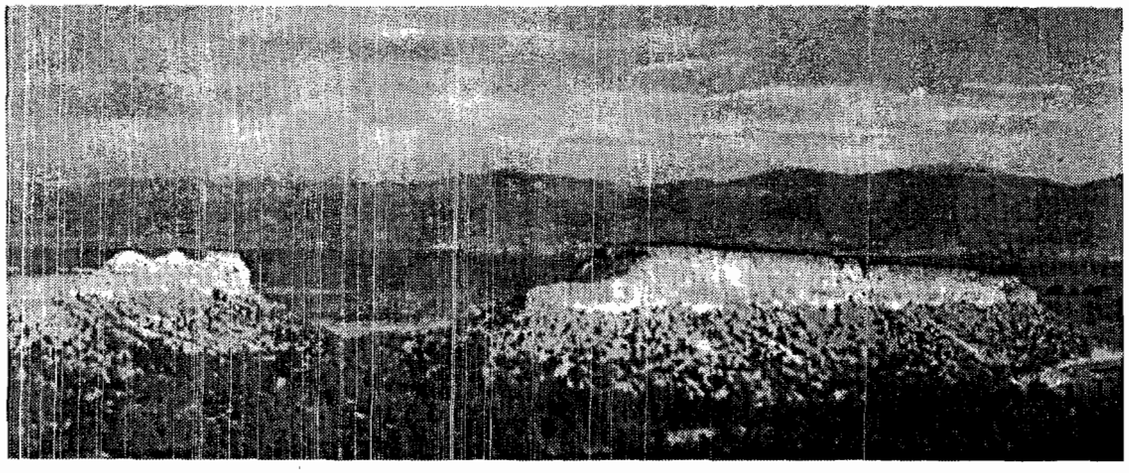

Fig. 3-24. Photograph across lower Pueblo Canyon to "gap of the eagle". Stop 3-4 is on mesa to right. Sangre de Cristo Range is in background.

Go my Sons, buy stout shoes, climb the mountains, search the valleys, the deserts, the sea shores, and the deep recesses of the earth . . . for in this way and in no other will you arrive at a knowledge of the nature and properties of things.

- P. Severinus (1778)

REFERENCES

Acklen, J. C., 1993, ed., Archaeological site testing for the Ojo Line Extension 345 kV transmission project in the Jemez Mountains, New Mexico: Albuquerque, Mariah Associates, Inc., report for The Public Service Company of New Mexico, 485 p. plus appendices.

Aldrich, M. J., Jr., 1986, Tectonics of the Jemez lineament in the Jemez Mountains and Rio Grande rift: Journal of Geophysical Research, v. 91, p. 1753-1762.

Aldrich, M. J., Jr., and Dethier, D. P., 1990, Stratigraphic and tectonic evolution of the northern Española basin, Rio Grande rift, New Mexico: Geological Society of America Bulletin, v. 102, p. 1695-1705.

Aldrich, M. J., Jr., and Harrington, C. D., 1995, Importance of understanding surface processes at environmental cleanup sites in obtaining representative samples: Geological Society of America, Abstracts with Programs, v. 27, no. 6, p. A-88.

Allen, B. D., 1991, Effect of climatic change on Estancia Valley, New Mexico: Sedimentation and landscape evolution in a closed-drainage basin: in Julian, B., and Zidek, J., Field Guide to Geologic Excursions in New Mexico and Adjacent Areas of Texas and Colorado, New Mexico Bureau of Mines and Mineral Resources Bulletin 137, p. 166-171.

Allen, C. D., 1989, Changes in the landscape of the Jemez Mountains, New Mexico: unpublished Ph.D. thesis, Berkeley, University of California, 346 p.

Allen, C. D., and Breshears, D. D., 1995, A drought-induced shift in a forest/woodland ecotone: Rapid response to variation in climate: Bulletin of the Ecological Society of America, Supplement, Program and Abstracts, 80th Annual ESA Meeting, p. 3.

Allen, C. D., Hanson, B., and Mullins, C., eds., 1993, Cochiti Reservoir reregulation, interagency biological report: unpublished report.

Allen, C. D., Touchan, R., and Swetnam, T. W., 1995, Landscape-scale fire history studies support fire management action at Bandelier: Park Science, v. 15, no. 3, p. 18-19.

Allen, C. D., Touchan, R., and Swetnam, T. W., 1996, Overview of fire history of the Jemez Mountains, New Mexico, *in* Goff, F., Kues, B. S., Rogers, M. A., McFadden, L. D., and Gardner, J. N., eds., The Jemez Mountains region: New Mexico Geological Society Forty-Seventh Annual Field Conference Guidebook (in press).

Anderson, R. S., 1993, A 35,000 year vegetation and climate history from Potato Lake, Mogollon Rim, Arizona: Quaternary Research, v. 40, p. 351-359.

Anderson, R. S., Repka, J. L., Dick, G. S., 1996, Explicit treatment of inheritance in dating deposits using in situ ^{10}Be and ^{26}Al: Geology, v. 21, p.47-51.

Aubele, J. C., 1978, Geology of the Cerros del Rio volcanic field, New Mexico: unpublished M.S. thesis, Albuquerque, University of New Mexico, 136 p.

Aubele, J. C., 1979, The Cerros del Rio volcanic field: New Mexico Geological Society, Guidebook 30, p. 243-252.

Bailey, R. A., and Smith, R. L., 1978, Volcanic geology of the Jemez Mountains, New Mexico, *in* Hawley, J. W., ed., Guidebook to Rio Grande Rift in New Mexico and Colorado, New Mexico Bureau of Mines and Mineral Resources Circular 163, p. 184-196.

Bailey, R. A., Smith, R. L., and Ross, C. S., 1969, Stratigraphic nomenclature of volcanic rocks in the Jemez Mountains, New Mexico, *in* Contributions to stratigraphy: U.S. Geological Survey Bulletin 1274-P, p. 1-18.

Baldridge, W. S., Ferguson, J. F., Braile, L. W., Wang, B., Eckhardt, K., Evans, D., Schultz, C., Gilpin, B., Jiracek, G. R., and Biehler, S., 1994, The western margin of the Rio Grande rift in northern New Mexico: An aborted boundary?: Geological Society of America Bulletin, v. 105, p. 1538-1551.

Baltz, E. H., Abrahams, J. H., and Purtymun, W. D., 1963, Preliminary report on the geology and hydrology of Mortandad Canyon near Los Alamos, New Mexico, with reference to disposal of liquid low-level radioactive waste: U.S. Geological Survey Open File Report, Albuquerque, New Mexico.

Becker, N. M., 1991, Influence of hydraulic and geomorphologic components of a semi-arid watershed on depleted uranium transport: unpublished Ph.D. thesis, University of Wisconsin, Madison, Wisconsin, 237 p.

Betancourt, J. L., 1990, Late Quaternary biogeography of the Colorado Plateau; *in* Betancourt, J. L., Van Devender, T. R., and Martin, P. S., eds., Packrat middens—The last 40,000 years of biotic change: Tucson, University of Arizona Press, p. 259-292.

Bierman, P. R. and Steig, E. J., 1996, Estimating rates of denudation using cosmogenic isotope abundances in sediment: Earth Surface Processes and Landforms, v. 21, p. 125-139.

Blagbrough, J. W., 1984, Fossil rock glaciers on Carrizo Mountain, Lincoln County, New Mexico: New Mexico Geology, v. 6, p. 65-68.

Blagbrough, J. W., and Brown, H. G., III, 1983, Rock glaciers on the west slope of South Baldy, Magdalena Mountains, Socorro County, New Mexico, *in* Chapin, C. E., ed., Socorro Region II: New Mexico Geological Society Thirty-Fourth Annual Field Conference Guidebook, p. 299-302.

Blagbrough, J. W., and Farkas, S. E., 1968, Rock glaciers in the San Mateo Mountains, south-central New Mexico: American Journal of Science, v. 266, p. 812-823.

Blake, W. D., Goff, F., Adams, A. I., and Counce, D., 1995, Environmental geochemistry for surface and subsurface waters in the Pajarito Plateau and outlying areas, New Mexico: Los Alamos National Laboratory Report LA-12912-MS, Los Alamos, New Mexico, 43 p.

Bowen, B. M., 1990, Los Alamos climatology: Los Alamos National Laboratory Report LA-11735-MS, 254 p.

Bowen, B. M., 1992, Los Alamos climatology summary: Los Alamos National Laboratory Report LA-12232-MS, 42 p.

Broxton, D. E., and Reneau, S. L., 1995, Stratigraphic nomenclature of the Bandelier Tuff for the Environmental Restoration Project at Los Alamos National Laboratory: Los Alamos National Laboratory Report LA-13010-MS, Los Alamos, New Mexico, 21 p.

Broxton, D. E., and Reneau, S. L., 1996, Buried early Pleistocene landscapes beneath the Pajarito Plateau, northern New Mexico, *in* Goff, F., Kues, B. S., Rogers, M. A., McFadden, L. D., and Gardner, J. N., eds., The Jemez Mountains region: New Mexico Geological Society Forty-Seventh Annual Field Conference Guidebook (in press).

Broxton, D. E., Heiken, G. H., Chipera, S. J., and Byers, F. M., Jr., 1995a, Stratigraphy, petrography, and mineralogy of Bandelier Tuff and Cerro Toledo deposits, *in* Broxton, D. E., and Eller, P. G., eds., Earth science investigations for environmental restoration—Los Alamos National Laboratory Technical Area 21: Los Alamos National Laboratory Report LA-12934-MS, Los Alamos, New Mexico, p. 33-63.

Broxton, D. E., Vaniman, D., Byers, F. M., Jr., Chipera, S. J., Kluk, E. C., and Warren, R. G., 1995b, Stratigraphy, mineralogy and chemistry of bedrock tuffs at Pajarito Mesa, *in* Reneau, S. L., and Raymond, R., Jr., eds., Geological site characterization for the proposed Mixed Waste Disposal Facility, Los Alamos National Laboratory: Los Alamos National Laboratory Report LA-13089-MS, Los Alamos, New Mexico, p. 5-30.

Bull, W. B., 1991, Geomorphic responses to climatic change: New York, Oxford University Press, 326 p.

Carter, K. E., and Gardner, J. N., 1995, Quaternary fault kinematics in the northwestern Española basin, Rio Grande rift, New Mexico, *in* Bauer, P. W., Kues, B. S., Dunbar, N. W., Karlstrom, K. E., and Harrison, B., eds., Geology of the Santa Fe region, New Mexico: New Mexico Geological Society Forty-Sixth Annual Field Conference Guidebook, p. 97-103.

Carter, K. E., and Winter, C. L., 1995, Fractal nature and scaling of normal faults in the Española basin, Rio Grande rift, New Mexico: Implications for fault growth and brittle strain: Journal of Structural Geology, v. 17, p. 863-873.

Cerling, T. E., Poreda, R. J., Rathburn, S. L., 1994, ^{3}He and ^{21}Ne ages of the Big Lost River flood, Snake River Plain, Idaho: Geology, v. 22, p. 227-230.

Chapin, C. E., 1988, Axial basins of the northern and central Rio Grande rift; *in* Sloss, L. L., ed., Sedimentary cover—North American craton: U.S.: Geological Society of America, Geology of North America, v. D-2, p. 165-170.

Chapin, C. E., and Cather, S. M., 1994, Tectonic setting of the axial basins of the northern and central Rio Grande rift; *in* Keller, G. R., and Cather, S. M., eds., Basins of the Rio Grande rift: Structure, stratigraphy, and tectonic setting: Geological Society of America Special Paper 291, p. 5-25.

Chapman, R. C., 1979a, Archaic settlement and the vegetative diversity model, *in* Biella, J. V., and Chapman, R. C., eds., Archaeological investigations in Cochiti Reservoir, New Mexico, Volume 4: Adaptive change in northern Rio Grande valley: Office of Contract Archeology, Department of Anthropology, University of New Mexico, p. 75-102.

Chapman, R. C., 1979b, The Archaic occupation of White Rock Canyon, *in* Biella, J. V., and Chapman, R. C., eds., Archaeological investigations in Cochiti Reservoir, New Mexico, Volume 4: Adaptive change in northern Rio Grande valley: Office of Contract Archeology, Department of Anthropology, University of New Mexico, p. 61-73.

Clark, D. H., Bierman, P. R., Larsen, P., 1995, Improving in situ cosmogenic chronometers: Quaternary Research, v. 44, p. 367-377.

Cordell, L. S., 1979, Cultural Resources Overview of the Middle Rio Grande Valley, New Mexico: U. S. Government Printing Office, Washington, D.C., 198 p.

Cordell, L. S., 1984, Prehistory of the Southwest: Orlando, Academic Press, 409 p.

Dahlgren, R. A., 1994, Quantification of allophane and imogolite, *in* Quantitative methods in soil mineralogy, Soil Science Society of America Miscellaneous Publication.

Davenport, D. W., 1993, Micromorphology, mineralogy, and genesis of soils and fracture fills on the Pajarito Plateau, New Mexico: unpublished Ph.D. thesis, Texas Tech University, Lubbock, 109 p.

Davenport, D. W., Wilcox, B. P., and Allen, B. L., 1995, Micromorphology of pedogenically derived fracture fills in Bandelier Tuff, New Mexico: Soil Science Society of America Journal, v. 59, p. 1672-1683.

Davis, O. K., and Shafer, D. S., 1992, A Holocene climatic record for the Sonoran Desert from pollen analysis of Montezuma Well, Arizona, USA: Palaeogeography, Palaeoclimatology, Palaeoecology, v. 92, p. 107-119.

Dethier, D. P., 1996, Geologic map of the White Rock quadrangle: New Mexico Bureau of Mines and Mineral Resources (in press).

Dethier, D. P., and Reneau, S. L., 1996, Lacustrine chronology links late Pleistocene climate change and mass movements in northern New Mexico: Geology, v. 24, p. 539-542.

Dethier, D. P., and McCoy, W. D., 1993, Aminostratigraphic relations and age of Quaternary deposits, northern Española basin, New Mexico: Quaternary Research, v. 39, p. 222-230.

Dethier, D. P., Harrington, C. D., and Aldrich, M. J., 1988, Late Cenozoic rates of erosion in the western Española basin, New Mexico: Evidence from geologic dating of erosion surfaces: Geological Society of America Bulletin, v. 100, p. 928-937.

Dixon, J. B., 1989, Kaolin and serpentine minerals, in Dixon J. B. and Weed, S. B. eds., Minerals in soil environments (2nd Edition), Soil Science Society of America Book Series, no. 1., p. 467-526.

Drake, P., and Inoue, C., 1993, Geomorphic characterization of Operable Unit 1079 (OU-1079), formerly Technical Area 10, Los Alamos National Laboratory, New Mexico: unpublished report, Glorieta Geoscience, Inc., Santa Fe.

Drakos, P., and Inoue, C., 1994, Geomorphic characterization of Operable Unit 1098 (OU-1098), Technical Areas 2 and 41, Los Alamos National Laboratory, New Mexico: unpublished report, Glorieta Geoscience, Inc., Santa Fe.

Drakos, P., Lazarus, J., and Inoue, C., 1996, Holocene evolution of canyons and implications for contaminant transport, Pajarito Plateau: *in* Goff, F., Kues, B. S., Rogers, M. A., McFadden, L. D., and Gardner, J. N., eds., The Jemez Mountains region: New Mexico Geological Society Forty-Seventh Annual Field Conference Guidebook (in press).

Dransfield, B. J., and Gardner, J. N., 1985, Subsurface geology of the Pajarito Plateau, Española basin, New Mexico: Los Alamos National Laboratory Report LA-10455-MS, 15 p.

Eberly, P., McFadden, L. D., and Watt, P. M., 1996, Eolian dust as a factor in soil development on the Pajarito Plateau, Los Alamos area, New Mexico: *in* Goff, F., Kues, B. S., Rogers, M. A., McFadden, L. D., and Gardner, J. N., eds., The Jemez Mountains region: New Mexico Geological Society Forty-Seventh Annual Field Conference Guidebook (in press).

Ferguson, J. F., Baldridge, W. S., Braile, L. W., Biehler, S., Gilpin, B., and Jiracek, G. R., 1995, Structure of the Española basin, Rio Grande rift, New Mexico, from SAGE seismic and gravity data, *in* Bauer, P. W., Kues, B. S., Dunbar, N. W., Karlstrom, K. E., and Harrison, B., eds., Geology of the Santa Fe region, New Mexico: New Mexico Geological Society Forty-Sixth Annual Field Conference Guidebook, p. 105-110.

Fisher, R. V., 1979, Models for pyroclastic surges and pyroclastic flows: Journal of Volcanology and Geothermal Research, v. 6, p. 305-318.

Foxx, T. S., compiler, 1984, La Mesa fire symposium: Los Alamos National Laboratory Report LA-9236-NERP.

Foxx, T. S., and Tierney, G. D., 1984, Status of the flora of the Los Alamos National Environmental Research Park: A historical perspective: Los Alamos National Laboratory Report LA-8050-NERP, v. 2, 50 p.

Friedman, L., Carrara, P., and Gleason, J., 1988, Isotopic evidence of Holocene climatic change in the San Juan Mountains, Colorado: Quaternary Research, v. 30, p. 350-353.

Galusha, T., and Blick, J. C., 1971, Stratigraphy of the Santa Fe Group, New Mexico: American Museum of Natural History Bulletin 144, 127 p.

Gardner, J. N., and Goff, F., 1984, Potassium-argon dates from the Jemez volcanic field: Implications for tectonic activity in the north-central Rio Grande rift, *in* Baldridge, W. S., Dickerson, P. W., Riecker, R. E., and Zidek, J., eds., Rio Grande rift: Northern New Mexico: New Mexico Geological Society Guidebook, 35th Field Conference, p. 75-81.

Gardner, J. N., and House, L., 1987, Seismic hazard investigations at Los Alamos National Laboratory, 1984-1985: Los Alamos National Laboratory Report LA-11072-MS, 76 p.

Gardner, J. N., and House, L., 1994, Surprisingly high intensities from two small earthquakes, northern Rio Grande rift, New Mexico: EOS, v. 75, p. 240.

Gardner, J. N., Goff, F., Garcia, S., and Hagan, R. C., 1986, Stratigraphic relations and lithologic variations in the Jemez volcanic field, New Mexico: Journal of Geophysical Research, v. 91, p. 1763-1778.

Gardner, J. N., Baldridge, W. S., Gribble, R., Manley, K., Tanaka, K., Geissman, J. W., Gonzalez, M., and Baron, G., 1990, Results from Seismic Hazards Trench #1 (SHT-1) Los Alamos Seismic Hazards Investigations: unpublished report, Memorandum EES1-SH90-19, Los Alamos National Laboratory, Los Alamos, New Mexico.

Gile, L., Peterson, F. F., Grossman, R. B., 1966, Morphologic and genetic sequences of carbonate accumulation in desert soils: Soil Science, v. 101, p. 347-360.

Goff, F., 1995, Geologic map of Technical Area 21, *in* Broxton, D. E., and Eller, P. G., eds., Earth science investigations for environmental restoration—Los Alamos National Laboratory Technical Area 21: Los Alamos National Laboratory Report LA-12934-MS, Los Alamos, New Mexico, p. 7-18.

Goff, F., Gardner, J. N., Baldridge, W. S., Hulen, J. B., Nielson, D. L., Vaniman, D., Heiken, G., Dungan, M. A., and Broxton, D., 1989, Volcanic and hydrothermal evolution of Valles caldera and Jemez volcanic field, *in* Chapin, C. E., and Zidek, J., eds., Field excursions to volcanic terranes in the western United States, Volume 1: Southern Rocky Mountain region: New Mexico Bureau of Mines & Mineral Resources Memoir 46, p. 381-434.

Goff, F., Kues, B. S., Rogers, M. A., McFadden, L. D., and Gardner, J. N., eds., 1996, The Jemez Mountains region: New Mexico Geological Society Forty-Seventh Annual Field Conference Guidebook (in press).

Golombek, M. P., 1983, Geology, structure, and tectonics of the Pajarito fault zone in the Española basin of the Rio Grande rift, New Mexico: Geological Society of America Bulletin, v. 94, p. 192-205.

Golombek, M. P., McGill, G. E.,, and Brown, L., 1983, Tectonic and geologic evolution of the Española basin of the Rio Grande rift: Structure, rate of extension, and relation to the state of stress in the western U.S.: Tectonophysics, v. 94, p. 483-507.

Gonzalez, M. A., 1993, Geomorphic and neotectonic analysis along a margin of the Colorado Plateau and Rio Grande rift in northern New Mexico: unpublished Ph.D. thesis, Albuquerque, University of New Mexico, 302 p.

Gonzalez, M. A., 1995, Use of erosional features for tectonic reconstructions and interbasin correlation: An example from the Rio Grande rift, northern New Mexico, *in* Bauer, P. W., Kues, B. S., Dunbar, N. W., Karlstrom, K. E., and Harrison, B., eds., Geology of the Santa Fe region, New Mexico: New Mexico Geological Society Forty-Sixth Annual Field Conference Guidebook, p. 139-145.

Gonzalez, M. A., and Dethier, D. P., 1991, Geomorphic and neotectonic evolution along the margin of the Colorado Plateau and northern Rio Grande rift, northern New Mexico, *in* Julian, B., and Zidek, J., eds., Field guide to geologic excursions in New Mexico and adjacent areas of Texas and Colorado: New Mexico Bureau of Mines and Mineral Resources Bulletin 137, p. 29-45.

Gonzalez, M. A., and Gardner, J. N., 1990, Geomorphic history and neotectonic analysis of Rendija and Cabra Canyons, Los Alamos County, New Mexico: unpublished report, Los Alamos National Laboratory, 30 p.

Gosse, J. C., Reedy, R., Harrington, C. D., Gillespie, A. R., 1996, Terrestrial cosmogenic nuclide dating: Tested and ready for action: EOS, v. 77, p. 275-276.

Graf, W. L., 1994, Plutonium and the Rio Grande: New York, Oxford University Press, 329 p.

Graf, W. L., 1995, Fluvial dynamics of plutonium in the Los Alamos Canyon system, New Mexico: unpublished report, Tempe, Arizona State University, 89 p.

Graf, W. L., 1996, Transport and deposition of plutonium contaminated sediments, Los Alamos Canyon, New Mexico: Geological Society of America Bulletin (in press).

Granger, D. E., Kirchner, J. W., Finkel, R., 1996, Spatially averaged long-term erosion rates measured from in situ-produced cosmogenic nuclides in alluvial sediment: Journal of Geology, v. 104, p. 249-257.

Griggs, R. L., 1964, Geology and groundwater resources of the Los Alamos area, New Mexico: U.S. Geological Survey Water-Supply Paper 1735, 107 p.

Hall, S. A., 1985, Quaternary pollen analysis and vegetational history of the Southwest; *in* Bryant, V. M., Jr., and Holloway, R. G., eds., Pollen records of late-Quaternary North American Sediments: Dallas, American Association of Stratigraphic Palynologists, p. 95-123.

Harden, J.W., 1982, A quantitative index of soil development from field descriptions: examples from a soil chronosequence in central California: Geoderma, v. 28, p. 1-28.

Harden. J. W., 1990, Soil development of stable landforms and implications for landscape studies: *in* Knuepfer, P. L. K., and McFadden, L.D., eds., Soils and landscape evolution: Geomorphology, v. 3, p. 391-398.

Harden, J. W., and Taylor, E. M., 1983, A quantitative comparison of soil development in four climatic regimes: Quaternary Research, v. 20, p. 342-359.

Harden, J. W., Taylor, E.M., Hill, C., Mark, R. L., McFadden, L. D., Reheis, M. C., Sowers, J. M., and Wells, S. G., 1991, Rates of soil development from four soil chronosequences in the southern Great Basin: Quaternary Research, v. 35, p. 383-399.

Hay, R. L., 1978, Geologic occurrences of zeolites, *in* Sand, L. B., and Mumpton, F. A., eds., Natural zeolites: Occurrences, properties, use: Elmsford, New York, Pergamon Press, p. 135-143.

Heiken, G., Goff, F., Stix, J., Tamanyu, S., Shafiqullah, M., Garcia, S., and Hagan, R. C., 1986, Intracaldera volcanic activity, Toledo caldera and embayment, Jemez Mountains, New Mexico, Journal of Geophysical Research, v. 91, p. 1799-1815.

Heiken, G., Goff, F., Gardner, J. N., Baldridge, W. S., Hulen, J. B., Nielson, D. L., and Vaniman, D., 1990, The Valles/Toledo caldera complex, Jemez volcanic field, New Mexico, *in* Annual Review of Earth and Planetary Science, v. 18, p. 27-53.

Heiken, G., Wohletz, K., Fisher, R. V., and Dethier, D. P., 1996, Maar volcanoes of White Rock Canyon—Interaction of ground and surface water with basaltic volcanoes of the Rio Grande rift, New Mexico, *in* Field excursions to the Jemez Mountains, New Mexico: New Mexico Bureau of Mines & Mineral Resources Bulletin 134, p. 56-72.

Hewett, E. L., 1938, The Pajarito Plateau and its ancient people: Albuquerque, University of New Mexico.

Hoard, D., 1981, Los Alamos outdoors: The Los Alamos Historical Society, Los Alamos, New Mexico, 120 p.

Ingersoll, R. V., Cavazza, W., Baldridge, W. S., and Shafiqullah, M., 1990, Cenozoic sedimentation and paleotectonics of north-central New Mexico: Implications for initiation and evolution of the Rio Grande rift: Geological Society of America Bulletin, v. 102, p. 1280-1296.

Irwin-Williams, C., 1973, The Oshara tradition: Origins of Anasazi culture: Eastern New Mexico University Contributions in Anthropology, v. 1, no. 4, p. 48-54

Izett, G. A., and Obradovich, J. D., 1994, $^{40}Ar/^{39}Ar$ age constraints for the Jaramillo Normal Subchron and the Matuyama-Brunhes geomagnetic boundary: Journal of Geophysical Research, v. 99, p. 2925-2934.

Keefer, D. K., 1984, Landslides caused by earthquakes: Geological Society of America Bulletin, v. 95, p. 406-421.

Keller, M. D., ed., 1968, Geologic studies and material properties investigations of Mesita de Los Alamos: Los Alamos Scientific Laboratory Report LA-3728.

Kelley, V. C., 1952, Tectonics of the Rio Grande depression of central New Mexico: New Mexico Geological Society Guidebook 3, p. 93-105.

Kelley, V. C., 1979, Tectonics, middle Rio Grande rift, New Mexico; *in* Riecker, R. E., ed., Rio Grande rift: Tectonics and magmatism: Washington, D.C., American Geophysical Union, p. 57-70.

Kelson, K. I., and Olig, S. S., 1995, Estimated rates of Quaternary crustal extension in the Rio Grande rift, northern New Mexico, *in* Bauer, P. W., Kues, B. S., Dunbar, N. W., Karlstrom, K. E., and Harrison, B., eds., Geology of the Santa Fe region, New Mexico: New Mexico Geological Society Forty-Sixth Annual Field Conference Guidebook, p. 9-12.

Kelson, K. I., and Wells, S. G., 1987, Present-day fluvial hydrology and long-term tributary adjustments, northern New Mexico; *in* Menges, C., ed., Quaternary tectonics, landform evolution, soil chronologies and glacial deposits—northern Rio Grande rift of New Mexico: Friends of the Pleistocene-Rocky Mountain Cell Field Trip Guidebook, p. 95-109.

Kelson, K. I., Hemphill-Haley, M. A., Olig, S. S., Simpson, G. D., Gardner, J. N., Reneau, S. L., Kolbe, T. R., Forman, S. L., and Wong, I. G., 1996, Late Pleistocene and possibly Holocene displacement along the Rendija Canyon fault, Los Alamos County, New Mexico, *in* Goff, F., Kues, B. S., Rogers, M. A., McFadden, L. D., and Gardner, J. N., eds., The Jemez Mountains region: New Mexico Geological Society Forty-Seventh Annual Field Conference Guidebook (in press).

Kohl, C. P. and Nishiizumi, K., 1992, Chemical isolation of quartz for measurement of in-situ-produced cosmogenic nuclides: Geochimica et Cosmochimica Acta, v. 56, p. 3583-3587.

Kolbe, T., Sawyer, J., Gorton, A., Olig, S., Simpson, D., Fenton, C., Reneau, S., Carney, J., Bott, J., and Wong, I., 1994, Evaluation of the Potential for Surface Faulting at the Proposed Mixed Waste Disposal Facility, TA-67: unpublished report, Woodward-Clyde Federal Services, Oakland, California, 3 volumes.

Kolbe, T., Sawyer, J., Springer, J., Olig, S., Reneau, S., Hemphill-Haley, M., and Wong, I., 1995, Evaluation of the Potential for Surface Faulting at TA-63: unpublished report, Woodward-Clyde Federal Services, Oakland, California.

Longmire, P. A., Reneau, S. L., Watt, P. M., McFadden, L. D., Gardner, J. N., Duffy, C. J., and Ryti, R. T., 1996, Natural background geochemistry, geomorphology, and pedogenesis of selected soil profiles and Bandelier Tuff, Los Alamos, New Mexico: Los Alamos National Laboratory Report LA-12913-MS, Los Alamos, New Mexico, 176 p.

Luedke, R.G., and Smith, R.L., 1978, Map showing distribution, composition and age of late Cenozoic volcanic centers in Arizona and New Mexico: U.S. Geological Survey Miscellaneous Investigations Map I-1091A.

Manley, K., 1976, The late Cenozoic history of the Española basin, New Mexico (Ph.D. dissertation): University of Colorado, Boulder, 171 p.

Manley, K., 1979, Stratigraphy and structure of the Española basin, Rio Grande rift, New Mexico, *in* Riecker, R. E., ed., Rio Grande rift: Tectonics and magmatism: American Geophysical Union, Washington, D.C., p. 71-86.

Markgraf, V., and Scott, L., 1981, Lower timberline in central Colorado during the past 15,000 yr: Geology, v. 9, p. 231-234.

McCalpin, J. P., 1995, Frequency distribution of geologically determined slip rates for normal faults in the western United States: Bulletin of the Seismological Society of America, v. 85, p. 1867-1872.

McDonald, E. V., Longmire, P. A., Watt, P. M., Ryti, R. T., and Reneau, S. L., 1996a, Natural major and trace element background geochemistry of selected soil profiles, Los Alamos, New Mexico, *in* Goff, F., Kues, B. S., Rogers, M. A., McFadden, L. D., and Gardner, J. N., eds., The Jemez Mountains region: New Mexico Geological Society Forty-Seventh Annual Field Conference Guidebook (in press).

McDonald, E. V., Reneau, S. L., and Gardner, J. N., 1996b, Soil-forming processes on the Pajarito Plateau: Investigation of a soil chronosequence in Rendija Canyon, *in* Goff, F., Kues, B. S., Rogers, M. A., McFadden, L. D., and Gardner, J. N., eds., The Jemez Mountains Region: New Mexico Geological Society Forty-Seventh Annual Field Conference Guidebook (in press).

McFadden, L. D., Watt, P. M., Reneau, S. L., and McDonald, E. V., 1996, General soil-landscape relationships and soil-forming processes in the Pajarito Plateau, Los Alamos National Laboratory, New Mexico, *in* Goff, F., Kues, B. S., Rogers, M. A., McFadden, L. D., and Gardner, J. N., eds., The Jemez Mountains region: New Mexico Geological Society Forty-Seventh Annual Field Conference Guidebook (in press).

McFaul, M., and Doering, W., 1993, Geoarchaeologic reconnaissance and testing program, *in* Acklen, J. C., ed., Archaeological site testing for the Ojo Line Extension 345 kV transmission project in the Jemez Mountains, New Mexico: Albuquerque, Mariah Associates, Inc., report for The Public Service Company of New Mexico, p. 39-115.

Muehlberger, W. R., 1979, The Embudo fault between Pilar and Arroyo Hondo, New Mexico: An active intracontinental transform fault: New Mexico Geological Society, Guidebook 30, p. 77-82.

Newman, B. D., 1996, Geochemical investigations of calcite fracture fills and mesa-top water dynamics on the Pajarito Plateau, New Mexico: unpublished Ph.D. thesis, New Mexico Institute of Mining and Technology, Socorro, 254 p.

Niedermann, S., Graf, T., Kim, J. S., Kohl, C. P., Marti, K., Nishiizumi, K., 1994, Cosmic-ray-produced ^{21}Ne in terrestrial quartz: The neon inventory of Sierra Nevada quartz separates: Earth and Planetary Science Letters v. 125, p. 341-355.

Nordin, C. F., Jr., and Beverage, J. P., 1965, Sediment transport in the Rio Grande, New Mexico: U.S. Geological Survey Professional Paper 462-F, 35 p.

Nyhan, J. W., Hacker, L. W., Calhoun, T. E., and Young, D. L., 1978, Soil Survey of Los Alamos County, New Mexico: Los Alamos Scientific Laboratory Informal Report LA-6779-MS, 102 p.

Olig, S. S., Kelson, K. I., Gardner, J. N., Reneau, S. L., and Hemphill-Haley, M., 1996, The earthquake potential of the Pajarito fault system, *in* Goff, F., Kues, B. S., Rogers, M. A., McFadden, L. D., and Gardner, J. N., eds., The Jemez Mountains region: New Mexico Geological Society Forty-Seventh Annual Field Conference Guidebook (in press).

Orcutt, J. D., 1991, Environmental variability and settlement changes on the Pajarito Plateau, New Mexico: American Antiquity, v. 56, p. 315-332.

Parfitt, R. L., and Childs, C. W., 1988, Estimation of forms of Fe and Al: A review, and analysis of contrasting soils by Dissolution and Mossbauer methods, Australian Journal of Soil Research, v. 26, p. 121-144.

Parfitt, R. L., Saigusa, M., and Cowie, J. D., 1984, Allophane and halloysite formation in a volcanic ash bed under different moisture conditions, Soil Science, v. 138, p. 360-364.

Phillips, F. M., Campbell, A. R., Kruger, C., Johnson, P., Roberts, R., and Keyes, E., 1992, A reconstruction of the response of the water balance in western United States lake basins to climatic change: New Mexico Water Resources Research Institute Report No. 269, v. 1, 167 p.

Phillips, W. M., in preparation, Applications of noble gas cosmogenic nuclides in geomorphology: University of Arizona, Tucson [Ph.D. dissertation].

Purtymun, W. D., 1995, Geologic and hydrologic records of observation wells, test holes, test wells, supply wells, springs, and surface water stations in the Los Alamos area: Los Alamos National Laboratory Report LA-12883-MS, Los Alamos, New Mexico, 339 p.

Purtymun, W. D., and Adams, H., 1980, Geohydrology of Bandelier National Monument, New Mexico: Los Alamos National Laboratory Informal Report LA-8461-MS, 25 p.

Purtymun, W. D., and Kennedy, W. R., 1971, Geology and hydrology of Mesita del Buey: Los Alamos Scientific Laboratory Report LA-4660, 12 p.

Purtymun, W. D., Peters, R. J., and Owens, J. W., 1980, Geohydrology of White Rock Canyon of the Rio Grande from Otowi to Frijoles Canyon: Los Alamos Scientific Laboratory Report LA-8635-MS, Los Alamos, New Mexico, 15 p.

Reneau, S. L., 1995a, Geomorphic studies at DP Mesa and vicinity, *in* Broxton, D. E., and Eller, P. G., eds., Earth science investigations for environmental restoration—Los Alamos National Laboratory Technical Area 21: Los Alamos National Laboratory Report LA-12934-MS, p. 65-92.

Reneau, S. L., 1995b, Potential mesa-edge instability at Pajarito Mesa, *in* Reneau, S. L., and Raymond, R., Jr., eds., Geological site characterization for the proposed Mixed Waste Disposal Facility, Los Alamos National Laboratory: Los Alamos National Laboratory Report LA-13089-MS, Los Alamos, New Mexico, p. 87-100

Reneau, S. L., and Dethier, D. P., 1996a, Late Pleistocene landslide-dammed lakes along the Rio Grande, White Rock Canyon, New Mexico: Geological Society of America Bulletin (in press).

Reneau, S. L., and Dethier, D. P., 1996b, Pliocene and Quaternary history of the Rio Grande, White Rock Canyon and vicinity, New Mexico, *in* Goff, F., Kues, B. S., Rogers, M. A., McFadden, L. D., and Gardner, J. N., eds., The Jemez Mountains region: New Mexico Geological Society Forty-Seventh Annual Field Conference Guidebook (in press).

Reneau, S. L., Gardner, J. N., Kelson, K. I., and Hemphill-Haley, M. A., 1993, Holocene stream aggradation and degradation, Pajarito Plateau, northern New Mexico: Geological Society of America Abstracts With Programs, v. 25, no. 5, p. 138.

Reneau, S. L., Dethier, D. P., and Carney, J. S., 1995a, Landslides and other mass movements near Technical Area 33, Los Alamos National Laboratory: Los Alamos National Laboratory Report LA-12955-MS, Los Alamos, New Mexico, 48 p.

Reneau, S. L., Kolbe, T., Simpson, D., Carney, J. S., Gardner, J. N., Olig, S. S., and Vaniman, D. T., 1995b, Surficial materials and structure at Pajarito Mesa, *in* Reneau, S. L., and Raymond, R., Jr., eds., Geological site characterization for the proposed Mixed Waste Disposal Facility, Los Alamos National Laboratory: Los Alamos National Laboratory Report LA-13089-MS, Los Alamos, New Mexico, p. 31-69.

Reneau, S. L., Gardner, J. N., and Forman, S. L., 1996a, New evidence for the age of the youngest eruptions in the Valles caldera, New Mexico: Geology, v. 24, p. 7-10.

Reneau, S. L., McDonald, E. V., Gardner, J. N., Kolbe, T. R., Carney, J. S., Watt, P. M., and Longmire, P. A., 1996b, Erosion and deposition on the Pajarito Plateau, New Mexico, and implications for geomorphic responses to late Quaternary climatic changes, *in* Goff, F., Kues, B. S., Rogers, M. A., McFadden, L. D., and Gardner, J. N., eds., The Jemez Mountains region: New Mexico Geological Society Forty-Seventh Annual Field Conference Guidebook (in press).

Rogers, D. B., 1994, Expanded Los Alamos area isohyetal map: unpublished report, Memorandum ESH-18/WQ&H-94-142, Los Alamos National Laboratory, Los Alamos, New Mexico.

Rogers, M. A., 1995, Geologic map of the Los Alamos National Laboratory Reservation: New Mexico Environment Department, Santa Fe.

Rothman, H. K., 1992, On rims and ridges: The Los Alamos area since 1880: University of Nebraska Press, Lincoln.

Schaafsma, P., 1975, Rock art in the Cochiti Reservoir district: Museum of New Mexico Papers in Anthropology, No. 16, Santa Fe.

Schaafsma, P., 1980, Indian rock art of the Southwest: Albuquerque, University of New Mexico Press, 379 p.

Schwertmann, U., and Taylor, R. M., 1989, in Dixon J. B. and Weed, S. B. eds., Minerals in soil environments (2nd Edition), Soil Science Society of America Book Series, no. 1., p. 379-426.

Self, S., and Sykes, M. L., 1996, Field guide to the Bandelier Tuff and Valles caldera, *in* Field excursions to the Jemez Mountains, New Mexico: New Mexico Bureau of Mines & Mineral Resources Bulletin 134, p. 7-55.

Self, S., Goff, F., Gardner, J. N., Wright, J. V., and Kite, W. M., 1986, Explosive rhyolitic volcanism in the Jemez Mountains: Vent locations, caldera development, and relation to regional structure: Journal of Geophysical Research, v. 91, p. 1779-1798.

Self, S., Gardner, J. N., and Goff, F., 1987, A field guide to the Jemez Mountains volcanic field, New Mexico, *in* Davies, G. H., and VadenDolder, E. M., eds., Geologic diversity of Arizona and its margins—excursions to choice areas: Arizona Bureau of Geology and Mining Technology, Special Paper 5, p. 95-112.

Self, S., Kircher, D. E., and Wolff, J. A., 1988, The El Cajete Series, Valles caldera, New Mexico: Journal of Geophysical Research, v. 93, p. 6113-6127.

Self, S., Wolff, J. A., Spell, T. L., Skuba, C. E., and Morrissey, M. M., 1991, Revisions to the stratigraphy and volcanology of the post-0.5 Ma units and the volcanic section of VC-1 core hole, Valles caldera, New Mexico: Journal of Geophysical Research, v. 96, p. 4107-4116.

Singer, B. S., and Kudo, A. M., 1986, Assimilation-fractional crystallization of Polvadera Group rocks in the northwestern Jemez volcanic field, New Mexico: Contributions to Mineralogy and Petrology, v. 94, p. 374-386.

Smith, R. L., and Bailey, R. A., 1966, The Bandelier Tuff: A study of ash-flow eruption cycles from zoned magma chambers: Bulletin Volcanologique, v. 29, p. 83-103.

Smith, R. L., and Bailey, R. A., 1968, Resurgent cauldrons, *in* Coats, R. R., Hay, R. L., and Anderson, C. A., eds., Studies in volcanology—a memoir in honor of Howell Williams: Geological Society of America Memoir 116, p. 613-662.

Smith, R. L., Bailey, R. A., and Ross, C. S., 1970, Geologic map of the Jemez Mountains, New Mexico: U.S. Geological Survey Miscellaneous Geologic Investigations Map I-571.

Soil Survey Staff, 1981, Examination and description of soils in the field, *in* Soil Survey Manual (USDA-ARS): U.S. Government Printing Office, Washington, D.C.

Spaulding, W. G., 1992, Late Quaternary paleoclimates and sources of paleoenvironmental data in the vicinity of Los Alamos National Laboratory—Final Report: unpublished report, Dames and Moore, Las Vegas, Nevada, 32 p.

Spaulding, W. G., Leopold, E.B., and Van Devender, T.R., 1983, Late Wisconsin paleoecology of the American Southwest: in Porter, S.C., ed., Late-Quaternary Environments of the United States, Vol. I, The Late Pleistocene, p. 259-293.

Spell, T. L., 1987, Geochemistry of Valle Grande Member ring fracture rhyolites, Valles caldera, New Mexico: unpublished M.S. thesis, New Mexico Institute of Mining and Technology, Socorro, 212 p.

Spell, T., Kyle, P., and Thirlwall, M., 1995, $^{40}Ar/^{39}Ar$ dating and geochemical evolution of the Cerro Toledo Rhyolite, Jemez volcanic field, New Mexico: Geological Society of America Abstracts With Programs, v. 27, no. 6, p. A-108.

Spiegel, Z., and Baldwin, B., 1963, Geology and water resources of the Santa Fe area, New Mexico: U.S. Geological Survey Water-Supply Paper 1525, 258 p.

Steen, C. R., 1977, Pajarito Plateau Archaeological Survey and Excavations: Los Alamos Scientific Laboratory Report LASL-77-4, 70 p.

Steen, C. R., 1982, Pajarito Plateau Archaeological Survey and Excavations, II: Los Alamos National Laboratory Report LA-8860-NERP, 60 p.

Stoker, A. K., Ahlquist, A. J., Mayfield, D. L., Hansen, W. R., Talley, A. D., and Purtymun, W. D., 1981, Radiological survey of the site of a former radioactive liquid waste treatment plant (TA-45) and the effluent receiving areas of Acid, Pueblo, and Los Alamos Canyons, Los Alamos, New Mexico: Los Alamos National Laboratory Report LA-8890-ENV, 252 p.

Stoker, A. K., Purtymun, W. D., McLin, S. G., and Maes, M. N., 1991, Extent of saturation in Mortandad Canyon: unpublished report, LA-UR-91-1660, Los Alamos National Laboratory, Los Alamos, New Mexico.

Stuart, D. E., 1989, The Magic of Bandelier: Santa Fe, Ancient City Press, 113 p.

Stuart, D. E., and Gauthier, R. P., 1981, Prehistoric New Mexico: Background for Survey. Albuquerque, University of New Mexico Press, 459 p.

Stuiver, M., and Reimer, P. J., 1993, Extended ^{14}C data base and revised CALIB 3.0 ^{14}C age calibration: Radiocarbon, v. 35, p. 215-230.

Switzer, P.S., Harden, J.W., and Mark, R.K., 1988, A statistical method for estimating rates of soil development and ages of geologic deposits: A design for soil-chronosequence studies: Mathematical Geology, v. 20, p. 49-61.

Thompson, R. S., Whitlock, C., Bartlein, P. J., Harrison, S. P., and Spaulding, W. G., 1993, Climatic changes in the western United States since 18,000 yr B.P.; *in* Wright, H. E., Jr., Kutzbach, J. E., Webb, T., III, Ruddiman, W. F., Street-Perrott, F. A. and Bartlein, P. J., eds., Global climates since the last glacial maximum: Minneapolis, University of Minnesota Press, p. 468-513.

Toyoda, S., Goff, F., Ikeda, S., and Ikeya, M., 1995, ESR dating of quartz phenocrysts in the El Cajete and Battleship Rock members of the Valles Rhyolite, Valles caldera, New Mexico: Journal of Volcanology and Geothermal Research, v. 67, p. 29-40.

Traylor, D., Wood, N., Hubbell, L., Scaife, R., and Waber, S., 1977, Bandelier excavations in the flood pool of Cochiti Lake, New Mexico: unpublished report, Southwest Cultural Resources Center, National Park Service, Santa Fe.

Turbeville, B. N., Waresback, D. B., and Self, S., 1989, Lava-dome growth and explosive volcanism in the Jemez Mountains, New Mexico: Evidence from the Plio-Pleistocene Puye alluvial fan: Journal of Volcanology and Geothermal Research, v. 36, p. 267-291.

Van Devender, T.R., Thompson, R.S., and Betancourt, J.L., 1987, Vegetation history of the deserts of southwestern North America; The nature and timing of the Late Wisconsin-Holocene transition, in Ruddiman, W.F., and Wright, H.E., Jr., eds., North America and adjacent oceans during the last deglaciation: Boulder, Colorado, Geological Society of America, The Geology of North America, v. K-3, p. 323-352.

Vaniman, D., and Chipera, S., 1995, Mesa-penetrating fractures, fracture mineralogy, and projected fault traces at Pajarito Mesa, *in* Reneau, S. L., and Raymond, R., Jr., eds., Geological site characterization for the proposed Mixed Waste Disposal Facility: Los Alamos National Laboratory Report LA-13089-MS, Los Alamos, New Mexico, p. 71-85.

Wada, K., 1989, Allophane and imogolite, 1989, in Dixon J. B. and Weed, S. B. eds., Minerals in soil environments (2nd Edition), Soil Science Society of America Book Series, no. 1., p. 1051-1087.

Waresback, D. B. and Turbeville, B. N., 1990, Evolution of a Plio-Pleistocene volcanogenic alluvial fan: The Puye Formation, Jemez Mountains, New Mexico: Geological Society of America Bulletin, v. 102, p. 298-314.

Watt, P. M., 1996, Landscape evolution and soil genesis on the Pajarito Plateau and the impact of soil chemical and physical properties on contaminant uranium migration, Los Alamos National Laboratory, New Mexico: unpublished Ph.D. thesis, University of New Mexico, Albuquerque, 353 p.

Weir, J. E., Jr., and Purtymun, W. D., 1962, Geology and hydrology of Technical Area 49, Frijoles Mesa, Los Alamos County, New Mexico: U.S. Geological Survey Administrative Release, Albuquerque, New Mexico.

White, W. D., and Wells, S. G., 1979, Forest-fire devegetation and drainage basin adjustments in mountainous terrain, *in* Rhodes, D. D., and Williams, G. P., eds., Adjustments of the fluvial system: Kendall/Hunt Publishing Company, Dubuque, Iowa, p. 199-223.

White, W. D., and Wells, S. G., 1984, Geomorphic effects of La Mesa fire; *in* Foxx, T. S., compiler, La Mesa fire symposium: Los Alamos National Laboratory Report LA-9236-NERP, p. 73-90.

Wilcox, B. P., 1994, Runoff and erosion in intercanopy zones of pinyon-juniper woodlands: Journal of Range Management, v. 47, p. 285-295.

Wilcox, B. P., Allen, C. D., Newman, B. D., Reid, K. D., Brandes, D., Pitlick, J., and Davenport, D. W., 1996a, Runoff and erosion on the Pajarito Plateau: Observations from the field, *in* Goff, F., Kues, B. S., Rogers, M. A., McFadden, L. D., and Gardner, J. N., eds., The Jemez Mountains region: New Mexico Geological Society Forty-Seventh Annual Field Conference Guidebook (in press).

Wilcox, B. P., Pitlick, J., Allen, C. D., and Davenport, D. W., 1996b, Runoff and erosion from a rapidly eroding pinyon-juniper hillslope, *in* Anderson, M. G., and Brooks, S., eds., Advances in hillslope processes: Chichester, John Wiley & Sons (in press).

Wilcox, B. P., Brandes, D., and Davenport, D. W., submitted, Runoff generation from a subhumid ponderosa pine hillslope in New Mexico: unpublished m.s., submitted to Water Resources Research.

Williams, J. L., ed., 1986, New Mexico in maps: University of New Mexico Press, Albuquerque, 2nd edition.

WoldeGabriel, G., 1993, K/Ar dating of clinoptilolites: Methods and preliminary results: Zeolite '93, 4th International Conference on the Occurrence, Properties, and Utilization of Natural Zeolites, Program and Abstracts, Boise, Idaho, p. 216-218.

WoldeGabriel, G., Laughlin, A. W., Dethier, D., and Heizler, M., 1996, Temporal and geochemical trends of volcanic rocks in White Rock Canyon and the Pajarito Plateau, Jemez volcanic field, New Mexico, USA, *in* Goff, F., Kues, B. S., Rogers, M. A., McFadden, L. D., and Gardner, J. N., eds., The Jemez Mountains region: New Mexico Geological Society Forty-Seventh Annual Field Conference Guidebook (in press).

Wolff, J. A., and Gardner, J. N., 1995, Is the Valles caldera entering a new cycle of activity?: Geology, v. 23, p. 411-414.

Wolff, J. A., Gardner, J. N., and Reneau, S. L., 1996, Field characteristics of the El Cajete pumice deposit and associated southwestern moat rhyolites of the Valles caldera, *in* Goff, F., Kues, B. S., Rogers, M. A., McFadden, L. D., and Gardner, J. N., eds., The Jemez Mountains region: New Mexico Geological Society Forty-Seventh Annual Field Conference Guidebook (in press).

Wong, I., Kelson, K., Olig, S., Kolbe, T., Hemphill-Haley, M., Bott, J., Green, R., Kanakari, H., Sawyer, J., Silva, W., Stark, C., Haraden, C., Fenton, C., Unruh, J., Gardner, J., Reneau, S., and House, L., 1995, Seismic Hazards Evaluation of the Los Alamos National Laboratory: unpublished report, Woodward-Clyde Federal Services, Oakland, California, 3 volumes.

Wong, I., Kelson, K., Olig, S., Bott, J., Green, R., Kolbe, T., Hemphill-Haley, M., Gardner, J., Reneau, S., and Silva, W., 1996, Earthquake potential and ground shaking hazard at the Los Alamos National Laboratory, New Mexico, *in* Goff, F., Kues, B. S., Rogers, M. A., McFadden, L. D., and Gardner, J. N., eds., The Jemez Mountains region: New Mexico Geological Society Forty-Seventh Annual Field Conference Guidebook (in press).

Wright, H. E., Jr., Brent, A. M., Hansen, B. S., and Mahler, L. J., Jr., 1973, Present and past vegetation of the Chuska Mountains, northwestern New Mexico: Geological Society of America Bulletin, v. 84, p. 1155-1180.

Table 1-1. Morphology for the Sandia Canyon soils (SC-1, SC-2) at Stop 1-2.

Horizon	Depth (cm)	Dry Color (Matrix)	Moist Color (Matrix)	Txt.*	Structure	Consistence Dry	Consistence Moist	Consistence Wet	Argillans	Mangans	% >2mm	Bdy**	Notes
SC-1													
Primary El Cajete Pumice													base of pumice
Etb1	0–10	10YR 7/3	10YR 4/3	l	2 c pr: 3-2 c,m pl: 1 c,m abk	h	fr	ss, vps	1nco, 1npo		3–5	as	
Bt1b1	10–25	10YR 6/3	7.5YR 5/4	sil	2 c pr: 2-1 c,m sbk	h	fi-fr	ss, ps	1n-mkpo, 1nco		2–5	cs	lamellae
Bt2b1	25–62	6.25YR 5/4	6.25YR 3/4	sil	2-1 c,m pr: 2 c,m sbk	h	fr	ss, p	2n-mkpf, 2n-mkpo	2n-mkpo	3–8	cs	
Bt3b1	62–75	7.5YR 6/4	7.5YR 4/4	l	2 c,m pr :2 c,m sbk	h	fr-vfr	ss, ps	1npf, 1npo		10–15	as-cs	
Etb2	75–84	7.5YR 7/4	7.5YR 4/4	l	2-1 c,m pr: 1 c,m sbk	h	fr	ss, ps	2n-mkpf, 1npo		5–10	as-cs	gravel-pebble colluvial layer
Btb2	84–93	6.25YR 5/4	6.25YR 4/4	l	1 c,m sbk + m	sh-h	fr-vfr	ss, vps	3n-mkbr	1npo	50–65	aw-as	
ABtb3	93–100	7.5YR 6/4	7.5YR 4/4	sil	2-3 m pr:2-1 c,m sbk	h	vfr	ss, ps	3n po, 1n-mkpr:pf		5–10	as	argillans increase with pore size
Bt1b3	100–118	7.5YR 7/4	7.5YR 5/6	sil	1 c,m pr: 1 c,m sbk	h-sh	fr-vfr	ss, ps-p	1npo	3npo	3–6	as	weak Bt, soil in overbank(?) deposits
BCb3	118–129	7.5YR 6/4	7.5YR 4/6	sil	m + 1 c,m sbk	h-sh	fr	ss, ps		1npo	2–4	aw-cw	krotovinas
Cb3	129–152	7.5YR 6/4	7.5YR 4/4	l	m	sh	vfr	ss, ps-vps			10–20	aw	stratified sands + silts
BAb4	152–170	7.5YR 6/4	7.5YR 4/4	l	2 m pr: 1-2 c,m sbk	sh	vfr	ss, ps		v1npo	5–10	cw	weak soil, noticeable structure and vertical pores
Bwb4	170–189	8.75YR 7/4	7.5YR 4/4	l	1-2 m pr: 1 c,m sbk	sh	vfr	vss, ps-vps		2n-mkpo	1–3	cs	floodplain and/or distal colluvium
BCb4	189–202	8.75YR 6/3	8.75YR 4/4	sl	1 c,m sbk	sh-so	vfr	vss, vps		1npo	5–10	as-aw	abundant krotovinas, burn layer
BAb5	202–216	7.5YR 6/4	7.5YR 4/4	l	1-2 m pr: 1 c,m sbk	sh	vfr	ss, vps		1n-mkpo	2–5	cs	
Bwb5	216–242	7.5YR 6/4	7.5YR 4/4	l	1 m pr: 1 c,m sbk	sh	vfr	ss, ps		v1npo	2–5	gs	
Cb5	242–268	7.5YR 6/4	7.5YR 4/4	sl	m	so	vfr	so, vps		1npo	5–15	as	stratified sands + silt stream deposits
ABb6	268–303	7.5YR 6/4	7.5YR 4/4	l	1 m pr: 1 c,m sbk	sh	vfr	ss, ps			2–5	cs	stratified stream deposits
C1b6	303–320	10YR 5/2	10YR 3/3	s	sg	lo	lo	so, po			10–20	cs	
C2b6	320+	10YR 5/2	10YR 3/3	s	sg	lo	lo	so, po			10–30		
SC-2													
A1	0–5	10YR 4/2	10YR 2/2	sl	2-1 m,f crb	so-lo	vfr-lo	so, vps			2–5	as	
A2	5–17	10YR 4/2	10YR 2/2	l	1 m,f sbk: 1m,f crb	so	vfr	so, vps			2–5	cs	krotovinas
Bw	17–30	10YR 5/2	10YR 3/2.5	sl	1 c pr: 1-2 m sbk	sh-so	vfr	so, vps			3–6	cs	krotovinas
BC	30–67	10YR 5/2	10YR 3/3	ls	1 m,f sbk + sg	so-lo	vfr-lo	so, vps-po			5–10	cs-cw	krotovinas
C1	67–88	10YR 5/2	10YR 3/3	ls	sg	so-lo	vfr-lo	so, vps-po			10–15	cs	
C2	88–113	10YR 5/2	10YR 3/3	s	sg	lo	lo	so, po			10–15	aw-cs	well stratified stream sands/pebbles
C3	113–136	10YR 5/2	10YR 3/3	s	sg	lo	lo	so, po			5–10	cs	well stratified stream sands/pebbles
C4	136–156+	10YR 5/2	10YR 3/3	s	sg	lo	lo	so, po			10–15		well stratified stream sands/pebbles

*Soil texture of the < 2mm fraction.

**Horizon boundary

Table 1-2. Morphology for Fence Canyon soils. Station 1-4b.

Horizon	Depth (cm)	Dry Color (Matrix)	Moist Color (Matrix)	Txt.*	Structure	Consistence			Argillans	% >2mm	Bdy**	CS***	% wt. Sand	% wt. Silt	% wt. Clay	Notes
						Dry	Moist	Wet								
A	0--6	10YR 6/3	10YR 4/4	l	1-2 m,f crb	so-lo	vfr-lo	vss, vps		2--5	as		57	41	2	1 cm O horizon on top
BA	6--21	7.5YR 5/4	7.5YR 3/4	l	1 c,m sbk: 1 m crb	so-lo	vfr-lo	vss, vps		2--5	cs		57	39	5	dominant root zone
Bw1	21--37	7.5YR 5.5/4	7.5YR 4/4	sil	1 m pr: 1-2 c,m sbk	sh-so	vfr-lo	ss, ps		5--10	cs		38	60	2	abundant bioturbation, filled insect burrows
BAb1	37--61	10YR 5/3	10YR 3/3	sil	1 m pr: 1-2 c,m sbk	sh-so	vfr-lo	ss, ps		10--15	cs-cw		32	67	2	v1 s-lt co on pr pf, filled insect burrows
Bwb1	61--85	10YR 5/3	10YR 3/4	sil	1 m pr: 1-2 c,m sbk	sh-so	vfr-lo	ss, ps		10--20	cs		28	70	2	filled insect burrows
BCkb1	85--104	10YR 5/3	10YR 3/4	l	1 m pr: 1-2 c,m sbk	sh-so	vfr-lo	ss, vps-ps		10--20	aw-ai	I	21	77	2	krotovina, filled insect burrows
ABkb2	104--118	8.75YR 6/4	7.5YR 4/4	sil	1 m,f pr: 2-3 m,f sbk	h-sh	vfr-fr	ss, ps	v1npf	5--10	cs	I	12	85	3	truncated in places due to bioturbation
Btkb2	118--141	7.5YR 6/4	7.5YR 4/4	sil	3-2 m,f pr: 2 m m,f sbk +abk	sh-h	vfr	ss-s, ps	1npr:pf, 1npo, v1mkpr:pf	2--8	cs	I	15	80	5	scattered EC pumice
Bt1b2	141--157	7.5YR 6/4	7.5YR 4/4	sil	1 m pr: 2-1 m,f sbk	sh	vfr	ss, ps	1npr:pf, 1nbr, 1npo	10--20	aw-ai		22	75	3	scattered EC pumice
Bt2b2	157--171	7.5YR 6/4	7.5YR 4/4	sil	m + 1 m,f sbk	h-sh	vfr-fr	ss, ps	3n-mkpo, 3n-mkbr + co	20--30	as		44	52	4	scattered EC pumice, lamellae sandy-pebble slopewash
Bt3b2	171--209	7.5YR 6/4	7.5YR 4/4	l	m + 1 m,f sbk	h-sh	vfr	ss, vps-ps	1n-mkbr + po, Lam: 3n-mkbr + po	30--40	cs		53	44	3	lamellae, sandy-pebble slopewash
BCb2	209--222	7.5YR 7/4	7.5YR 4/6	sil	m + 1 c,m sbk	sh	vfr	ss, vps-ps	vnfbr	10--20	cs		47	51	2	sandy-pebble slopewash
BAb3	222-235	7.5YR 7/4	7.5YR 4/5	l	1-2 m,f sbk	sh	vfr	ss, ps-vps	v1npo	10--20	cs		48	49	3	scattered EC pumice
Btb3	235--257	7.5YR 6/4	7.5YR 4/4	sil	1 c,m sbk	h	vfr-fr	ss, ps-vps	2n-mkpo, 1nbr	10--20	aw-ai		45	52	3	scattered EC pumice
Ekb4	257--264	10YR 7/3	8.75YR 5/4	sil	1-2 m,f pr: 2 m,f pl + 2-1 m,f sbk	h	fr-fi	vss, ps	v1npo + pf	2--5	as-aw	I	34	64	2	Soil locally overlain by EC
BEtkb4	264--275	7.5YR 6/5	7.5YR 4/6	sil	3 c,m pr: 2 c,m sbk + abk	h	fi	ss, ps	4mk-npo, 3n-mkpr:pf, 2n-mkbk:pf	2--5	cs	I	32	66	2	2 mk-n skeletans on pr:pf
Btkb4	275--290	7.5YR 6/4	7.5YR 4/6	sil	3-2 m pr: 2 c,m abk	h	fr-fi	ss, ps-p	4mk-npo, 2n-mkpr:pf, 2n-mkbk:pf	2--5	cs	I-	22	75	3	v1 n skeletans on pr:pf, lamellae
Bt1b4	290--314	7.5YR 6/5	7.5YR 4/6	sil	3-2 m pr: 2 c,m abk + sbk	h	fi-fr	ss, ps-p	4mkpo, 2n-mkpr:pf, 1n-mkbk:pf	5--10	cs		30	65	5	incipient lamellae
Bt2b4	314--329	7.5YR 6/4	7.5YR 4/4	sil	2-1 m pr: 2-1 c,m sbk	sh-h	fr-fi	ss-vs, ps	1npr:pf, 1npo, v1mkpr:pf	5--15	cs		42	54	4	incipient lamellae, tuff framents
Bt3b4	329--337	7.5YR 6/5	7.5YR 4/6	l	1-2 m pr: 2 c,m sbk	h-sh	fi-fr	ss, ps-vps	2n-mkpr:pf, 2n-mkpo, 1n-mkbk:pf	10--20	as-cs		49	48	3	stone line
Bt4b4	337--353	7.5YR 6/4	7.5YR 4/5	sil	1-2 m pr: 2 c,m sbk	sh-h	fr-fi	ss, vps-ps	1n-mkpr:pf + po, Lam: 3n-mk pr:pf + po	5--10	cs		36	60	4	lamellae, pebble layers, insect burrows
Bt5b4	353--377	7.5YR 6.5/4	7.5YR 4/4	sil	2-1 m pr: 2-1 c,m sbk	sh-h	vfr	ss, vps-ps	1npr:pf, Lam: 2n-mkpr:pf + po	5--10	cs		38	60	2	incipient lamellae
BCtb4	377--410	7.5YR 6.5/4	7.5YR 4/4	sil	1-2 m pr: 1 c,m sbk	sh	vfr	ss, ps	*Lam: 3mk-npr:pf + po*	2--5	cs		35	63	2	incipient lamellae
Cb4	410--430	7.5YR 4/5	7.5YR 4/5	sil	m	so	vfr	ss, ps-vps		10--20	aw-ai		46	52	2	Tuff fragments
R	430+								4mk-nco along top of tuff							Fractured tuff, unweathered

*Soil texture of the < 2mm fraction.
**Horizon Boundary.
***Secondary carbonate stage (Gile et al., 1965).

Lam = lamellae

EC = El Cajete pumice

Table 1-3. Morphology for the AC-1 soil, Stop 1-5.

Horizon	Depth (cm)	Dry Color (Matrix)	Moist Color (Matrix)	Txt.*	Structure	Consistence Dry	Consistence Moist	Consistence Wet	Argillans	% >2mm	Bdy	% wt. Sand**	% wt. Silt	% wt. Clay	OX:*** Fe2O3 (% wt)	CDB:*** Fe2O3 (% wt	Notes
A1	0--4	10YR 4/2	10YR 2/1	sl	1 m sbk: 1c,m crb	so	lo-vfr	so, ps-po		2--4	as	75	18	7	0.44	0.42	
A2	4--12	10YR 4.5/2	10YR 3/3	s	1 m,f sbk: 1 m,f crb	so	vfr	so, po		2--4	as	88	9	3	0.46	0.31	
Bw1	12--27	10YR 4/2	10YR 3/2	l	1-2 m pr: 1-2 m,f sbk	sh	vfr	ss, ps		5--10	cs	48	43	9	0.6	0.35	patchy silans on gravel
Bw2	27--56	10YR 5/4	10YR 4/3	sl	1 c,m sbk	sh	vfr	so, ps-po		10--15	aw	66	26	8	0.53	0.38	patchy silans on pf
C1	26--69	10YR 5/3	10YR 3/3	s	sg	lo	lo-vfr	so, po		5--10	as	88	8	3	0.47	0.22	
C2	69--90	10YR 5/2	10YR 3/3	s	sg	lo	lo-vfr	so, po		5--10	cw	93	5	2	0.32	0.34	
C3	90--109	10YR 5/2	10YR 3/3	s	sg	lo	lo-vfr	so, po		35--55	cs	94	5	1	0.28	0.32	patchy coatings of CaCO3 on clasts bottoms: Stage I-
C4	109--130	10YR 5/2	10YR 4/3	s	sg	lo	lo-vfr	so, po		10--15	as-aw	95	4	1	0.26	0.17	base of stream channel deposits
Buried Soil																	
Bt1b	130--151	10YR 5/4	8.25YR 4/3	sl	1 c,m sbk	h-sh	vfr	so, po-ps	2n-mkpf + po	5--10	cs	66	24	10	0.49	0.43	truncated top of buried soil
Bt2b	151--196	10YR 5/4	10YR 4/3	sl	1 c,m sbk	h-sh	vfr	ss-so, po-ps	1n-mkpf + po	10--20	cs	64	9	27	0.44	0.44	abundant pumice
BCb	196--236	10YR 5/3	10YR 4/3	sl	m + 1 c,m sbk	sh	vfr	ss-so, po-ps		10--20	cs			no data			
CBb	236--274	10YR 5/3	10YR 4/3	ls	m + 1 c,m sbk	sh-so	vfr	ss-so, po-ps		10--20	cs			no data			
Cb	274-300+	10YR 5/2	10YR 4/3	s	sg	lo	lo-vfr	so, po		5--15							

*Soil texture (<2mm fraction).
**Particle-size data from Longmire et al.(1996).
***Data from Longmire et al.(1996). CDB = dithionite extractabble Fe; OX = oxalate extractable Fe.

Table 1-4. Morphology for the FM-1 soil, Stop 1-6.

Horizon	Depth (cm)	Dry Color (Matrix)	Moist Color (Matrix)	Txt.*	Structure	Consistence			Argillans	% >2mm	Bdy**	Notes
						Dry	Moist	Wet				
A	0–4.5	10YR 4/2	10YR 2/1	l	1 m sbk: 1 c,m crb	so	lo-vfr	so, ps-po		3–5	as	
Bw1	4.5–16	10YR 5/3	10YR 3/3	l	1 m,f sbk	sh-so	vfr	so, ps-po	v1nco-pumice	4–6	cw	
Bw2	16–35	10YR 6/4	10YR 4/3	sl	1 m,c sbk	so	vfr	so, ps-po	v1nco-pumice	5–10	cs	
Bw3	35–49	10YR 6/4	10YR 4/3	ls	1 c,m sbk + sg	so-lo	vfr-lo	so, po		5–10	as-cs	
BC	49–60	10YR 6/3	10YR 4/3	ls	sg + 1 m,f sbk	so-lo	lo	so, po		2–6	aw	
2Bkqmb1	60–71	10YR 8/1	10YR 5/2	sl	m	vh-h	efi	so, po		2–4	as	Ash layer, platy, horizontal CaCO3 seams; weakly cemented
2Btkb1	71–79	7.5YR 4/6	7.5YR 4/4	s	sg	lo	lo	so, po	3mk-nco + br	90+	as	Top of pumice, disseminated CaCO3 and needle-shaped CaCO3 in some voids
2Btb1	79–139	7.5YR 3/4	7.5YR 3/3	s	sg	lo	lo	so, po	*Lam:* 2-1n-mkco + br	95+	ds	Abundant lamellae
2Cb1	139–267	10YR 8/0	10YR 7/2	s	sg	lo	lo	so, po		95+		Unaltered pumice
3BEb2	267–280	10YR 6.5/3	10YR 4/3	l	2-3 c pr: 1-2 c,m abk	h-sh	fi-fr	ss, ps	2n-mkpr:pf	2–5	as	Transtional E horizon, top of buried soil, abundant charcoal
3Btb2	280–300	7.5YR 6/4	7.5YR 4/4	sil	2 m,f sbk + abk	sh-h	fr	ss, ps	2npf + br, 1 mk pf + br	40–60	aw	Thin Bt horizon
R	300+											Fractured tuff

*Soil texture (<2mm fraction)

**Horizon boundary.

Lam: lamellae

Table 2-1. Morphology for the WJR-5 and WJR-7 soils at Stop 2-2a and 2-2b.

Horizon	Depth (cm)	Dry Color (Matrix)	Moist Color (Matrix)	Txt.*	Structure	Consistence Dry	Consistence Moist	Consistence Wet	Argillans	%** >2mm	Bdy***	Notes
WJR-5: Post-El Cejate Soil												
A	0--4	10YR 4/2	10YR 2/3	sil	2-1 m,f pl: 1-2 m sbk	sh-so	vfr	ss, ps		2--5	as	
Bw	4--23	10YR 6/3	10YR 4/3	sil	1 c,m sbk	sh-h	vfr	ss, ps		2--5	cs	
Bt1	23--39	10YR 6/3	8.75YR 4/3	sil	1 m pr: 1-2 c,m sbk	h-sh	fr	ss, ps	3npr:pf, 1npf	2--5	as	
Bt2	39--61	7.5YR 6/4	7.5YR 4/4	sil	2-3 m,f pr: 2.- m abk+sbk	h	fr-fi	ss, ps	4mk-npr:pf, 3n-mkbk:pf, 3n-mkpo	5--10	as-cs	
Bt3	61--84	7.5YR 6/3	7.5YR 4/3	sil	2 m pr: 2 c,m sbk+abk	h-sh	fr	ss, p	3n-mkpr:pf, 3n-mkpo, 2mk-nbk:pf	5--15	cs	
Bt4	84--106	7.5YR 6/4	7.5YR 4/4	sil	2-1 m pr: 2 c,m sbk	h	fr	ss, ps-p	4n-mkpo, 3mk-npr:pf, 1nbk:pf	10--20	cs	
Bt5	106--132	10 YR 6/3	7.5YR 4/3	sil	1 m pr: 2-1 c,m sbk	h-sh	fr	ss-s, ps-p	3n-mkpr:pf, 3n-mkpo, 1n-mkbk:pf	10--20	aw	
2Bt1	132--148	10 YR 8/2	10 YR 7/4	is	sg	so-lo	vfr	vss-ss, vps	1fco+br, lam:3mk-nco+br	30--50	cs	
2Bt2	148--203	10 YR 8/3	10 YR 7/4	scl	sg	so-lo	fr-lo	vss, vps	v1fco+br, lam:4mk-nco+br	30--50	cs	
2Bt3	203--221	10 YR 5/4	10 YR 4/4	sl	sg	so-lo	vfr-lo	vss-ss, vps	v1fco+br, lam:4mk-kco+br	30--50	aw	
3EBtb	221-230	10YR 6/4	10YR 4/3	ls	2-3 vc,c pr	vh-eh	efi	ss, ps-p		2--4	as	4n-mk skeletans pr:pf
3BEtb	230--243	10YR 6/4	10YR 4/3	sil	2-3 vc,c pr: 1 c,m sbk	vh-eh	efi	ss, ps-p	1npf	2--4	as	4n-mk skeletans pr:pf
3Bt1b	243--268	7.5YR 6/4	7.5YR 4/4	sil	2 m pr: 1-2 c,m sbk + abk	h	fr-fi	ss, ps-p	4mk-npo, 3n-mkpr:pf, 1nbk:pf	2--4	as	
3Bt2b	268--308	7.5YR 6/4	7.5YR 5/4	sil	3-2 m,f pr: 2 m,f abk + sbk	h	fr-fi	ss, p	4mk-npo, 3n-mkpr:pf, 1nbk:pf	4--8	cs	weak lamellae
WJR-7: Pre-El Cajete Soil												
A1	0--4	10YR 4/2	10YR 2/3	l	1 c,m pl: 2 m sbk + crb	so-lo	vfr	ss, ps		5--10	as	3n silans on pumice
A2	4--11	10YR 5/3	10YR 3/3	is	1 c,m sbk	so-sh	vfr	vss, vps		10--15	aw	3n silans on pumice
E	11--20	10YR 7/3	10YR 5/3	l	1 c sbk + sg	lo-so	lo	so, vps-po	v1nco on bottom of pumice	20--30	aw	pumice
Bt1	20--29	7.5YR 6/4	7.5YR 4/4	scl	1 m sbk + sg	so-lo	vfr	ss, vps	4 mk br + co on pumice	20--30	aw	pumice
Bt2	29--71	7.5YR 6/4	7.5YR 4/4	sl	1 m sbk + sg	so-lo	vfr	ss, vps	3 mk br + co on pumice	20--30	aw	pumice
Bt3	71--77	7.5YR 6/4	7.5YR 4/4	scl	1 m sbk + m	sh-h	vfr	ss, vps	4mk-kbr + co	15--25	as	pumice
2EBt1b	77--83	10YR 6/4	10YR 4/3	l	1-2 c,m pr: 1 c,m pl	vh-eh	vfi	ss, ps	4n-mkpr:pf	1--3	as	top of pre- El Cajete soil, colloidal stains as lamellae
2EBt2b	83--92	10YR 6/4	10YR 4/3	sil	2-1 c,m pr	vh-eh	vfi	ss, ps	3n-mkpr:pf	1--3	as	
2Bt1b1	92--101	7.5YR 6/4	7.5YR 4/4	sil	1 c,m pr	h	fr	ss, ps	3npr:pf	2--4	cs	former BA-Bw horizon
2Bt2b1	101--117	7.5YR 6/4	7.5YR 5/4	sil	1 m pr: 1-2 c,m sbk	h	fr-fi	ss, ps	4n-mkpo, 1npf	3--6	cs	
2Bt3b1	117--132	7.5YR 6/4	7.5YR 5/4	l	2 m pr: 2 c,m sbk + abk	h	fi	ss, p	2n-mkpf, 1n-mkpo	5--15	cs	
2Bt4b1	132--155	7.5YR 6/4	7.5YR 5/4	cl	2-3 m pr: 2-3 m abk + sbk	h	fi	ss, p	4mkpr:pf, 4mk-nbk:pf, 4mk-npo	10--20	cs-cw	stongest Bt in profile
2Bt5b1	155--203	7.5YR 6/4	7.5YR 5/4	l	1-2 c,m pr: 2-1 c,m abk + sbk	h	fr	ss, p	4n-mkpr:pf, 4mk-npo, 3n-mkbk:pf	15--30	cs-gs	abundant large clasts
2Bt1b2	203--234	7.5YR 6/4	7.5YR 5/4	sil	2-1 m pr: 2-1 c,m sbk	h	fi	ss, p	4mk-npr:pf, 4mk-npo, 3n-mkbk:pf	5--10	cs	1 pr:pf mangans
2Bt2b2	234--266	7.5YR 6/4	7.5YR 5/4	sil	2 m pr: 2-3 m abk + sbk	h-vh	fi	ss, p	4mkpr:pf, 4n-mkbk:pf, 4mk-npo	2--5	ai	1 pr:pf mangans
2Bt3b2	266--276	7.5YR 6/4	7.5YR 5/4	l	1-2 m sbk	h-vh	fr	ss, p-ps	4mkbr+ co, 4mkpo	15--30	ai	pressure faces on pf

*Soil texture of the < 2mm fraction.

**Field estimates of gravel % by volume

***Horizon boundary.

Lam: lamellae

Table 2-2. Laboratory data for the WJR-5 and WJR-7 soils at Stop 2-2a and 2-2b.

Horizon	Depth (cm)	Sand (% wt.)*	Silt (% wt.)	Clay (% wt.)	pH	Bulk Density (g/cm3)**
WJR-5						
A	0--4	34	61	5	5.5	1.13
Bw	4--23	30	61	9	5.6	1.33
Bt1	23--39	30	58	13	5.5	1.40
Bt2	39--61	25	51	24	5.7	1.56
Bt3	61--84	25	54	21	6.0	1.40
Bt4	84--106	21	57	22	6.1	1.23
Bt5	106--132	31	53	17	6.4	1.26
2Bt1	132--148	69	14	17	6.5	0.71
2Bt2	148--203	70	9	21	6.6	0.62
2Bt3	203--221	74	12	14	6.7	n.d.
3EBtb	221-230	33	48	18	6.8	1.83
3BEtb	230--243	26	55	19	6.9	1.72
3Bt1b	243--268	23	57	20	7.1	1.66
3Bt2b	268--308	20	59	21	7.1	1.56
WJR-7						
A1	0--4	46	45	8	5.2	1.03
A2	4--11	84	9	6	4.9	0.78
E	11--20	40	49	11	5.1	0.73
Bt1	20--29	49	18	33	5.9	0.87
Bt2	29--71	73	7	19	6.0	0.87
Bt3	71--77	52	20	28	6.2	1.03
2EBt1b	77--83	40	44	16	6.2	1.74
2EBt2b	83--92	25	60	15	6.3	1.63
2Bt1b1	92--101	28	60	12	6.5	1.71
2Bt2b1	101--117	31	54	15	6.6	1.64
2Bt3b1	117--132	33	45	22	6.8	1.73
2Bt4b1	132--155	36	37	27	6.9	1.79
2Bt5b1	155--203	44	34	22	7.1	1.59
2Bt1b2	203--234	31	51	18	7.1	1.86
2Bt2b2	234--266	14	63	23	7.2	1.74
2Bt3b2	266--276	42	35	23	7.4	1.67

*Particle-size distribution measured using standard pipette method.

**Bulk density measured by wax-coated clod method or by in-situ measurement of soil volume.

Table 2-3. Pyrophosphate, oxalate, and dithionite selective dissolution results for soils in mixed colluvium and fan deposits, western scarp area.

Horizon	Depth (cm)	% Alp	% Alo	% Feo	% Fed	% Sio	% wt. Fe2O3o	% wt. Fe2O3d	Fed/Feo	(Alo-Alp)/ SiO2*	% wt A + I**
WJR-7: ***Soil formed in Pleistocene El Cajete pumice/pre-El Cajete deposits***											
A1	0--4	0.18	0.33	0.33	0.34	0.13	0.19	0.49	0.38	1.18	0.91
A2	4--11	0.20	0.39	0.26	0.28	0.16	0.15	0.40	0.37	1.20	1.12
E	11--20	0.14	0.34	0.35	0.27	0.16	0.20	0.39	0.51	1.21	1.17
Bt1	20--29	0.55	0.57	0.36	0.67	0.30	0.21	0.95	0.22	0.06	2.13
Bt2	29--71	0.25	0.48	0.30	0.36	0.25	0.17	0.52	0.33	0.90	1.80
Bt3	71--77	0.50	0.60	0.37	0.55	0.30	0.21	0.78	0.27	0.35	2.15
2EBt1b	77--83	0.17	0.38	0.58	0.69	0.23	0.33	0.99	0.34	0.93	1.61
2EBt2b	83--92	0.11	0.26	0.34	0.73	0.18	0.19	1.05	0.19	0.83	1.25
2Bt1b1	92--101	0.08	0.21	0.28	0.65	0.17	0.16	0.93	0.17	0.75	1.23
2Bt2b1	101--117	0.11	0.24	0.30	0.60	0.18	0.17	0.86	0.20	0.71	1.31
2Bt3b1	117--132	0.09	0.27	0.29	0.54	0.24	0.17	0.78	0.21	0.74	1.75
2Bt4b1	132--155	0.11	0.34	0.29	0.59	0.30	0.17	0.84	0.20	0.78	2.13
2Bt5b1	155--203	0.08	0.27	0.29	0.56	0.24	0.16	0.80	0.20	0.79	1.72
2Bt1b2	203--234	0.07	0.26	0.37	0.58	0.23	0.21	0.83	0.25	0.83	1.66
2Bt2b2	234--266	0.07	0.29	0.24	0.58	0.28	0.14	0.83	0.17	0.81	1.99
2Bt3b2	266--276	0.05	0.29	0.27	0.52	0.25	0.15	0.75	0.20	0.96	1.77
WJR-6: ***Soil formed in ~Holocene fan deposits, Canon de Valle***											
A	0--5	0.26	0.31	0.37	0.41	0.07	0.21	0.59	0.36	0.75	0.53
Bw1	5--18	0.20	0.28	0.41	0.28	0.09	0.24	0.40	0.60	0.94	0.65
Bw2	18--57	0.11	0.21	0.44	0.18	0.09	0.25	0.26	0.95	1.19	0.62
BC1	57--100	0.16	0.28	0.64	0.22	0.12	0.36	0.31	1.17	1.05	0.84
C1	100--119	n.d.	n.d.	n.d.	n.d.	n.d.	n.d.	n.d.	n.d.	n.d.	n.d.
C2	119--149	0.14	0.26	0.45	n.d	0.12	0.25	n.d	n.d	1.01	0.85
C3	149--187	0.20	0.25	0.61	n.d	0.13	0.35	n.d	n.d	0.43	0.92

Notes: p = Pyrophosphate extraction (0.1M Na-pyrophosphate)
o = Acid-oxalate extraction (0.2 M oxalic + 0.2 M ammonium oxalate).
d = Dithionite-citrate extraction (0.3 M sodium citrate + Na-dithionite + Na-bicarbonate)

*Estimated Al/Si atomic ratio for allophane/imogolite (Parfitt and Childs, 1988).

**Estimated concentrations for allophane and imogolite as a function of % Sio (Parfitt and Childs, 1988).

Table 2-4. Morphology for the WJR-6 soil formed in alluvial fan deposits at Canon de Valle.

Horizon	Depth (cm)	Dry Color (Matrix)	Moist Color (Matrix)	Txt.*	Structure	Consistence			%** >2mm	Bdy***	Sand (% wt.)	Silt (% wt.)	Clay (% wt.)	Notes
						Dry	Moist	Wet						
A	0–5	10YR 3.5/2	10YR 3/1	sl	2-3 c,m sbk + crb	sh-so	vfr	ss, ps	20–15	as	57	36	8	
Bw1	5–18	10YR 6/3	10YR 4/2	sil	1 m sbk	so	vfr	so, vps	35–50	cs	36	55	8	1n silans co clasts
Bw2	18–57	10YR 7/2	10YR 4/2	ls	1 m sbk	so	vfr	so, vps	40–60	cs-gs	74	23	3	3n silans co clasts
BC1	57–100	10YR 6/2	10YR 4/2	s	sg	lo	lo	so, po	40–60	cs	87	9	3	1n silans co clasts
C1	100–119	10YR 6/4	10YR 6/6	s	sg	lo	lo	so, po	70–80	cw	88	9	2	oxidized coatings on clasts
C2	119–149	10YR 6/2	10YR 4/2	s	sg	lo	lo	so, po			89	8	3	
C3	149–187	10YR 6/2	10YR 4/2	s	sg	lo	lo	so, po			90	7	3	

*Soil texture (<2mm fraction)

**Field estimates of gravel % by volume

**Horizon boundary

Table 2-5. Estimated Ages of Rendija Canyon Stream Terraces

Stream Terrace	Height Above Channel (m)*	Estimated Age (ka) Gonzalez & Gardner (1990)	Wong et al. (1995)	McDonald et al. (1996b)**	This Guidebook ***
Qt1a	42, 32	-	-		?
Qt1	32, 22	180-250	150-300	-	>102-160
Qt2	27, 21	180-250	100-200	105-180	102-160
Qt4	11,7	60-130	20-100	70-80	67-74
Qt5	6.5, 5	60-130	-	-	9.6-10.0
Qt6	4.5, 4	6-25	6-7	5.2-7.0	5.7-7.9
Qt7	2.1, <1.6	6-25	2-3	3.2	3.0-4.6
Qt8	0.7, <-0.4	<6	-	0.5-1.1	0.5-1.7

Notes:

* Heights are the top and bottom of gravelly stream deposits, as measured at sites between the Guaje Mountain fault zone and Cabra Canyon, except for Qt1a which shows the range in observed heights of gravels associated with several buried terrace remnants. (Note that heights and thicknesses of stream deposits vary longitudinally within the canyon.)

** Holocene ages in McDonald et al. (1996b) are uncalibrated ^{14}C dates from soil pits used in developing the initial soil chronofunction.

*** Holocene ages presented here are calibrated ^{14}C ages indicating probable ages for the primary stream deposits associated with each terrace. Many terrace units include multiple discrete sedimentary packages and/or multiple terrace levels that are closely spaced in time or that have similar heights above the channel, and which have not been broken out as separate mapping units. Soil-based age estimates use a chronofunction that has been revised slightly from McDonald et al. (1996b), and incorporates soil descriptions from additional pits excavated in 1996.

Table 2-6. Morphology for representative soils on the Holocene Qt8, Qt7, and Qt6 surfaces.

Horizon	Depth (cm)	Dry Color (Matrix)	Moist Color (Matrix)	Txt.*	Structure	Consistence Dry	Consistence Moist	Consistence Wet	Argillans	% >2mm*	% wt. Sand	% wt. Silt	% wt. Clay
Qt8 RCT8-2													
A1	0--9	10YR 4/3	10YR 2/2	l	1 m sbk:1-2 m,f crb	sh-so	vfr	so, po		3--8	60	32	8
A2	9--14	10YR 4/2	10YR 2/1	sl	1 m sbk:1 m,f crb	sh-so	vfr	so, ps		3--8	77	17	6
BA	14--26	10YR 4/2	10YR 3/2	sl	1 m,f sbk	so	vfr	so, ps		5--10	77	18	5
Bw	26--39	10YR 4.5/2	10YR 3/2	ls	1 m sbk	sh-so	vfr	so, vps		5--10	83	19	3
CB	39--54	10YR 5/3	10YR 4/2	ls	sg	so-lo	lo	so, vps		10--20	90	8	2
C1	54--85	10YR 5.5/2	10YR 4/2	s	sg	lo	lo	so, po		25--40	98	2	1
C2	85--140	10YR 6/3	10YR 4/2	s	sg	lo	lo	so, po		25--40	97	2	1
Qt7 RCT7-1													
C	0--8	10YR 5/4	10YR 4/3	l	1 m,f pl	sh	fr	vss, ps		2--4	39	50	11
A	8--17	10YR 3/2	10YR 2/1	sl	1 m,f sbk	sh-so	vfr	vss, ps		5--15	72	22	6
Bw1	17--26	10YR 5/2.5	10YR 3/3	sl	1 c,m sbk	so	vfr	vo, pss		10--25	77	19	4
Bw2	26--69	10YR 5/2.5	10YR 3/2.5	sl	1 c,m sbk	so	vfr-lo	vo, pss		15--25	76	21	4
CB	69--95	10YR 5/3	10YR 3/2.5	sl	m + 1 c,m sbk	so	vfr-lo	vo, pss		15--25	77	20	4
C	95--155	10YR 5/3	10YR 3/3	ls	sg	lo	lo	so, po		40--60	86	12	2
Qt6 RCT6-2													
A	0--8	10YR 5.5/3	10YR 3/2	sil	1 m pr:1c,m,f sbk	so	vfr	ss, ps		3--8	40	51	9
BA	8--15	8.75YR 5/3	8.75YR 4/2	sil	2 m pl:1 m sbk	sh	vfr	s-ss, p-ps		3--8	19	64	16
Bw1	15--27	10YR 5/3	10YR 4/2	sil	1 m sbk	h	fr-vfr	ss, ps		3--8	60	30	11
Bw2	27--60	10YR 5/2	10YR 3/2	l	1 c,m sbk	sh	vfr	ss, ps-vps	vf f br	20--30	66	25	9
Bw3	60--79	10YR 6/3	10YR 4/2	sl	1 c,m sbk	sh	vfr	so, vps		25--40	81	14	5
BC	79--116	10YR 5.5/3	10YR 4/3	ls	sg	so-lo	vfr-lo	so, vps-po		35--50	80	15	5
C1	116--165	10YR 6/2	10YR 4/2	s	sg	lo	lo	so, po		50--70	86	13	1
C2	165--205	10YR 6/2	10YR 4/2	s	sg	lo	lo	so, po		5--15	98	2	0

*Soil textural class

**Field estimates of gravel % by volume

Table 2-7. Radiocarbon Ages From Rendija Canyon Soil Pits

Soil Pit	Field Sample Number(s)	^{14}C Age (yr B.P.)	Calibrated Age (cal yr. BP) **	Depth(s) (m)	Notes
Qt8 Terrace					
RCT8-1	GM-30, GM-32	1040 ± 35	940 (920-1050)	0.7, 1.7	average of 2 statistically indistinguishable dates from upper and lower parts of channel deposit
RCT8-2	GM-38, GM-39	500 ± 45	520 (490-550)	0.3, 0.7	average of 2 statistically indistinguishable dates from sandy floodplain deposit and underlying gravelly channel deposit
RCT8-3	GM-48, GM-52	1030 ± 20	940 (920-970)	0.6, 2.1	average of 2 statistically indistinguishable dates from sandy floodplain deposit and basal channel deposit
Qt7 Terrace					
RCT7-1	GM-29, GM-41	3210 ± 45	3400-3440 (3350-3480)	0.6, 1.5	average of 2 statistically indistinguishable dates from sandy floodplain deposit and underlying gravelly channel deposit
Qt6 Terrace					
RCT6-1	GM-28	6950 ± 80	7710 (7580-7910)	1.6	lower part of gravelly channel deposit
RCT6-2	GM-35	5280 ± 60	6000-6160 (5920-6260)	1.0	uppermost channel deposit
RCT6-3	GM-53	5040 ± 50	5750-5850 (5650-5920)	1.4	upper channel deposit
Qt4 Terrace					
RCT4-2	GM-46	13,820 ± 60	16,570 (16,340-16,800)	1.15	CaCO3-rich horizon in buried soil, below Holocene colluvium
Qt2 Terrace					
RCT2-1	RCT2-1	10,860 ± 70	12,790 (12,590-12,970)	0.7	lower part of upper colluvial deposit

Notes:

* Shown are "best estimates" for ages of soils at specific pits used in developing soil chronofunction. For sites with multiple dates, these are either: 1) an average of 2 statistically indistinguishable dates; or 2) the stratigraphically highest date, except in cases where the uppermost date is suspect. All radiocarbon dates are AMS analyses on disseminated charcoal fragments, and are corrected for $\delta^{13}C$. Uncertainties in original date are 1σ values reported by laboratory, or that obtained after averaging 2 similar dates.

** Calibrated ages use computer program CALIB 3.03 of Stuiver and Reimer (1993), with error multiplier of 2.0 and 2σ uncertainty. Ages in ( ) are 2σ range.

Table 2-8. Drainage Basin Parameters For Cabra and Rendija Canyons

Drainage Basin	Drainage Area (km^2)	Channel Gradient (deg.) **	Tschicoma Formation Outcrop (%) ***	Mean Elevation (m)	Basin Relief (m)
Cabra	4.7	1.4 (0.9)	26	2245	295
Rendija *	17.3	1.2	58	2400	895

Notes:
* Values for Rendija Canyon are for part upstream of confluence with Cabra Canyon.
** Channel gradient measured for reach immediately upstream of confluence of Cabra and Rendija Canyons. Number in parentheses for Cabra Canyon is estimated channel gradient at ca. 3.2 ka (see Fig. 2-33).
*** Percentage of drainage basin underlain by Tschicoma Formation dacite, based on map of Smith et al. (1970). Remainder of basins underlain by Bandelier Tuff, pumice beds and alluvium of Cerro Toledo interval, and Quaternary alluvium.

Table 2-9. Morphology for representative soils on the Pleistocene Qt4, Qt2, and Qt1 surfaces.

Horizon	Depth (cm)	Dry Color (Matrix)	Moist Color (Matrix)	Txt.*	Structure	Consistence Dry	Consistence Moist	Consistence Wet	Argillans	% >2mm**	CS***	% wt. Sand	% wt. Silt	% wt. Clay
Qt4 RCT4-1														
A	0--8	10YR 5.5/3	10YR 4/3	sil	2 m,f pl: 1 m sbk	sh	vfr	ss, ps		3--8		34	57	9
Bw1	8--34	8.75YR 6/4	8.75YR 4/3	sil	1-2 m pr: 1-2 c,m,f sbk	sh	vfr	ss, ps		3--8		34	51	15
Bw2	34--52	8.75YR 5/3	8.75YR 4/3	sil	1-2 m pr: 1-2 c,m,f sbk	sh-so	vfr	ss, ps		3--8		29	55	15
Bw3	52--69	10YR 5/3	10YR 4/3	sil	1-2 m pr: 2-1 c,m sbk	sh	fr	ss, ps-p		3--8		28	57	15
Batb	69--90	7.5YR 6/3	7.5YR 4/3	sil	1-2 m pr: 1-2 c,m,f sbk	h	fi-dr	ss, ps-p	3npr:pf, 2npo, 1nsbk:pf	5--10		34	53	13
Btb	90--109	7.5YR 6/3	7.5YR 4/3	sil	1-2 m pr: 1-2 c,m,f sbk	h	fr	ss, ps-p	3n-mkpo, 1npr:pf	10--15		38	54	7
Btk1b	109--126	10YR 4/3	10YR 5/3	l	1-2 m pr: 1-2 c,m sbk	vh-h	fi-fr	s-s, ps	3npo, 1npf	5--15	II-	44	46	10
Btk2b	126--162	10YR 5/3	10YR 4/3	l	2-1 m pr: 1-2 c,m sbk	vh-h	fi-fr	ss, ps-p	3npo	5--10	I	51	39	9
Btk3b	162--172	8.75YR 5/4	8.75YR 4/3	sl	1 m pr: 1 c,m sbk	vh-h	fr	ss, ps	3n-mkpo	15--20	I-	63	29	9
Btk4b	172--198	10YR 5/3.5	8.75YR 4/3	sl	1 m pr :1 c,m sbk	h	fi-fr	s-ss, ps	2npo, 1npf	15--20	I-	70	21	9
Btb'	198--226	8.75YR 6/3	7.5YR 4/3	sl	sg	so	vfr-io	so, ps	2nco	45--55		65	24	11
BCb	226--274	8.75YR 5/4	8.75YR 4/3	ls	sg	so	vfr	so, ps	1nco	45--55		80	12	9
Qt2 RCT2-2														
A	0--10	10YR 5/3	10YR 3.5/2	sil	1 m sbk	so	vfr	s, ps		2--5		18	68	13
BA	10--28	10YR 5/3	10YR 3/2	sil	1-2 c,m sbk	sh	fr	ss, ps		2--5		17	66	16
Bw1	28--49	10YR 5/3	8.75YR 3/3	sil	1-2 m pr :2-1 c,m sbk	sh	fr-vfr	ss, ps		3--8		19	67	15
Bw2	49--63	10YR 5.5/3	10YR 3/2	sil	1-2 m pr 2-1 c,m sbk	sh	fr-vfr	ss, ps		3--8		19	67	14
Bw3	63--77	10YR 6/3	10YR 4/3	sil	1-2 m pr: 2 c,m sbk	h	fr	s, ps	v1nco + po	3--8		24	63	13
Bt1b1	77--90	10YR 6/3	8.75YR 4/3	sil	1-2 m pr: 1-2 m pl+1-2 c,m sbk	h	fr-fi	s, p	3n-mkpf, 3n-mkpo	2--5		24	58	18
Bt2b1	90--107	10YR 6/3	10YR 4/3	sil	2-1 m pr: 2 c,m abk + sbk	h	fi	ss, p-ps	4mkpf + po	2--5		28	58	13
Etkb2	107--123	10YR 6/3	10YR 4/3	sil	1 c,m pr: 1-2 c,m abk	vh	fi	ss, p-ps	4mkpf + po	2--5	I	33	57	10
BEtkb2	123--143	10YR 6/3	10YR 4/3	sil	1 c,m pr: 1-2 c,m abk	vh	vfi	ss, ps	4n-mkpo, 4npr:pf	2--5	I	36	55	9
Bt1b2	143--177	7.5YR 5/4	6.25YR 4/3	sil	2-1 m,f pr: 3-2 c,m abk	h	fr	s-ss, p	4mkpf + po	10--20		28	50	22
Bt2b2	177--214	7.5YR 5/4	6.25YR 4/3	sil	2 m pr: 2 c,m abk + sbk	h	fi-fr	ss, p	4mkpo, 4n-mkpr:pf, 3n-mkbk:pf	15--25		33	50	16
Bt3b2	214--257	7.5YR 5.5/4	7.5YR 4/4	l	1 m pr: 2-1 c,m sbk	h	fi-fr	ss, p-ps	4n-mkpo, 3n-mkpr:pf, 1nbk:pf	10--20		38	49	14
Bt4b2	257--278	7.5YR 6/4	7.5YR 4/4	l	1 c,m sbk	h-sh	fr	s, ps-vps	3n-mkpo, 2nbr, 1npf	10--20		43	44	13
Bt5b2	278--319	10YR 6/4	8.75YR 4/3	l	1 c,m sbk + m	h-sh	fr-vfr	ss, p	3npo, 2nbr	25--40		47	40	12
BCb2	319--348	10YR 6/4	10YR 4/4	sl	m	h	fr-vfr	ss, vps	2fpo	15--25		64	30	6
Qt1 RCT1-2														
A	0--6	8.75YR 5/3	7.5YR 3/3	l	1-2 m pl: 1-2 m,f sbk	sh	vfr	ss, ps		2--5		48	43	9
BA1	6--19	8.75YR 5/4	7.5YR 3/3	l	1-2 m,f pl: 1-2 m,f sbk	so	vfr	ss, ps		2--5		37	49	14
BA2	19--41	7.5YR 6/4	7.5YR 4/3	l	1-2 m pl: 1-2 c,m sbk	sh	vfr-fr	ss, ps	1npr:pf	2--5		41	46	14
Bt1	41--51	7.5YR 6/4	7.5YR 4/4	l	1-2 c,m sbk	sh-h	fr	ss, ps	2n-mkpf	2--5		45	39	16
Bt2	51--68	7.5YR 6/4	7.5YR 4/3	sil	1-2 m pl: 1-2 c,m abk + sbk	h	fr	ss, ps	3n-mkpo, 3n-mkpf	5--10		32	50	17
Btkqm	68--85	8.75YR 6/3	7.5YR 4/3	sil	1-2 c,m pr: 2-1 c,m pl	vh	efi	ss, ps	3npo, 3npr:pf	10--30	II	38	51	11
Btk1	85--96	6.25YR 4/4	5YR 4/4	sl	1 c,m sbk	h	fr-vfr	ss-s, ps	4n-mkbr, 4n-mkbr	30--40	I	59	27	14
Btk2	96--111	6.25YR 4/4	5YR 4/4	sl	1-2 c,m sbk	h	fr-vfr	ss-s, ps	4mkpo	35--45	I	58	24	17
Btk3	111--137	7.5YR 6/4	7.5YR 4/4	ls	m	h	fr-vfr	ss, ps	1nbr, Lam:3n-mkbr	25--35	I	78	21	1
Btk4	137--190	7.5YR 6/4	7.5YR 3.5/4	ls	m	h	fr-vfr	ss, ps	1nbr, Lam:3n-mkbr	25--40	I-	80	13	7
BC	190--217	8.75YR 6/4	7.5YR 4/4	ls	m	sh-h	fr-vfr	vss, vps	1npo	2--5		84	16	1
CB1	217--245	8.75YR 6/4	7.5YR 5/4	s	m	sh	vfr	so, po	1nco	30--40		89	9	2
CB2	245--290	10YR 6/4	10YR 5/4	s	m	sh	vfr	so, po		10--15		86	10	3

*Soil textural class

**Field estimates of gravel % by volume

***Secondary carbonate stage (Gile et al., 1996).

Lam: = Lamellea

Table 2-10. Summary of soil B horizon thickness, PDI results, and estimated ages for non-dated surfaces.

Soil	Soil #	Total Bw Thickness (cm)	Total Bt Thickness (cm)	PDI	Mean PDI	Site Specific Age (ka)*	Age Range (ka)**	Estimated Age (ka) Using PDI***	Mean Age (ka) Using PDI***
Qt8	RCT8-1	16		3.9		9.4	0.5–1.7		
	RCT8-2	12		4.3		5.2	0.5–1.7		
	RCT8-3	19		4.4	4.2+0.3	9.4	0.5–1.7		
Qt7	RCT7-1	52		7.6	7.4	3	3.0–4.6		
Qt6	RCT6-1	67	13	18		7.7	5.7–7.9		
	RCT6-2	64		13.8		6.1	5.7–7.9		
	RCT6-3	68		16.1	16.0+2.1	5.8	5.7–7.9		
HCW****	RCT4-1-H	61		22.1			12.8, <16.6		
	RCT4-2-H	85		22.6		<16.6	12.8, <16.6		
	RCT2-1-H	45		21.4		12.8	12.8, <16.6		
	RCT2-2-H	49		22.1	22.1+0.5		12.8, <16.6		
Post-EC*****	WJR-5	23	182	69.4		50-60	50-60		
Qt4	RCT4-1		157	76.0			20-100	74.9	
	RCT4-2		124	71.4		>16.6	20-100	67.5	
	RCT4-3		174	77.9	75.1+3.3			76.7	73±9.8
Qt2	RCT2-1		276	95.0			100-200	102.7	
	RCT2-2		291	128.3			100-200	159.7	
	RCT2-3		202	115.3			100-200	136.5	
	RCT2-4		253	110.1				127.5	
	RCT2-5		211	105.8	110.9+12.3			120.3	129±42.0
Qt1	RCT1-1	41	149	71.7			150–300	>>67.9	
	RCT1-2		189	99.5	85.6+19.7		150–300	>>109.9	

*Radiocarbon dates from Table 2-8.

**Range for: (1)Qt8-Qt6 from ~30 radiocarbon dates from Rendija Canyon (Reneau, unpubl., 1995), (2) HCW from Table 2.8, (3) Qt4-Qt1 from Wong et al. (unpubl., 1995) based on relative comparisons of soil development.

***Soil ages calculated from linear regression results in Fig. 2-46.

****Soils formed in Holocene colluvial cap overlying Qt2 and Qt4 soils.

*****Soil formed in colluvium and loess overlying the ca. 50-60 ka El Cajete Tephra. Date for El Cajete from Reneau et al. (1995)

Table 2-11. Results of selective dissolution, pH, and clay mineralogy for select soils formed along Rendija Canyon.

Horizon	Depth (cm)	% Alp	% Alo	% Slo	% wt. Fe2O3o	% wt. Fe2O3d	Fed/Feo	(Alo-Alp)/ SiO2*	% wt A + I**	pH	Clay Minerals***		
											I	K	I-S
RCT8-1													
C	0--10	0.06	0.54	0.28	0.49	0.68	0.72	1.72	1.97	6	X	X	
A	10--20	0.05	0.43	0.26	0.42	0.50	0.84	1.49	1.83	6.1			
Bw	20--36	0.06	0.24	0.14	0.40	0.39	1.04	1.34	0.97	6.3	XX	XX	
BC	36--54	0.04	0.23	0.15	0.38	0.40	0.96	1.23	1.09	6.6			
C1	54--84	0.03	0.17	0.13	0.35	0.37	0.93	1.10	0.90	6.7			
C2	84--174	0.03	0.33	0.23	0.32	0.29	1.10	1.34	1.61	6.7	X	X	
RCT7-1													
C	0--8	0.36	0.46	0.19	0.50	0.72	1.35	0.54	1.35	6.1			
A	8--17	0.07	0.38	0.17	0.54	0.50	1.09	1.87	1.19	6.4			
Bw1	17--26	0.06	0.34	0.19	0.50	0.41	1.20	1.48	1.35	6.6			
Bw2	26--69	0.07	0.37	0.21	0.46	0.39	1.18	1.41	1.52	6.8	X	X	
BC	69--95	0.06	0.38	0.23	0.35	0.38	0.92	1.45	1.61	6.9			
C	95--155	0.05	0.34	0.23	0.36	0.46	0.80	1.24	1.66	7			
RCT6-2													
A	0--8	0.14	0.26	0.13	0.14	0.29	0.50	0.87	0.95	5.4			
BA	8--15	0.19	0.32	0.17	0.14	0.43	0.33	0.80	1.22	5.5			
Bw1	15--27	0.07	0.30	0.16	0.14	0.28	0.49	1.38	1.16	5.8			
Bw2	27--60	0.06	0.28	0.17	0.15	0.34	0.44	1.27	1.21	6	X	XX	
Bw3	60--79	0.05	0.26	0.16	0.13	0.26	0.49	1.29	1.14	6.2			
BC	79--116	0.04	0.25	0.18	0.19	0.27	0.70	1.18	1.30	6.3			
C1	116--165	0.04	0.19	0.15	0.14	0.17	0.83	1.01	1.07	6.4			
C2	165--205	0.04	0.18	0.14	0.13	0.14	0.93	0.99	0.99	6.3			
RCT4-1													
A	0--8	0.16	0.25	0.13	0.30	0.78	0.39	0.27	0.89	5		X	X
Bw1	8--34	0.09	0.33	0.18	0.33	0.92	0.36	0.51	1.30	5.8	X	X	
Bw2	34--52	0.12	0.36	0.22	0.35	0.95	0.36	0.76	1.60	6.3			
Bw3	52--69	0.10	0.28	0.17	0.33	0.83	0.40	0.58	1.24	6.2			
Bt1b	69--90	0.05	0.30	0.19	0.35	0.83	0.42	0.67	1.38	6.4	XX	XX	X
Bt2b	90--109	0.06	0.35	0.23	0.34	0.83	0.41	0.87	1.64	6.9			
Btk1b	109--126	0.07	0.36	0.23	0.36	0.83	0.43	0.83	1.67	7.4	X	X	X
Btk2b	126--162	0.07	0.39	0.26	0.32	0.72	0.44	0.82	1.89	7.6			
Btk3b	162--172	0.06	0.30	0.22	0.19	0.59	0.32	0.77	1.58	7.6			
Btk4b	172--198	0.05	0.30	0.20	0.16	0.55	0.28	0.80	1.40	7.6			
Btb	198--226	0.06	0.44	0.28	0.17	0.72	0.24	0.89	1.98	7.6	X	X	XX
BCb	266--274	n.d.	0.32	0.21	0.15	0.45	0.33	0.81	1.48	7.6	X	XX	
RCT2-1													
A	0--7	0.14	0.23	0.12	0.23	0.63	0.37	0.39	0.85	5.6			
BA	7--20	0.05	0.36	0.20	0.29	0.75	0.38	0.86	1.46	6.2			
Bw1	20--51	0.05	0.37	0.22	0.28	0.78	0.37	0.88	1.58	6.4			
Bw2	51--65	0.06	0.34	0.22	0.26	0.77	0.34	0.83	1.58	6.8	X	X	X
Btk1b	65--75	0.05	0.46	0.30	0.32	0.80	0.40	0.89	2.18	7.3	X	XX	
Btk2b	75--92	0.04	0.40	0.29	0.26	0.70	0.37	0.90	2.10	7.5			
Btk3b	92--107	0.06	0.50	0.35	0.20	0.72	0.28	0.87	2.50	7.6	X	XX	X
Btk4b	107--131	0.08	0.41	0.28	0.15	0.64	0.24	0.81	2.01	7.7			
Bt1b	131--180	n.d.	0.38	0.25	0.12	0.58	0.21	1.00	1.81	7.6			
Bt2b	180--206	n.d.	0.38	0.22	0.13	0.49	0.26	1.00	1.60	7.6			
Bt3b	206--234	n.d.	0.34	0.20	0.11	0.46	0.25	1.00	1.45	7.5			
Bt4b	234--296	n.d.	0.35	0.19	0.12	0.43	0.28	1.00	1.35	7.4	XX	XX	
BC	296--341	n.d.	0.17	0.11	0.21	0.29	0.72	1.00	0.81	7.3	XX	XX	

Notes: p = Pyrophosphate extraction (0.1M Na-pyrophosphate)
o = Acid-oxalate extraction (0.2 M oxalic + 0.2 M ammonium oxalate).
d = Dithionite-citrate extraction (0.3 M sodium citrate + Na-dithionite + Na-bicarbonate)

*Estimated Al/Si atomic ratio for allophane/imogolite (Parfitt and Childs, 1988).

**Estimated concentrations for allophane and imogolite as a function of % Slo (Parfitt and Childs, 1988).

***Preliminary XRD results: I = illite, K = kaolinite, I-S = illite-smectite interstratified clay. X = moderately to slightly abundant; XX = strongly abundant.

Appendix A-1. Key to symbols used in Tables of soil morphology.

Structure

Grade	Size	Type	Other
1 = weak	c = coarse	sbk = subangular blocky	: = parting to (e.g. pr:pf)
2 = moderate	m = medium	abk = angular blocky	
3 = strong	f = fine	pr = prismatic	
		pl = platy	
		sg = singles grain	
		m = massive	

Consistence

Dry	Moist	Wet - Stickiness	Wet - Plasticity
lo = loose	lo = loose	so = non sticky	po = non-plastic
so = soft	vfr = very friable	vss = very slightly sticky	vps = very slightly plastic
sh = slightly hard	fr = friable	ss = sticky	ps = slightly plastic
h = hard	fi = firm	s = sticky	p = plastic
vh = very hard	vfi = very firm		

Argillans (Mangans, Skeltans)

Abundance	Thickness	Location/Type
v1 = very few (< 5%)	n = thin	po = along pores
1 = few (2 - 25%)	mk = moderately thick	co = coating gravel, ped faces
2 = common (25 - 50%)	k = thick	br = bridging grains
3 = many (50 - 75%)		pf = along ped faces (co + br)
4 = nearly continuous (90%+)		pr:pf along prismatic ped faces
		bk:pf along blocky ped faces
		Lam = lamellae
		si = silt coatings

Horizon Boundary

Thickness	Topography
a =abrupt (< 2cm)	s = smooth
c = clear (2 - 5cm)	w = wavy
d = diffuse (> 5 cm)	i = irregular

Texture

s = sand	sil = silt loam
ls = loamy sand	scl = sandy clay loam
sl = sandy loam	sicl = silty clay loam
l = loam	cl = clay loam

Library Materials Processing Form

From: Initials NS
Date 10/9/96

The attached item was checked against the online catalog and it is:

✓ New title

____ Related title (Call #:_____)

____ Added copy/vol.
(Call #:_____)

To: Collection

___ Rush catalog

✓ For REF REF-IA (MAIN) REPT REPREF
other _____

___ Transfer
____

___ Make r Nancy:

_____

___ Withdr For library.

Steve

!.95